



# AUTOMATIC INTRAMYOCARDIAL STEM CELL INJECTION DEVICE

---

FINAL REPORT

DECEMBER 14TH, 2022

BME 400

Team: Heartthrob

Lab Section 304

Team Members:

Parker Esswein (Leader)

Macy Frank (Communicator)

Lars Krugel (BPAG)

Vanessa Obrycki (BWIG)

Gab Zuern (BSAC)

Client: Dr. Amish Raval, Department of Medicine and Biomedical Engineering

Advisor: Dr. Aviad Hai, Department of Biomedical Engineering

## Abstract

Treating heart failure by injecting mesenchymal stem cells (MSC) into the myocardium via an injection device and a needle-tipped catheter is a novel approach that can improve quality of life. The procedure is currently performed manually with 10 - 14 sequential injections of a 0.5 mL MSC aliquot solution over a 30 or 60 second duration. Unfortunately, manual injections result in an uncontrolled flow rate, inconsistent cell delivery, and operator fatigue. This can limit cell retention and induce cell reflux, damage, or clumping. Automating the injections can improve stem cell delivery and enhance the clinical success of intramyocardial MSC injections. Existing automatic injection devices are insufficient since they can not display intramyocardial MSC injection forces and are not approved or tailored for this procedure. As a result, a novel automatic injection device was fabricated that integrates with the procedural syringe-catheter system, limits operator intervention, provides controlled injection rates, maintains standard cell viability, constantly displays injection forces, and alerts the operator if catheter obstruction is imminent. Extensive validation testing was performed and the results confirmed that MSC viability does not decrease by more than 5% from initial viability, the force feedback system is accurate and consistent, and the device delivers 0.5 mL of solution in 30 and 60 second intervals. Thus, the device has the potential to enhance procedural success. Bovine steak and *ex vivo* heart testing determined typical injection forces for different tissue and stiffness values, demonstrating the injector's ability to function as a research device.

## Table of Contents

<b>Abstract</b>	<b>2</b>
<b>Introduction</b>	<b>7</b>
Motivation	7
Problem Statement	8
<b>Background</b>	<b>9</b>
Current Cardiovascular Disease Treatment	9
Mesenchymal Stem Cells	9
Intramyocardial Stem Cell Injection Procedure	9
Flow Rate Impact	10
Existing Devices and Current Methods	11
Standards and Regulations	15
Client Information	16
Design Specifications	16
<b>Preliminary Designs</b>	<b>17</b>
Overview	17
Cellringe Pump: Thread Regulated Injections	17
Visual Feedback System	19
Design Ideas	20
FSR 400 Series Round Force Sensing Resistor	20
FSG020WNPB Series Force Sensor	22
LCMKD-10N Load Cell with NanoShield	24
P30 Non-Invasive Pressure Sensor	25
<b>Preliminary Design Evaluation</b>	<b>28</b>
Design Evaluations	28
Proposed Final Design	32
<b>Fabrication/Development Process</b>	<b>33</b>
Materials	33
Overview	33
Force Sensor	34
Microcontroller and Software	34
Visual Feedback Display and Circuitry	35
Ultimaker PLA Injector Components	36
Injector Force Application Materials	37

Methods	39
Final Prototype	43
Testing	45
Feedback System Force Detection Accuracy Testing	45
Feedback System Testing	46
Syringe Clamp Connection and Locking Testing	46
Injection Rate Testing	47
Cell Viability Testing	47
Overall Device Testing	48
25 Gauge Injection Testing	48
Clinical Simulation Testing	48
Catheter Backup Testing	49
Bovine Steak Injection Testing	49
Ex Vivo Cervine Heart Injection Testing	50
Viscosity Testing	50
Pressure Sensing Catheter Testing	50
<b>Results</b>	<b>51</b>
Feedback System Force Detection Accuracy	51
FSR Force Detection Accuracy	51
FSG Force Detection Accuracy	53
FSR vs FSG Force Accuracy Results	55
FSR Feedback System Results	57
Syringe Clamp Connection and Locking Results	58
Injection Rate Results	59
Cell Viability Results	59
Overall Device Results	63
25 Gauge Injection Results	63
Clinical Simulation Results	64
Catheter Backup Results	65
Bovine Steak Injection Results	67
Deer Heart Injection Results	70
Viscosity Testing Results	72
Pressure Sensing Catheter Results	74
<b>Discussion</b>	<b>75</b>
Discussion of Results	75



Feedback System Force Detection Accuracy Testing	75
FSR Feedback System Testing	76
Syringe Clamp Connection and Locking Testing	76
Cell Viability Testing	77
25 Gauge Needle Testing	77
Catheter Backup Testing	78
Bovine Steak Injection Testing	79
Ex Vivo Heart Cervine Injection Testing	79
Viscosity Testing	80
Pressure Sensing Catheter Testing	80
Ethical Considerations of Design	81
Sources of Error	82
<b>Conclusion</b>	<b>84</b>
Overview	84
Future Work	85
<b>References</b>	<b>88</b>
<b>Appendix</b>	<b>96</b>
Section 1: Product Design Specifications	96
Section 2: Material Information and Calculations	112
Section 2.1: Arduino Uno Rev 3 Technical Data Sheet	112
Section 2.2: FSR 400 Series Round Force Sensing Resistor Technical Data Sheet	113
Section 2.3: FSG020WNPB Series Force Sensor Technical Data Sheet	115
Section 2.4: LCMKD-10N Load Cell Technical Data Sheet	117
Section 2.5: Pressure Range Calculations	119
Section 2.6: P30 Non-Invasive Pressure Sensor Technical Data Sheet	120
Section 2.7: LED Serial 7-Segment Digital Display Technical Data Sheet	121
Section 2.8: INA129 Instrumentation Amplifier Technical Data Sheet	122
Section 2.9: Ultimaker PLA Technical Data Sheet	123
Section 2.10: NEMA-17 Stepper Motor Technical Data Sheet	124
Section 2.11: Grainger Zinc Coated Aluminum Fully Threaded Bolt Technical Data Sheet	125
Section 2.12: Grainger Nylon Hex Nut Technical Data Sheet	126
Section 2.13: Maximum Stress Calculations	127
Section 2.14: Materials List and Budget Table	128
Section 3: Fabrication Protocols	131

Section 3.1: NEMA-17 Stepper Motor Circuit and General Fabrication	131
Section 3.2: Cellringe Pump Fabrication	136
Section 3.3: FSR Feedback System Circuit and General Fabrication	140
Section 4: SolidWorks Drawings	146
Section 5: Testing Protocols	149
Section 5.1: Sensor Calibration Curve Testing Protocol	149
Section 5.2: Feedback System Force Detection Accuracy Testing Protocol	153
Section 5.3: Feedback System Testing Protocol	156
Section 5.4: Syringe Clamp Connection and Locking Testing Protocol	157
Section 5.5: Injection Rate Testing Protocol	160
Section 5.6: Cell Viability Testing Protocol	161
Section 5.7: Catheter Obstruction Testing Protocol	162
Section 5.8: Bovine Steak Injection Testing Protocol	163
Section 5.9: Ex Vivo Cervine Heart Injection Testing Protocol	165
Section 5.10: Viscosity Testing Protocol	166
Section 6: Testing Results and Data Analysis	167
Section 6.1: FSR Feedback System Force Detection Accuracy Results	167
Section 6.2: FSG Feedback System Force Detection Accuracy Results	169
Section 6.3: FSR vs FSG Feedback System Force Detection Accuracy Comparison Results	171
Section 6.4: FSR Feedback System Testing Results	172
Section 6.5: Syringe Clamp Connection and Locking Results	174
Section 6.6: Injection Rate Testing Results	175
Section 6.7: Cell Viability Testing Results and Analysis	177
Section 6.8: Overall Device - 25 Gauge Needle Testing Results	184
Section 6.9: Overall Device - Clinical Simulation Testing	189
Section 6.10: Catheter Backup Data and Analysis	193
Section 6.11: Bovine Steak Injection Testing Results	195
Section 6.12: Viscosity Testing Injection Results	199
Section 6.13: Pressure Sensing Catheter Data and Analysis	201

## Introduction

### Motivation

Cardiovascular disease is the leading cause of death in the United States. There were 696,962 deaths in 2020 alone and this number continues to increase every year [1]. Heart failure affects around 5 million people per year, killing over 250,000 of those affected [2]. This high mortality rate is due to cardiac tissue having a very limited regeneration capacity compared to other tissues in the body. Following a myocardial infarction (heart attack), regions of cardiac muscle get replaced by scar tissue. This causes the heart to experience more stress because the scar tissue can not contract to distribute blood throughout the body. In order for the heart to still pump and supply blood to the body, the healthy cardiac tissue must work much harder, eventually leading to heart failure [3]. Despite current clinical interventions, the mortality rate of heart failure is still 20% within one year of diagnosis and 80% within eight years of diagnosis [4], demonstrating the importance of a new high efficacy novel approach.

The risk of heart failure increases with age and people over 65 years old are the most susceptible. Men have a higher chance of experiencing heart failure than women and the ethnicity that is most at risk is African-Americans. There is also an increased risk of heart failure based on genetics and family history, demonstrating that if there is a history of heart disease, other members within the family are more likely to experience similar problems. Other risk factors include diabetes, obesity, and high blood pressure as well as living a sedentary lifestyle or drug and alcohol abuse [5].

Mesenchymal stem cell (MSC) delivery treatment is a novel approach that has been developed to aid in repairing damaged heart tissue following myocardial infarction. MSC therapy is currently in clinical trials and has been proven to be useful in improving the function of the heart. MSCs had a positive safety profile meaning that they caused limited safety issues with people in various clinical trials. Additionally, autologous and allogeneic MSCs showed improvements in left ventricle function, stroke volume and myocardial mass and a decrease in adverse remodeling. Allogeneic MSCs, particularly, had even more benefits and resulted in major improvements in quality of life [4]. More information about the procedure, doses, etc., can be found in the *Intramyocardial Stem Cell Injection Procedure* section of the report.

An automatic intramyocardial stem cell injection device will provide a more accurate and efficient way to deliver MSCs into the heart, specifically the myocardium, as this device would inject stem cells at a controlled rate. This accurate rate regulation can improve the chances of regenerating the dead cardiac tissue, improving its function, through stem cell modification as it will improve cell retention during injections [6]. The automatic delivery system will help renew the tissue through the injection of healthy MSCs that can assist with pro-angiogenic and immune-modulatory properties, improving heart function. Integrating a feedback system into the device that measures the force of the stem cell injections into the myocardium throughout each procedure will improve clinical efficacy, as it will assist the clinician in determining the medium

the MSCs are being injected into (body cavity, healthy tissue, or ideally, the diseased/scarred tissue) and if there is a potential for catheter back-up and cell reflux.

The force detection system can also be used to conduct force and cell viability testing to determine a maximum threshold value for an effective injection procedure. Developing this understanding and boundary is critical to the success of each injection since the force range that is associated with lower cell viability will increase the likelihood of complications from the surgery. If cells die due to violence or disease, the defense and repair mechanisms within the body become mobilized, initiating an inflammatory response. As myocardial infarctions are characterized by an exaggerated inflammatory response that overworks the heart and can lead to cardiac arrest, delivering cells that experience necrosis and thus promote this inflammatory response in the body will make the injection procedure therapeutically ineffective [7]. The treatment can thus pose health risks to patients. As a result, utilizing the device to establish the proper force range for each injection in order to increase cell viability will enable high efficacy intramyocardial MSC injection procedures. Ultimately, the surgeon can use the automatic injection device to gauge how the cells and body will react during each injection and thus minimize cell death and complications.

Currently, there is not an automatic injection device on the market targeted toward assisting in MSC delivery to the myocardium, demonstrating the importance and impact this high efficacy injector can have on intramyocardial stem cell injection procedures. The automated stem cell injector device will improve procedural accuracy by controlling the delivery of the stem cells which can lead to clinical success and improved patient recovery and survival, making this device a critical component of improving the treatment of myocardial infarction and heart failure.

## Problem Statement

Treating heart failure by injecting mesenchymal stem cells (MSC) into the myocardium via an injection device and a needle-tipped catheter is a novel approach that can improve quality of life. Unfortunately, the procedure is currently performed manually (10 - 14 sequential injections), so MSCs are delivered into the myocardium at an uncontrolled flow rate with susceptibility to rapid injections that reduce cell retention in the myocardium and induce cell reflux and damage [8]. While slower injection rates improve cell retention, they incite operator hand fatigue, resulting in inconsistent cell delivery which can cause therapeutically ineffective MSC clumping, cell reflux, lower cell retention, and even cell damage/death. As a result, a novel automatic injection device that integrates with the procedural syringe and catheter, limits operator intervention, and provides a slow, controlled, and adjustable injection rate is required to improve stem cell delivery, maximize cell retention, and enhance clinical success. A force detection mechanism that tracks the amount of force applied to the cells is also needed to promote the effectiveness of the system. By providing live feedback during the injections, the operator can ensure that the cells are not compromised, leading to increased efficacy of the procedure.

## Background

### Current Cardiovascular Disease Treatment

The current treatments for heart failure include left ventricular assist devices (LVAD), medications such as beta blockers and heart transplants, but they do not assist in full recovery of the heart function. A left ventricular assist device (LVAD) mechanically unloads the portion of the heart in addition to neurohormonal blockade heart failure medications which can improve the patient's likelihood of recovery [9]. Beta blockers are able to cause neurohormonal alterations, specifically they can work by blocking the effects of epinephrine, which can help slow down the heart [10]. Another current treatment is a heart transplant, but this is a very invasive procedure, and there is a critical organ shortage not allowing everyone eligible to receive a heart transplant [11]. The survival rate after receiving a heart transplant decreases below 85% after just one year. Heart transplants are typically considered last if other treatments are not working, but due to the risks associated, the limited number of donors and the complications that can follow the procedure, it is not the best treatment [12]. Nanotechnology drug delivery systems have also been used to treat cardiovascular diseases. This type of treatment has the ability to enhance bioavailability by prolonging blood residence, deliver a wide range of payloads, and sustain release of therapeutic agents over time [13]. Unfortunately, although these current cardiovascular disease treatments can help lower the mortality rate from heart failure, they are not long-term solutions and thus do not increase life expectancy by an impactful amount.

### Mesenchymal Stem Cells

Mesenchymal stem cells are multipotent progenitor cells with pro-angiogenic and immune-modulatory properties. They can be isolated from multiple sources, such as bone marrow, adipose, and cardiac tissue [14]. These stem cells are one of the most frequently used cell types for regenerative medicine due to their controlled differentiation capabilities. MSCs have been seen to treat many different pathologies including neurological disorders, cardiac ischemia, diabetes, and bone and cartilage diseases. MSCs have been successful therapeutically due to their ability to divide and differentiate into a variety of cell types, enabling the growth of specific cells in regions where they were lost or damaged as a result of disease [15]. Through inflammatory regulation, anti-fibrosis, neovascularization and differentiation into cardiomyocyte-like cells, MSCs are able to help heal cardiovascular diseases [16]. The delivery of MSCs into the myocardium as a mechanism for tissue regeneration and thus heart failure recovery is a novel approach with the potential to provide a more effective and long-term solution compared to current treatments.

### Intramyocardial Stem Cell Injection Procedure

Assessment of the patient is required to ensure they are eligible before the procedure occurs. If the patient has heart failure after a myocardial infarction and they are receiving stable,

guideline-directed medical therapy with a left ventricular ejection fraction between 20 and 40%, they are eligible for the procedure [6]. To perform the intramyocardial stem cell injection procedure, a 60 mL bone marrow aspiration is initially taken from the patient prior to injection and the MSCs are isolated for further use. The intramyocardial injection procedure begins with an introducer sheath placed into the femoral artery followed by a left ventriculogram that combines with a 17-segment polar map of the myocardial wall motion and thickness from the patient's echocardiogram in order to provide a patient-specific road-map. This road-map helps operators move the catheter around to specific injection points. Operators target myocardial segments where wall thickness is greater than 6 mm which indicates a peri-infarct zone. After the route to the target tissue is identified, a needle-tipped catheter is inserted into the myocardium region of interest. Surgeons ensure that the catheter needle is properly inserted and engaged with the myocardium by observing appropriate, stable fixation of the catheter tip via x-ray fluoroscopy and through visualization of a transient arc adjacent to the endocardial surface when a bolus of radio-contrast is injected. The catheter is either connected directly to the syringe containing the MSC solution that will be injected, or it is connected to medical grade tubing, which is directly connected to the procedural syringe. The target dose of stem cells per procedure is about 200 million. After appropriate catheter insertion is confirmed, bone marrow-derived MSCs are delivered into the myocardial tissue, typically through a Helix™ transendocardial injection catheter and a Morph® deflectable guiding catheter. Each injection transports 0.5 mL of MSC solution and a typical procedure requires 10 to 14 injections (using a new syringe for each injection) [6]. These procedures normally display a MSC injection force value range of 0.14 N to 3.00 N, where 2.40 N corresponds to the force characteristic of potential obstruction [17]. Each injection targets a rate of 30 seconds or 60 seconds followed by a 60 second maximum dwell time between each MSC injection into the myocardium. However, all injections are performed manually, making them susceptible to rapid injections (less than 30 seconds) that lead to the reflux of cells through the needle tract and cell damage. While slower injection rates improve cell retention, they insight operator discomfort and hand cramping, reducing the efficacy of the delivery [6]. In both cases, the success of the treatment is severely restrained as the chances of complications occurring during the procedure is high which limits the potential of this novel treatment.

## Flow Rate Impact

Unfortunately, the current injection devices used to perform this stem cell delivery are manually controlled and are unable to regulate cell flow rate through the catheter and into the myocardium. As a result, this procedure is susceptible to rapid injections (less than 30 seconds) that lead to the reflux of cells through the needle tract and cell damage. The cells can also be damaged during fast injections due to the possibility of a fluid shear force of more than  $6.23 \times 10^{-6}$  N being applied onto the cells [18]. The calculation of this shear force can be seen in Equation 1 below [19]. The cells could also end up off-target and not within the targeted myocardium tissue, overall reducing the cell retention. Slower injection rates can insight operator

discomfort and hand cramping, reducing the efficacy of the delivery. Cell clumping can also occur with too slow of an injection rate, which can cause catheter obstruction and issues with the cells being delivered to the myocardium. Rate inconsistency through the injections can lead to rejection of the cells within the heart.

$$\begin{aligned} [1] \text{ Catheter Radius} &= 0.115 \text{ cm} = 0.00115 \text{ m} \\ \text{Catheter Area} &= \pi * (0.115)^2 = 0.0415 \text{ cm}^2 = 4.15 \times 10^{-6} \text{ m}^2 \\ \text{Apoptosis Inducing Fluid Shear Stress} &= 1.5 \text{ Pa} = \text{N/m}^2 \\ \text{Required Force to Induce Apoptosis} &= \text{Shear Stress} * \text{Area} = 1.5 * 4.15 \times 10^{-6} = \mathbf{6.23 \times 10^{-6} \text{ N}} \end{aligned}$$

The myocardial stiffness can also affect the pressure being applied to the syringe during the procedure. The average myocardial stiffness for healthy individuals is  $6.08 \pm 1.06$  kPa whereas  $12.68 \pm 2.91$  kPa is the myocardium stiffness associated with an individual who experienced a myocardial infarction. The greater the stiffness, the more force required to inject the MSCs into the myocardium, which can slow down the rate at which the stem cells are injected. The flow rate at which the stem cells are injected into the myocardium can have a great impact on the outcome of the procedure and can affect the retention of stem cells [20].

## Existing Devices and Current Methods

There are currently products on the market that involve similar concepts to the automated stem cell injector, but no device has all of the components that will be included in the final design for this device.

One type of device that is a competitor to the injector is an automated syringe pump. These systems are used by anesthesiologists to inject a controlled volume of anesthesia into the patient over time. The Baxter Infus OR Syringe Pump ABC 4100, is an infusion pump device that is compatible with 1, 3, 5, 10, 20, 30, 60 and 140 mL syringe sizes. To operate the device, the syringe is front loaded and locked into place. The anesthesiologist would then enter a flow rate and the type of drug being used, clicking start to initiate the injection. The advantage to the Baxter device is that it is able to sense syringe plunger force and movement and has a system to detect and monitor delivery accuracy as well as alarms with audio and LED lights [21]. The disadvantages and limitations include that this system is not tailored to eject fluid at the rate that is needed for intramyocardial stem cell delivery and has not been proven to maintain cell viability for MSCs. See Figure 1 below for this Baxter Syringe Pump along with an additional Baxter Syringe Pump.



Figure 1: The “Baxter Infus OR Syringe Pump ABC 4100” that is sold for ~\$3000 using the trade-in program (left image) [21] and the “Baxter Infus O.R. Syringe Pump Refurbished” that is sold for ~\$4000 (right image) [22].

Another competing device is the apparatus used to inject IV fluids into patients. This device is able to transfer fluids from a bag directly into the person through connection tubing at a programmed rate. There is also another similar device called the Contract Delivery System from ACIST Medical Group that is used for angiographic procedures to deliver an iopamidol injection. The advantages to this device include a controlled flow rate system that is compatible with catheters and has been used in procedures involving cardiology and radiology [23]. The disadvantages, however, is that this device is not tailored to eject the 0.5 mL volume of stem cells from a 1 mL syringe for 10 - 14 injections over a period of 30 - 60 seconds. In addition, similar to the Baxter device, the IV machines were not proven to be compatible with stem cells. This product can be seen in Figure 2 below.



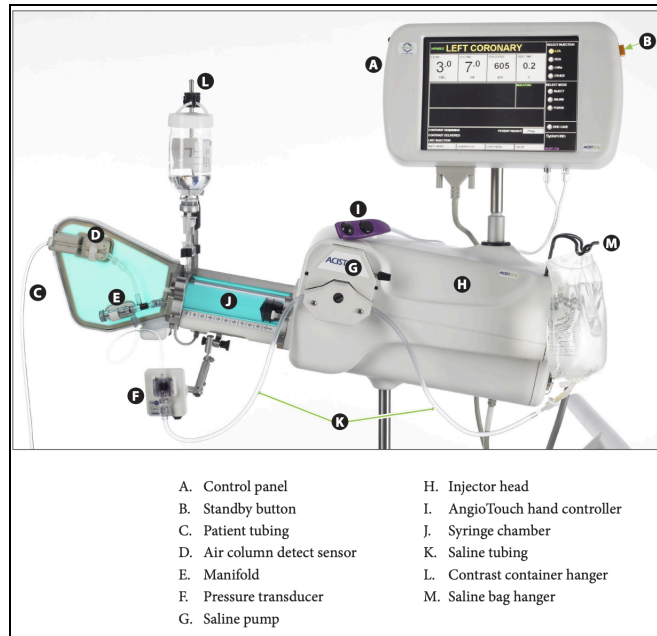


Figure 2: Diagram of the important user components in the Acist Contrast Delivery System [23].

Additionally, there was a device in preclinical trials in 2017 that was fabricated to deliver cells. This product was called an “automated injection device for intradermal delivery of a cell-based therapy”. The current status of the product is unknown and the device is not currently patented or on the market. The limitation to this device is that it delivers solutions directly into a patient via the hypodermic needle and has not been proven to be compatible with the connection tubing-catheter system that is needed for the injections. Although it may be easy to operate by pushing the trigger button, the flow rate of the solution is not tailored to the 30 and 60 second injection times for 0.5 mL of solution in the 1 mL syringe which is required for intramyocardial stem cell injection procedures. The device can be seen in Figure 3 below.

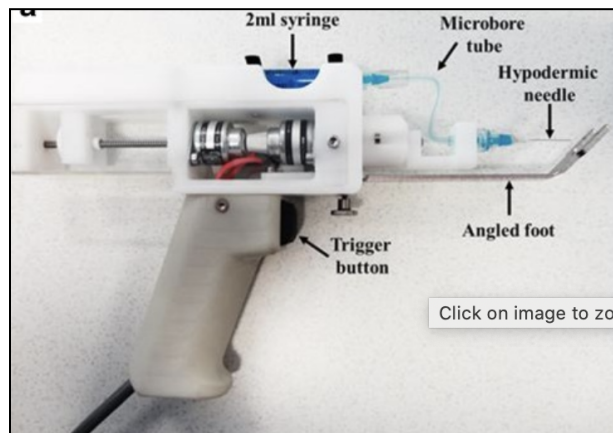


Figure 3: Automated injector device that was in preclinical development in 2017 [24].

Although these infusion pump systems and injection devices have positives when it comes to injecting a solution into a patient, they have not been proven to work well with stem cell delivery and in conjunction with the catheter system that goes into the myocardium. These features are important because MSC viability must be maintained for the intramyocardial stem cell injection procedures to be successful and the MSC aliquot solution must be able to transport through the catheter and into the heart. Additionally, the devices on the market do not contain force detection systems that provide accurate algorithms for determining the pressure needed for injecting cells into the myocardium.

The JP2019069165A patent (see Figure 4 below) involves a system which has an automatic injector device that uses cassettes to hold the injectate. This is an automatic device that could be engaged by the push of a button via its superior end. However, this apparatus is not extremely similar to the cardiac repair injector device that will be fabricated since it does not have syringe or catheter compatibility, it does not have a controlled injection rate, and does not have a pressure-detecting system that can trigger visual feedback [25].

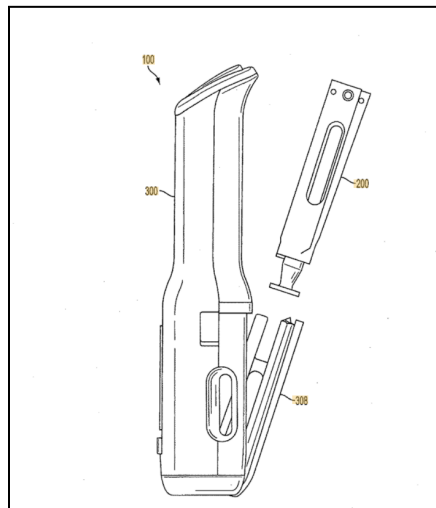


Figure 4: The cassette automatic injector device [25].

Lastly, the US Patent US4759750A (see Figure 5 below) is relevant to the current objective of detecting the force and / or pressure the cells are experiencing during the injections [26]. Specifically, the patent is for a Pressure Sensing Syringe which has a pressure sensitive piston between the syringe plunger and the thumb. The device also provides a tactile signal when a specified pressure is applied so that a person directing fluid somewhere can be alerted when a certain preset pressure is reached. This patent is interesting because it allows for a direct way to sense pressure in a fluid filled syringe. There are, however, other similar devices on the market that can also be used to get pressure readings.

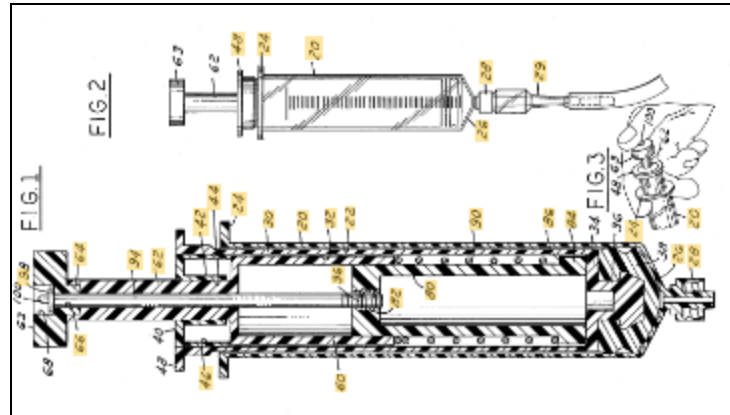


Figure 5: US Patent US4759750A [26]

## Standards and Regulations

The fabrication of the automatic injector and the product itself should adhere to various standards and regulations in order to allow for the development of a successful product that interacts accurately, effectively, and safely with operators and patients and can be commercialized. The Code of Federal Regulations (CFR) Title 21 Part 820 provides quality system regulations, including the requirements related to the methods used in designing, manufacturing, packaging, labeling, storing, installing, and servicing of medical devices intended for human use [27]. As the injector will be used in conjunction with syringes, medical grade tubing, and catheters that interact directly with patients, it should follow and meet the quality guidelines outlined in the CFR. This will allow good standard operating procedures to be followed in relation to the fabrication and commercialization of the product. The CFR Title 21 Part 870 identifies a Percutaneous Transluminal Coronary Angioplasty Catheter used for the treatment of acute myocardial infarctions as a Class II medical device (includes all components associated and utilized in conjunction with the catheter) and specifies the procedure required for this class [28]. As the injector will be used to treat heart failure induced by myocardial infarctions (via syringe-catheter integration) and it provides an intermittent risk to patients (controls MSC injections into the myocardium), the injector can also be categorized as a Class II medical device and thus needs to adhere to the procedures outlined by this CFR. Current injection devices and syringe pumps used for drug delivery are identified as Class II medical devices [29]. This further supports the classification of the injector as a Class II device that must adhere to the process provided in CFR Title 21 Part 870, as MSC delivery will require considerations consistent with drug delivery.

The CFR Title 21 Part 3.2 categorizes the injector device as a combination product, due to its interaction with a medical device (syringe) and biological product (MSCs) in order to achieve its intended therapeutic effect. This standard provides the procedure for properly identifying the designated agency component and preparing it for premarket review and regulation [30]. If the injector device is pursued as a combination product rather than focusing on

its design individually, this CFR will have to be followed in order to allow adequate agency designation and to meet premarket review requirements.

The CFR Title 21 Part 610 provides the performance, testing, and safety requirements, labeling standards, and sterility expectations for biological products, such as MSCs [31]. As the injector will interact with a syringe that contains MSCs, it is important to have familiarity with the MSCs themselves and the performance and safety requirements they must adhere to. The CFR Title 21 Part 1271 describes the current good tissue practices that must be followed for cells, tissues, and cellular- and tissue-based products, including their processing, manipulation, and associated manufacturing procedures, facilities, and equipment [32]. The intramyocardial stem cell injections utilize MSCs as a therapeutic that reduces the exaggerated inflammatory response and characteristic aberrant extracellular matrix remodeling experienced following a myocardial infarction (see the *Mesenchymal Stem Cells* section above) [16]. This demonstrates that the MSCs are a cellular therapy product used to treat heart failure. As the injector will deliver the MSCs into the myocardium, it must be designed in a manner that maintains the viability of the MSCs, limits the induction of cell apoptosis, and prevents the introduction, transmission, and spread of communicable diseases in order to meet the requirements associated with cellular products.

## Client Information

The client is Dr. Amish Raval, a faculty member in the Division of Cardiovascular Medicine within the Department of Medicine at the University of Wisconsin-Madison. He also holds an affiliate appointment with the Department of Biomedical Engineering in the College of Engineering. Dr. Raval specializes in interventional cardiology, specifically working on reducing the effects of coronary artery disease and valvular heart disease. He performs different procedures including heart catheterizations to correct valvular and congenital defects and cardiomyopathies, coronary angiography, coronary revascularization and related coronary and pulmonary procedures. Clinical trials are currently being performed for this procedure with Dr. Raval as one of the operators. Dr. Eric Schmuck works closely with Dr. Amish Raval, acting as an additional client for the design. He is an associate Scientist and Director of Translational Research for the Dr. Amish Raval Laboratory.

## Design Specifications

The client seeks a product that is capable of treating heart failure by automatically injecting MSCs into the myocardium via an injection device and a needle-tipped catheter. The client requests a device that will electronically inject mesenchymal stem cells into the myocardium and have less than 5% cell death relative to post-thawing cell viability, as this matches current procedures. The injector must be compatible with the standard catheters, medical grade tubing, and 1 mL procedural syringes currently used in practice. The stem cell injection flow rate must be adjustable, consisting of a 16.7  $\mu\text{L}/\text{sec}$  rate and a 8.33  $\mu\text{L}/\text{sec}$  rate capable of introducing the required 0.5 mL stem cell solution into the myocardium [6]. The

injector also needs to complete 10 - 14 injections throughout the entire procedure. Each injection rate must be able to be performed within one second of the target time (30 seconds and 60 seconds). The volume of solution delivered from the syringe after the completion of either of these injection rates must be within 5% of the 0.5 mL volume of solution inserted into the syringe, with this error margin taking into account the inherent and inevitable dead space present in the distal tip of each syringe (see the *25 Gauge Injection Results* section below). A force sensing device must be included in the design that reads the force applied to the MSCs during the injection. Force values above a threshold of 2.40 N, as read from the syringe plunger, must cause the device to visually alert the user that the catheter or syringe is potentially clogged with solution or exhibiting aliquot back flow [17]. The applied force needs to be displayed throughout the entire procedure with less than 5% error. The injector should also have the ability of being used for research purposes. The device also must withstand the three year life in service requirement. The client has a budget of \$3000 and a manufacturing cost of \$500 [33]. A complete outline of the product design specifications can be found in the Section 1 of the Appendix.

## Preliminary Designs

### Overview

As discussed in the *Design Specifications* section above, the automatic injection device needs to consist of a force sensor, a visual feedback system, an automation apparatus to inject MSCs into the medical grade tubing and catheter system and thus the myocardium, and a syringe insertion and locking mechanism. The injector base, force application mechanism, 1 mL syringe mold, and visual feedback system are standardized across each design idea. As a result, the four concepts considered in the *Design Ideas* section below vary only in their force detection device and method.

### Cellringe Pump: Thread Regulated Injections

The automatic injection device fabricated during the Spring 2022 semester, the Cellringe Pump, will be preserved for this semester's injector, except for its force detection sensor. This design consists of a  $27.50 \times 10.00 \times 7.50$  cm base that includes a NEMA-17 stepper motor, a zinc coated aluminum threaded bolt injection regulator, an Ultimaker PLA force application block, and a 1 mL syringe mold (see Figure 6 below). The Ultimaker PLA base is a rectangular structure that contains and stores all injector components, including the required circuitry. A NEMA-17 stepper motor controls the automated injections and is housed in the  $6.00 \times 9.00 \times 9.00$  cm gray compartment, depicted in Figure 6 below. This motor performs 200 steps per revolution ( $1.8^\circ$  turn per step), is compatible with a maximum current of 350 mA, can be controlled by a 0 - 12 V rated voltage supply, and is driven by an Arduino Uno microcontroller [34]. This step rate and Arduino Uno microcontroller regulation allows for a very precise and controlled rotation of the stepper motor that correlates to a delivery of 0.5 mL of MSC aliquot

solution (within the required 5% error margin) across 30 and 60 second rates via a threaded bolt-force application block system. The compartment this motor is stored within contains an opening on its dorsal side in order to allow for the motor to interface with the microcontroller housed within the interior of the base. The motor's rotation shaft connects to a zinc coated aluminum threaded rod that penetrates through a nut sitting within the Ultimaker PLA force application block. The movement of the motor rotates the threaded rod, driving the block toward the syringe plunger in a very controlled manner, applying a specified force to the syringe that results in the delivery of the MSCs. The force block will completely compress the syringe plunger, injecting the 0.5 mL MSC solution into the medical grade tubing and catheter. The Arduino Uno motor revolution control and the threaded rod force application system allows for accuracy and consistency when compressing the syringe plunger. This enables the injector to apply 30 and 60 second injection rates with a high degree of efficacy, delivering the 0.5 mL MSC aliquot solution within the required 5% error margin. The performance of the injector was thoroughly tested in the Spring 2022 semester (see the *Injection Rate Results and Overall Device Results* sections below), demonstrating that this system effectively and successfully performs the 30 and 60 second injections that are required for therapeutically impactful intramyocardial MSC injection procedures. The motor can also be rotated in the opposite direction, causing the threaded rod to drive the force block away from the syringe and its plunger. This is critical when another injection needs to be performed. Two additional unthreaded aluminum rods are located on either side of the threaded bolt (offset slightly above the bolt) and are built into the support structure (between the force application block and syringe mold), penetrating through the force application block to provide stability within the syringe compression system. To ensure the procedural 1 mL syringes properly integrate with the device, the injector contains a syringe mold that is permanently attached to its superior face, located on the anterior side of the device. It is fitted to the clinical 1 mL syringes, so it securely holds each syringe in place following insertion, preventing any displacement or movement during each injection. This promotes the overall efficacy of the device and procedure and it displays the injector's compatibility with the required 1 mL procedural syringes. Syringes have to be manually inserted into and removed from the syringe molds before and after each injection (10 - 14 injections per procedure). Within this design, the medical grade tubing and catheter easily connect to the distal end of the syringe without experiencing any hindrance, allowing for proper MSC injection through the tubing-catheter system and into the myocardium.

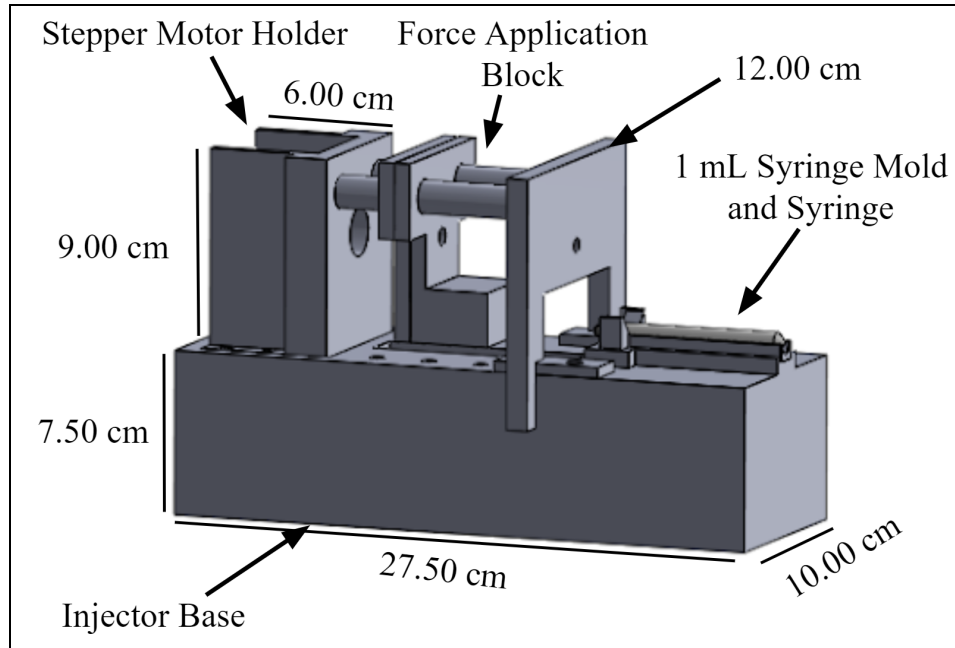


Figure 6: Cellringe Pump SolidWorks drawing highlighting the force application block, stepper motor force application control, and the 1 mL syringe mold. The injector base is  $27.50 \times 10.00 \times 7.50$  cm.

## Visual Feedback System

The injector's visual feedback system consists of a light emitting diode (LED) signal that alerts the operator of potential catheter backup and cell reflux as well as a digital display that constantly outputs the force value applied to the syringe throughout each injection, promoting procedural success. This system consists of a force detection device that connects to an Arduino Uno microcontroller via circuitry. The Arduino Uno microcontroller contains a 4.88 mV resolution over a 0.00 V - 5.00 V range [35]. As a result, the visual feedback system must contain a circuit (utilized with the selected force detection device) that outputs a voltage range between 0.00 V and 5.00 V across the 0.00 N - 3.00 N force application range characteristic of a typical intramyocardial stem cell injection procedure [17]. During each injection, all voltage changes delivered to the Arduino Uno microcontroller as a result of force application variance to the force sensor must correspond to deviations greater than 4.88 mV to enable accurate force detection. The technical data sheet for the Arduino Uno microcontroller can be found in Section 2.1 of the Appendix.

The Arduino IDE software program is used in conjunction with the Arduino Uno microcontroller to receive the voltage input from the feedback circuit. The calculations used to establish the force applied by the injector to the syringe will be based on an experimentally determined standard calibration curve for the force detection device and circuit (see the *Final Design and Methods* section below). The procedure followed to develop the calibration curve for the Force Sensing Resistor utilized last semester (Spring 2022) and the graph itself can be found in the *Methods* section below. A conversion equation will also be developed via empirical data to

record the force applied to the MSCs during each procedure based on the values detected by the force sensor. Using the calibration curve and force conversion algorithm, the Arduino IDE program will identify the force value applied to the syringe and MSCs throughout each injection and constantly display it on an LED Serial 7-Segment Digital Display (see Figure 7 below) for easy operator visibility [36]. This will allow the operator to ensure that a proper injection is taking place within the desired tissue and without catheter blockage and cell reflux. To support this injection administration, the feedback system will also consist of a red LED signal that illuminates when the 2.40 N threshold is reached or exceeded, demonstrating that catheter obstruction or cell reflux is imminent [17]. Arduino IDE code to control the feedback system will be developed. During each injection, this system will enable proper catheter insertion and placement as well as it will help promote successful MSC delivery by accurately depicting the injection force throughout each procedure. As a result, the visual feedback system will increase the efficacy of the intramyocardial stem cell injection procedures, enhancing clinical success and thus improving quality of life.

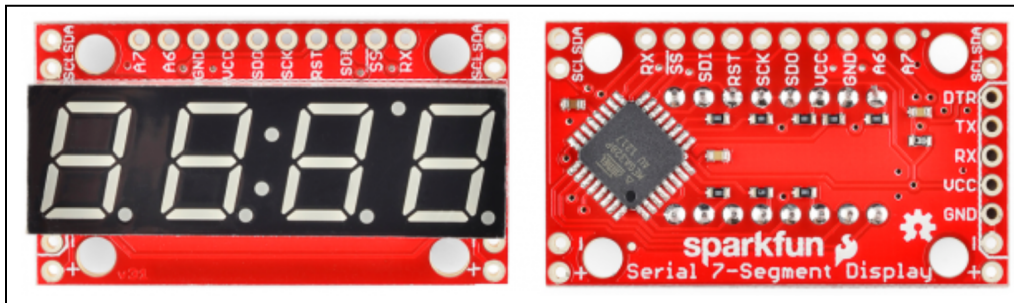


Figure 7: Top (left) and Bottom (right) view of the LED Serial 7-Segment Digital Display that is used in conjunction with the Arduino Uno microcontroller and FSR sensor voltage divider circuit. This display constantly outputs the force applied by the injector to the syringe plunger throughout each injection [36].

## Design Ideas

### FSR 400 Series Round Force Sensing Resistor

The FSR 400 Series Round Force Sensing Resistor (FSR) was used as the force sensor within the injection device to detect the force applied between the injector and the syringe plunger during the Spring 2022 semester (see Figure 8 below). It is a 56.40 mm long sensor with a 0.55 mm nominal thickness, making the FSR a relatively small sensor that should not interfere with the overall functionality of the injector [37].



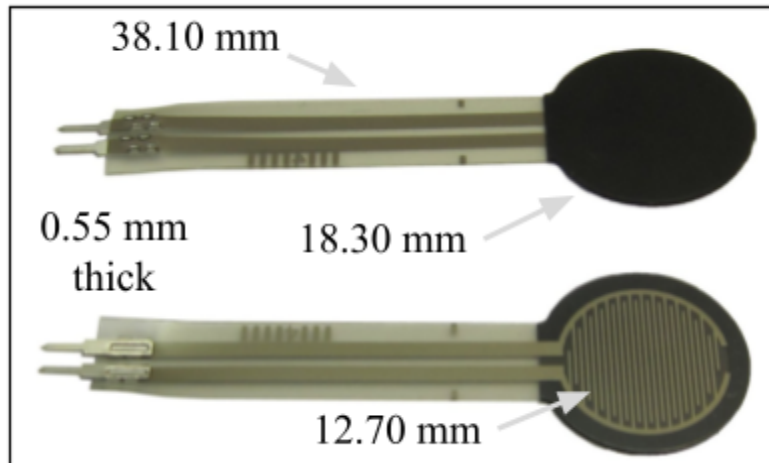


Figure 8: FSR 400 Force Sensing Resistor highlighting its 12.70 mm active zone (patterned circle), 0.55 mm thickness, and 38.10 mm length as well as its two prong connectors that allow breadboard and circuit integration [37].

The FSR will be attached with adhesive to the force application block of the injector at the location that comes into contact with the syringe plunger, allowing for a constant force value to be detected throughout each injection (see Figure 9 below). The active zone (detects force application) is about 12.70 mm in diameter, allowing it to adequately receive the entire force applied by the standard 1 mL clinical syringes (plunger diameter is  $\sim 10.24$  mm [38]). The FSR sensor has an actuation force of 0.10 N and a force sensitivity range from 0.00 N to 10.00 N [37]. This demonstrates that the sensor will provide a relatively accurate force detection reading throughout each injection, as the anticipated force range during a typical intramyocardial stem cell injection procedure is 0.14 N to 3.00 N, with forces expected to reach no larger than 10.00 N (see the *Intramyocardial Stem Cell Injection Procedure* section above) [17]. However, its 0.10 N sensitivity limits its ability to pick up small changes in force application throughout each injection. Its susceptibility to altering the force value it detects based on the location of force application to the active zone reduces its precision and reliability over repeated injections. The FSR's resistance changes with the force applied, decreasing in resistance with increasing pressure, providing a mechanism to determine force application when the FSR is used in conjunction with a circuit and microcontroller. The FSR will have a resistance of approximately 100 k $\Omega$  at 0.14 N of applied force and about 2 k $\Omega$  at 3.00 N of force. As seen in Figure 8 above, two wires connect from the active zone to two metal prongs. These prongs allow the FSR sensor to connect with electrical wires in order to carry the resistance generated by force application to the active zone into a circuit [37]. As a result, the FSR sensor can integrate with the feedback system and its Arduino microcontroller and Arduino IDE program (see the *Visual Feedback System* section above), allowing force detection to take place throughout the injection in adherence with the design specifications. The technical data sheet for the FSR sensor can be found in Section 2.2 of the Appendix.

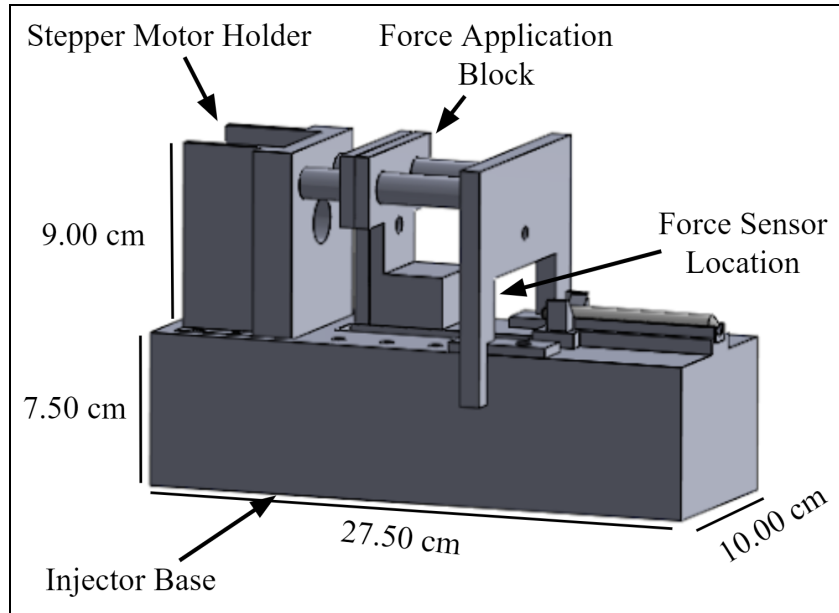


Figure 9: SolidWorks drawing of the current automatic injector, labeling key features and displaying the location the force sensor will be placed on the force application block.

#### ESG020WNPB Series Force Sensor

The FSG020WNPB Series Force Sensor (FSG) utilizes a piezoresistive micro-machined silicon sensing element to detect force and provide reliable and stable voltage outputs (see Figure 10 below). The sensor has a 12.70 mm width, 7.98 mm length, and a 9.04 mm height. While the FSG sensor is bulkier than the FSR sensor, it is still relatively small and thus should not disrupt the functionality of the injector and its force application mechanism [39].

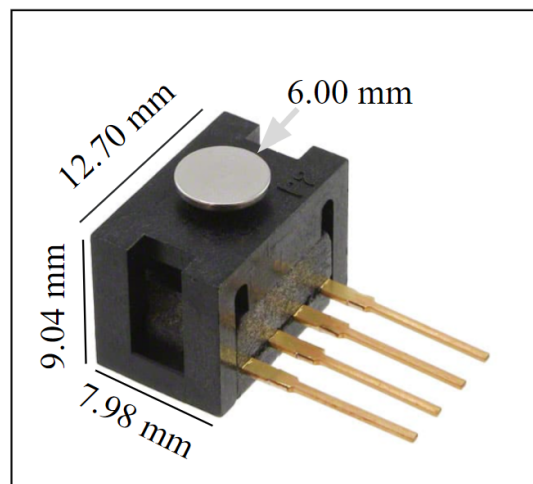


Figure 10: FSG020WNPB Series Force Sensor highlighting its four prong connectors that allow breadboard and circuit integration, 6.00 mm active zone, and elevated sensor promoting complete force reception [39].

The FSG sensor will be positioned on the force application block of the injector to enable the syringe plunger to come into contact with its sensor, allowing a constant force value to be detected throughout each injection (see Figure 10 above). The FSG sensor can be attached to the force block with adhesive or it can be integrated with the force application block via the mount that comes with the device. If the latter is chosen, the force application block will have to be updated to allow for a proper interaction between the block and the FSG sensor mount. Although the sensor's 6.00 mm active zone is smaller than the diameter of a typical 1 mL syringe plunger (~ 10.24 mm [38]), the FSG will still be able to receive and thus detect the entire force applied by the injector to the syringe plunger as it has a  $1.31 \pm 0.27$  mm actuator height between the active zone and the superior side of the FSG. This will prevent the syringe plunger from interacting with any other surface besides the sensor [39]. As the syringe plunger is composed of sturdy plastic, minimal deformation is expected when delivering force to the sensor, enabling the plunger to only connect with the sensor [38]. The FSG sensor has a sensitivity of 3.6 mV/V/N and a resolution of 0.0098 N over a 0.00 N to 10.00 N force range. It also contains a low repeatability error of  $\pm 0.2\%$  and an accuracy of  $\pm 0.5\%$  when comparing the detected force to the actual force [39]. The sensor will thus provide an accurate force detection reading throughout each injection over multiple injections and procedures across the anticipated force range (0.14 N to 3.00 N [17]). This will increase the overall efficacy and safety of the injector as the system will provide reliable and correct force values for the operator to monitor throughout a procedure, enabling proper determination of the potential for catheter obstruction, cell reflux, or MSC lysis. The high 3.6 mV/V/N sensitivity illustrates that each change in force applied to the sensor corresponds to a 3.6 mV variance in voltage output by the system. While this is below the 4.88 mV Arduino Uno resolution, a simple amplification circuit will enable the voltage delivered to the Arduino Uno microcontroller to be within the required resolution [35]. The FSG sensor operates on the principle that the resistance of the silicon-implanted piezoresistors will increase when the resistors flex under an applied load. The sensor concentrates force from the application, through the sensor, directly to the silicon-sensing element. The amount of resistance within the device changes in proportion to the amount of force applied, resulting in a corresponding voltage output change. The piezoresistors are also patterned in a Wheatstone bridge topology, enabling the FSG to be very sensitive to small force application changes while also providing a stable mV output for these pressures, enhancing the success of the injector. As seen in Figure 10 above, four metal prongs protrude from the interior of the force sensor. These prongs allow the FSG sensor to connect with electrical wires in order to carry the resistance generated by force application to the active zone into a circuit [39]. As a result, the FSG sensor can integrate with the feedback system and its Arduino microcontroller and Arduino IDE program (see the *Visual Feedback System* section above), allowing force detection to take place throughout the injection in adherence with the design specifications. The technical data sheet for the FSG sensor can be found in Section 2.3 of the Appendix.

## LCMKD-10N Load Cell with NanoShield

The LCMKD-10N Load Cell will work in conjunction with a Nanoshield to provide a high resolution detection of the force applied by the syringe plunger to the force application block (see Figure 11 below). The load cell will utilize circuitry wires in order to connect to the Nanoshield via its load cell connector terminal [40, 41].

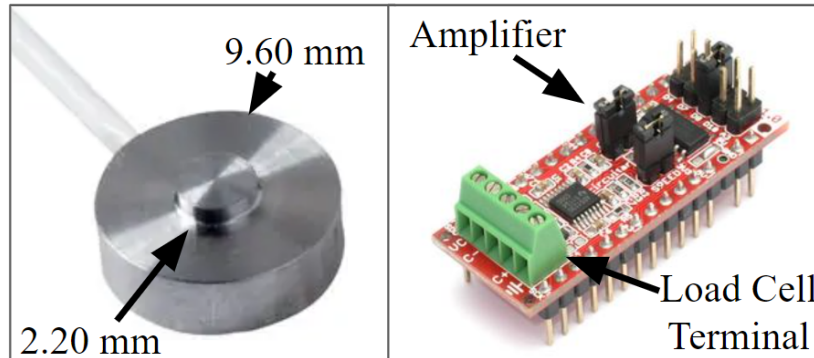


Figure 11: LCMKD-10 N load cell highlighting its one wire that allows breadboard and circuit integration as well as its 2.20 mm active zone and 9.60 mm diameter base (left) [40]. The right depiction is of the Nanoshield, which contains an amplifier to increase the input voltage, a load cell terminal that enables load cell integration, and a voltage source [41].

As the force detection system is used to measure the force applied by the injector to the syringe plunger, the load cell will be permanently attached (via adhesive) to the application block in the same position as discussed in the *FSG020WNPB Series Force Sensor* and *FSR 400 Series Round Force Sensing Resistor* sections above (see Figure 11 above). The load cell has an active zone diameter of 2.20 mm, which is smaller than a typical 1 mL syringe plunger (~ 10.24 mm [38]). However, the 0.76 mm projection height of the sensor from the superior face of the load cell will enable it to receive and detect the entire force applied by the injector to the syringe plunger [40]. As the syringe plunger is composed of sturdy plastic, minimal deformation is expected when delivering force to the sensor, enabling the plunger to only connect with the load cell's active zone [38]. Its overall 9.60 mm diameter is not large and thus should not interfere with the functionality of the injector and its force application mechanism. The wire extension protruding from the load cell will connect with the load cell terminal of the nanoshield, enabling a proper interface between the load cell and Nanoshield. This connection will take place within the interior of the injector base, preventing interference between the system and the force application mechanism and thus mitigating any disturbances to the efficacy of the injector. The Nanoshield will also provide a 5.0 V voltage supply and ground to the load cell through the connection terminal in order to support its functionality. The load cell's resistance increases with force application to its sensor, resulting in the voltage delivered to the Nanoshield being proportional to the force applied during each injection. Using jumper wires, the Nanoshield will integrate with the Arduino Uno microcontroller that regulates the feedback system, delivering the voltage values provided by the load cell directly to the Arduino Uno microcontroller for

further manipulation and force determination [40, 41]. The load cell and Nanoshield device can thus integrate with the feedback system and its Arduino microcontroller and Arduino IDE program (see the *Visual Feedback System* section above), allowing force detection to take place throughout the injection in adherence with the design specifications.

The Nanoshield contains an effective output range of up to 100,000 points (increases Arduino Uno bit size), a power supply of 5.0 V, an ADS1230 integrated circuit, an integrated amplifier, a noise filtering circuit, and a high-resolution ADC converter. As a result, its integration with the LCMKD-10N load cell and intermediate role between the load cell and Arduino Uno microcontroller generates a high precision and resolution force detection system. The overall force detection device (load cell and Nanoshield) contains a sensitivity of 2.0 mV/V/N, an accuracy of  $\pm 0.25\%$ , and a repeatability error of  $\pm 0.1\%$  over a 0.00 N to 10.00 N force range [40, 41]. Across the anticipated 0.14 N to 3.00 N force range [17], the load cell system will thus provide reliable and accurate force detection readings throughout each injection over multiple procedures, significantly enhancing the safety of the injector. The precision, resolution, and consistency displayed in this system over time will ensure the operator is correctly able to determine when catheter obstruction, cell reflux, or MSC lysis is imminent. While the 2.0 mV/V/N sensitivity within the system is very high, it provides a greater resolution compared to the 4.88 mV Arduino Uno resolution [35]. As a result, the Arduino Uno microcontroller will need to be manipulated and its bit size increased by the Nanoshield to ensure that it can detect all voltage alterations corresponding to force application changes, limiting the overall feasibility of the design. The technical data sheet for the load cell can be found in Section 2.4 of the Appendix.

### P30 Non-Invasive Pressure Sensor

The P30 Non-Invasive Pressure Sensor consists of a disposable flow module and pressure sensor that detects the pressure applied by the MSCs within the aliquot solution (see Figure 12 below). The sensor is located directly beneath the flow module, contacting the tube's ventral surface, and contains a 30.50 mm sensing diameter with a total height of 23.80 mm [42].

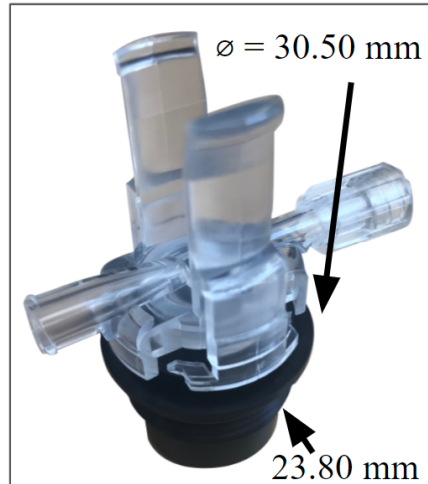


Figure 12: P30 Non-Invasive Pressure Sensor highlighting its disposable flow module and pressure sensor components as well as its 30.50 mm diameter sensor (height of 23.80 mm) [42].

As the system contains a pressure sensor rather than a force sensor, it will need to interact with the intramyocardial MSC injection procedure's MSC aliquot solution directly rather than attaching to the force application block and recording the force applied by the system to the syringe plunger. The sensor operates by detecting the flow of solution through the flow module (known diameter), altering the resistance it outputs based on the pressure detected. To properly detect the pressure applied by the solution to the MSCs throughout each injection, the inlet of the flow module tube (left side based on Figure 12 above) will connect to the distal tip of the 1 mL syringe and its outlet (right side based on Figure 12 above) will interface with the medical grade tubing (see Figure 13 below). The flow module will be modified to ensure that both the inlet and outlet are the proper size to create a secure and reliable connection with the syringe and medical grade tubing and thus enable proper flow of the aliquot solution through the system without leakage or avoidable residual solution remaining in the system [42]. As a result, the pressure sensor will integrate with the syringe-medical grade tubing-catheter system, demonstrating that it is compatible with the clinical and procedural set-up and can be implemented without disrupting the system.

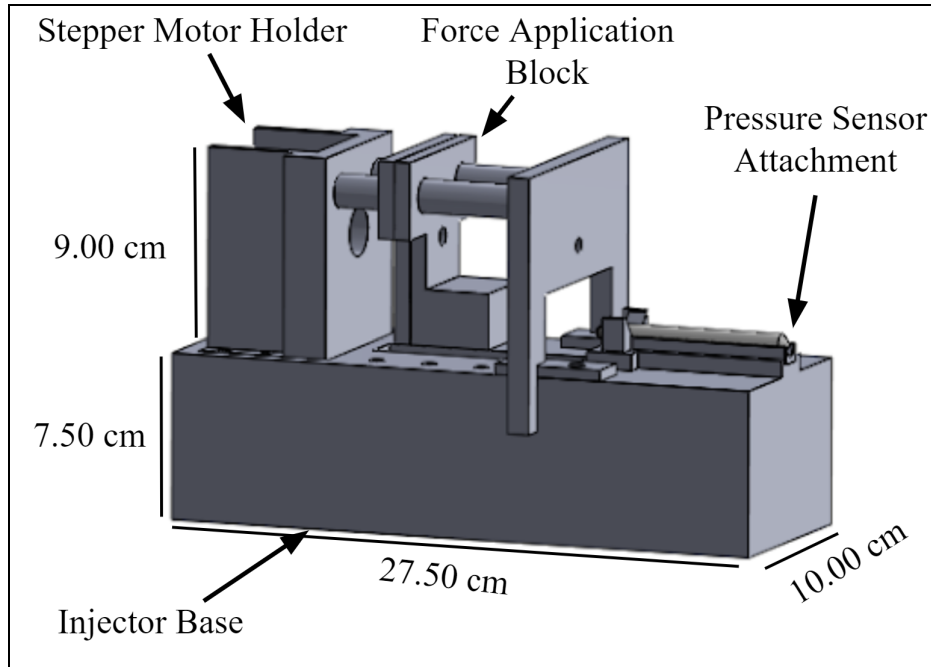


Figure 13: SolidWorks drawing of the current automatic injector, labeling key features and displaying the attachment location of the pressure sensor with the injector.

The pressure sensor has a pressure range of 0.00 kPa - 207.00 kPa [42], which is well within the expected 0 kPa - 188.63 kPa pressure range for a typical procedure, confirming that it will be able to establish the pressure applied to the MSCs throughout each injection and procedure [17]. These pressure calculations can be found in Section 2.5 of the Appendix. As the P30 sensor is directly measuring the pressure applied to the MSCs during each injection, it will inherently provide a high degree of accuracy when measuring the force applied directly to the MSCs. The system is directly measuring the stress experienced by the MSCs rather than utilizing an indirect force detection technique, as seen with the previous three designs. To establish the pressure and ultimately the force applied to the MSCs, the sensor contains a set of pins on its inferior surface. Jumper wires can interface with these pins and the feedback system circuitry to connect the sensor to the Arduino Uno microcontroller and enable the resistance values provided by the sensor (proportional to the applied pressure) to be read by the microcontroller. As a result, the P30 Non-Invasive Pressure Sensor can integrate with the feedback system and its Arduino microcontroller and Arduino IDE program (see the *Visual Feedback System* section above), allowing stress detection to take place throughout the injection in adherence with the design specifications [42]. Despite the increased accuracy associated with this design, it has safety concerns due to the flow module's direct interaction with the MSC aliquot solution. While the disposable flow module that interacts with MSCs is composed of a medical grade plastic, it still poses a risk of damaging the cells, inducing the MSCs to perform lysis, or contaminating the stem cells. The presence of any of these situations will present health risks to the patient, reducing the treatment capabilities of the current intramyocardial stem cell injection procedure

[43]. The constant shear force and stress applied to the pressure sensor over repeated uses reduces the overall durability of the system due to the homogeneous shearing experienced throughout the entire system in addition to continual compressive and bending forces. This limits the sensor's life in service, increasing its susceptibility to failure during the required three year life cycle (see the *Design Specifications* section above and Section 1 of the Appendix) [44]. The technical data sheet for the pressure sensor can be found in Section 2.6 of the Appendix.

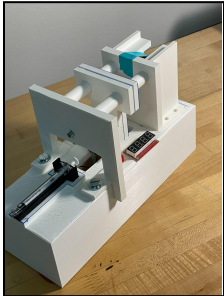
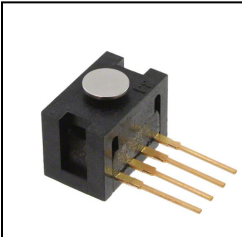
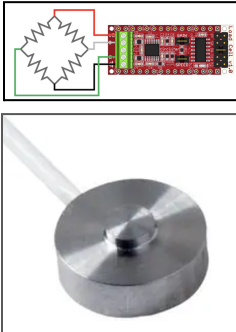

## Preliminary Design Evaluation

### Design Evaluations

All four force detection design ideas were placed into a design matrix consisting of carefully weighed criteria that helped determine the design that will be fabricated (see Table 1 below). As discussed in the *Design Ideas* section above, the injector base, force application system, 1 mL syringe mold, and visual feedback system for the injections will remain the same for each force detection system design. The method of integration for the feedback sensor and display will not change unless additional components are needed to implement the design idea. The details and functions of each design are described in the *Design Ideas* section above. The designs consist of components that are similar to or the same as those addressed in the *Materials* section below.



Table 1: Stem Cell Injector Force Detection System Design Matrix. Consists of seven design criteria to evaluate each design. The FSG Series Force Sensor design won as the best choice with a total of 86/100, while the Load Cell with Nanosheild scored 80/100, the Non-Invasive Pressure Sensor design scored 76/100 and the Cellringe Pump FSR Force Sensor Based System scored 69/100.

Automated Injection System Force Detection Designs									
Design Criteria	Weight	Cellringe Pump FSR Force Sensor Based System		FSG Series Force Sensor		LCMKD-10N Load Cell with Nanosheild		Non-Invasive Pressure Sensor	
									
Accuracy	25	2/5	10	4/5	20	4/5	20	5/5	25
Sensitivity	25	2/5	8	5/5	25	5/5	20	4/5	20
Feasibility	20	5/5	20	4/5	16	3/5	16	3/5	12
Safety	10	4/5	8	5/5	10	5/5	10	3/5	6
Cost	10	5/5	10	3/5	6	2/5	4	3/5	6
Ease of Operation	5	5/5	5	5/5	5	5/5	5	4/5	4
Durability	5	4/5	4	4/5	4	4/5	4	3/5	3
<b>Total (100)</b>	<b>100</b>	<b>Sum</b>	<b>65</b>	<b>Sum</b>	<b>86</b>	<b>Sum</b>	<b>80</b>	<b>Sum</b>	<b>76</b>

Winner	Tie
--------	-----

To ensure proper scoring and evaluation of the three design ideas, each criterion was carefully and conscientiously selected and weighed based on its importance to the overall injector design and the design specifications (see the *Design Specifications* section above and

Section 1 of the Appendix). Accuracy and sensitivity were each given the highest weight (25) compared to the other criteria since the main goal of the project is to improve the functionality of the injection device's force detection system. Accuracy relates to the sensor's ability to measure the force or pressure experienced by the MSC's in the syringe. As each sensor is able to read the applied force or pressure differently, this criteria strictly addresses one of the primary goals of this project, significantly contributing to the determination of the winning design. The sensitivity of each sensor determines how well each system can detect minimal amounts of variance in the force or pressure applied to the device itself, rather than the MSCs. As injection forces will be tested to determine how much pressure and force applied to the syringe causes cell damage and lysis, a highly sensitive design is necessary to develop a precise range of values that result in damage to the cells. Both the accuracy and sensitivity of the sensor designs were graded using the technical specifications provided for each individual device along with the judgment of how well the design measures the force and pressure experienced by the cells. Feasibility is weighted highly (20) as it reflects the ability to implement the component into the current design from a prototypical level within the required semester time frame. The sensor device needs to be calibrated and implemented into the device in a single semester. This criteria evaluates the complexity of each design and its integration requirements. While complex sensors may have higher accuracy and sensitivity, they could also require special circuitry that delays the prototype fabrication process. Safety has a lower rating (10) which is rationalized by the designs' interactions with the MSCs. As all materials used to hold and deliver the MSCs within each design are fully biocompatible with the MSCs, the Safety score was graded based on any additional factors the sensor may pose as a threat to the patient, operator, or the MSCs themselves, such as bubble formation within the MSC solution or inducing cell lysis (see the *Ethical Considerations of Design* section below). Cost was also weighted on the lower end of the scale (10). The Cost grades were based on how expensive the feedback sensor device is, along with any potential additions to the prototype that may be required. This weight is lowered because all the sensors are under the project budget of \$3000. This criteria thus grades the cost of each sensor in comparison to the target manufacturing cost of \$500. Ease of operation and durability rank the lowest (5) on the criteria scale due to the goal of the feedback system improvement project. The ease of operation was already maximized in the prototype's button interface system and easy loading of syringes, so this criteria looks at any additional steps that may be added to the operator's procedure. Durability also is assumed to not pose a problem as the low forces applied to the syringe will likely not damage the sensor. The durability criteria thus looks at the strength of the device's materials, how well the sensor will fit within the current prototype, and each sensor's susceptibility to failure during an injection.

Accuracy was scored highest in the Non-Invasive Pressure Sensor (5). This outranked the other designs, as the pressure sensor is the only device to directly measure the pressure of the MSC aliquot solution. (via its flow module) The FSG Series Force Sensor and Load Cell with Nanoshield designs scored high (4) due to their very high accuracy ratings, being  $\pm 0.5\%$  and  $\pm 0.25\%$  respectively [39], [40]. They are able to measure force from the syringe plunger much

more accurately than the FSR Force sensor on the current prototype design. However, as this is an indirect measurement of the force or pressure applied to the MSCs, they did not receive the high score for this criterion. The FSG Series Force Sensor and Load Cell with Nanoshield designs both scored highest in sensitivity (5). The sensitivity of the FSG Series Force Sensor has a rating of 3.60 mV/V/N, which allows the device to detect extremely small changes in applied force within its range of 0.00 N - 10.00 N [39]. The Load Cell with Nanoshield sensor has a slightly lower sensitivity rating of 2 mV/V/N [40]. While this is lower than the 4.88 mV resolution of the Arduino Uno microcontroller [35], the Nanoshield incorporated within this design raises the resolution of the Arduino Uno microcontroller processor, enabling the detection of these smaller voltage changes from the sensor itself [41]. Although the Pressure Sensor also ranks high in sensitivity (4), the additional benefits of precise sensitivity and increased resolution from the FSG Force Sensor and the Load Cell Nanoshield system results in their higher scores in the sensitivity category. The FSR Force Sensor displayed the lowest ranking (2) as the placement of the syringe plunger on the FSR's active zone controls the sensitivity the device provides, resulting in an inconsistent sensitivity. The FSR Force Sensor ranked highest in feasibility (5) as the simple device is able to be easily implemented into the Arduino Uno microcontroller, using the same power supply provided by the microcontroller itself. The device is also already integrated with the current injector, so no additional fabrication is required with this design. The FSG Force Sensor also ranked high (4) due to its simplicity of implementation to the prototype's microcontroller. The FSG just needs to adhere to the force application block and connect via jumper wires to the feedback system circuitry. The FSG ranked lower, however, due to the change in required input voltage (requires a 10.0 V supply rather than the FSR's 5.0 V supply [39, 37]) and thus output voltage. This will consequently require modifications to the feedback circuitry in order to implement the FSG into the injector. The Load Cell Nanoshield system and the P30 Non-Invasive Pressure Sensor scored lower (3) due to the additional components within each device that will induce complications when integrating the sensors with the feedback circuitry, Arduino Uno microcontroller, and Arduino IDE software. They will also alter the physical structure of the prototype. The FSG Force Sensor and Load Cell with Nanoshield design scored highest in safety (5) as their high scores in accuracy and sensitivity demonstrates that they will improve the detection of force and pressure applied to the cells. Their high repeatability of  $\pm 0.2\%$  and  $\pm 0.1\%$ , respectively [39, 40, 41], will also result in correct and reliable force values being displayed across multiple injections and procedures, further increasing the safety of the device. Applying too much force to the cells can cause harmful effects to the MSCs, disrupting the injection procedure and harming the patient (see *Motivation* section above). Although the Non-Invasive Pressure sensor also scored higher in accuracy and sensitivity, it scored lower in the safety category (3) due to the device interacting with the MSC aliquot solution directly. The sensor could damage the MSCs, induce lysis within the cells, or contaminate the stem cells, presenting a greater concern with the impact the device will have on the patients and the efficacy of the intramyocardial MSC injections [7]. The FSR Force Sensor scores the highest in cost, (5) as this sensor is currently within the design and thus does not present any additional costs. The

FSG Force Sensor and Non-Invasive Pressure Sensor rank lower (3) with the Load Cell with Nanoshield design ranking the lowest (2). The price of the FSG Force Sensor is \$163.12 [39] and the P30 Non-Invasive Pressure Sensor is in a similar price range [42]. These designs are not too costly and are still within the required \$500 manufacturing cost, putting them at a score of three. They are not ranked higher since their \$163.12 price is still relatively large compared to the FSR sensor which does not represent any financial burden. The Load Cell with Nanoshield Design costs \$775.50 [40, 41]. As this sensor costs the highest and is above the desired \$500 manufacturing cost, it was ranked the lowest with a score of two. Ease of operation scored highest (5) in all designs besides the Non-Invasive Pressure Sensor. All other designs do not affect the operator procedure, as they will be identical to what is already implemented in the prototype. As the Non-Invasive Pressure Sensor is integrated with the distal tip of the 1 mL syringe (see Figure 13 above) and the flow module is disposable and thus replaceable after each injection, the operator will have to constantly attach and detach the sensor to the procedural system. These are additional steps that decrease the overall ease of operation of this device, which is reflected in its lower score. Durability also ranked high (4) in all categories besides the Non-Invasive Pressure Sensor (3). The pressure sensor will experience constant shear force and stress throughout each injection in addition to continual compressive and bending forces, limiting its overall durability. These constant forces reduce the sensor's life in service, increasing its susceptibility to failure during the required three year life cycle (see the Design Specifications section above and Section 1 of the Appendix) [44]. The other three designs will only receive a minimal compressive force (maximum assumed force of 3.00 N [17]) during each injection, so they will not display the same durability concerns as the pressure sensor. Based on this evaluation, the top force detection design was determined to be the FSG Series Force Sensor, making it the system that will be moved forward with.

## Proposed Final Design

The force detection design with the highest score in the Design Matrix was the FSG Series Force Sensor, with an overall score of 86. The design was followed by the Load Cell with Nanoshield with a score of 80, the Non-Invasive Pressure Sensor with a score of 76, and the original FSR Force Sensor with a score of 65. The FSG Series Force Sensor scored highest in sensitivity, safety, ease of operation, and durability, validating its score and ability to successfully meet all of the design specifications and the goal for the advancement of the prototype by increasing the efficacy of the feedback system and thus the device and injection procedure (see the *Design Specifications* section above). The FSG Series Force Sensor also scored high in feasibility, proving this sensor can be implemented into the injector within the allotted semester time. Although it did not have the high score for one of the heaviest weighted categories, accuracy, the  $\pm 0.5\%$  error associated with the FSG sensor is still within the required 5% error specification [39]. As a result, the sensor thus has a high enough accuracy to provide the operator with reliable force values throughout each injection that enable proper detection of the force supplied to the syringe for high efficacy procedures. The FSG Force Sensor will be incorporated

within the current Cellringe Pump prototype in the same manner that the FSR Force sensor was (see the *Preliminary Design* section above), placing the sensor inside a modified force application block, aligned with the syringe plunger. The FSG Series Force Sensor will also be integrated with circuitry to connect the sensor to the Arduino Uno microcontroller and the LED digital display. Once the sensor is properly included within the circuit, known forces will be applied to the sensor in order to experimentally develop a calibration curve. The resulting equation associated with the curve will be utilized in conjunction with the Arduino Uno IDE program (see the *Methods* section below) to detect and display the force values throughout each injection on the digital display. This will be visible to the operator, enabling them to confirm the success of each injection.

## Fabrication/Development Process

### Materials

#### Overview

The force sensor based visual feedback system consists of an FSG020WNPB Series Force Sensor [39], an Arduino Uno microcontroller [35], Arduino IDE [34], an LED Serial 7-Segment Digital Display [36], an INA129 Instrumentation Amplifier [45], and standard circuitry wires, resistors, an LED, and an adhesive breadboard [46]. See Section 2.3, Section 2.1, Section 2.7, and Section 2.8 of the Appendix for the technical data sheets of the FSG sensor, Arduino Uno microcontroller, LED Serial 7-Segment Digital Display, and INA129 Instrumentation Amplifier, respectively. The injector base, stepper motor storage compartment, support block, force application block, and syringe clamp were fabricated with Ultimaker PLA via 3D printing (see Section 2.9 of the Appendix for the technical data sheet of the PLA) [47]. The automated injection is controlled by a NEMA-17 stepper motor [48], an Arduino Uno microcontroller [35], Arduino IDE [34], a fully threaded zinc coated aluminum bolt [49], and three tactile buttons [50]. See Section 2.10 and Section 2.11 of the Appendix for the technical data sheets of the stepper motor and threaded bolt. A nylon hex nut (see Section 2.12 of the Appendix for the technical data sheet of the nut) [51] is embedded within the Ultimaker PLA force application block to allow for the threaded rod to control its movement and thus syringe plunger compression. Two aluminum support rods are attached to the stepper motor storage compartment and the support block, penetrating through the force application block in order to maintain its upright position and assist with its movement and enhance its syringe plunger compression capabilities. Standard 1 mL clinical syringes, medical grade tubing, and therapeutic catheters are compatible with the Cellringe Pump, but as they are not part of the fabrication process and the actual injector design, their material composition will not be incorporated in the discussion.

## Force Sensor

The FSG sensor is only 12.70 mm wide with a 7.98 mm length and a 9.04 mm height, making it a small sensor that will not interfere with injector functionality [39]. Typical 1 mL standard syringes used within the intramyocardial MSC injection procedure have a 10.24 mm plunger diameter [38]. Despite the FSG sensor's 6.00 mm active zone, its  $1.31 \pm 0.27$  mm actuator height makes the FSG sensor a great fit for the injector force sensor as it will allow the entire force applied by the 1 mL standard syringes to be adequately received throughout each procedure. This force reception will be read with a high degree of accuracy as the FSG sensor has a sensitivity of 7.2 mV/V/N, resolution of 0.0098 N, repeatability error of  $\pm 0.2\%$ , and an accuracy of  $\pm 0.5\%$  over a 0.00 N to 10.00 N force range [39], which is well within the expected 0.14 N to 3.00 N injector force range during a typical intramyocardial stem cell injection procedure (see the *Intramyocardial Stem Cell Injection Procedure* section above) [17]. The high sensitivity and accuracy of the force sensor over repeated uses allows force values to be detected during each injection with a high degree of efficacy, a critical component that will impact the success of each procedure. The ability for the FSG sensor to contribute to the visual feedback system via its integration with standard circuitry, breadboards, and an Arduino Uno microcontroller further promotes its use as the injector force sensor [39]. Alternative force sensors, such as the LCMKD-10N Load Cell, a TFX292X-040B-0025-L compact compression load cell, or a MS5611 Barometric Sensor, require additional circuitry components in addition to just typical electrical wires to integrate with the Arduino Uno microcontroller [40, 43, 44]. The FSG sensor also costs only 163.12 dollars while the Nanoshield and LCMKD-10N Load Cell system costs 775.50 dollars [39, 40, 41]. As a result, the FSG sensor is a cost effective choice that can properly and adequately detect the entire force applied by the injector to the 1 mL syringes during each injection due to its 6.00 mm diameter elevated active zone, confirming that this sensor is the appropriate force identification device.

## Microcontroller and Software

The Arduino Uno microcontroller has a very high sensitivity to voltage change with a resolution of 4.88 mV [35]. This allows the microcontroller to pick-up very slight changes in voltage input, with one ADC value representing every 4.88 mV input into the board. This resolution allows for accurate microcontroller ADC value designations based on the voltage input from the voltage divider circuit, that is used to establish force. This demonstrates the effectiveness of using the Arduino Uno as the feedback system's microcontroller. This microcontroller is also compatible with the NEMA-17 stepper motor, connecting to it via an adafruit Motor Shield v2.3. This allows the microcontroller to easily drive and accurately control the revolution rate of the motor through Arduino code and thus the force application (to the syringe plunger) and injection rates [52, 34]. The Arduino Uno has a length of 68.6 mm, a width of 53.4 mm, and a weight of 25 g, so it is a small microcontroller that fits within the  $27.50 \times 10.00 \times 7.50$  cm injector base, is easy to transport, and does not create a burden during procedures and storage [35]. One of the main benefits of using the Arduino Uno microcontroller

is the Arduino IDE software program that is coupled with it. This program takes the precise and accurate voltage readings from the microcontroller and utilizes algorithms to perform calculations that convert these inputs into force values based on a standard calibration curve (see the *Methods* section below). These values are then displayed in real-time to the operator throughout the injections via an LED Serial 7-Segment Digital Display that integrates with the software and microcontroller, assisting in the success of the procedure. Code also illuminates an LED signal based on the force value that is being output by the program, enabling the visual feedback system to function properly. The IDE software program contains additional code that regulates the stepper motor via the microcontroller, controlling its step rate and rotation velocity and thus the application of force to the syringe plunger. As a result, this Arduino Uno and Arduino IDE system controls and maintains the success of the injector. See Section 3.1 of the Appendix for the stepper motor Arduino IDE code.

### Visual Feedback Display and Circuitry

The circuit jumper wires, resistors, and adhesive breadboard are used in combination to form a circuit that integrates the FSG sensor with the Arduino Uno microcontroller, allowing for a visual feedback system to be fabricated with the use of a red LED and an LED Serial 7-Segment Digital Display. The jumper wires are used to connect the FSG sensor to the breadboard, power and ground the circuit, connect the voltage output from the force detection circuit to the microcontroller, link the digital display and the microcontroller, and connect the microcontroller to the red LED. These connections allow for the circuit and visual feedback system to function. The force detection feedback circuit consists of an INA129 Instrumentation Amplifier that acts as an intermediate between the FSG sensor and the Arduino Uno microcontroller. It amplifies the voltage difference delivered from the FSG sensor by 23.45, delivering the output to the Arduino Uno microcontroller in order to enable proper detection of the system's output voltage. This amplifier was selected due to its ability to provide a large gain of 23.45 while maintaining a proper current to deliver the voltage to the microcontroller [45]. The FSG sensor only changes its voltage by a total of 360 mV across the entire 0.00 N - 10.00 N force range, correlating to a sensitivity of 3.6 mV/V/N, which is not within the 4.88 mV resolution of the Arduino Uno microcontroller [39, 35]. To allow proper voltage values to be delivered to the Arduino Uno microcontroller for accurate detection, the 23.45 gain from the INA129 amplifier is required. The instrumentation amplifier also contains a 50  $\mu$ V sensitivity, so it will detect all voltage differences delivered by the FSG sensor, allowing proper force detection throughout each injection, generating a high efficacy feedback system [45]. A 200  $\Omega$  resistor is connected in series with the LED to prevent the LED from burning out when the Arduino Uno delivers 5.0 V. The resistors utilized within the force detection section of the feedback system will be selected to provide a large enough voltage output range (taking into account the expected FSG resistance values over the anticipated force range) for proper Arduino Uno microcontroller detection and response. The Sparkfun resistors were also used due to their greater lead thickness compared to typical resistors, promoting their durability and resistance to cyclic fatigue, as well

as its low  $\pm 5\%$  tolerance that will reduce error [53]. The Sparkfun adhesive breadboards were specifically chosen as they are relatively small ( $83.5 \times 54.5 \times 8.5$  mm) and can strongly adhere to the bottom of the injector base [54]. The small size minimizes the interference of the breadboard with the overall injector functionality and MSC injection procedure as well as enables it to fit within the  $27.50 \times 10.00 \times 7.50$  cm injector base. The sturdy connection to the injector will prevent any displacement of the breadboard throughout each injection, limiting the susceptibility to loose connections and thus feedback system error. The LED Serial 7-Segment Digital Display outputs the force provided to the syringe throughout each injection on a  $41 \text{ mm} \times 23 \text{ mm}$  screen. This allows the operator to easily track the force being applied by the injector throughout each procedure, assisting in clinical success. It is compatible with the Arduino Uno microcontroller, contains a baud rate of 9600, and can provide two decimal places when displaying force values. As a result, the display can easily integrate with the microcontroller-Arduino IDE system, displaying a highly accurate force output in real-time (as the force is applied to the FSG sensor) [36]. While there are additional digital displays that can connect with an Arduino Uno microcontroller, such as a common cathode 7-Segment display, they require additional components in order to properly connect with the microcontroller and they consist of complex interfaces, increasing their susceptibility to error during display system fabrication [55]. As a result, the LED Serial 7-Segment Digital Display is the most cost effective option as well as it provides an accurate system that can integrate with the Arduino Uno system with minimal error, demonstrating that it is the correct display device. The red LED is used to provide the visual feedback for the operator and is controlled by the Arduino Uno microcontroller and its IDE software. These components are all from the BME 201 kit, so there was no additional cost to the design.

### Ultimaker PLA Injector Components

Ultimaker PLA contains a detailed surface quality and supports the creation of high-resolution parts, enabling the injector base, stepper motor storage compartment, support block, force application block, and syringe clamp mold to be fabricated with a high degree of detail, complexity, and accuracy. This allows these features to interact together successfully and correctly, producing controlled injection rates that meet the 30 and 60 second requirements. The high quality generation of the syringe clamp mold enables it to properly interact with the 1 mL syringes, preventing any movement or displacement of the syringe during force application and the injection. The Ultimaker PLA has excellent ultimate strength (49.5 MPa), is highly resistant to deformation over time and cyclic fatigue, and has very high stiffness (2,346.5 MPa) [56]. This allows for a durable and strong injector base, stepper motor storage, support block, force application block, and syringe clamp that will be able to withstand all repeated forces applied to the injector throughout each procedure. As the syringe clamp is permanently attached to the injector base, it should not experience failure at its connection site as this attachment will be reliable and permanent, rather than exchangeable, integrating the clamp into the base to make one cohesive syringe insertion complex. The clamp will not display the weakness and



susceptibility to failure that a replaceable and exchangeable mold would display as it is fully and permanently attached to the injector base rather than just clipped or temporarily locked into the base. Testing confirmed the durability and strength of the syringe clamp as seen in the *Syringe Clamp Connection and Locking Testing* and *Syringe Clamp Connection and Locking Results* sections below. Although forces may be applied throughout the injector as a result of operator interaction with the device, the main point of force reception will be where the force application block comes into contact with the syringe plunger. In order to confirm that the force application block will be able to withstand the expected maximum force of 10.00 N (see the *FSR 400 Series Round Force Sensing Resistor* section above), the stress generated on this block (cross-sectional area of contact  $6.362 \times 10^{-5} \text{ m}^2$ ) at the maximum applied force was calculated using Equation 2 below [56].

$$[2] \sigma = F / A$$

Under the maximum applied force of 10.00 N, the force application block will experience 0.16 MPa of stress based on its geometry, which is much less than its 49.5 MPa ultimate strength. As a result, the force application block will be able to withstand all applied forces during each injection, demonstrating its success as a force application block. This durability demonstrates that the Ultimaker PLA model will last for at least three years, meeting the shelf-life client requirement. These mechanical properties will also allow the stepper motor storage, force application block, and syringe clamps to act as stable and reliable holders for the motor, threaded rod, and syringes, respectively. While Tough Ultimaker PLA and Formlabs' Clear Resin have comparable ultimate strengths to Ultimaker PLA (37 MPa and 38 MPa respectively), the Tough Ultimaker PLA has a stiffness of only 1,820 MPa and both materials are not resistant to deformation over time and cyclic fatigue [56, 57]. Ultimaker PLA has thus the optimal mechanical properties to be able to withstand the cyclic nature of each injection procedure, solidifying this material as an adequate choice to use throughout the injector that will allow for successful injections and enable it to meet the three year life specification.

### Injector Force Application Materials

A NEMA-17 stepper motor is used to control the automated injection due to its compatibility with the high resolution Arduino Uno microcontroller and the very precise and controlled rotation it can provide as a result of its 200 steps per revolution and 0 - 12 V rated voltage revolution rate dependence [48]. The accuracy this motor can provide will allow it to regulate the force application and thus injection rates with a high degree of efficacy, allowing the 30 and 60 second injection rate design requirements to be met. A zinc plated aluminum fully threaded bolt was chosen to control the force application of the block to the syringe plunger as a result of its durability, corrosion and fatigue resistance, and strength relative to typical aluminum, steel, and stainless steel bolts (do not contain a zinc coat), which have limited corrosion resistance, strength, and cyclic durability. The aluminum threaded bolt also has a much greater tensile strength and Young's Modulus compared to nylon bolts [49, 58]. These are critical

features for generating consistent and reliable injections, displaying the zinc coated aluminum bolt's ability to perform accurate and successful injection procedures. A nylon hex nut was chosen to mediate the threaded bolt's rotation and ultimately the force application as it contains higher strength and durability compared to typical metal fasteners, corrosion resistance, decreased wear on mating parts, and good bearing properties [59]. The bolt and nut are also lightweight and the nut is nonconductive, increasing the portability of the injector and eliminating any concerns associated with the circuitry from the feedback system or stepper motor interacting with the threaded rod system [51]. The properties characteristic of the zinc plated aluminum bolt and nylon hex nut will allow the threaded rod system to resist fatigue from cyclic loading and provide a better connection between the bolt and hex nut, increasing the accuracy and precision of the force application system over a greater amount of uses and thus decreasing its susceptibility to cyclic stress compared to traditional metal bolts and hex nuts. The support rods used to hold the force application block in its proper vertical alignment throughout each injection are composed of aluminum due to its ability to assist with the functionality and accuracy of the force application system over repeated uses. The aluminum rods have a much smoother finish than the inevitable roughness of Ultimaker PLA (due to the nature of 3D printing) as well as typical metals, such as steel, nickel, and zinc (generated from impurities induced by surface coating) [60, 56, 61]. The smoothness of the aluminum rods generates a tight and polished interface with the force application block, providing minimal friction between the two surfaces as the force application block moves laterally during an injection. This will thus improve the consistency and efficacy of the force application system, enabling precise and accurate injections to take place throughout each procedure. The high cyclic ultimate and shear strength of aluminum (110 MPa and 80 MPa, respectively) compared to Ultimaker PLA (49.5 MPa) further increases the reliability and durability of the injections, validating the use of aluminum for the support rods [62, 63, 56]. As the force application block applies shearing force to the support rods during each procedure in addition to the constant compression experienced at the ends of the rods, long-term resistance to cyclic loads of shearing force are critical to the success of the system and its ability to function properly for the required three year shelf-life. A 5 mm to 6.35 mm coupler is used to securely connect the bolt to the stepper motor [64], enabling the stepper motor to control the rotation rate of the bolt with a high degree of accuracy. Three 12 mm tactile buttons control the stepper motor via the Arduino Uno microcontroller. Standard jumper wires (see the *Visual Feedback Display and Circuitry* section above) connect the tactile buttons to the microcontroller and a simple click of the button results in either a 30 second or 60 second injection or a reset of the injection (in case an issue arises during the procedure). These buttons integrate with the Arduino Uno microcontroller and are 12.00 × 12.00 × 8.50 mm, so they easily fit within the injector base and do not disrupt the system [50].

The full list of materials used for the injector, the budget, and all calculations related to mechanical properties can be found in Section 2 of the Appendix.

## Methods

The injector base fabrication process relied on using Ultimaker PLA in conjunction with the NEMA-17 stepper motor and zinc plated aluminum threaded bolt (see the *Materials* section above for more information on the described materials). The different features within the injector are on the centimeter scale with some detail that is required on the millimeter scale. Therefore, the design and fabrication method must be able to account for this precision and complexity. The SolidWorks Computer Aided Design (CAD) software allows for the development of detailed and complex designs and provides a SimulationXpress Analysis Wizard extension that determines the location of the weakest points and thus where failure is imminent. This software was used to ensure that the entirety of the final design will be able to withstand the maximum expected force of 3.00 N, which includes critical points such as the force application block and syringe clamp mold. The outer base, force application block, and force block outer rods were all designed using the CAD software SolidWorks and fabricated out of the Ultimaker PLA material that is created through the Ultimaker 3D printers at the University of Wisconsin-Madison MakerSpace [56]. 3D printing through the UW-MakerSpace was easily accessible and allowed for the creation of all the necessary parts needed to fabricate the prototype through the use of the CAD created part files. All CAD created components of the base were compiled into an assembly with each other to confirm correct dimensioning and to take into account tolerances applied to the 3D printed products. Each 3D printed piece serves an essential function, requiring the resolution, precision, and accuracy associated with SolidWorks and all parts were created so they can easily assemble together with all base features. The outer base that was designed to hold and conceal the NEMA-17 Stepper Motor was updated to better secure the motor in place using 1 cm diameter screws. The stepper motor holder was also designed to allow for the connecting wires to flow down into the base and easily connect with the Arduino. A 1.0 mL syringe mold was designed to hold the syringe firmly in place during injections and allow the syringe to be easily replaceable in between injections. The zinc plated aluminum threaded bolt was connected with a coupler to fit over the stepper motor in a way that allows for a complete transition of power from the motor to the threaded rod, and from the threaded to the force application block. To enable proper fitting of the bolt within the force application system and between the support block and coupler, a drop saw was used to accurately and precisely cut the bolt down to a length of 3.50 cm. The force application block is prevented from spinning and thus promotes horizontal motion by the use of the aluminum cylinder rods that are easily detachable to allow for easy adjustments to be made to the positioning of the force application block. The force application cylinder rods were updated from being 3D printed using Ultimaker PLA to now implemented aluminum coated rods. This change was made in order to decrease the friction between the force application block and the support rods during injections. The cylinder rod holder was also updated to hold the aluminum rods and fit securely in place on the outer base. The force application block was also manipulated to house the FSG series force sensor within the block and mitigate any changes to the code in the Arduino IDE software. The exact fabrication protocols for the development of the FSG force sensor feedback system (includes code), NEMA-17 Stepper Motor circuitry, and overall device

can be found in Section 3 of the Appendix and all associated SolidWorks part files and drawings can be found in Section 4 of the Appendix.

To provide an equation to accurately and reliably establish the injector force applied to the syringe plunger throughout each injection, a calibration curve was created based on the FSG feedback system testing force and voltage data. Using the schematic to determine the function and pin-outs of the FSG series force sensor [39], the sensor was powered using the 5.00 V power supply from the Arduino Uno Microcontroller, while an INA129 instrumentation amplifier is incorporated into the circuitry to amplify the difference in voltage that is output from the FSG sensor's internal wheatstone bridge circuit. The instrumentation amplifier increased the FSG's voltage difference with a gain of 23.45, found by using the gain equation (Equation 3 below) provided by the instrumentation amplifier's datasheet and the 2.2 k $\Omega$  gain resistor [45].

$$[3] \text{ Voltage Gain} = 1 + (49.4\text{k}\Omega / R_G)$$

The instrumentation amplifier was powered using the 5.00 V supplied by the Arduino, as well as a -5.00 V supply from an external power supply. The -5.00 V was used to ensure there is no offset voltage and the Arduino IDE software reads 0.00 V when there is no force applied to the FSG force sensor. The technical datasheet for the INA129 instrumentation amplifier can be found in Section 2.8 of the Appendix. The voltage level that is output by the instrumentation amplifier when a force is applied is then sent to the Arduino, where a line of best fit equation was identified that correlates the difference in voltage from the FSG sensor (V) to known force applications (N), allowing the force to be determined based on each voltage input to the Arduino Uno microcontroller. The purpose of the calibration curve is primarily to derive a linear trendline which can then be used to calculate the unknown applied force during the injections. This equation was implemented into the feedback system's Arduino IDE code and allowed the force to be constantly output to the operator through the LED Serial 7-Segment Digital Display (see Figure 7 above) for easy operator visibility [36]. This will assist in the accuracy of each injection, mitigating MSC reflux and catheter obstruction as well as establishing catheter tissue location, and thus promote the efficacy of the intraoperative stem cell injection procedure. The independent variable (x) in the line of best fit equation represents the applied force and the dependent variable (y) describes the output voltage. A 5th degree polynomial (Figure 14) was created to calculate the force values for voltage readings between 0.00 and 5.00 volts. The curves were created dependent on residuals, the correlation coefficients and the distribution of residuals. The complete FSG calibration curve testing protocol can be seen in Section 5.1 of the Appendix. The calibration curves developed for the FSR from the Spring 2022 semester followed the same procedure outlined in Section 5.1 of the Appendix and the curves can be seen at the bottom of Section 5.1 of the Appendix.

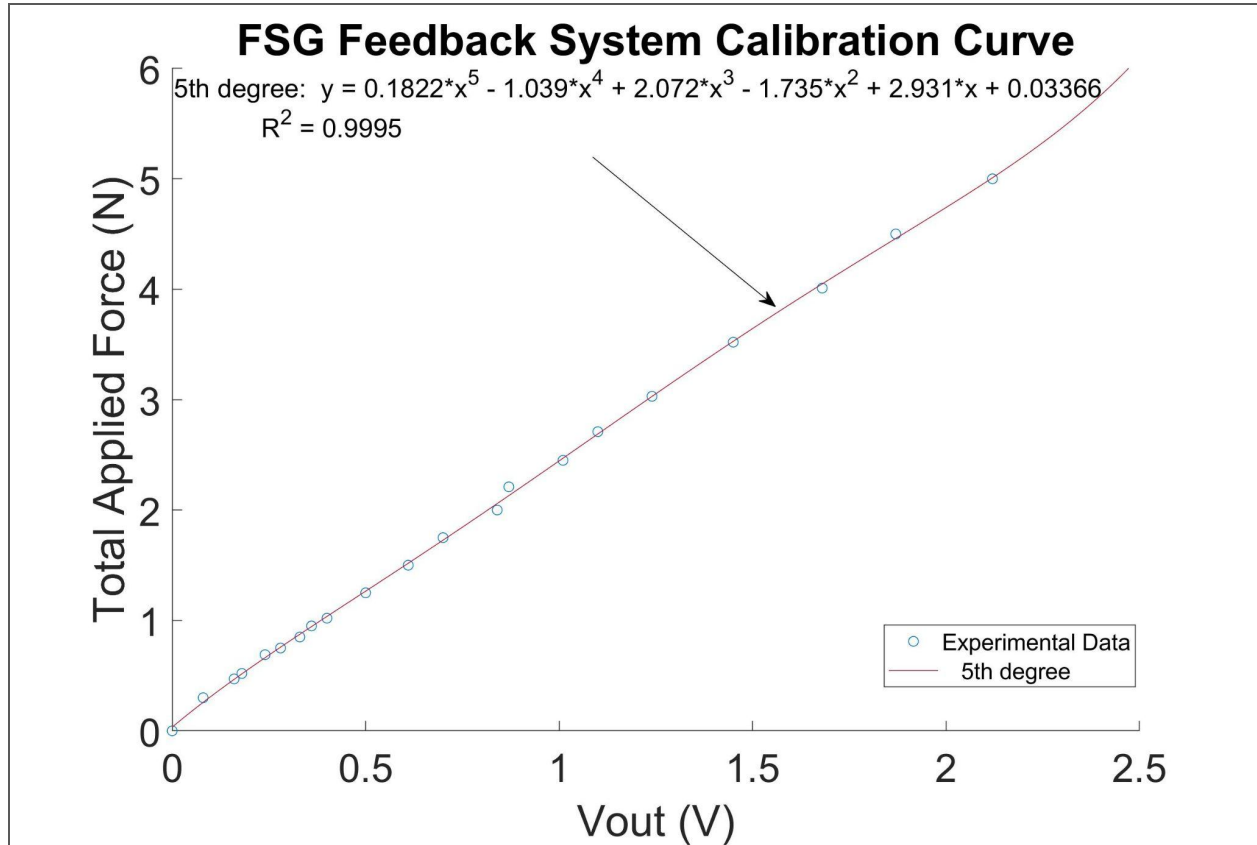


Figure 14: Calibration curve for the FSG feedback system under various loading enabling applied force calculation.

A calibration curve and equation was also created to implement the correct speed and travel distance into the Arduino code controlling the Stepper Motor. To create an equation for the distance traveled per step number applied within the code, a plot was created to differentiate the step size number versus the distance traveled by the nylon nut up the threaded rod. Taking the average of each step size versus distance traveled created the equation as seen in Equation 4 below that was used to calculate the step size needed to have the device fully travel the length of a 0.5 mL filled 1.0 mL syringe.

[4] Distance Traveled = (Step Size Number) \* 0.0064 mm

This equation works for any step size number and will allow for accurate and reliable injection travel distance. This equation can then be correlated with the speed setting of the motor within the code to have the device. The speed equation used to determine the speed number coded in the Arduino program for the 30 and 60 second injections was determined by testing known speeds to find the time it took to travel a known distance. The Stepper Motor rotating times were hand timed using a stopwatch and plotted against the same distance each test to

determine the mm/sec equation. The plot can be seen below in Figure 15, as the logarithmic equation can be solved to find the necessary step speed number for the velocities of the push block during the 30 and 60 second injections. The equation developed through the line of best fit can be seen below in Equation 5. This equation was used to find the motor speed implemented in the Arduino when the 30 and 60 second velocity requirements were determined. The code for controlling the Stepper Motor can be found in Section 3.1 of the Appendix.

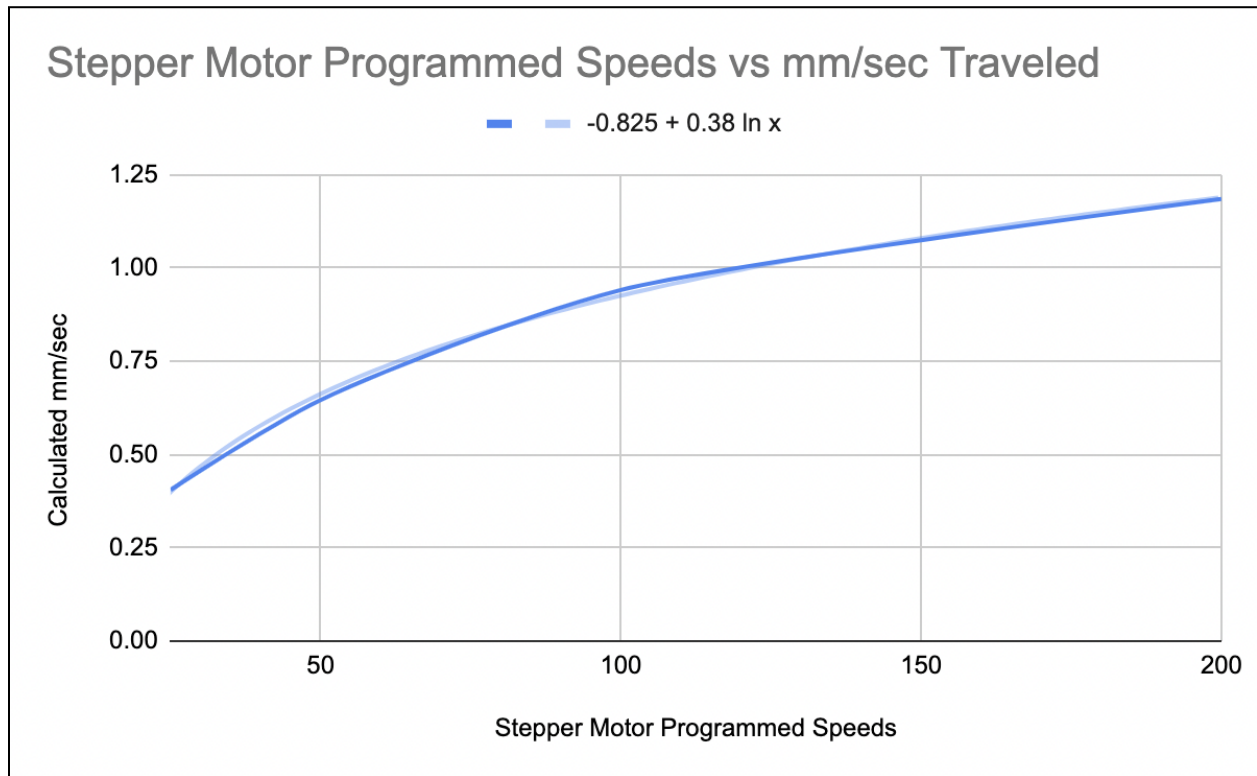


Figure 15: The plotted Stepper Motor programmed speeds versus the velocity of the nylon nut during testing. A line of best fit was applied to generate the implemented equation used in the Arduino coding.

$$[5] \text{ Velocity (mm/sec) } = -0.825 + 0.38 \cdot \ln(\text{Motor Speed})$$

The circuitry of the FSG feedback system and Stepper Motor were assembled and designed to serve all the requirements necessary to enable the automatic syringe injection system to perform the injections and display the force at the same time. The Stepper Motor utilizes the Arduino Uno Microcontroller (see *Microcontroller and Software*) and integrates a Motor Shield and buttons to allow for easy fabrication and testing of the injection rate components.

## Final Prototype

The updated prototype injection device was designed to meet the Product Design Specifications and client requirements in order to maximize efficiency, accuracy, and reliability during each myocardium stem cell injection. The 1 mL Syringe Mold secures the placement of the loaded syringe during injections, while also allowing the operator to easily remove and replace the syringe in between injections. The three buttons are utilized to control the device through connections to the Arduino and Motor Shield, which thus power the NEMA-17 Stepper Motor with the buttons' respective commands. Pressing either the 30 or 60 second button will initiate the start of the injection. Pressing the same button that was pressed to start the injection will pause the device for the duration of however long the button is held. The Force Application Block returns to its' starting position either after a successful 30 or 60 second injection, or if the reset button is pressed while the device is still injecting. The use of three buttons minimizes user control to maximize the device's ease of operation.

During each injection, the FSG Series Force Sensor attached within the Force Application Block sends a voltage through the instrumentation amplifier to send a different voltage to the Arduino Uno microcontroller that is then calculated into force and is displayed on the LED Digital Display. This allows the operator to constantly monitor the amount of force being applied to the syringe and have an idea of when there is any catheter obstruction, clogging, or incorrect placement of the catheter during the procedure. The LED Threshold Light illuminates red when the FSG picks up a force above 2.40 N. This specifically alerts the operator that there is a potential for catheter obstruction or cell reflux. The device does not automatically shut off when this value is reached as the obstruction may not be significant enough to require device stoppage. The light serves as a warning to the user, who can easily stop or pause the device to further assess the situation without needing to reset the procedure whenever the 2.40 N threshold is reached. Figure 16 and Figure 17 below display these features.

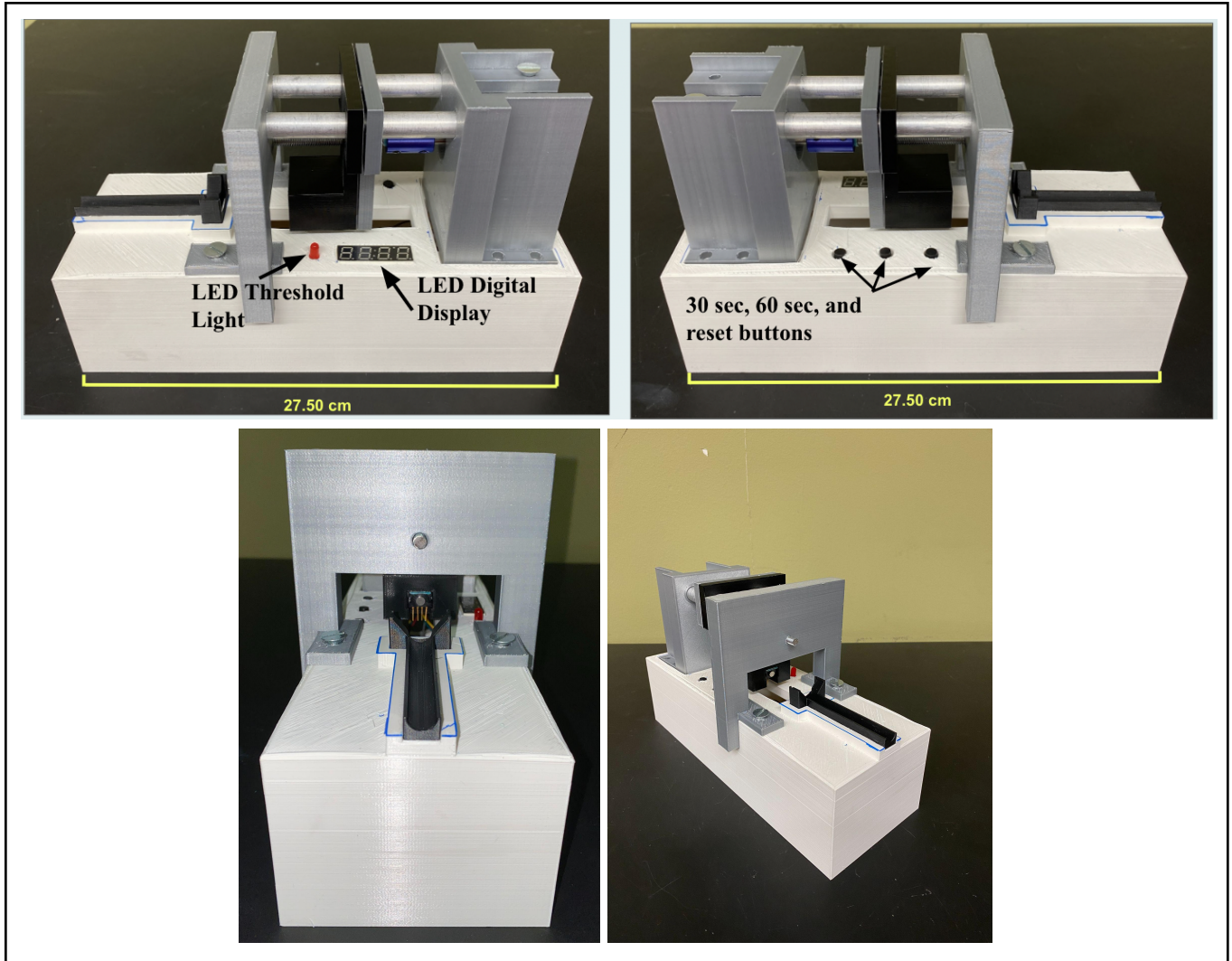


Figure 16: Right end (top left), Left end (top right), front (bottom left), and isometric (bottom right) views of the final prototype with labeled features and 31 cm ruler for scale.

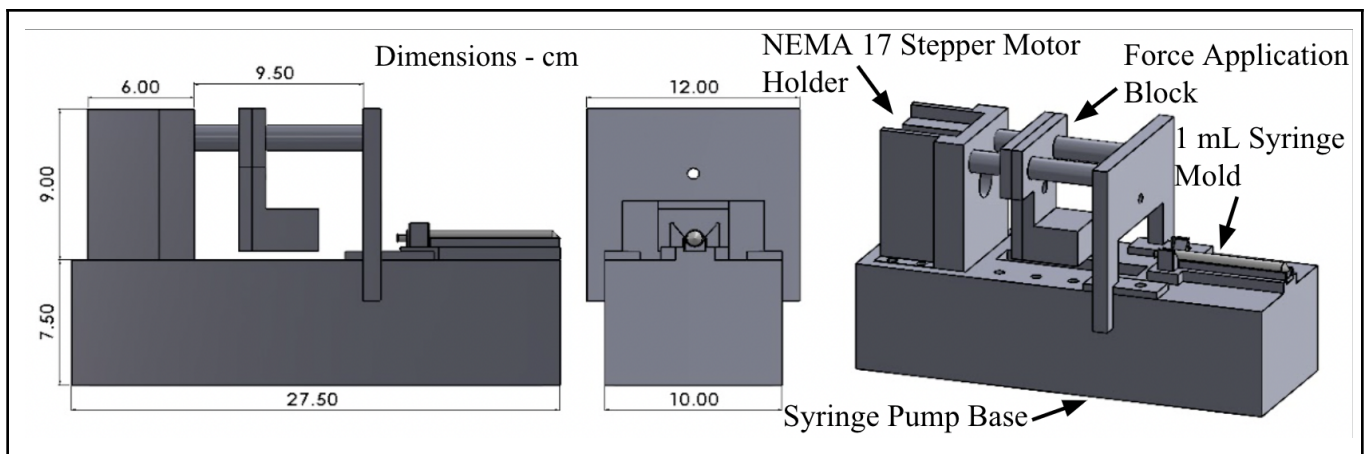


Figure 17: Dimensional depictions of the final prototype as seen in Solidworks with labeled components.



The Syringe Pump Base was designed to hold all components together and house the circuitry underneath. This allows for easier assembly and disassembly of the prototype. When the prototype is put together, the pieces and motor are held firmly in place by 6.25 mm bolts. This allows for successful injections to be performed and the device to be taken completely apart if needed. The base components of the prototype other than the aluminum rods are all made of Ultimaker PLA via the 3D printers at the University of Wisconsin-Madison MakerSpace Lab, (see *Materials: Ultimaker PLA Injector Components*, and *Methods* sections). Further figures and dimensions of the device can be found in Section 4 of the Appendix.

## Testing

The testing discussed below includes all testing performed on the Cellringe Pump prototype during the Spring and Fall 2022 semesters. Of note, the injector from Spring 2022 contained an FSR sensor as the force detection device rather than the FSG sensor that was implemented this semester. As a result, force testing relates to the FSR sensor and the FSG device.

### Feedback System Force Detection Accuracy Testing

Feedback System Force Detection Accuracy Testing of the FSR sensor was completed during the Spring 2022 semester. The percent error was calculated to determine if the force value output by the feedback system was within a 15% error margin of the actual applied force (calculated by the weight of the bottle for all applied forces) for values below 1.00 N and an error margin of 15% for all forces greater than or equal to 1.00 N. Force values less than 1.00 N during a typical injection correspond to an error margin of 20% rather than 15% as very small changes (less than  $\pm 0.1$  N) can correlate to errors greater than 15% while these same force variations for values greater than or equal to 1.00 N correspond to an error less than 15%. Using the percent error equation seen in Equation 6 below [65], for the lowest expected force of 0.14 N, if the feedback system detects a force of 0.17 N, the error between the two values is  $\sim 21.4\%$ . If the feedback system provides force values within the 20% and 15% error margins, the system will thus be capable of providing accurate force outputs required for the operator to adequately determine the efficacy of each injection. The 20% and 15% error margins were only for the Spring 2022 semester as these margins provided a reasonable accuracy level based on the FSR sensor being used. However, this error margin was not acceptable for this semester's specifications hence the 5% error margin was created for the FSG sensor.

$$[6] \text{ Percent Error} = (|V_{\text{theoretical}} - V_{\text{experimental}}| / V_{\text{theoretical}}) * 100$$

Feedback System Force Accuracy Testing of the FSG sensor was performed this semester to test the accuracy of the feedback system and if it was within the required error margin relative to the actual applied force to the FSG sensor (5% error margin). This testing was completed by choosing a specified force value within the range of 0.00 N - 5.00 N. The required amount of

water was then added to an empty water bottle based on the force value chosen. The water bottle was then placed on the FSG and the force and voltage value was read from the spiral monitor. After recording the values, the percent error was calculated to determine if the force value output by the feedback system was within a 5% error margin of the actual applied force (calculated by the weight of the bottle for all applied forces). This error margin has been selected as the force applied throughout each injection will assist the operator in determining where the injection is taking place, the susceptibility to cell damage, and if catheter obstruction or reflux is imminent. The force detection accuracy is thus critical to the success of the device, resulting in a stringent error margin requirement of 5% as this correlates to the resolution and accuracy necessitated for proper determination of injection efficacy [17]. As a result, adhering to the 5% error margin will increase the overall success of the intramyocardial MSC injection procedures. The complete protocol can be found in Section 5.2 of the Appendix below. This testing procedure made sure the device met the required error margins as specified in the *Design Specifications* section above. The results should show that the device is able to meet these standards and forces applied are within the correct error margin.

### Feedback System Testing

Testing of the feedback system was performed to ensure that the system and display were working properly. The feedback system needs to accurately display the force being applied throughout the procedure with less than 5% difference and light the red LED if the force applied is greater than 2.40 N, as specified by the design criteria. To test this system, different amounts of water in increments of 50 - 200 mL was added to a water bottle. The water bottle was then placed on the FSR sensor and the values were read and recorded from both the serial monitor and the LED digital display. After recording the values, the percent difference was calculated between the value read from the serial monitor and the value read from the LED digital display. A force greater than 2.40 N was applied to the sensor to ensure that the red LED would light up. The complete protocol can be seen in Section 5.3 of the Appendix. The design specifications required the force on the LED digital display to be within 5% of the force on the serial monitor as well as a force of 2.40 N or greater would light up the red LED. This testing should be able to conclude that both of these specifications were met and the feedback system is functioning properly.

### Syringe Clamp Connection and Locking Testing

Testing of the 1 mL Syringe Clamp Mold was performed to ensure the stem cell loaded syringe can withstand the forces provided by the injection device when undergoing 30 and 60 second injections. This test also ensures that the syringe can be easily removed and replaced in between injections, as timeliness of the injection procedure is crucial to success. Using the 1.0 mL Syringe Mold, a 1.0 mL syringe, and medical grade tubing, the syringe was exposed to forces that are normally higher than that of an injection with the device. Applying a 5.00 N force to the syringe plunger and ensuring it stays in place will validate the design, as it is predicted the

syringe will not see above 5.00 N of force when being used in the injection device. Following each successful application of 5.00 N of force, the syringe will be tested on removability from the mold. The syringe should easily slide out of the mold without sticking, scraping, or having any unnecessary force applied in order to remove the syringe. Results of this testing procedure provides validation for use of the 1.0 mL Syringe Mold in the injection device during clinical procedures. The complete Syringe Clamp Connection and Locking Testing protocol can be found in Section 5.4 of the Appendix.

### Injection Rate Testing

Testing of the injection rates was completed to ensure the device will completely empty the syringe in the correct time frame. The device and incorporated Stepper Motor must cause the nylon nut on the threaded rod to travel the required distance needed to empty out 0.5 mL of liquid from the syringe in both 30 and 60 seconds. The device needs to finish injections within 5% of 30 or 60 seconds, while also traveling within 5% of the required distance of 30.5 mm that would completely empty a 1 mL syringe loaded with 0.5 mL of solution. To begin, the nylon nut was placed in the center of the threaded rod with this starting point being marked with tape. The circuit controlling the Stepper Motor was then powered on. Both the 30 and 60 second injection rates were recorded using a stopwatch, being sure to start and stop the stopwatch as soon as the motor starts and finishes spinning. After each test, the recorded time on the stopwatch was compared to the expected time of 30 or 60 seconds. During the time the motor was spinning, the nylon nut was held in place by the user to prevent it from spinning, thus allowing it to travel up the threaded rod. After each test, the distance the nylon nut traveled up the threaded rod was recorded and compared to the value of 30.5 mm. The percent errors and standard deviations in each testing group was calculated to validate the injection rate times and nylon nut distance traveled. The overall results of this testing should ensure that the injection rate components of the device were ready to be moved forward with and incorporated into the final prototype. The complete injection rate testing protocol can be found in Section 5.5 of the Appendix.

### Cell Viability Testing

Cell viability testing was completed to ensure there was not more than 5% cell death from starting viability after completing 30 and 60 second automatic injections, as specified by the design criteria. Porcine-derived MSCs were thawed and prepped to get a 40 mL of solution that was used throughout the entire testing process. A 1 mL syringe with a 25 gauge needle attached was loaded with 0.5 mL of the solution and placed in the syringe holder on the device, the button to start the 30 second injection was then pressed. The solution was collected in a small vial in order to test viability after injection. This was repeated five times total for 30 second automatic injections as well as five times total for 60 second automatic injections. Manual injections were also performed in order to compare the automatic injection vs manual injection cell viability. Manual injections were performed three times at 30 seconds and an additional three times at 60 seconds, collecting the solution in a small vial after each injection. Rapid injection

(less than one second) was also performed three times. Using trypan blue, cell suspension, and a hemocytometer, cell viability was measured and recorded. The cell viability was then compared to the starting viability to determine if there was any cell death from the injection. The cell viability testing should be able to conclude if there is less than 5% cell death during the 30 and 60 second automatic injections. The complete cell viability protocol can be found in Section 5.6 of the Appendix.

## Overall Device Testing

### *25 Gauge Injection Testing*

Once the final prototype was assembled and confirmed to work, finalizing tests were performed to ensure all components of the device worked during each injection rate. To further validate the design, the 1.0 mL syringe was loaded with 0.5 mL of water and placed into the syringe mold. The 1.0 mL syringe had an attached 25 gauge needle to allow the water to be collected into the collecting dish and mimic the connection tubing and catheter forces. After each 30 and 60 second injection, the water emptied from the syringe was collected, weighed, and compared to the expected value. Along with testing how well the device empties the syringe, the injection times and force ranges were also recorded. The injection times were then compared to the expected injection times of 30 and 60 seconds, while the force ranges were recorded and compared with each test to determine the repeatability of each injection's force production. Similar to the *Injection Rate Testing*, the times for each injection are expected to be within 5% of the expected value. The force values were observed from the LED Display, with the smallest and largest observed values being recorded. It is anticipated that the volume of water delivered from the syringe will be within 5% of the required 0.5 mL value, as the injector is expected to be accurate and this 5% error margin accounts for water that is inherently and inevitably present in the dead space of the needle and distal tip of the syringe following each injection.

### *Clinical Simulation Testing*

The Clinical Simulation Testing procedure is set up the same way as the *25 Gauge Injection Testing*. The 1.0 mL syringe loaded with 0.5 mL of water was hooked up to the provided connection tubing and catheter system to mimic the conditions the syringe will go through during stem cell injection procedures. The 30 and 60 second injection times were recorded and compared to their original values to ensure the times were within 5% error margin of the expected time. The volume of fluid ejected from the syringe was not recorded, as most of the fluid will be within the connection tubing and catheter after the injection. Visually observing the syringe being completely emptied will validate that the device can perform the stem cell injection procedure using the appropriate tools. The force ranges were also recorded again to determine the repeatability of each injection's force production.

### Catheter Backup Testing

This test was performed to evaluate the force value that is observed by the feedback system within the device when the catheter is backed up and determine what values correlate to an obstructed catheter. In 2022 spring each injection rate was performed once while this semester three trials were performed, where the 1.0 mL syringe loaded with 0.5 mL of water was hooked up to the medical grade tubing and catheter system. After proper system set-up and connection of the syringe to the catheter system, the distal end of the catheter was then blocked with a finger applying force and preventing any liquid from escaping. However, during the Spring 2022 semester, the 30 second and 60 second injection rates were both only tested once with a catheter obstruction modeled by physically kinking the catheter. This catheter system was entirely filled with solution prior to the attachment of the syringe to the medical grade tubing in order to enable proper flow of solution through the system during each injection and to mimic the procedural setting utilized during clinical trials. The recorded values for this test were the force range values, peak force, and if the 2.40 N threshold value was exceeded, causing the LED threshold light to signal to the operator the threshold value was passed. This test will provide data establishing the force values that correspond to an obstructed catheter and whether or not the 2.40 N threshold correctly indicates catheter obstruction susceptibility. This test will also determine the strength of the Stepper Motor and whether or not the injection device is powerful enough to reach the 2.40 N threshold. The full testing protocol can be found in Section 5.7 of the Appendix.

### Bovine Steak Injection Testing

The Bovine Steak Injection Test was performed in order to determine force values corresponding to various states of heart tissue: healthy, diseased, and scarred. Through literature research it was concluded that the Young's Modulus of a healthy human heart is 8 - 15 kPa and increases to more than 100 kPa for scar tissue [66]. Cooking bovine steak with various temperatures achieves various stiffnesses. Young's Modulus for raw steak is around 70 kPa and cooked steak is around 260 kPa [67]. To create this approximate model, steak was obtained from the grocery store then cut into eight sections. Two sections were left raw, two sections were cooked rare, two were cooked medium, and two well done. MTS compression testing was performed for each steak condition to determine a more accurate Young's Modulus.

For each trial 1 mL syringe filled with 0.5 mL of DI water connected to a procedural catheter was placed into the syringe mold of the Cellringe Pump integrated with the FSG Sensor. The needle-tipped end of the procedural catheter was inserted into the meat of each bovine steak condition and tested at 30 and 60 second injection rates for three trials each. Before the injections began it was ensured that the force detected by the FSG sensor was being properly plotted by Arduino into a file. Finally, the force data was collected throughout each injection for future analysis. The full testing protocol can be found in Section 5.8 of the Appendix.

### Ex Vivo Cervine Heart Injection Testing

*Ex Vivo* Cervine Heart Injection Testing was performed in order to gauge the typical force ranges seen during an intramyocardial stem cell injection procedure. The Young's modulus of a healthy human heart is below 50 kPa and increases to more than 100 kPa for scar tissue [66]. Cervine hearts mimic the anatomy of human hearts as they are very similar in size, structure, and function. Once the cervine heart is obtained and thawed this test can begin. The procedure is the same as *Bovine Steak Injection Testing* with the exception of the cervine heart being injected into rather than bovine steak. Three trials are performed for the 30 and 60 second injection rates and force data is collected throughout each injection for future analysis. The full testing protocol can be found in Section 5.9 of the Appendix.

### Viscosity Testing

The viscosity correlation testing was performed to determine the force values associated with different solutions of different viscosities. Viscosity corresponds to the concept of 'thickness' while also providing a measure of the resistance of a fluid to deformation or flow with application of shear or tensile stress [68]. By obtaining various solutions ranging in different viscosities, tests were conducted with the Cellringe Pump integrated with the FSG sensor at 30 and 60 seconds. Solutions with a known viscosity used during this testing were water ( $10^{-3}$  Pa.s) and canola oil (46.2 mPa.S) [69]. Before completing the tests, it was confirmed that the force detected by the FSG Sensor was being properly plotted by the Arduino. For the first set of trials, 0.5 mL of water was loaded into a 1 mL syringe with a 25 gauge needle attached. The injections were into air, with the solutions collected in a petri dish. A total of six trials were completed, three at 30 seconds and three at 60 seconds. Once the trials with water were completed, the procedure was repeated with canola oil. After each trial, the data was named appropriately and saved to be used for future analysis. The full testing protocol can be found in Section 5.10 of the Appendix.

### Pressure Sensing Catheter Testing

Pressure Sensing Catheter Testing was performed in order to correlate the force values detected at the distal end of the 1 mL syringe to the pressure experienced by the MSCs inside of the catheter. This data will be used to determine an equation that is able to accurately predict the pressure inside of the syringe-catheter system from the force detected by the FSG at the distal end of the syringe. To perform the Pressure Sensing Catheter Testing, the Cellringe pump integrated with the FSG sensor was set-up on the bedside countertop and a 1 mL syringe with 0.5 mL of DI water was inserted into the syringe mold. Next, the pressure sensing catheter was connected to the proximal end of the syringe, laying across the length of the countertop. The proximal end of the catheter was inserted into an aortic arch biomimetic 3D structure and the outlet tip was placed in a petri dish for the water to feed into. This set-up mimicked the clinical procedures, enabling the results generated from the testing to be accurate and properly resemble the force-pressure correlation expected during typical intramyocardial injections. Three trials

were performed for the 30 and 60 second injection rates and the peak pressure and force range was recorded for each trial for future analysis.

## Results

The results provided and analyzed below are from the Spring and Fall 2022 semesters. Of note, during the Spring 2022 semester, the injector contained an FSR sensor as the force detection device rather than the FSG sensor that was implemented this semester. Some force results thus correlate to the FSR sensor instead of just the FSG device. Specifically, the *FSR Force Detection Accuracy*, *FSR Feedback System Results*, *Cell Viability Results*, and *Overall Device Results* sections below contain data that was generated with the FSR sensor.

### Feedback System Force Detection Accuracy

#### FSR Force Detection Accuracy

The FSR Feedback System Force Detection Accuracy testing (see the *Feedback System Force Detection Accuracy Testing* section above) was used to establish the force identification efficacy of the feedback system during the Spring 2022 semester, when the injector contained the FSR sensor. As the sixth-degree polynomial line of best fit equation and 4th-degree polynomial line of best fit equation from the system's calibration curves (Section 5.1 of the Appendix) was utilized to calculate the force applied by the injector to the syringe plunger, the tests also verified the accuracy and reliability of the calibration curves. Forces across the initial expected injector range (0.14 N - 3.00 N [17]) were tested following the force detection testing protocol described in the *Feedback System Force Detection Accuracy Testing* section above and in Section 5.2 of the Appendix. To determine if the feedback system met the required error margin specifications (see the *Design Specifications* section above), the percent error between the force detected by the feedback system (experimental value) and the actual applied force (theoretical value) was calculated using Equation 6 above [65].

Establishing the discrepancy between the force displayed by the feedback system and the actual applied force via percent error determines if the injector accurately detects force and thus properly assists the operator throughout each injection. As a result, calculating the percent error between the feedback system and the applied force identified the efficacy of the feedback system throughout the intramyocardial MSC injection procedure and the system's ability to correctly determine when catheter obstruction is imminent or present. The feedback system's percent difference across the injector force range and thus its accuracy can be seen in Figure 18 below.

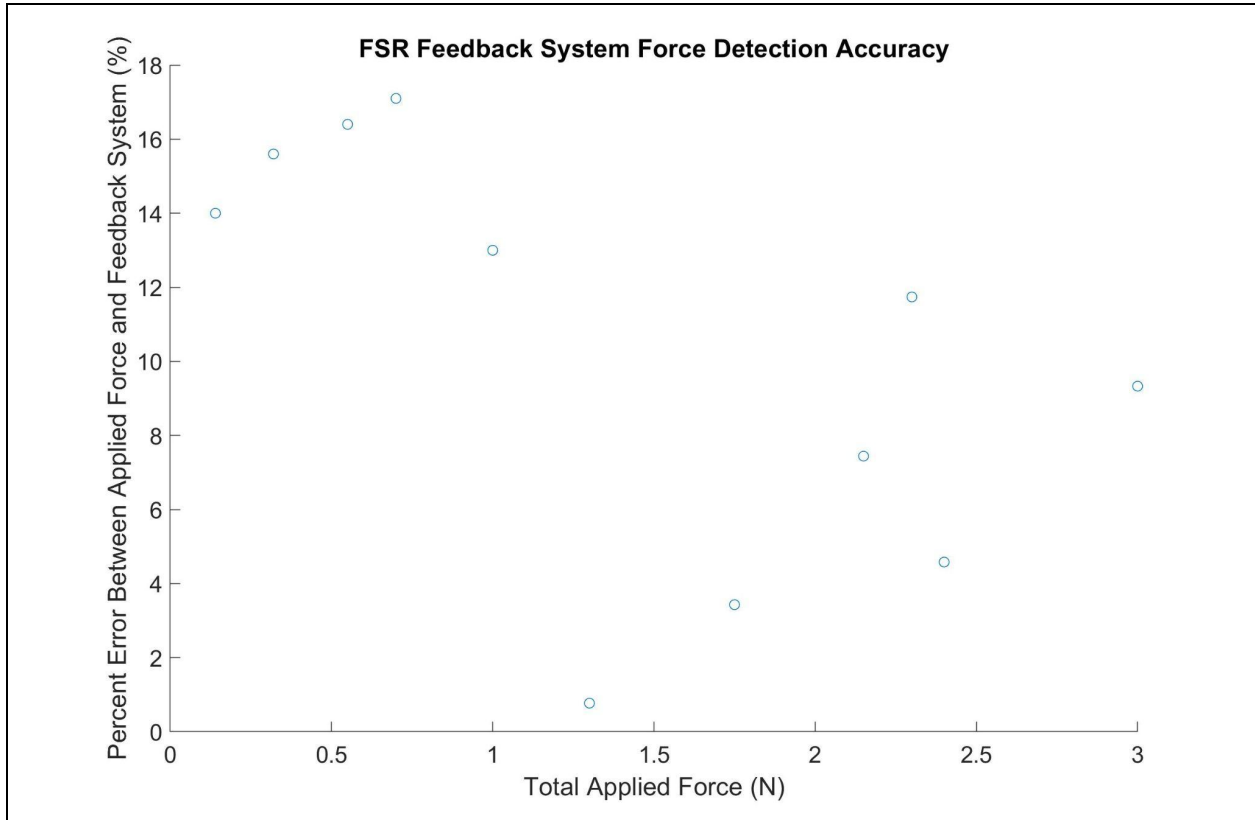


Figure 18: FSR-based feedback system’s force output error margin relative to their respective applied forces over the typical 0.14 N - 3.00 N [17] injector force range.

As seen in Figure 18 above, all output force values less than 1.00 N were accurate within an 18% error margin, averaging an error of  $15.78 \pm 1.33\%$ . All detected force values at or above 1.00 N displayed an average error of  $7.18 \pm 4.50\%$ . When combining all of the data, the average error was  $10.31 \pm 5.61\%$ . All force values output by the feedback system over the initial expected 0.14 N - 3.00 N injector force range met the Spring 2022 required 20% and 15% error margin, for values less than 1.00 N and greater than or equal to 1.00 N, respectively, demonstrating that the FSR incorporated injector was able to display force values throughout each procedure with relative accuracy. See the *Feedback System Force Detection Accuracy Testing* section above for the justification of having two error margins. Despite being within the required specifications from the Spring 2022 semester, these error margins are still high, especially in a clinical therapeutic injection setting, so the device does not contain the desired force detection efficacy (5% error margin) when utilizing the FSR force sensor (see the *Feedback System Force Detection Accuracy Testing* section above). Confirming the success of the injector at lower force values (0.14 N - 2.50 N) is pertinent as they represent the most common forces exhibited on the syringe plunger throughout each injection [14]. To account for this force dominance and establish the device’s accuracy over this range, a relatively large number of tests were performed on the lower force values (4 tests/N). The FSR feedback system contained an average error of  $10.40 \pm 5.90\%$  for force application values between 0.14 N and



2.50 N. While this is a seemingly low error percentage, it does not meet the required 5% error margin for the semester, so the feedback system is not as accurate as desired. This will ultimately limit the operator's ability to adequately determine the efficacy of each injection, reducing the success of the entire procedure when using the FSR-based feedback system.

While it is important to correctly detect the force applied to the injector throughout each injection, it is critical that the feedback system can establish when the 2.40 N threshold is reached and catheter obstruction or cell reflux is imminent. The feedback system needs to identify when this value is reached with a high degree of accuracy in order to motivate the operator to monitor the injection and stop it if catheter obstruction or cell backflow is present (determined by operator). If the injection continues while the catheter is obstructed, the cells will build-up in the catheter and the increasing pressure within the catheter will induce cell damage and lysing, drastically reducing the efficacy of the intramyocardial MSC injection procedure [70]. As seen in Figure 18 above, there is only a 4.58% difference between the feedback system and actual applied force when 2.40 N of force is delivered to the FSR sensor, confirming the accuracy associated with detecting catheter obstruction and cell reflux susceptibility. All force accuracy detection data can be found in Section 6.1 of the Appendix below.

#### FSG Force Detection Accuracy

To provide an injector capable of significantly increasing conversance about intramyocardial stem cell injections as well as the efficacy of the procedure, the error margin for the force detection system output compared to the actual applied force is much more stringent this semester, requiring 5% error (see *Design Specifications* section above). As a result of this requirement, the force detection system is utilizing an FSG sensor due to its high degree of sensitivity, resolution, and accuracy (see *FSG020WNPB Series Force Sensor* section above). To establish the force identification efficacy of the FSG sensor feedback system, Feedback System Force Detection Accuracy testing was performed as outlined in the *Feedback System Force Detection Accuracy Testing* section above and Section 5.2 of the Appendix. As the fifth-degree polynomial line of best fit equation from the system's calibration curve was utilized to calculate the force applied by the injector to the syringe plunger, the tests also verified the accuracy and reliability of the calibration curves. While the applied force did not reach 2.40 N during Spring 2022 semester testing, injections were only performed into air. To account for the increase in applied force when delivering the aliquot solution into tissue with varying stiffness, the typical expected injector force range for tissue injections was increased to 0.14 N - 5.00 N, with a maximum expected force of 10.00 N [17]. The 0.14 N - 5.00 N range was tested following the force detection testing protocol (see *Feedback System Force Detection Accuracy Testing* section above and in Section 5.2 of the Appendix) in order to ensure that all forces within this interval could be properly identified throughout each injection. To determine if the feedback system met the required error margin specifications (see the *Design Specifications* section above), the percent error between the force detected by the feedback system (experimental value) and the actual applied force (theoretical value) was calculated using Equation 6 above [65]. Establishing

the discrepancy between the force displayed by the feedback system and the actual applied force via percent error determines if the injector accurately detects force and thus properly assists the operator throughout each injection, increasing procedural success. The feedback system's percent difference across the injector force range and thus its efficacy can be seen in Figure 19 below.

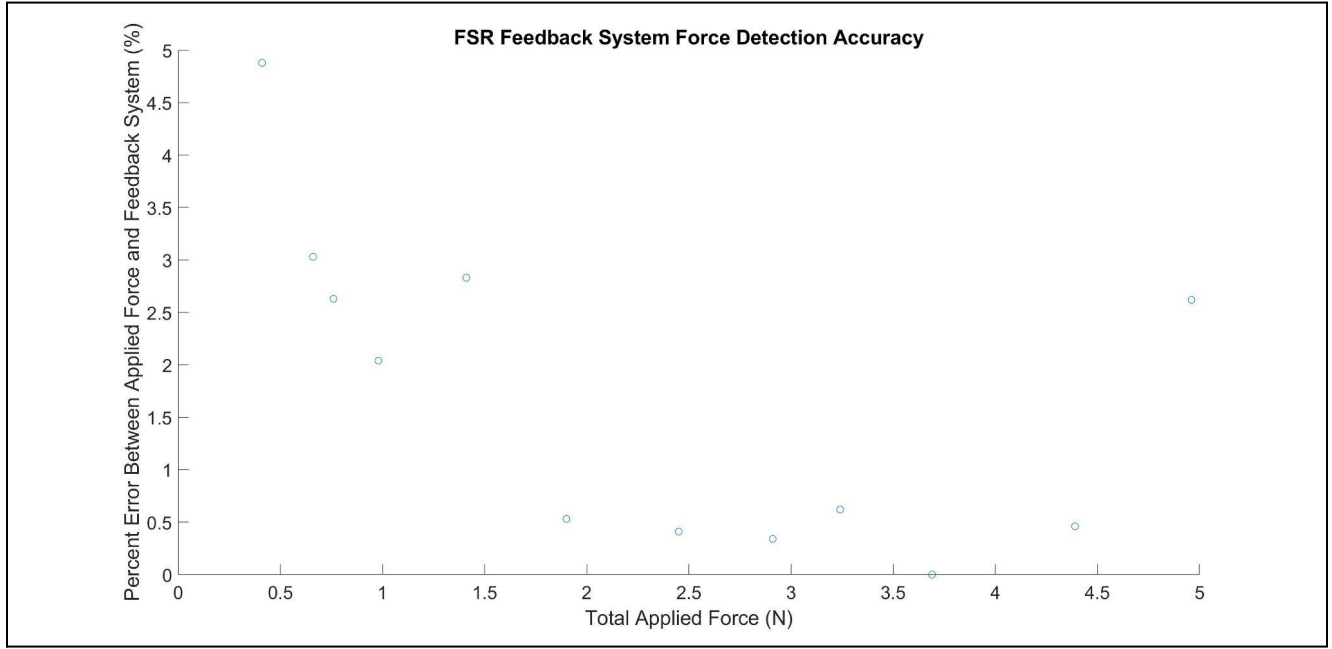


Figure 19: FSG-based feedback system's force output error margin relative to their respective applied forces over the typical 0.14 N - 5.00 N [17] injector force range.

As seen in Figure 19 above, all output force values were accurate within the required 5% error margin, averaging an error of  $1.70 \pm 1.52\%$ . The force values output by the feedback system over the expected 0.14 N - 5.00 N injector force range met the required error margin, demonstrating the FSG-based injector's ability to accurately display force values throughout each procedure and thus its high force detection efficacy. Confirming the success of the injector at lower force values (0.14 N - 2.50 N) is critical as they represent the most common forces exhibited on the syringe plunger throughout each injection [14]. To account for this force dominance and ensure that the device was very accurate over this range, a large number of tests were performed on the lower force values ( $\sim 3$  tests/N). The 5% error margin represents the proper force magnitude difference between the feedback system's output and the actual applied force to enable accurate and proper injection success identification for the high resolution clinical procedures (see the *Feedback System Force Detection Accuracy Testing* section above). The FSG feedback system contained an average error of  $2.34 \pm 1.55\%$  for force application values between 0.14 N and 2.50 N. As all of the percent errors are less than the 5% error margin, the feedback system is accurate, enabling the operator to adequately determine the efficacy of each injection. This demonstrates that the feedback system will properly assist each injection.

Detecting when the 2.40 N threshold is reached and catheter obstruction or cell reflux is imminent is a vital feature of the feedback system that promotes procedural efficacy. As a result, the device needs to identify when this value is reached with a high degree of accuracy in order to motivate the operator to monitor the injection and stop it if catheter obstruction or cell backflow is present (determined by operator). Properly establishing when the threshold value is reached or exceeded will increase the therapeutic impact of each injection and reduce clinical complications, as it will prevent cell damage and lysis as well as enable adequate operator intervention. As depicted in Figure 19 above, there is only a  $0.43 \pm 0.10\%$  difference between the feedback system and the actual applied force to the FSG sensor for values within the 2.40 N range (1.90 N - 2.91 N), confirming the accuracy associated with detecting catheter obstruction susceptibility. This minimal error generates confidence in the device and its ability to detect as soon as 2.40 N is reached or exceeded, alerting the operator that catheter obstruction or cell reflux is imminent. All FSG force accuracy detection data can be found in Section 6.2 of the Appendix below.

#### FSG vs FSR Force Accuracy Results

To confirm that the feedback system containing the FSG sensor was much more precise and accurate compared to the system with the FSR sensor, the percent error between each sensor's force output and the applied force was statistically compared. As the FSG sensor had an overall average error margin of only  $1.70 \pm 1.52\%$ , while the FSR sensor displayed an average error of  $10.31 \pm 5.61\%$ , the sensors are expected to display a difference in accuracy due to the large discrepancy in error margins. To determine if there is a statistically significant difference between the two sensors, a two-sample Student t-test was utilized to compare the force detection accuracy values as the two samples are independent of each other. If there is a statistically significant difference between the force detection data as determined via a two-sample Student t-test, the FSG sensor is more accurate than the FSR sensor and thus corresponds to a high efficacy injection device, as it contains the lowest average percent error between the two sensors and does not exceed the 5% error margin requirement (see *Design Specifications* section above). The force detection accuracy results for the FSR and FSG sensors can be seen in Figure 20 below. The rectangles represent the interquartile range and the whiskers display the full range of force identification error for each force application value and sensor modality (FSR and FSG).

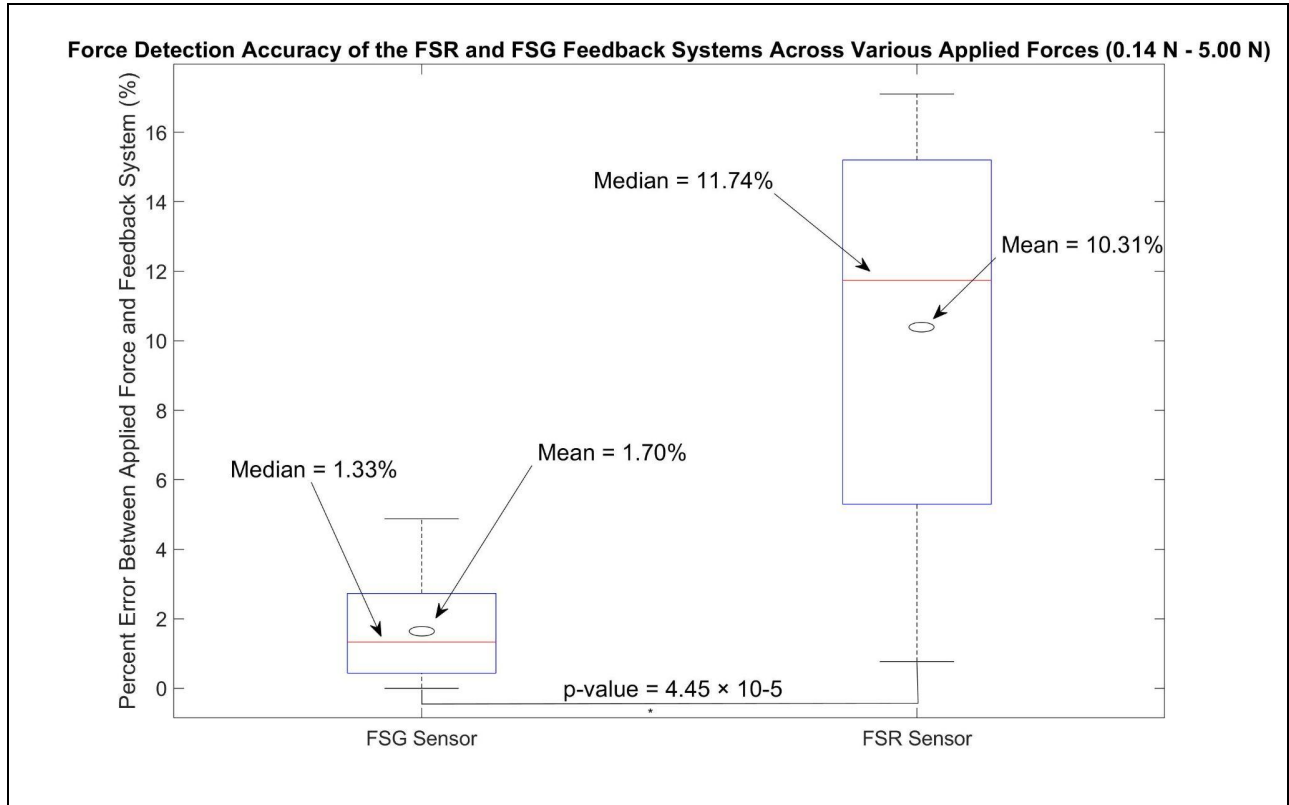


Figure 20: Boxplot comparing the percent error between applied forces and the output values for the FSR and FSG sensor feedback systems to each other. The rectangles represent the interquartile range, the whiskers display the full range of error, the red lines locate the median, and the circles identify the mean for each force application value and sensor modality (FSR and FSG).

As seen in Figure 20 above, the average error between the applied force and the feedback system's output was  $1.70 \pm 1.52\%$  for the FSG, while it was  $10.31 \pm 5.61\%$  for the FSR sensor. A two-sample Student t-test was performed on these percentages, yielding a p-value of  $\sim 4.45 \times 10^{-5}$ . Using a significance value of  $p = 0.05$ , it can be concluded that the  $10.31 \pm 5.61\%$  FSR error has a statistically significant difference relative to the FSG's  $1.70 \pm 1.52\%$  error. As a result, the two sensors have a discrepancy in their resolution and sensitivity, with the FSG sensor displaying the greatest accuracy and precision of the two (lowest error). This confirms that the FSG sensor produces the highest efficacy injection device compared to the FSR sensor, enabling proper and high resolution force detection throughout each injection. The operator will be able to identify the applied injection force with confidence, allowing catheter obstruction and cell reflux to be appropriately determined. The FSG-based system will thus generate effective clinical intramyocardial injection procedures. All of the calculations and statistical analyses can be found in Section 6.3 of the Appendix.

## FSR Feedback System Results

As outlined in the Feedback System Testing Protocol, this test compares the force output value outputted on the scoreboard display with the force printed by the serial monitor. The test also confirms that the LED light turns on when the force exceeds 2.4 N. In order to interpret the results, the average and standard deviation of the 15 force output values (from the three sets of five second samples where each measurement was taken one second apart) for both the display and serial monitor was calculated. This was repeated for each of the five aliquots of water. Next, the percent difference between the scoreboard display and the serial monitor was calculated using the formula in Equation 7 below [71].

$$[7] (|SM_{avg} - Display_{avg}| / (((SM_{avg} + Display_{avg})/2))) * 100 = \text{Percent Difference}$$

SM = Serial Monitor  
Display = Scoreboard

The results of the testing concluded that the FSR Feedback System is functioning accurately because there is less than 5% difference between the scoreboard display output and the serial monitor. The average percent difference between the two was 0.137% so this means that for the most part, the serial monitor and scoreboard display will be similar to each other. This result means that the surgeon can rely on the scoreboard display to accurately output the approximate force that is being applied on the syringe which corresponds to how much the cells are experiencing. In addition, the results confirmed that the LED light does turn on and stay on when the force exceeds 2.4 N. The raw data and explanation for how the mean, standard deviation and percent error were calculated can be found in Section 6.4 of the Appendix.

Table 2: Results for the difference between the readings on the scoreboard display and the serial monitor output.

	Scoreboard Display Average (N)	Serial Monitor Average (N)	Percent Difference (%)	Was the LED on?
Aliquot of water #1	0.213 ± 0.0140	0.213 ± 0.0145	0%	No
Aliquot of water #2	0.679 ± 0.00743	0.681 ± 0.00743	0.387%	No
Aliquot of water #3	1.21 ± 0.00737	1.21 ± 0.00862	0.166%	No
Aliquot of water #4	1.93 ± 0.00594	1.93 ± 0.00594	0.104%	No
Aliquot of water #5	2.48 ± 0.00676	2.48 ± 0.00704	0.0283%	Yes
Average Percent Difference: 0.137%				

### Syringe Clamp Connection and Locking Results

The Syringe Clamp Connection and Locking tests confirmed that the syringe was able to be easily swapped as well as lock and stay in place when force is applied. The force testing was passed because the syringe clamp was able to securely hold the syringe in place when any force above 5 N was applied. In addition, the average time for swapping the syringes with the syringe clamp was  $13.50 \pm 1.74$  seconds. This result is less than the 60 second maximum that is required for surgeons to be able to change the syringes during the course of the surgery. Even with the standard deviation, the time for swapping the syringes is much less than 60 seconds. Of note, despite the standard deviation demonstrating that the syringe exchange may take up to 15.24 seconds, for all five trials performed, the exchange time was never greater than 14.78 seconds, so the optimal 15 second dwell time was obtained for each procedure. The syringe clamp successfully provides an easily exchangeable mechanism that is sturdy enough to support well above the maximum amount of force that it may experience during the course of the procedure. All syringe clamp testing data can be found in Section 6.5 of the Appendix below.

## Injection Rate Results

The Injection Rate testing proved that the motor was set at an accurate setting for both the 30 second and 60 second injection rates and moved the appropriate distance to deliver 0.5 mL of solution. The average injection times for the 30 second and 60 second groups were recorded along with the distance the motor was able to “travel” during each injection. Although the motor itself does not move, the distance that the motor can displace an object via the rotation of the bolt is important since it will drive the force application block forward at a certain distance, compressing the syringe plunger over this distance as well. The plunger must travel 30.50 mm in order to deliver the full 0.5 mL solution. To establish the accuracy of the stepper motor, Equation 6 above was used to calculate the percent error between each injection time and their desired target time as well as the distance “traveled” by the motor relative to the required 30.5 mm distance. The results can also be seen in Table 3 below.

Table 3: Results of the Injection Rate Testing performed for the two rates (30 seconds and 60 seconds). Both the injection time and the distance traveled was evaluated.

		Mean	Standard Deviation	Percent Error (%)
30 Second Rate	Injection Time	30.32 seconds	$\pm 0.14$ seconds	1.067%
	Distance Traveled	30.48 mm	$\pm 0.23$ mm	0.06557%
60 Second Rate	Injection Time	60.80 seconds	$\pm 0.84$ seconds	1.333%
	Distance Traveled	30.49 mm	$\pm 0.15$ mm	0.03279%

As seen in Table 3 above, the 30 second injection rate had an average time of  $30.32 \pm 0.01$  seconds, representing a percent error of 1.067%. For this rate, the distance traveled was  $30.48 \pm 0.23$  mm, corresponding to a percent error of 0.06557%. For the 60 second rate sample, the mean speed measured was  $60.80 \pm 0.84$  seconds and the average distance traveled was  $30.49 \pm 0.15$ . The percent error for the injection duration and travel distance was 1.333% and 0.03279%, respectively. The raw data and explanation for how the mean, standard deviation and percent error were calculated can be found in Section 6.6 of the Appendix.

## Cell Viability Results

Cell viability testing using Trypan Blue staining was performed as outlined in the *Cell Viability Testing* section above to determine if cell viability was reduced by more than 5% following each injection of 0.5 mL of MSC aliquot solution relative to the initial viability

immediately after MSC thawing. The cell viability testing followed the standard procedure utilized by Dr. Raval during clinical trials [14], so the results from these tests confirm how well the injector will maintain MSC viability during intramyocardial MSC injection procedures and thus its ability to perform successful injections without reducing therapeutic potential. The cell viability results for 30 second and 60 second automatic and manual injections can be seen in Figure 21 below. The rectangles represent the interquartile range and the whiskers display the full range of MSC viability for each rate and injection modality (manual and automatic).

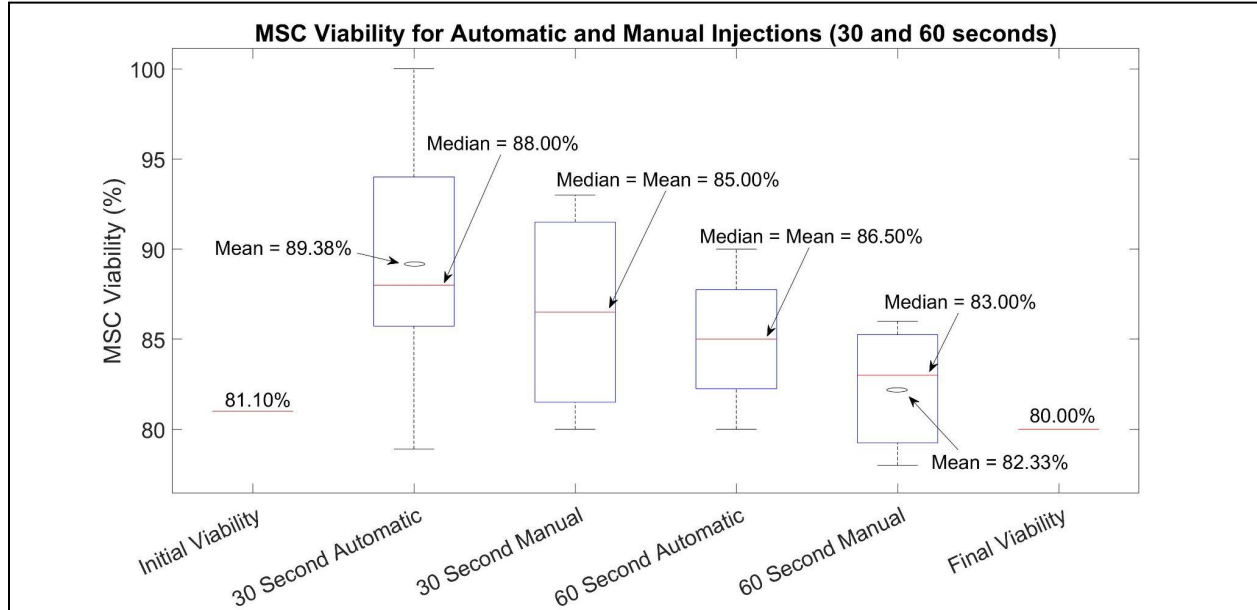


Figure 21: Boxplot comparing the viability of MSCs following automatic and manual 30 and 60 second injections to each other and to the starting and final MSC viability. The rectangles represent the interquartile range, the whiskers display the full range of MSC viability, the red lines locate the median, and the circles identify the mean (if it is not the same as the median) for each rate and injection modality (manual and automatic).

As seen in Figure 21 above, the initial MSC viability after thawing was 81.10% and the final viability at the conclusion of the testing was 80.00%. A Student paired t-test was performed on these viabilities, yielding a p-value of  $\sim 0.634$ . Using a significance value of  $p = 0.05$ , it can not be concluded that the 80.0% end viability has a statistically significant difference relative to the starting 81.10% viability. As a result, the cells did not experience any substantial death during the course of the testing due to sitting out in typical laboratory benchtop conditions, so the results collected throughout the experiment do not need to be normalized prior to comparison and all the data for each injection rate and delivery modality can be statistically analyzed. For the automatic injections, the average cell viability was  $89.38 \pm 7.64\%$  and  $85 \pm 3.81\%$  for the 30 second and 60 second injection rates respectively. Out of these two groups, the 30 second injection rate had the lowest cell viability value for all five trials, 78.90%, which is not a 5% reduction in cell viability relative to the initial 81.10% starting viability. This confirms that the



automatic injections do not reduce cell viability by greater than 5% during each MSC delivery and thus the injections meet the MSC viability design specifications.

After confirming the efficacy of each automatic injection in terms of cell viability, the automatic injections were compared to the 30 second and 60 second manual injections in order to determine how the automatic MSC delivery compares to current manual procedures. The average cell viability for the 30 second manual injections was  $86.50 \pm 6.02\%$  while the average viability was  $82.33 \pm 4.04\%$  for the 60 second manual injections group. To compare the four groups, an ANOVA was performed with each injection rate and delivery modality corresponding to a separate group. The ANOVA p-value was 0.41, verifying that there is not a statistically significant difference between the four groups when comparing their MSC viabilities following each injection (significance value of 0.05). Student paired t-tests were also performed on all groups, further establishing that MSC viability is not significantly different between any pair of injection groups (see Section 6.7 of the Appendix for these additional comparisons). This confirms that the automatic injections are able to maintain the cell viability seen in typical intramyocardial MSC injection procedures, demonstrating that the automatic injections can be implemented clinically without reducing the therapeutic potential of each injection. All of the cell viability data, calculations, and statistical analyses can be found in Section 6.7 of the Appendix.

Rapid injections were also performed during the cell viability testing, with an average injection rate of  $0.748 \pm 0.400$  seconds and an average MSC viability of  $86.25 \pm 6.65\%$  following each injection. Similar to the 30 and 60 second injections, an ANOVA was performed to compare the cell viability between the 30 second, 60 second, and rapid injections with each injection rate and delivery modality (automatic and manual) corresponding to separate groups. Interestingly, while one of the rapid injection trials had the lowest cell viability relative to all other groups and trials (77.0%), this viability still did not exceed a 5% reduction in cell viability relative to the initial 81.10% that is not acceptable based on the design specifications. Consequently, the ANOVA p-value was 0.59, demonstrating that there is not a statistically significant difference between the five groups when comparing their MSC viabilities following each injection (significance value of 0.05). Student paired t-tests were performed on all groups, confirming that MSC viability is not significantly different between any pair of injection groups, including the rapid injection group. The data and analysis related to the rapid injection cell viability is in Section 6.7 of the Appendix. The implications of these results are described in the *Discussion of Results* section below.

Throughout the MSC viability testing, the force value range for the 30 second and 60 second injections and both manual and automatic delivery mechanisms were collected. The variation across each set of maximum and minimum force values that were consistently cycled between during each injection was calculated in order to determine the force application consistency across each injection and thus the stability of the cell flow rate through the catheter system and into the myocardium. The more consistent the slow flow rate at the desired 30 and 60 second injection rates compared to inconsistent rates containing rapid injection intervals during

the 30 and 60 seconds, the greater the cell retention at the localized site of interest within the myocardium and thus the greater the therapeutic impact [72]. Only the values that were part of the constant cycling of force experienced throughout each procedure are included in this analysis without taking into account the peak force experienced at the end of each injection, as this force is a result of the syringe plunger experiencing applied pressure directly after being fully compressed. Thus, the 0.5 mL of solution was delivered prior to the peak force being applied, so this force does not correlate to injecting any MSCs and is excluded from analysis. The average maximum and minimum force values that were consistently cycled between throughout each injection can be seen in Table 4 below.

Table 4: 30 second and 60 second injection maximum and minimum force values, including their variation, for both automatic and manual injections.

Injection Type	Average Minimum Force (N)	Average Maximum Force (N)	Variance Across Maximum and Minimum Values (N)
30 Second Automatic	0.194	0.264	$\pm 0.00528$
30 Second Manual	0.438	0.475	$\pm 0.0310$
60 Second Automatic	0.230	0.260	$\pm 0.00435$
60 Second Manual	0.333	0.493	$\pm 0.00573$

The variance across the maximum and minimum values (within the consistent cycle of values seen during the injection without including the peak force experienced at the end of each injection) for each 30 second automatic and manual injection as well as each 60 second automatic and manual injection was  $\pm 0.00528$  N,  $\pm 0.0310$  N,  $\pm 0.00435$  N, and  $\pm 0.00573$  N, respectively. This demonstrates that the variance across the manual injections is the highest relative to their respective automatic injection rates as well as that the manual injections have the two highest variances overall. As a result, the automatic injections have a greater force and MSC flow rate consistency throughout their injections relative to their respective manual injections. The p-value between the two 30 second injection groups (automatic and manual) from a Student paired t-test is 0.0193. With a significance level of 0.05, the variance between these two rates is significantly different, further supporting the greater force and thus MSC flow rate consistency within the 30 second automatic injections relative to the 30 second manual injections. This increased MSC delivery rate stability provided by the automatic injections compared to the manual injections will enable greater cell retention at the site of interest within the myocardium, which could improve the therapeutic potential of each injection. All of the cell viability force data, calculations, and statistical analyses can be found in Section 6.7 of the Appendix.

## Overall Device Results

### 25 Gauge Injection Results

Upon final assembly of the device, testing was completed to ensure the device was functioning properly and meeting the design criteria. The system was set up as if it were going to be used in a procedure except for a 2.22 cm 25 gauge needle was used to mimic the medical grade tubing-catheter system. This needle was selected as it has a similar radius relative to the procedural catheter system and thus generates forces that correspond to the values experienced when utilizing the clinical catheter system. The 25 gauge needle was used for the first round of testing to check for volume injection levels because all of the fluid immediately comes out of the needle with the exception of minimal fluid left within the dead space. The device was able to inject approximately 0.5 mL of solution in the allotted 30 or 60 second intervals with an average error of less than 5%. The volume injection values did display some variation from the desired 0.5 mL solution amount because there is dead space present in the distal tip of the syringe and in the needle. There is inherent dead space at the distal tip of every syringe and within each needle that can not be avoided, even during manual injections. As a result, the volume delivered will be reduced and the entire 0.5 mL of solution will not be delivered during each injection. The expected injected volume was approximately 0.5 mL, but due to the dead space, not all of the fluid was accounted for after each injection. To account for the dead space, the delivery volume needs to be within 5% of 0.5 mL, corresponding to a maximum dead space of ~0.025 mL throughout the entire syringe-needle system. The mean of the injected volume was established and then a percent error was calculated between the injector's delivery volume and the desired 0.5 mL injection amount, establishing the accuracy of each injection. The force that was applied by the system to inject the fluid did not exceed 2.40 N, demonstrating that there was not any backup or obstruction experienced during the tests. The injection time, injection volume, and force ranges, as well as the serial plotter were measured and can be seen in Table 5 below and Section 6.8 of the Appendix respectively. A box plot displaying the percentage difference between the injection times and delivery volumes to their respective target values can also be seen in Section 6.8 of the Appendix.

Table 5: Results of the Overall Device Testing performed for the two rates (30 seconds and 60 seconds) with a 2.22 cm, 25 gauge needle. The injection times, volumes, and force ranges were evaluated.

		Mean	Standard Deviation	Percent Error (%)
30 Second Rate	Injection Time (seconds)	30.6	$\pm 0.121$ seconds	$1.88 \pm 0.410$
	Volume Injected (mL)	0.486	$\pm 0.0134$	$3.60 \pm 1.67$
	Force Range (N)	0.164 - 0.498	-	-
60 Second Rate	Injection Time (seconds)	60.2	$\pm 0.150$ seconds	$0.260 \pm 0.250$
	Volume Injected (mL)	0.480	0	4.00
	Force Range (N)	0.156 - 0.462	-	-

### Clinical Simulation Results

The assembled device was then tested while connected to the catheter and connection tubing system to simulate the clinical use of the device. The same tests were performed as with the 25 gauge needle except the ejected volume was not collected because there would be an inaccurate amount due to bubbles in the tubing systems and dead space. Simply verifying if all of the solution was out of the syringes was all that was done to ensure enough of the fluid was injected. These tests were done to ensure that the force values when the syringe was connected to the rest of the system were still within range, that the device was able to exert enough force to push the fluid through the thin connection tubing and catheter system, and that the times for the ejections were still accurate. The results confirmed that there was less than 5% error with the ejection times and that the force range was still well under 2.4 N indicating that there was no catheter backup. The 30 and 60 second serial plotter results with the force values over time can be seen in Section 6.9 of the Appendix. It should be noted that although the serial plot was taken for each trial, the exact force values cannot be interpreted for them so the force value ranges in the Table 6 below were obtained by looking at the display. This is because the serial monitor and serial printer can not be on at the same time.

Table 6: Results of the Overall Device Testing performed for the two injection rates (30 seconds and 60 seconds) with the connection tubing and catheter system utilized during clinical trials.

The injection times, volumes, and force ranges were evaluated.

		Mean	Standard Deviation	Percent Error (%)	Was the syringe empty at the end of the injection?
30 Second Speed	Injection Time	30.6 seconds	$\pm 0.176$ seconds	$2.04 \pm 0.58$	Yes, for all trials
	Reverse Time	23.6 seconds	$\pm 0.359$ seconds	-	
	Force Range	$(0.236 \pm 0.049) - (0.484 \pm 0.043)$ N		-	
60 Second Speed	Injection Time	60.3 seconds	$\pm 0.187$ seconds	$0.55 \pm 0.31$	Yes, for all trials
	Reverse Time	24.5 seconds	$\pm 0.224$ seconds	-	
	Force Range	$(0.168 \pm 0.038) - (0.448 \pm 0.040)$ N		-	

### Catheter Backup Results

Following the Catheter Backup Testing Protocol discussed in the *Catheter Backup Testing* section above and outlined in Section 5.7 of the Appendix, the force values corresponding to the onset of catheter obstruction were tested to confirm the accuracy of the 2.40 N catheter backup literature value. However, during the Spring 2022 semester, the 30 second and 60 second injection rates were both only tested once with a catheter obstruction indicator force value of 1.51 N and 1.81 N respectively. Only one trial was performed for each rate as it was determined that the force value associated with catheter back-up for each rate during the Spring 2022 set-up was not characteristic of catheter obstruction forces, as the aliquot solution was still able to leak through the finger block at the distal tip of the catheter, flowing into the petri dish. The catheter was not completely occluded, preventing a proper detection of catheter obstruction. As a result, the catheter obstruction protocol was updated to incorporate a kink within the middle of the catheter that fully blocked flow (see the *Catheter Backup Testing* section above and Section 5.7 of the Appendix). Additional testing was performed this semester, following the new protocol, to provide more accurate catheter obstruction values and thus enable proper determination of the accuracy associated with the 2.40 N catheter blockage literature value. The peak force experienced during the testing correlates to the threshold value indicative of catheter obstruction as it resembles the force reached as soon as the aliquot solution contacts the occluded catheter, coinciding with blockage. When the build-up was reached, the syringe was removed immediately to prevent any damage to the injector, validating that the peak force displayed prior

to syringe removal represents catheter blockage. The catheter obstruction force values can be seen in Figure 22 below.

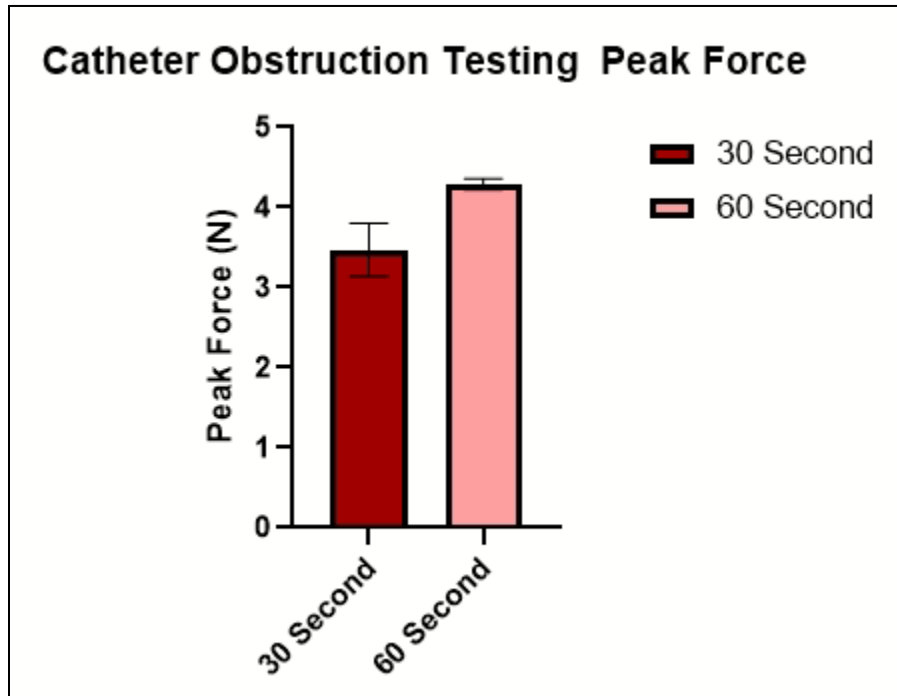


Figure 22: Bar graph depicting the threshold forces that correspond to catheter obstruction for both the 30 second and 60 second injection rates (n = 3).

As illustrated in Figure 22 above, the average peak threshold force indicative of catheter obstruction for the 30 and 60 second injection rates is  $3.47 \pm 0.33$  N and  $4.29 \pm 0.07$  N, respectively. A two-sample Student t-test was used to compare the force values for the two injection rates, generating a p-value of 0.013. Using a significance value of  $p = 0.05$ , the 30 and 60 second injection rates have a statistically significant difference when comparing their catheter obstruction values. As a result, the catheter obstruction forces for the 30 second and 60 second injections are different, demonstrating that the applied force characteristic of occlusion will vary based on the injection rate utilized. While the  $3.47 \pm 0.33$  N and  $4.29 \pm 0.07$  N threshold values for 30 and 60 second injections, respectively, are larger than the 2.40 N literature value and thus do not align with the theoretical threshold, these values were produced using the set-up implemented during clinical intramyocardial injection procedures. This generates confidence that the experimental values are correct and the literature value (2.40 N) is not accurate for intramyocardial MSC injections and the syringe-medical grade tubing-catheter set-up it consists of. The catheter obstruction value will thus need to be adjusted accordingly within the feedback system to properly alert the operator when occlusion is immediate.

The  $3.47 \pm 0.33$  N and  $4.29 \pm 0.07$  N threshold values for 30 and 60 second injections, respectively, are still lower than injections into myocardium tissue, as seen with the peak forces displayed during *ex vivo* cervine heart testing (see Figure 26 below). The peak force for the 30

second injection was  $\sim 9.01$  N, while it was  $\sim 4.69$  N for the 60 second injection. As the catheter obstruction testing was performed by delivering water into the air (dripping into a petri dish), the threshold values correspond to obstruction when injecting into the air. These values are lower than the forces that will be experienced during a typical clinical MSC injection into the myocardium. The 8 - 15 kPa healthy myocardium stiffness as well as  $100 \text{ kPa} \pm 2.91$  myocardium Young's Modulus value associated with an individual who experienced a myocardial infarction [73 ,66 ] will increase the force required to inject the MSCs into cardiac tissue relative to the current testing that was performed with the medical grading tubing-catheter system delivering the solution into a petri dish. This will correlate to a higher force value indicating the onset of catheter obstruction during clinical procedures compared to the blockage force values picked up during testing. As a result, the force values identified during the catheter backup testing do not correlate to the catheter obstruction force values that will be picked up during a clinical intramyocardial MSC injection procedure, preventing these tests from providing information that correctly identifies catheter obstruction susceptibility. All of the obstruction force value data, calculations, and statistical analyses can be found in Section 6.10 of the Appendix.

## Bovine Steak Injection Results

The steak testing was performed using a round cut steak at different levels of doneness. Details regarding the testing can be found in the *Bovine Steak Injection Testing* section. The steak was cooked to be well done, medium well, medium or left raw. Mechanical testing was performed on the steak to determine the mechanical properties of the steak at the varying doneness levels. Mechanical testing was performed to determine if the stiffness of the injection material alters the amount of injection force required for a solution. Compression testing was performed on the steak using the MTS Insight - Model 5kN in the Teaching Lab of ECB [74] and it was found that the well done steak had the highest Young's Modulus with a value of 666.77 kPa. This was followed by the next highest Young's Modulus value for medium well at 634.04 kPa, then medium at 428.26 kPa, and lastly raw at 284.37 kPa (see Figure 23 for the Stress vs Strain curves). These values are higher relative to those found in literature which are between 70 kPa and 260 kPa ranging from raw to cooked bovine steak [67].

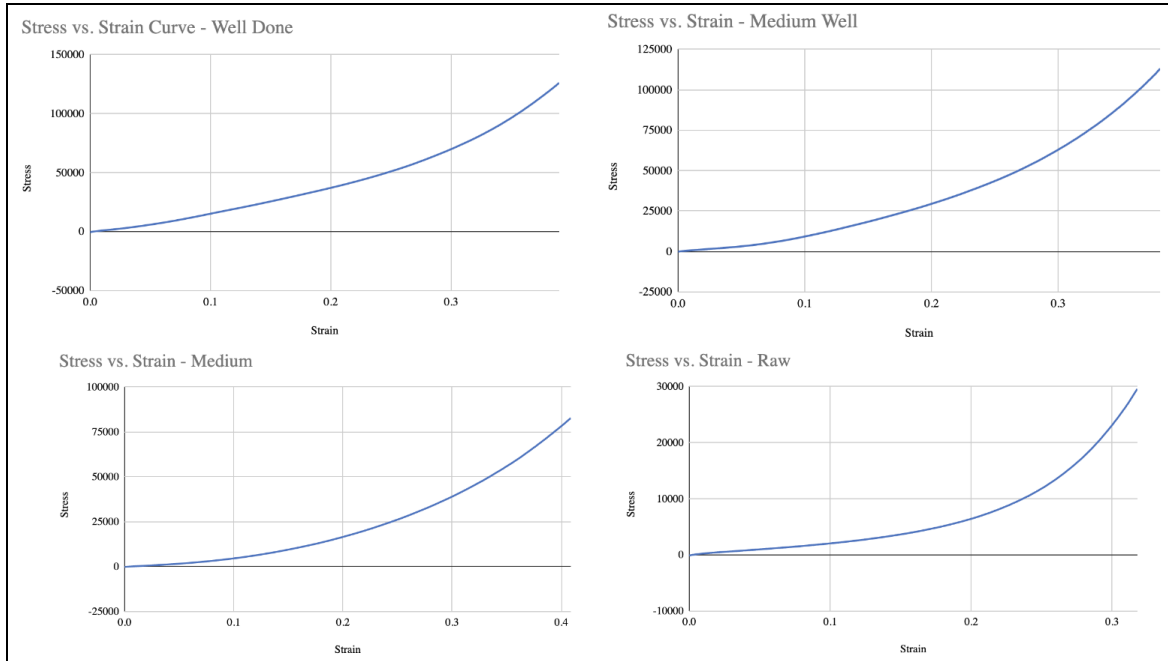


Figure 23: Stress vs. Strain Curves for four levels of steak doneness (well done, medium well, medium and raw).

After verifying that the Young's Modulus values increased as the steak was cooked more, injection testing was performed to determine the approximate forces that are required to inject a solution into the steak. It was hypothesized that the injection forces would increase with increasing steak doneness because the material was tougher. However, the force values did not correspond with the mechanical testing, because as the Young's Modulus increased, the peak force did not always increase. The results for the steak testing include the typical force ranges (upper and lower boundaries), peak force, and injection rate and can be seen in Table 7. Values for the individual trials can be found in Appendix Section 6.11.



Table 7: Final Results for the Bovine Steak Injection Testing including averages for the force range (lower and upper boundaries), peak force and injection rate.

	Steak Doneness	Lower Boundary of Force Range (N)	Upper Boundary of Force Range (N)	Peak Force (N)	Rate (s)
30 Seconds	Well Done	1.27 ± 0.058	1.63 ± 0.058	1.95 ± 0.0379	30.91 ± 0.0173
	Medium Well	1.40 ± 0.100	2.03 ± 0.153	2.26 ± 0.203	30.70 ± 0.205
	Medium	1.13 ± 0.115	2.20 ± 0.173	2.51 ± 0.0493	30.65 ± 0.293
	Raw	1.13 ± 0.0265	1.50 ± 0.100	1.69 ± 0.0265	30.64 ± 0.267
60 Seconds	Well Done	1.01 ± 0.161	1.39 ± 0.193	1.58 ± 0.233	60.52 ± 0.253
	Medium Well	1.37 ± 0.115	1.70 ± 0.100	2.02 ± 0.0404	60.57 ± 0.0458
	Medium	1.20 ± 0.346	2.03 ± 0.252	2.42 ± 0.0961	60.58 ± 0.124
	Raw	1.03 ± 0.230	1.28 ± 0.107	1.36 ± 0.125	60.40 ± 0.228

The graphs for the peak force values for the steak types at 30 and 60 seconds can be seen in Figures 24 and 25. In these figures, it is clear that the results were not consistent with what was expected because the peak force when injecting into the medium steak was the highest rather than the well done steak which had the highest mechanical properties.

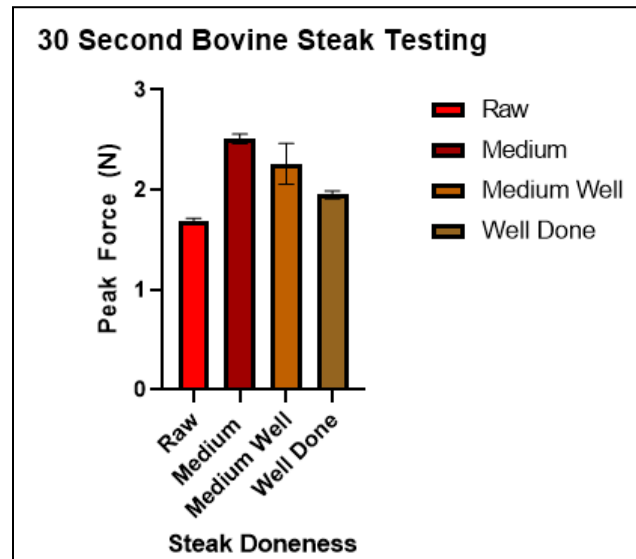


Figure 24: Bovine Steak Testing Results for the peak force during 30 second injections of water into steaks with various doneness levels.

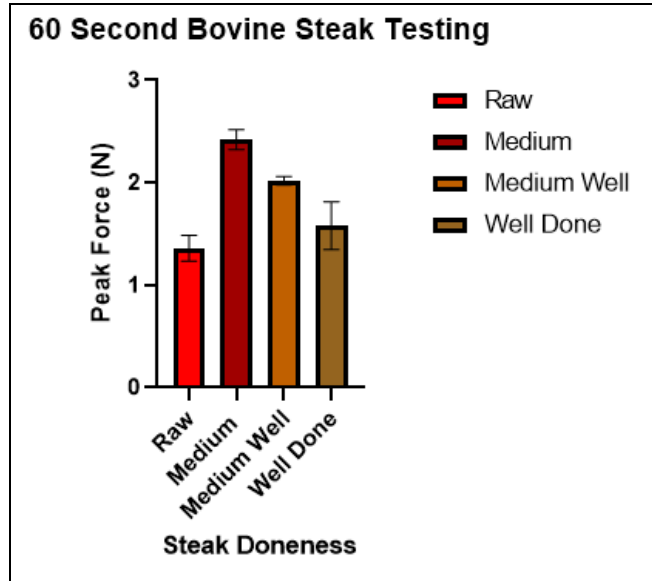


Figure 25: Bovine Steak Testing Results for the peak force during 60 second injections of water into steaks with various doneness levels.

Ultimately, the results were generally inconclusive due to the fact that there was no trend in the data. The inconclusive results were likely due to increasing amounts of resistance or obstruction in the catheter during testing because the raw steak trials were done first followed by the well done, medium well and the medium steaks. Further explanation of the results can be found in the *Discussion* Section of the report.

### Deer Heart Injection Results

The deer heart testing was performed to obtain data on how much force is required to inject solution into the myocardium. An overview of the procedure can be found in the *Deer Heart Injection Testing* section. The results were obtained by looking at the force values throughout the course of the procedure and then averaging the values from the three trials for both the 30 second and 60 second injection rates as well as performing a standard deviation calculation. Tables 8 and 9 depict the results for the deer heart testing including the typical force ranges (upper and lower boundaries), and peak force. A visual depiction of the data can also be seen in Figure 26.

Table 8: 60 second Deer Heart Myocardium Injection Testing Results with the Force Range (lower and upper boundaries), and peak force.

	Lower Boundary of Force Range (N)	Upper Boundary of Force Range (N)	Peak Force (N)
Trial 1	3.5	4.5	4.53
Trial 2	3.6	4.6	4.8
Trial 3	3.5	4.6	4.74
Average $\pm$ Standard Deviation	$3.53 \pm 0.0577$	$4.57 \pm 0.0577$	$4.69 \pm 0.142$

Table 9: 30 second Deer Heart Myocardium Injection Testing Results with the Force Range (lower and upper boundaries), and peak force.

	Lower Boundary of Force Range (N)	Upper Boundary of Force Range (N)	Peak Force (N)
Trial 1	5.60	6.50	7.68
Trial 2	4.50	8.00	11.10
Trial 3	4.70	6.50	8.26
Average $\pm$ Standard Deviation	$4.93 \pm 0.586$	$7.00 \pm 0.866$	$9.013 \pm 1.83$

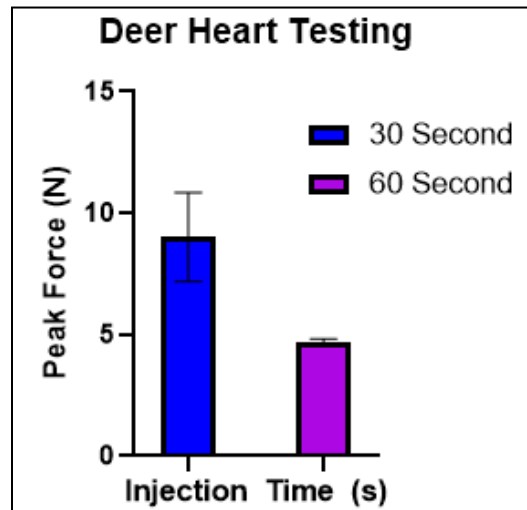


Figure 26: Deer Heart Myocardium Injection Testing Results for the peak force (N) at the 60 and 30 second injection rates.

Given the above data from the deer heart testing, it can be reasonably concluded that it takes significantly more force to inject into the myocardium with a 30 second rate than the 60 second rate. An unpaired t-test was performed and a p-value of 0.0151 was found. Due to the fact that  $p < 0.05$ , this indicates a significant difference in the amount of force required to inject cells into the myocardium at varying injection rates. These results only confirm that it requires more force to inject at a faster injection rate, but it cannot be concluded whether these higher force values at higher injection rates correspond with lower cell viability compared to the lower injection rate. Therefore, further testing should be performed to determine whether these significantly different injection force values will alter cell viability.

Lastly, it should be noted that force values above 5 N may not have less than 5% error associated with the readings because the calibration curve only included values up to 5N. The FSG calibration was fairly linear, however, so it can be reasonably assumed that the values are accurate, but further confirmation should be performed in the future (see the *Future Work* section for more information).

## Viscosity Testing Results

The viscosity testing was performed in order to determine the relative difference in force that is required to inject a solution. This testing could correspond with the force cells would experience at different concentrations as the viscosity levels vary. Both oil and water were tested. Water has a known viscosity of 1.0016 mPa\*s at 20 degrees C [75] and the oil that was used had a viscosity of 46.2 mPa\*s [69]. The results were obtained by looking at the force values throughout the course of the procedure followed by averaging the values from a set of three trials. Both 30 and 60 second injection rates to test water and only 60 second injection rate testing was performed with oil. Although 30 second trials with the oil were conducted, ultimately the results were found to be inconclusive due to increasing obstruction in the syringe / needle system over time and the injector device not being able to eject all of the oil. Lastly] standard deviation calculations were performed to determine the amount of variability in the results. The final results for the testing can be seen in Table 10 and Figures 27 and 28 below. Values for the individual trials can be found in Appendix Section 6.12.

Table 10: Final Results for the Viscosity Testing including averages for the force range (lower and upper boundaries) and peak force for water at 30 and 60 second injection rates and oil at a 60 second injection rate.

	Lower Boundary of Force Range (N)	Upper Boundary of Force Range (N)	Peak Force (N)
30 Seconds - Water	$0.803 \pm 0.17$	$1.23 \pm 0.49$	$1.44 \pm 0.54$
60 Seconds - Water	$0.65 \pm 0.13$	$0.917 \pm 0.104$	$1.12 \pm 0.077$
60 Seconds - Oil	$1.46 \pm 0.048$	$1.78 \pm 0.076$	$2.03 \pm 0.045$

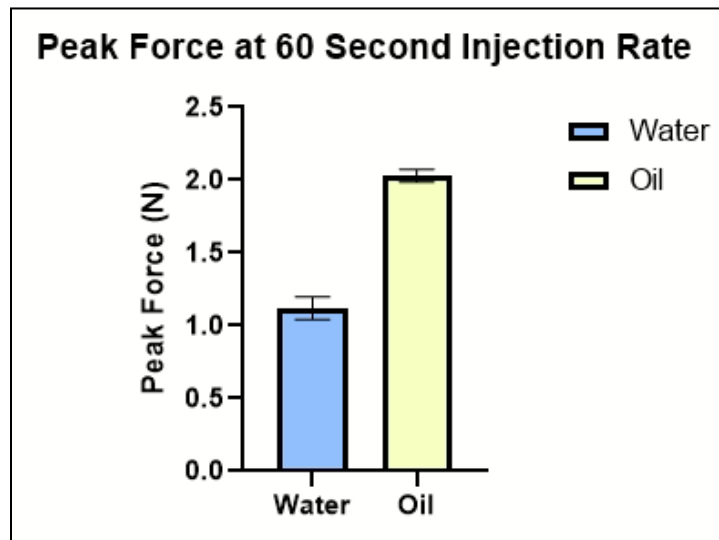


Figure 27: Viscosity Injection Testing Results for water compared to oil peak forces (N) at the 60 second injection rate.

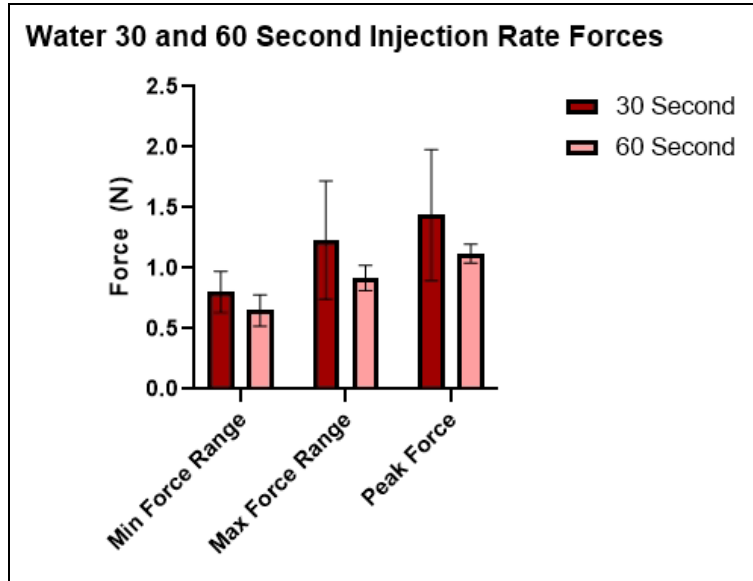


Figure 28: Viscosity Injection Testing Results for water compared to oil peak forces (N) at the 60 second injection rate.

Based on these results in Figure 27, it can be concluded that higher viscosities require more force to inject. The results comparing oil and water specifically show that solutions that are more viscous reach a higher peak force during injections. Thus, higher concentrations of cells (a higher viscosity solution), will require more force to inject the solution into the myocardium. Additionally, the testing results depicted in Figure 28 further proved that injecting the cells at a higher injection rate will also require more force. This implies that the cells will likely experience more force at higher injection rates as well. Further discussion of results can be found in the *Discussion* Section and future viscosity testing can be found in *Future Work*.

### Pressure Sensing Catheter Results

Utilizing the injector as a research tool in the realm of academia and industry was one of the main focuses of the semester. Currently, the correlation between the force applied to the syringe plunger and the pressure experienced by the aliquot solution being injected in a typical clinical injection procedure is not known [6]. As a result, the pressure sensing catheter testing was performed (outlined in the *Pressure Sensing Catheter Testing* section above) to establish the relationship between the applied injector force (to the syringe plunger) and the pressure received by the injectate. During testing, the applied force rose continuously throughout each injection, while the pressure experienced by the aliquot solution reached a plateau and stayed at that value for the remainder of the injection. This behavior thus prevented a proper correlation to be made between the applied syringe plunger force and the internal solution pressure throughout the injection that can be displayed on the visual feedback display, as a changing force value does not relate to a constant pressure value via a mathematical equation. However, there was consistency between the onset of peak pressure and the applied force value it correlated to. The peak pressure

and its corresponding applied force value (displayed right at the onset of peak pressure) can be seen in Table 11 below.

Table 11: Average force value that corresponds to the onset of peak pressure for the 30 second and 60 second injection rates (n = 2).

Injection Rate	Average Force Value (N)	Standard Deviation (N)	Onset Peak Pressure (mmHg)
30 Second	2.21	± 0.01	429
60 Second	2.22	± 0.06	429

As displayed in Table 11 above, the average force value that corresponds to reaching the 429 mmHg peak pressure during a typical injection is  $2.21 \pm 0.01$  N and  $2.22 \pm 0.06$  N for the 30 and 60 second injection rates, respectively. A Student paired t-test was performed on these peak force values, yielding a p-value of ~0.87. Using a significance value of  $p = 0.05$ , it can not be concluded that the 30 second peak pressure indicator forces have a statistically significant difference relative to the 60 second peak pressure identification force values. As a result, the average force values corresponding to the onset of peak pressure for either injection rate can be utilized to determine when peak pressure is reached. This will enable the operator to understand when the peak pressure is reached for injections into air and thus determine the success of each injection. See the *Pressure Sensing Catheter Testing* section below for further discussion about the implications this force-peak pressure correlation has, especially in relation to injection efficacy. All of the pressure sensor data, calculations, and statistical analyses can be found in Section 6.13 of the Appendix.

## Discussion

### Discussion of Results

#### Feedback System Force Detection Accuracy Testing

FSG Force Detection Accuracy Testing was performed in order to establish the force identification efficacy of the feedback system using a line of best fit equation from the calibration curve that was developed. This testing confirmed that all output force values over the typical injector force range were accurate within the required 20% error margin in accordance with the design specifications. The error associated with the FSG sensor was determined to be  $1.70 \pm 1.52\%$  for all force values which is greatly improved from the error seen last semester with the FSR sensor. Last semester with the FSR the output force values less than 1.00 N had an error of  $15.78 \pm 1.33\%$  and all force values above 1.00 N had an average error of  $7.18 \pm 4.50\%$ . The lower error margin of the new FSG sensor provides an improved estimate of the forces experienced by the MSCs and thus increases the effectiveness of the procedure. Meeting this

client requirement to provide an accurate force detection system is important because the device will be used by surgeons to see approximately how much force they are applying to the cells. The feedback system will also identify the type of tissue the MSCs are being injected into as healthy heart tissue requires a different applied force range than diseased tissue. Having an accurate force detection system is therefore going to provide the surgeon with feedback on the efficacy of the injections and indicate potential concerns associated with the procedure. This feedback system is also a method that is not present in injection devices on the market, displaying its novelty and the groundbreaking impact the injector can have on intramyocardial MSC injections.

### FSR Feedback System Testing

Last semester FSR Feedback System Testing was performed in order to compare the force output value displayed with the force printed by the serial monitor along with LED illumination when 2.4 N is exceeded. The results from this test successfully validated that the LED turned on when the FSR received at least 2.40 N of force and that the FSR Feedback System is functioning accurately due to the less than 5% difference between the scoreboard display output and the serial monitor with a 0.14% difference on average. These results are important because they show that the feedback system is thus able to accurately receive and display the force throughout each injection and alert the user when catheter obstruction is imminent, helping the operator to perform successful injections.

### Syringe Clamp Connection and Locking Testing

Syringe Clamp Connection and Locking tests were also performed last semester to confirm that the syringe was able to be easily swapped as well as lock and stay in place when force is applied. In compliance with design specifications, the results from this testing validated that the syringe clamp is stable enough to support well above the maximum amount of force that it may experience during the course of the procedure. This is important because the syringe must stay in place throughout the course of the injections while also being easily swappable so that the surgeon can deliver the cells in a timely manner. Injection Rate testing was performed to ensure that the device is capable of providing the 30 second and 60 second injection rates requested by the client and also moved the appropriate distance to deliver 0.5 mL of solution. The 30 second injection rate resulted in a percent error of 1.08% for the injection rate timing and a 0.0721% error for distance traveled. The 60 second injection rate resulted in a percent error of 1.33% for the injection rate timing and a 0.0328% error for distance traveled. These percent errors are well within the desired 15% error margin. These results exemplify the accuracy of the injection device in accordance with design specifications. This is important because one of the main goals of the project was to be able to accurately deliver cells in a controlled manner at the two specified rates that the client uses in clinical trials. Although the best rate for this therapy has not been determined, the 30 and 60 second rates have been proven to work well with this therapy so it was important to be able to inject the cells at these rates.



## Cell Viability Testing

Following assembly of the entire injector, MSC viability testing using Trypan Blue staining was performed to determine if cell viability was reduced by more than 5% following 30 second, 60 second, and rapid manual injection. This verified that each automatic injection rate kept MSC viability within 5% of initial cell survival, in congruence with typical intramyocardial injections. This confirms that the automatic device did not have a lower cell viability than the manual injections and thus does not reduce the therapeutic impact of the current procedure. This is important because having a device with similar cell viability compared to the manual injections means that the device can deliver the cells in a way that will allow for similar procedural success (or potentially more success) than if the injections were done manually. Although the results showed that there is not a statistically significant difference between the four groups when comparing their MSC viabilities following each injection, automatic injections are expected to aid in improved cell retention in comparison to manual. Manual injections had inconsistent force values across their injections with force ranges that did not display a steady pattern throughout each injection as some manual injections had high force values early within the injection and then lower force applications at later times, other injections started out with low force application values and then the force application peaked at the end. As a result, there is less consistency across the manual injections in terms of syringe plunger force application compared to the consistency seen in the automatic injections which all displayed about the same force range value across each set of trials for each respective injection rate (minimal variation seen in the *Cell Viability Results* Section above). As automatic injections have a greater force and flow rate consistency at the desired, slow 30 second and 60 second rates throughout their injections relative to manual injections, their MSC delivery should enable greater localization at the myocardium site of interest, which can enable greater cell retention in the myocardium that will improve the therapeutic impact [72]. Additional bovine steak and *ex vivo* porcine heart testing will need to be performed to confirm the cell retention differences between the automatic and manual injections and thus the greater clinical success the automatic injections can promote.

## 25 Gauge Needle Testing

Additional testing was performed with the fully assembled device to ensure that it was functioning properly along with meeting the design criteria. 25 Gauge Injection Testing was performed using a 25 gauge needle to mimic the connection between the tubing and the catheter system and validate the volume ejected. The device was successfully able to eject approximately 0.5 mL of fluid with an average error of less than 5% with the consideration that dead space is present in the needle. This is important because the device needs to be able to inject all of the fluid so that the stem cells will all be delivered in full within the preferred time (either 30 or 60 seconds). Finally, clinical simulation testing and catheter backup testing was performed to confirm the overall design functionality which was important because the device must be able to still operate when connected to the connection tubing/catheter system because that is what will be used when delivering the stem cells into the myocardium with patients. The force ranges for

the clinical simulation testing also confirmed that the force value ranges for injecting the cells stayed well below the 2.4 N indicating that there is no backup in the system and too much force is not being applied on the cells. Catheter Backup testing was performed with the 30 and 60 second injection rates resulting in catheter obstruction force value of 1.51 N and 1.81 N respectively. During clinical simulation testing the entire device was assembled and connected to the catheter via tubing and the same tests were performed as the 25 gauge needle testing without collection of the ejected volume. The results confirmed that there was less than 5% error with the ejection times and that the force range was still well under 2.4 N. However, the force values identified during the catheter backup testing cannot properly simulate the catheter obstruction force values during a clinical intramyocardial MSC injection procedure. Thus Catheter Backup testing results cannot provide information that correctly identifies catheter obstruction susceptibility.

### Catheter Backup Testing

The Catheter Obstruction Testing performed this semester followed an updated protocol in order to provide more accurate obstruction values. The average peak threshold forces observed during obstruction testing for the 30 and 60 second injection rates were  $3.47 \pm 0.33$  N and  $4.29 \pm 0.07$  N, respectively. These results correlated to higher force values than the previously used 2.40 N catheter backup literature value, however these values are more accurate for potential catheter obstruction during an intramyocardial MSC injection with a 1 mL syringe integrated with medical grade tubing connected to the procedural catheter. Given this higher value, the feedback system will thus need to be adjusted accordingly in order to properly alert the operator when catheter obstruction may be occurring. Further catheter obstruction testing injecting into myocardial tissue is required in order to provide a more accurate determination of the threshold values. This is because the catheter obstruction testing performed this semester injected water into the air, dripping into a petri dish, rather than directly into myocardium tissue. These values are expected to be lower than the forces that will be experienced during a typical clinical MSC injection into the myocardium as the resistance provided by tissue stiffness is much greater than air. A healthy myocardium stiffness is 8 - 15 kPa while the stiffness of an individual who experienced a myocardial infarction is  $100 \text{ kPa} \pm 2.91$  [73,66] will increase the force required to inject the MSCs into these tissues. This will correlate to a higher force value indicating the onset of catheter obstruction during clinical procedures compared to the blockage force values picked up during testing. The values obtained during this test may also be unreliable as the obstruction in the catheter was not standardized between each test and there may have been inconsistent flow profiles in each test. Another observation from the results was that the 60 second tests had a higher peak average force ( $4.29 \pm 0.07$  N) than the 30 second tests ( $3.47 \pm 0.33$  N). This is inconsistent with the force trends found in other data, but may prove viable as higher forces may be necessary to better overcome the obstruction in the catheter. This would thus cause faster injections, within a viable range, to have a decrease in required force throughout the injection. This will be further researched when using a standardized testing protocol for future catheter

obstruction tests. As a result, the force values identified during the catheter backup testing do not correlate to the catheter obstruction force values that will be picked up during a clinical intramyocardial MSC injection procedure, preventing these tests from providing information that correctly identifies catheter obstruction susceptibility.

### Bovine Steak Injection Testing

Results from the bovine steak injection testing were intended to prove that increasing the stiffness of the material that is injected into will increase the force required to perform the injection for each rate. It was seen that increasing the stiffness did not correlate with higher forces for steak preparations “raw” through “medium-well” (see *Results: Bovine Steak Injection Results*). It was also seen that the tests done on the “well done” section of bovine steak did not have the highest required force that would have been expected. It was seen throughout the procedure that the average force values for each injection kept climbing in sequential order of the tests, indicating there may have been a problem with the testing system as a whole. A way to avoid this problem and obtain more reliable results in future testing with different myocardial tissue mimicking material is to use separate catheters for each different material. This will remove the implication that further testing on the same catheter will automatically raise the required force independent of the stiffness of the material. These tests were able to prove that the device is successful at delivering the expected solution amount at the expected times, further demonstrating the ability for the injector to perform successful intramyocardial MSC injections into a wide variety of stiffness values, as expected within the myocardium. A healthy myocardium stiffness is 8 - 15 kPa while the stiffness of an individual who experienced a myocardial infarction is  $100 \text{ kPa} \pm 2.91$  [73,66]. It will be important to ensure the catheter is properly positioned within the tissue that is most replicable of how the procedure is performed. This will ensure the force values obtained are reliable and will further help determine the force range that should be expected when delivering MSC's into the myocardium.

### Ex Vivo Heart Cervine Injection Testing

The results obtained from the deer heart injections further confirm that it requires more force to inject at faster injection rates. There was a significant difference between the peak forces given that the p-value was below 0.05 after performing a t-test. However, it cannot be concluded whether these higher force values at the higher injection rates will correspond with lower cell viability when compared to the lower injection rates. Further testing should be performed using the same experimental setup to determine whether these significantly different injection force values will alter cell viability. Mechanical properties of the tissue used for the testing should also be determined in order to relate varying force values with the different tissue stiffness values that occur throughout the myocardium. These observations will further help determine the force range that should be expected when performing injections into the myocardium tissue. It should also be noted that the obtained force values above 5 N may not have less than 5% error associated with these readings because the calibration curve only accounted for values up to 5N.

The FSG calibration was fairly linear, however, so it can be reasonably assumed that the values are reliable, but further confirmation should be performed in the future (see the *Future Work* section for more information).

### Viscosity Testing

Based on these results from the data displayed in the *Viscosity Testing Results* Section, it can be concluded that higher viscosities require more force to inject. Therefore, if there are higher concentrations of cells, and thus a higher viscosity solution, more force will be required to inject the solution into the myocardium. Additionally, the testing results also further proved that injecting the cells at a higher injection rate will also require more force meaning that the cells will likely experience more force at higher injection rates as well. Testing should be done to determine the viscosities of various cell concentrations and the corresponding injection forces. Further discussion of future viscosity testing can be found in *Future Work*.

### Pressure Sensing Catheter Testing

As seen in the *Pressure Sensing Catheter Results* Section above, the force values that correspond to the onset of peak pressure are relatively consistent for each injection rate, indicating that the pressure values reached during the injection are independent of injection rate, but dependent on force application when increasing toward the pressure plateau. This demonstrates that the feedback system will enable the operator to determine when the peak pressure is reached and what the peak pressure corresponds to when injecting into the air, based on the nature of the testing (see the *Pressure Sensing Catheter Testing* section above). This will assist the operator throughout the intramyocardial MSC injection procedure, enabling confirmation of the location and thus success of each injection, significantly improving the efficacy of the procedures. The injection rates are expected to influence the time it takes the peak pressure to be acquired and the rate of pressure increase while the applied force is assumed to control the specific internal pressure experienced by the aliquot solution throughout an injection until the pressure plateau is reached. While current testing demonstrates that force correlates to the onset of peak pressure, additional testing will need to be performed to verify this rate and force pressure dependence as the internal pressure moves toward its plateau. While the testing provided important peak pressure data for aliquot injections into the air, more testing will need to be performed where the aliquot solution is delivered into myocardium tissue. This will generate results that correlate to the expected pressure and force values that will be identified during clinical intramyocardial MSC injection procedures. Injections into tissue will raise the force application values and consequently pressure experienced by the internal solution, as read from the pressure sensing catheter (see the *Catheter Backup Results* section above). To provide more accurate pressure results that establish the force applied to the aliquot solution throughout each injection, the clinical procedure needs to be simulated completely. As a result, future pressure sensing catheter testing needs to be performed where the injectate is delivered into myocardium tissue to enable correct pressure readings that will correlate to the clinical intramyocardial MSC

injection procedures. This will thus promote the efficacy of the procedures as the operator will be able to determine if the appropriate force and thus pressure is applied for the injection location of interest. Of note, the current peak pressure values for injections into air are still critical data. If injections values are low during a intramyocardial MSC injection procedure, the operator can utilize the 2.21 - 2.22 N force values to establish how close the internal applied pressure is to the 429 mmHg peak pressure of air throughout the injection and thus establish if the aliquot is being delivered into air or a body cavity rather than the desired myocardium tissue. Coupling these values with the peak pressure for myocardium injections after future testing will provide a high efficacy injector capable of determining where each injection is taking place.

## Ethical Considerations of Design

One area of ethical considerations that needs to be taken into account is safety. The device must have both operator and patient safety. In terms of operator safety, if the system were exposed to liquid or malfunctions there should be no harm to the operator from the moving parts or from the electrical components. Regarding patient safety, the risk of bubble formation in the catheter tubing must be reduced as much as possible. Air bubbles in the arteries due to catheter removal or insertion can lead to lethal coronary air embolism [76]. A manual design was chosen instead of a fully automated design to reduce this risk. Additionally, the device must ensure that two flow rates, a 30 second rate and a 60 second rate, reliably and consistently inject 0.5 mL of stem cell solution into the myocardium with dwell time in between. If the injection rate is too fast it can lead to the reflux of cells through the needle tract and cell damage. Furthermore the device must be capable of notifying the user of a potential clog in the catheter tubing. If the user encounters a clog and the injection device does not notify the user, it could potentially lead to damage of the system or an improper volume of stem cells injected into the myocardium. The system also must be sustainable and withstand everyday use. The impact that each material will have on the environment must also be taken into consideration.

Another important ethical consideration is the ethics of animal testing. The device will first be tested in the animal cath lab for porcine procedures before it is used during human procedures. In all animal testing it is essential that research has a sufficient purpose to justify the use of animals. Humane consideration for the well-being of the animals must be incorporated into the design and procedure and all animal testing testing must approved prior by the Institutional Animal Care and Use Committee (IACUC). During a procedure, animals must remain under anesthesia for the entirety of the procedure and aseptic technique must be used whenever possible [77]. All personnel involved in the procedure must be properly trained and receive instruction in the care, maintenance, and handling of the species being studied. Procedures where the research animal is anesthetized and is euthanized before regaining consciousness are generally acceptable. Animals also should not be subjected to successive survival surgical procedures, except as required by the nature of the research or surgery. Multiple surgeries on the same animal must receive approval from the IACUC [78]. Additionally, animals that were raised in a laboratory must not be released into the wild because it is likely they cannot survive.

Euthanasia must be performed in a humane manner to ensure immediate death, ensuring that no animal is discarded until its death is verified. Euthanasia is often accomplished by injection of a death-inducing drug that stops brain function and is not painful to the animal [79].

Ethical concerns in relation to stem cells for use in both the procedure and for testing is also relevant. Concerns for clinical application of MSCs are unwanted differentiation of the transplanted MSCs and their potential to suppress anti-tumor immune response and generate new blood vessels that may promote tumor growth and metastasis. In the case of injection into the myocardium it is desired that the MSCs differentiate into cardiac muscle cells, unwanted differentiation or tumor formation could lead to a serious safety issue. Another major concern with injecting MSCs into the body is the possibility for an inflammatory response. MSCs can adopt a pro-inflammatory phenotype and produce neutrophils and activate T-cells invoking an inflammatory response [80]. Chronic inflammation can lead to further health complications. On the other hand, if stem cell-based interventions live up to their therapeutic potential, it will be important to ensure equitable access to these treatments. As cell therapies are cost and labor intensive, the automatic intramyocardial MSC injection procedures will presumably be costly [81]. As a result, an equitable distribution of this new therapy is a significant consideration for clinical usage. Non-infectious porcine derived MSCs will be used in testing that were derived from euthanized pigs, one must ensure that these cells were obtained in an ethical manner.

## Sources of Error

Possible sources of errors during the testing from the Spring 2022 semester could be due to the variability of force detection with the FSR 400 Force Sensing Resistor, count-to-count variability during stem cell viability testing, injection time variability, volume injection value inconsistencies, and 3D printing errors. The variability with the FSR led to relatively high errors of margin with force detection. Despite the error margins being still below the requirements (less than 20% error for force values less than 1.00N and less than 15% error for force values greater than 1.00N), ideally this margin of error should be lowered. In the Fall 2022 semester the error margin associated with the FSR was reduced. This was completed by integrating the FSG Series Force Sensor. This new sensor was able to reduce this  $10.31 \pm 5.61\%$  error to a  $1.70 \pm 1.52\%$  error. Additionally Spring 2022 semester, another source of error occurred during overall device testing with the 25 gauge needle. The volume ejection values measured were not extremely precise due to the dead space present in the needle and where the needle connects to the syringe. The expected delivery volume was 0.5 mL but typically only 0.49 mL - 0.48 mL of solution was measured demonstrating that there is 0.01 mL - 0.03 mL of dead space that accounts for this error. This was taken into consideration when establishing the error margin of 5% for injection volume. Possible sources of error in stem cell viability testing could be due to count-to-count variability. Count-to-count variability of a single sample by an experienced cell biologist is commonly 10% or more and when comparing variation of single-sample counts across multiple scientists, counting variability can exceed 20% [82]. Other sources of error last semester may include injection time outside the specified range of 60 seconds  $\pm$  0.5 seconds and 30 seconds  $\pm$

0.5 seconds, and volume dispensed must be within 0.5% of 0.5 mL. During 25 Gauge Injection Testing error in the volume dispensed could be due to the inaccuracy of the scales used to weigh the water ejected, miss-consideration of the dead space present, and inaccurate uptake of the water by hand.

This semester potential sources of error that occurred during testing include human error associated with catheter obstruction testing, potential catheter occlusion during bovine steak testing, catheter needle issues, and coupler concerns. Catheter obstruction testing was not standardized across trials as the procedural catheter connected to medical grade tubing was kinked in various places to mimic obstruction using various different methods. This human error could account for error during catheter obstruction testing and can be avoided in the future by creating a standardized method of creating catheter obstruction. Furthermore, during bovine steak testing catheter occlusion could have resulted in increased error. The needle of the catheter was inserted into each bovine steak but occlusion may have occurred as the entire distal end of the catheter was inserted into each steak instead of just the needle. The implication of this is that the forces measured during bovine steak testing may have been higher due to this potential occlusion. The needle-tipped end of the catheter that was used for various testing including bovine steak and *ex vivo* heart injection testing became bent with usage leading to potential error. It became difficult for the needle to eject fully and became more damaged with increased usage. The coupler connecting the NEMA-17 stepper motor to the threaded rod became loose with repeated high force testing causing the entire device to either fail or become stuck. This error was especially present during pressure sensing catheter testing because the screws became completely loose causing the injection to fail multiple times leading to error. This error will be addressed next semester by purchasing a new coupler or sanding the grooves in the threaded rod to allow for a better connection to the stepper motor. There will also be errors associated with each component that is fabricated from 3D printed Ultimaker PLA. The Ultimaker S5 3D printer that was used to print each Ultimaker PLA component contains a tolerance, resulting in slight variations in precision and accuracy during each 3D print [83]. This difference across each 3D printed part will result in dimensional errors across components that may hinder the cohesiveness and mating of the injector. However, the dimensional difference between parts should be minimal, so the overall functionality of the injector should not be impacted to any significant degree, especially since the connections within the force application threaded system will not be impacted. After the integration of the FSG Series Force Sensor with the current system, there will still be associated error within this force sensor. The FSG Series Force Sensor has an accuracy of  $\pm 0.5\%$  and a repeatability of  $\pm 0.2\%$  [39], demonstrating that a minimal amount of variance from the actual applied force is inevitable.

## Conclusion

### Overview

The client, Dr. Amish Raval, requests an automatic injection device for use during stem cell delivery procedures to the myocardium. The device must integrate with 1 mL procedural syringes, medical grade tubing and a clinical catheter. Its aim is to limit operator intervention and provide a 60 and 30 second injection rate. The current procedure is susceptible to rapid injections that lead to the reflux of cells through the needle tract and cell damage. Thus it is imperative that the injector maintain the desired injection rates as well as maximize cell viability throughout the entirety of the procedure. The Cellringe Pump, the current prototype, won the design matrix due to its efficacy, feasibility, and cost. This design consists of a base that includes a stepper motor, a threaded rod injection regulator, an Ultimaker PLA force application block, and adjustable syringe clamp molds. To achieve accurate injections, the injector consists of a stepper motor that autonomously rotates a fully threaded metal bolt to drive a force application block toward the procedural syringe, injecting 0.5 mL of MSC solution into the catheter tubing and into the myocardium at a 30 or 60 second injection rate. A syringe clamp mold within the injector base fastens the required 1 mL syringe in place, preventing any displacement during each injection. Following each successful injection, the force application block moves back to the starting position, allowing syringe removal and insertion to take place within a maximum 60 second dwell time between injections. An LED built into the feedback circuit signals when the 2.40 N threshold is reached to indicate potential catheter obstruction. The injector feedback system is controlled by an Arduino Uno microcontroller and detects force via an FSG series force sensor attached to the force application block, receiving and displaying the force applied by the injector to the syringe throughout each injection on the scoreboard. The FSG Series Force Sensor had the highest score in the Design Matrix, followed by the Load Cell with Nanoshield, the Non-Invasive Pressure Sensor, and lastly the original FSR Force Sensor. The FSG Series Force Sensor was the chosen force detection system due to its sensitivity, safety, ease of operation, and durability. It was also tested and results found that the sensor successfully meets all of the design specifications and greatly advances the force sensing accuracy and repeatability of this prototype.

In Spring Semester 2022 the overall design functionality was confirmed with a clinical MSC injection procedure simulation that demonstrated 0.5 mL of MSCs were properly delivered with both injection rates and that the FSR feedback system correctly displayed force values and alerted the user when threshold was exceeded. This semester injection testing into bovine steak, *ex vivo* cervine heart tissue, and obstructed catheters further proved the applicability of the Cellringe Pump prototype and gathered viable force range data relevant to the discovery of an expected force range value. The design specification testing results validate the efficacy of the injection device, confirming its reliability and accuracy. The injector provides the required slow, consistent injection rates, maintaining cell viability and maximizing cell retention. Its automatic MSC delivery at the required flow rates and dwell time limits operator intervention, meeting



design specifications and promoting its clinical applicability. The new FSG feedback system accurately receives and displays the force throughout each injection, correctly alerting the operator when catheter obstruction is imminent with reduced error compared to the previous FSR feedback system. As a result, it meets all feedback system requirements, providing a simplistic interface that assists the operator with each injection, increasing MSC injection procedural success. With the injection device, the user is no longer subject to hand fatigue and the susceptibility to rapid injections is removed, promoting procedural efficacy. This device is thus a critical component of improving the treatment of myocardial infarction and mitigating cardiac arrest risk.

## Future Work

With the FSG Series Force Sensor implemented within the prototype, further testing can be pursued to determine different force values that correlate with different scenarios within an intramyocardial MSC injection procedure. As the force values from the *ex vivo* cervine heart testing were close to or over the FSG calibration curve's maximum applied testing force of 5.00 N (see *Methods* section above), a new calibration curve will need to be generated from force testing across a 0.00 N - 15.00 N range. This will result in a curve that has an accurate line of best fit equation for force applications ranging from 0.00 N to 10.00 N, aligning with the force values obtained during cervine heart testing and thus the expected myocardium tissue injection force values. Along with recalibration to obtain a higher max force value, recalibration will also be necessary to discard the -5.00 V power that is needed for the instrumentation amplifier to work within the system (see *Methods* section above). Obtaining a new calibration curve with the correct force range and proper power supply will allow the prototype to conduct a wider range of tests and become a more marketable product.

Wider range of tests that will be conducted to ultimately find a force range that accurately represents the range expected when performing MSC injection procedures include porcine clinical validation testing, procedural tests in different locations within the myocardium, differing solution viscosity testing, and further pressure sensor testing. Porcine clinical validation testing will allow the prototype to undergo a current clinical procedure to validate its design and function. Proving this device works in current clinical practice will allow the device to be potentially incorporated into further clinical testing and operations. The purpose of the steak injection testing (see *Results: Bovine Steak Injection Results*) was to gain an idea of how different tissue stiffness values will correlate to different forces required to perform the procedure. By replicating these tests and finding test material with more similar mechanical property values as the myocardial tissue within the human heart, more specific tests inclined to find the force value range that will be experienced in real clinical operation will be performed. Using solutions with different viscosities such as vegetable oil or glycerol in tests will broaden the range of force values that will be used to find the correct force range experienced during clinical procedures. Ultimately, the goal of this test will be to find the viscosity of the MSC solution and be able to replicate that in a different solution to perform tests without the need of

the actual MSC solution. Another goal of this device is to effectively correlate values found from a pressure sensor with the force detected from the syringe plunger. Further testing to prove there is correlation by forming an equation to relate the two different force detections will be conducted. The final validation of the device's functionality in a clinical setting will be confirmed via *in vivo* porcine model testing. This will ensure that the feedback system properly detects catheter obstruction and the entire injection device correctly functions, delivering 0.5 mL of the MSC aliquot solution through the catheter and into the myocardium at the 30 and 60 second specified rates.

Adding to the prototype to improve its functionality and increase the variety of application will not only allow for different tests and procedures outside of the current clinical practice, but also increase its marketability and potential to be seen as a staple for all stem cell related injections. Adding functions to allow the user to input different syringe sizes and request different injection rates based on the amount of solution needed to be dispensed will be incorporated within the prototype. This implementation will greatly expand the use of the prototype and allow for more tests to be run to determine the force ranges for all different types of procedures. Along with furthering the interface system, the prototype aims to become completely portable to ease the use of operation and transportation during or between procedures. The goal is to switch the device and all of its internal components to be battery powered. Adding batteries will remove the need for an external power supply and allow the device to be used anywhere in the procedural room, unrestricted from power cord length and power outlet location. Furthermore, the prototype's shape and overall design will be modified to alleviate all functional failures and restrictions that occur during testing procedures. The new design will better transport the force application block during the procedure and be shaped to fit different syringe sizes and solution amounts.

All mentioned accomplishments and design implementations were accounted for in an invention disclosure report that was filed to the Wisconsin Alumni Research Foundation and is awaiting further approval for the potential of filing for a patent. Further steps following approval will include meeting with an attorney to discuss the completion of the device patent.

Moving forward, the FSG Series Force Sensor will be integrated with the current design to replace the FSR 400 Force Sensing Resistor in order to improve the overall accuracy and sensitivity of the device. The FSG Series Force Sensor will be used to detect the external forces on the plunger with a high degree of efficacy. These forces will then be correlated to the internal force experienced by the MSCs via calculations and algorithms within the Arduino IDE software. To ensure the force value displayed from the feedback system corresponds to the force applied to the MSCs rather than the syringe plunger, calculations and equations converting the force applied to the syringe plunger to the stress experienced by the MSCs will be developed through experimentation. Furthermore, the current design will be optimized by making small improvements to the injector, such as reducing the friction between the force application block and the support rods (see *Final Prototype* section above) in order to increase the accuracy and reliability associated with the force application system or printing all of the circuitry onto a chip

or breadboard to make the system more compact (see *Methods* section above). These modifications will improve the overall efficacy and reliability of the device, increasing the clinical success associated with intramyocardial stem cell injection procedures. After submitting an invention disclosure to the Wisconsin Alumni Research Foundation to initiate the process of filing for a patent, a decision will be made shortly that will determine whether to move forward with the design. If chosen, a patent application will be filed with WARF's assistance.

After the device is optimized and the new force sensor is installed, testing will be done to establish force ranges associated with different myocardium locations: diseased or scarred tissue, healthy tissue, and body cavity. A bovine steak model of different densities and properties will be used to determine the expected force values that correspond to healthy tissue and the pressure difference between healthy and unhealthy tissue. Then, testing will be performed utilizing solutions of different viscosities and MSC aliquot solutions with various cell concentrations to ensure the device's accuracy in detecting correct force values over a range of different situations. In addition, there will be *ex vivo* catheter obstruction testing to simulate the catheter obstruction force values during a clinical intramyocardial MSC injection procedure as this was not achieved during the Catheter Backup testing. To make this device easier to incorporate in a clinical setting, the injector should transition into battery operation in order to minimize the amount of wires present and thus the space required for the device during procedures.

## References

- [1] Centers for Disease Control and Prevention, “Leading Causes of Death,” *Centers for Disease Control and Prevention*, 2019.  
<https://www.cdc.gov/nchs/fastats/leading-causes-of-death.htm>.
- [2] G. F. Tomaselli and D. P. Zipes, “What Causes Sudden Death in Heart Failure?,” *Circulation Research*, vol. 95, no. 8, pp. 754–763, Oct. 2004, doi: 10.1161/01.res.0000145047.14691.db.
- [3] J. Duan, I. Pillai, Y. Lu, J. Huang, and R. Fritz, “Cardiac Repair and Regeneration Research Unit | Heart and Vascular Services at UCLA,” *Uclahealth.org*, 2019.  
<https://www.uclahealth.org/heart/cardiac-repair-regeneration>.
- [4] M. Rheault-Henry, I. White, D. Grover, and R. Atoui, “Stem cell therapy for heart failure: Medical breakthrough, or dead end?,” *World Journal of Stem Cells*, vol. 13, no. 4, pp. 236–259, Apr. 2021, doi: 10.4252/wjsc.v13.i4.236.
- [5] “Heart Failure: Risk Factors | University Health Care System,” *www.universityhealth.org*.  
<https://www.universityhealth.org/heart-failure/risk-factors/>.
- [6] A. N. Raval et al., “Point of care, Bone Marrow Mononuclear Cell Therapy in Ischemic Heart Failure Patients Personalized for Cell potency: 12-month Feasibility Results from CardiAMP Heart Failure roll-in Cohort,” *International Journal of Cardiology*, vol. 326, pp. 131–138, Mar. 2021, doi: 10.1016/j.ijcard.2020.10.043.
- [7] Kono, Hajime, and Kenneth L Rock. “How dying cells alert the immune system to danger.” *Nature reviews. Immunology* vol. 8,4 (2008): 279-89. doi:10.1038/nri2215
- [8] M. H. Amer, F. R. A. J. Rose, L. J. White, and K. M. Shakesheff, “A Detailed Assessment of Varying Ejection Rate on Delivery Efficiency of Mesenchymal Stem Cells Using Narrow-Bore Needles,” *Stem Cells Translational Medicine*, vol. 5, no. 3, pp. 366–378, Mar. 2016, doi: 10.5966/sctm.2015-0208.
- [9] Lenneman AJ, Birks EJ. Treatment strategies for myocardial recovery in heart failure. *Curr Treat Options Cardiovasc Med*. 2014 Mar;16(3):287. doi: 10.1007/s11936-013-0287-9. PMID: 24492922.
- [10] R. N. Doughty, S. MacMahon, and N. Sharpe, “Beta-blockers in heart failure: Promising or proved?,” *Journal of the American College of Cardiology*, vol. 23, no. 3, pp. 814–821, Mar. 1994, doi: 10.1016/0735-1097(94)90773-0.
- [11] M. J. Everly, “Cardiac transplantation in the United States: an analysis of the UNOS registry,” *Clinical Transplants*, pp. 35–43, 2008, [Online]. Available: <https://pubmed.ncbi.nlm.nih.gov/19708444/>.

- [12] M. J. Wilhelm, “Long-term outcome following heart transplantation: current perspective,” *Journal of thoracic disease*, vol. 7, no. 3, pp. 549–51, 2015, doi: 10.3978/j.issn.2072-1439.2015.01.46.
- [13] J. H. Park, D. Dehaini, J. Zhou, M. Holay, R. H. Fang, and L. Zhang, “Biomimetic nanoparticle technology for cardiovascular disease detection and treatment,” *Nanoscale Horizons*, vol. 5, no. 1, pp. 25–42, 2020, doi: 10.1039/c9nh00291j.
- [14] E. G. Schmuck et al., “Intravenous Followed by X-ray Fused with MRI-Guided Transendocardial Mesenchymal Stem Cell Injection Improves Contractility Reserve in a Swine Model of Myocardial Infarction,” *Journal of Cardiovascular Translational Research*, vol. 8, no. 7, pp. 438–448, Oct. 2015, doi: 10.1007/s12265-015-9654-0.
- [15] A. Hmadcha, A. Martin-Montalvo, B. R. Gauthier, B. Soria, and V. Capilla-Gonzalez, “Therapeutic Potential of Mesenchymal Stem Cells for Cancer Therapy,” *Frontiers in Bioengineering and Biotechnology*, vol. 8, no. 43, Feb. 2020, doi: 10.3389/fbioe.2020.00043.
- [16] Y. Guo, Y. Yu, S. Hu, Y. Chen, and Z. Shen, “The therapeutic potential of mesenchymal stem cells for cardiovascular diseases,” *Cell Death & Disease*, vol. 11, no. 5, May 2020, doi: 10.1038/s41419-020-2542-9.
- [17] A. Vo, M. Doumit, and G. Rockwell, “The Biomechanics and Optimization of the Needle-Syringe System for Injecting Triamcinolone Acetonide into Keloids,” *Journal of Medical Engineering*, vol. 2016, 2016, doi: 10.1155/2016/5162394.
- [18] Y. Huang, J.-Y. Qian, H. Cheng, and X.-M. Li, “Effects of Shear Stress on Differentiation of Stem Cells into Endothelial Cells,” *World Journal of Stem Cells*, vol. 13, no. 7, pp. 894–913, Jul. 2021, doi: 10.4252/wjsc.v13.i7.894.
- [19] F. P. Beer, E. R. Johnston Jr., J. T. DeWolf, and D. F. Mazurek, *Mechanics of Materials*, 8th Edition. McGraw Hill Education, 2020.
- [20] O. Villemain et al., “Myocardial Stiffness Evaluation Using Noninvasive Shear Wave Imaging in Healthy and Hypertrophic Cardiomyopathic Adults,” *Jacc. Cardiovascular Imaging*, vol. 12, no. 7, pp. 1135–1145, Jul. 2019, doi: 10.1016/j.jcmg.2018.02.002.
- [21] “Baxter Infus or Syringe Pump ABC 4100 Trade in Program.” Wilburn Medical Equipment and Supplies, <https://wilburnmedicalusa.com/baxter-infus-or-syringe-pump-abc-4100-trade-in-program/>
- [22] “Infus O.R. Syringe Pump Refurbished,” *4MD Medical Solutions*. [https://www.4mdmedical.com/index.php/catalog/product/view/id/253457/s/infusor-syringe-pump-refurbished?CAWELAID=120141310000056386&%3BCAGPSPN=pla&%3Bgclid=CjwKCAiAo4OQBhBBEiwA5KWu\\_8f3uyspUWEZJ9eX8-duXozZ5qbgAjz8DOYtmfDnjlz8zi4LdJ5RxoCcriQAvD\\_BwE](https://www.4mdmedical.com/index.php/catalog/product/view/id/253457/s/infusor-syringe-pump-refurbished?CAWELAID=120141310000056386&%3BCAGPSPN=pla&%3Bgclid=CjwKCAiAo4OQBhBBEiwA5KWu_8f3uyspUWEZJ9eX8-duXozZ5qbgAjz8DOYtmfDnjlz8zi4LdJ5RxoCcriQAvD_BwE) (accessed Mar. 01, 2022).

- [23] “User’s Guide ACIST | CVi® Contrast Delivery System,” Acist Medical Group, Aug. 2019. Accessed: Feb. 07, 2022. [Online]. Available: <http://acist.com/wp-content/uploads/2019/09/901418-00301-Users-Guide-CVi-MU-English-USA.pdf>.
- [24] Leoni, G., Lyness, A., Ginty, P., Schutte, R., Pillai, G., Sharma, G., Kemp, P., Mount, N., & Sharpe, M. (2017). Preclinical development of an automated injection device for intradermal delivery of a cell-based therapy. *Drug delivery and translational research*, 7(5), 695–708. <https://doi.org/10.1007/s13346-017-0418-z>
- [25] P. Mounce et al., “Medicament cassette, automatic injector, and automatic injector system,” May 09, 2019.
- [26] J. H. DeVries and R. J. VanPopering, “Pressure sensing syringe,” US4759750A, Jul. 26, 1988 Accessed: Oct. 03, 2022. [Online]. Available: <https://patents.google.com/patent/US4759750A/en>.
- [27] Food and Drug Administration, “CFR - Code of Federal Regulations Title 21,” Fda.gov, 2019. <https://www.accessdata.fda.gov/scripts/cdrh/cfdocs/cfCFR/CFRSearch.cfm?CFRPart=820> (accessed Feb. 09, 2021)
- [28] F. and D. Administration, “CFR - Code of Federal Regulations Title 21 Part 870,” [www.accessdata.fda.gov](http://www.accessdata.fda.gov), Jan. 06, 2022. <https://www.accessdata.fda.gov/scripts/cdrh/cfdocs/cfcfr/cfrsearch.cfm?fr=870.5100> (accessed Feb. 08, 2022).
- [29] U. S. Food and Drug Administration, “Product Classification,” <https://www.accessdata.fda.gov>, 2020. <https://www.accessdata.fda.gov/scripts/cdrh/cfdocs/cfPCD/classification.cfm?ID=FRN> (accessed May 01, 2022).
- [30] F. and D. Administration, “CFR - Code of Federal Regulations Title 21 3.2,” Code of Federal Regulations, Feb. 07, 2022. <https://www.ecfr.gov/current/title-21/chapter-I/subchapter-A/part-3/subpart-A/section-3.2> (accessed Feb. 08, 2022).
- [31] F. and D. Administration, “CFR - Code of Federal Regulations Title 21 Part 610,” U.S. Food and Drug Administration, Jan. 06, 2022. <https://www.accessdata.fda.gov/scripts/cdrh/cfdocs/cfcfr/cfrsearch.cfm?cfrpart=610> (accessed Feb. 08, 2022).
- [32] F. and D. Administration, “CFR - Code of Federal Regulations Title 21 Part 1271,” [www.accessdata.fda.gov](http://www.accessdata.fda.gov), Mar. 29, 2022. <https://www.accessdata.fda.gov/scripts/cdrh/cfdocs/cfcfr/CFRSearch.cfm?CFRPart=1271> (accessed Sep. 19, 2022).

- [33] Dr. A. Raval, "Manufacturing cost of final automatic injection system product," Jan. 2022
- [34] Arduino, "Arduino - H," [www.arduino.cc](http://www.arduino.cc), 2022. <https://www.arduino.cc/en/math/h>.
- [35] A. Staff, "Arduino Uno Rev3," [Arduino.cc](http://Arduino.cc), 2019.  
<https://store.arduino.cc/usa/arduino-uno-rev3> (accessed Feb. 25, 2021).
- [36] J. Blom, "Using the Serial 7-Segment Display," [learn.sparkfun.com](http://learn.sparkfun.com), 2022.  
<https://learn.sparkfun.com/tutorials/using-the-serial-7-segment-display/introduction>.
- [37] I. Electronics, "FSR 400 Data Sheet Figure 1 -Typical Force Curve Industry Segments Interlink Electronics -Sensor Technologies FSR 400 Series Round Force Sensing Resistor," 2021. Accessed: Feb. 15, 2022. [Online]. Available:  
<https://cdn.sparkfun.com/datasheets/Sensors/ForceFlex/2010-10-26-DataSheet-FSR400-Layout2.pdf>.
- [38] C. Inc., "BD Plastic Syringe | Maximum & Minimum Flow Rates," Chemyx Inc, Dec. 21, 2017.  
<https://www.chemyx.com/uncategorized/bd-plastic-syringe-minimum-maximum-flow-rates/> (accessed Feb. 15, 2022).
- [39] H. Sensing and Productivity Solutions, "FSG020WNPB," Digi-Key Electronics, 2022.  
<https://www.digikey.com/en/products/detail/honeywell-sensing-and-productivity-solutions/FSG020WNPB/3884049> (accessed Sep. 26, 2022).
- [40] Omega, "LCKD-1KG Load Cell," Newark, 2022.  
<https://www.newark.com/omega/lckd-1kg/load-cell-2mv-v-2-2lb-5vdc-rohs/dp/69AJ0415>
- [41] C. Eletronicos, "Load Cell - High Resolution Measurement for Load Cells - Arduino-compatible Shields - Circuitar," [www.circuitar.com](http://www.circuitar.com), 2018.  
<https://www.circuitar.com/nanoshields/modules/load-cell/index.html> (accessed Oct. 03, 2022).
- [42] S. M. Devices, "NonInvasive Pressure Sensor," Strain Measurement Devices, 2017.  
<https://www.smdsensors.com/products/type/non-invasive-pressure-sensor/> (accessed Oct. 03, 2022).
- [43] 14:00-17:00, "ISO 10993-1:2018," ISO, Oct. 2018.  
<https://www.iso.org/standard/68936.html>.
- [44] M. Inc., "Strength of Materials | Mechanics of Materials | MechaniCalc," [Mechanicalc.com](http://Mechanicalc.com), 2020. <https://mechanicalc.com/reference/strength-of-materials> (accessed Oct. 10, 2022).
- [45] T. Instruments, "INA129P," Digi-Key Electronics, 2022.  
<https://www.digikey.com/en/products/detail/texas-instruments/INA129P/254674>

- [46] S. Electronics, "UW-Madison BME Supply List (BME 310 and BME 201) - SparkFun Electronics," [www.sparkfun.com](http://www.sparkfun.com), 2021. [https://www.sparkfun.com/wish\\_lists/122199](https://www.sparkfun.com/wish_lists/122199).
- [47] Ultimaker, "Technical Data Sheet - PLA," Nov. 2018. Accessed: Dec. 02, 2021. [Online]. Available: <https://ultimaker.com/materials/pla>.
- [48] A. Industries, "Stepper Motor - NEMA-17 Size - 200 steps/rev, 12V 350mA," [www.adafruit.com](http://www.adafruit.com), 2022. [https://www.adafruit.com/product/324?gclid=Cj0KCCQiAjc2QBhDgARIsAMc3SqQi\\_8rpHenYK-iXt9KMn2Y-33zOxCpePZHOu\\_C26oTAriVpTp67CgQaArgPEALw\\_wcB](https://www.adafruit.com/product/324?gclid=Cj0KCCQiAjc2QBhDgARIsAMc3SqQi_8rpHenYK-iXt9KMn2Y-33zOxCpePZHOu_C26oTAriVpTp67CgQaArgPEALw_wcB) (accessed Feb. 21, 2022).
- [49] W. W. Grainger, Inc, "Fully Threaded Rod, Aluminum, 1/4"-20, 3 Ft Length," Grainger, 2022. <https://www.grainger.com/product/GRAINGER-APPROVED-Fully-Threaded-Rod-10P782>
- [50] S. Electronics, "Tactile Button - SMD (12mm) - COM-12993," [www.sparkfun.com](http://www.sparkfun.com), 2020. <https://www.sparkfun.com/products/12993>
- [51] W. W. Grainger, "Hex Nut, Machine Screw Nut, Nylon, Not Graded, Black Nylon coat, 1/4"-20 Dia./Thread Size," Grainger, 2022. <https://www.grainger.com/product/GRAINGER-APPROVED-Hex-Nut-4AGF9> (accessed Feb. 26, 2022).
- [52] "Adafruit Motor Shield V2," Adafruit Learning System, Jul. 09, 2013. [https://learn.adafruit.com/adafruit-motor-shield-v2-for-arduino/overview?gclid=Cj0KCCQjwpcOTBhCZARIsAEAYLuUmq5hpSgWHPxJN3gcg\\_1hCnajEPIIkC-C\\_myxJ159J0US\\_X8sUk50aAk7dEALw\\_wcB](https://learn.adafruit.com/adafruit-motor-shield-v2-for-arduino/overview?gclid=Cj0KCCQjwpcOTBhCZARIsAEAYLuUmq5hpSgWHPxJN3gcg_1hCnajEPIIkC-C_myxJ159J0US_X8sUk50aAk7dEALw_wcB) (accessed May 04, 2022).
- [53] S. Electronics, "Resistor Kit - 1/4W (500 total) - COM-10969 - SparkFun Electronics," [www.sparkfun.com](http://www.sparkfun.com), 2021. <https://www.sparkfun.com/products/10969>.
- [54] S. Electronics, "Breadboard - Self-Adhesive (White) - PRT-12002 - SparkFun Electronics," [www.sparkfun.com](http://www.sparkfun.com), 2021. <https://www.sparkfun.com/products/12002>.
- [55] S. Electronics, Inc., "7-Segment Display - 20mm (Blue) - COM-11408 - SparkFun Electronics," [www.sparkfun.com](http://www.sparkfun.com), 2022. <https://www.sparkfun.com/products/11408>
- [56] Ultimaker, "Technical Data Sheet - Tough PLA," Sep. 2018. Accessed: Dec. 02, 2021. [Online]. Available: <https://ultimaker.com/materials/tough-pla>.
- [57] Formlabs, "Standard Materials for High-Resolution Rapid Prototyping," Formlabs, Apr. 2016. Accessed: May 03, 2022. [Online]. Available: <https://formlabs-media.formlabs.com/datasheets/1801089-TDS-ENUS-0P.pdf>



- [58] W. W. G. Inc., “Fully Threaded Rod, Nylon, 1/4"-20, 2 Ft Length, Off-White,” Grainger, 2022.  
<https://www.grainger.com/product/GRAINGER-APPROVED-Fully-Threaded-Rod-2KA63>.
- [59] C. Plastics, “Nylon Plastic | Strong, Stiff, Bearing & Wear Material | Curbell Plastics,” Curbellplastics.com, 2022.  
<https://www.curbellplastics.com/Research-Solutions/Materials/Nylon#:~:text=Nylon%20is%20a%20strong%2C%20stiff> (accessed Feb. 27, 2022).
- [60] Everbilt, “Everbilt 1/2 in. X 36 in. Aluminum round Rod 801637,” The Home Depot, 2022.  
<https://www.homedepot.com/p/Everbilt-1-2-in-x-36-in-Aluminum-Round-Rod-801637/204273968> (accessed Dec. 10, 2022).
- [61] W. J. Smith and F. E. Goodwin, “Hot Dip Coatings,” ScienceDirect, Jan. 01, 2017.  
<https://www.sciencedirect.com/science/article/pii/B9780128035818092146> (accessed Dec. 10, 2022).
- [62] Engineering ToolBox, “Young’s Modulus - Tensile and Yield Strength for Common Materials,” Engineeringtoolbox.com, 2003.  
[https://www.engineeringtoolbox.com/young-modulus-d\\_417.html](https://www.engineeringtoolbox.com/young-modulus-d_417.html) (accessed Dec. 10, 2022).
- [63] A. Materials, “Aluminium: Specifications, Properties, Classifications and Classes,” AZoM.com, May 17, 2005.  
<https://www.azom.com/article.aspx?ArticleID=2863#:~:text=Mechanical%20Properties%20of%20Aluminium&text=Alloying%2C%20cold%20working%20and%20heat> (accessed Dec. 10, 2022).
- [64] Uxcell, “Uxcell 5mm to 1/4 Inch Bore Rigid Coupling Set Screw L25XD14 Aluminum Alloy, Shaft Coupler Connector, Motor Accessories, Dark Blue : Industrial & Scientific,” www.amazon.com, 2022.  
<https://www.amazon.com/uxcell-Coupling-Aluminum-Connector-Accessories/dp/B08H26NP3T?th=1>
- [65] Dr. A. M. Helmenstine, “How to Calculate Percent Error,” ThoughtCo, Nov. 02, 2020.  
<https://www.thoughtco.com/how-to-calculate-percent-error-609584> (accessed Dec. 03, 2021).
- [66] Allijn, Iris, Marcelo Ribeiro, André Poot, Robert Passier, and Dimitrios Stamatialis. “Membranes for Modeling Cardiac Tissue Stiffness In Vitro Based on Poly(Trimethylene Carbonate) and Poly(Ethylene Glycol) Polymers.” *Membranes* 10, no. 10 (October 3, 2020): E274. <https://doi.org/10.3390/membranes10100274>.
- [67] James, Bryony, and Seo Won Yang. “Testing Meat Tenderness Using an in Situ Straining Stage with Variable Pressure Scanning Electron Microscopy.” *Procedia Food Science*, 11th International Congress on Engineering and Food (ICEF11), 1 (January 1, 2011): 258–66.  
<https://doi.org/10.1016/j.profoo.2011.09.041>.

- [68] Poon, Christine. “Measuring the Density and Viscosity of Culture Media for Optimized Computational Fluid Dynamics Analysis of in Vitro Devices.” bioRxiv, August 25, 2020. <https://doi.org/10.1101/2020.08.25.266221>.
- [69] L. M. Diamante and T. Lan, “Absolute Viscosities of Vegetable Oils at Different Temperatures and Shear Rate Range of 64.5 to 4835 s<sup>-1</sup>,” *Journal of Food Processing*, vol. 2014, pp. 1–6, Aug. 2014, doi: 10.1155/2014/234583.
- [70] W. Luo et al., “Laminar Shear Stress Delivers Cell Cycle Arrest and anti-apoptosis to Mesenchymal Stem Cells,” *Acta Biochimica Et Biophysica Sinica*, vol. 43, no. 3, pp. 210–216, Mar. 2011, doi: 10.1093.
- [71] “Percent Difference Calculator - with Step-by-Step Guide,” Inch Calculator. <https://www.inchcalculator.com/percent-difference-calculator/> (accessed May 03, 2022).
- [72] F. van den Akker et al., “Intramyocardial Stem Cell injection: go(ne) with the Flow,” *European Heart Journal*, vol. 38, no. 3, pp. 184–186, Jan. 2017, doi: 10.1093/eurheartj/ehw056.
- [73] R. Emig et al., “Passive Myocardial Mechanical properties: meaning, measurement, Models,” *Biophysical Reviews*, vol. 13, no. 5, pp. 587–610, Oct. 2021, doi: 10.1007/s12551-021-00838-1.
- [74] “BME Shared Lab Resources.” BME Lab - 1002 ECB - Biomedical Experimental Teaching Lab, <https://sharedlab.bme.wisc.edu/labs/1002/>.
- [75] Alambra, Kenneth. “Water Viscosity Calculator.” Omni Calculator, Omni Calculator, 14 Mar. 2022, <https://www.omnicalculator.com/physics/water-viscosity>.
- [76] S. H. Mun, D. A. An, H. J. Choi, T. H. Kim, J. W. Pin, and D. C. Ko, “Lethal coronary air embolism caused by the removal of a double-lumen hemodialysis catheter: a case report,” *Korean Journal of Anesthesiology*, vol. 69, no. 3, pp. 296–300, Jun. 2016, doi: 10.4097/kjae.2016.69.3.296.
- [77] M. Ghasemi and A. R. Dehpour, “Ethical considerations in animal studies,” *Journal of medical ethics and history of medicine*, vol. 2, p. 12, 2009, [Online]. Available: <https://www.ncbi.nlm.nih.gov/pmc/articles/PMC3714121/>.
- [78] American Psychological Association, “Guidelines for Ethical Conduct in the Care and Use of Animals,” <https://www.apa.org>, 2012.
- [79] “Euthanasia,” American Veterinary Medical Association, 2007. <https://www.avma.org/resources/pet-owners/petcare/euthanasia>.
- [80] V. Volarevic et al., “Ethical and Safety Issues of Stem Cell-Based Therapy,” *International Journal of Medical Sciences*, vol. 15, no. 1, pp. 36–45, Jan. 2018, doi: 10.7150/ijms.21666.

[81] J. Lowenthal and J. Sugarman, “Ethics and Policy Issues for Stem Cell Research and Pulmonary Medicine,” *Chest*, vol. 147, no. 3, pp. 824–834, Mar. 2015, doi: 10.1378/chest.14-1696.

[82] “Accuracy and Precision With the Countess II FL Automated Cell Counter - US,” [www.thermofisher.com](http://www.thermofisher.com).  
<https://www.thermofisher.com/us/en/home/life-science/cell-analysis/cell-analysis-learning-center/cell-analysis-resource-library/cell-analysis-application-notes/accuracy-precision-countess-ii-fl-automated-cell-counter.html#:~:text=When%20manually%20counting%20cells%20using> (accessed Feb. 27, 2022).

[83] Ultimaker, “Ultimaker S5: Reliability at Scale,” [ultimaker.com](http://ultimaker.com), 2022.  
<https://www.ultimaker.com/3d-printers/ultimaker-s5> (accessed Feb. 28, 2022).

## Appendix

### Section 1: Product Design Specifications

#### **Product Design Specification**

#### **Automatic Intraoperative Stem Cell Injection Device**

Team Heartthrob  
Lab 304  
December 14th, 2022

Team Members:	Parker Esswein	Team Leader
	Macy Frank	Communicator
	Vanessa Obrycki	BWIG
	Lars Krugel	BPAG
	Gab Zuern	BSAC

#### **Function:**

Treating heart failure by injecting mesenchymal stem cells (MSCs) into the myocardium via an injection device and a needle-tipped catheter is a novel approach that can save lives and significantly improve quality of life. Unfortunately, this procedure is currently performed manually utilizing a 1 mL syringe (10 - 14 sequential injections), so stem cells are delivered through the catheter and into the myocardium at an uncontrolled injection and flow rate. To improve stem cell delivery and cardiac repair, an automatic injection device that integrates with 1 mL procedural syringes, medical grade tubing, and a clinical catheter is desired. This device will limit operator intervention and provide a slow, controlled, and adjustable injection rate to maximize cell retention and enhance clinical success. The device will operate at two different injection rates, 30 seconds and 60 seconds, and complete 10 - 14 injections, each containing 0.5 mL of a MSC solution, per procedure. The injector will also maintain standard cell viability throughout the procedure as determined by current manual intramyocardial MSC injection procedures. The device must contain a force detection system that reads the force from the syringe and visually alerts the user if the force threshold value of 2.40 N is reached (represents potential catheter obstruction or cell backflow). This automatic injector will result in less labor-intensive intramyocardial stem cell injection procedures, enhancing the accuracy, efficiency, and efficacy of each operation.

#### **Client requirements:**

- Injector must be compatible with the standard catheters, medical grade tubing, and procedural 1 mL syringes currently used in practice
- The injector must be able to integrate with standard 1 mL syringes, securely locking each syringe in place during the intramyocardial injection procedure
- Non-infectious porcine derived MSCs will be used for cell viability testing (must display less than 5% cell death relative to post-thawing cell viability) and procedural injections
- The injector will consist of two different injection rates (30 and 60 seconds) that deliver

- 0.5 mL of a MSC solution per injection
- The force detection system must display less than 5% error relative to the actual applied force
- Volume of solution delivered from the syringe after the completion of each injection must be within 5% of the 0.5 mL MSC aliquot solution volume, taking into account the dead space within the distal tip of the syringe
- Injection automation should begin and end with a single start/stop button click and be electrically controlled
- Visual feedback must be provided to the operator when the force threshold value (2.40 N) is read from the syringe to indicate the potential for catheter obstruction or MSC aliquot solution backflow
- Ability to be used as a research device
- The project's budget is \$3000
- The injector should cost no more than \$500 to manufacture

## **Design requirements:**

### 1. Physical and Operational Characteristics

#### *a. Performance requirements:*

The automatic injection device must be electronically controlled and capable of injecting MSCs into the myocardium. The stem cell injection flow rate must be adjustable, consisting of a 30 second rate and a 60 second rate capable of introducing the required 0.5 mL MSC solution into the myocardium [1]. The 30 second rate correlates to an injection of 16.7  $\mu\text{L}/\text{sec}$  while the 60 second rate represents a delivery of 8.33  $\mu\text{L}/\text{sec}$  when transmitting 0.5 mL of solution. These two dispensary rates will be produced in 1 mL standard syringes integrated within the injector. In standardized 1 mL syringes, a 30 second flow rate corresponds to the syringe plunger traveling 1 mm/sec while it travels 0.5 mm/sec for a 60 second flow rate. The flow rate must be controlled within the device and capable of repeatability throughout the procedure. Syringes 1 mL in volume must be securely locked into the device, receiving the entire force provided by the injector without exhibiting displacement. The syringes must also be easily replaceable within the device, allowing for rapid reloading (less than 60 seconds) of MSC loaded syringes. The syringes within the device will connect to medical grade tubing that is integrated with the procedural catheter, allowing the catheter to move without hindrance or obstruction. During a typical intramyocardial injection procedure, the injector will perform 10 - 14 injections, each consisting of 30 second or 60 second injection rates followed by a maximum 60 second dwell time [1]. Any blockage or backflow within the syringe or catheter must be monitored. As a result, force values above a threshold of 2.40 N, as read from the syringe, must cause the device to visually notify the user that there is a potential for catheter or syringe obstruction or aliquot backflow. A LED light will illuminate to alert the user that the 2.40 N threshold has been reached or exceeded and the catheter may be backed up [2].

b. *Safety:*

The International Organization for Standardization (ISO) describes medical device risks that must be considered while the device of interest is undergoing its intended use in standard 14971. All risk factors must be mitigated in order to decrease the potential for accidental injury or injection caused by the device [3]. ISO 60601 states that any electrical components within the medical device should present no potential risks to either the healthcare professional or the patient [4]. The device must be fabricated in a manner that effectively covers all wired components and is free of any sharp items in order to ensure the well-being of the user and patient. All electrical components within the device will be properly labeled. Each item in contact with the MSCs can not present biological hazards, chemical altering materials, or mechanically disrupting forces that may change and modify the biological components of the individual stem cells per ISO 10993 [5]. This also requires that the materials in contact with the stem cells are mechanically stable, capable of enduring any applied force from the injector without breaking, preventing potential harmful contact with the MSCs. Each component within the device must be able to perform each injection without exhibiting deformation. Instructions for the device will be provided and labels will be printed on the device to prevent any confusion and mitigate risk of endangerment to the user. These labels and instructions will also ensure the device is not damaged by misuse. Liability will not be charged if damage is a result of misuse. The injector can not be toxic, carcinogenic, and harmful upon touch.

c. *Accuracy and Reliability:*

Provided the contents within the syringe are of identical fluid and viscosity properties to each other, all recorded injection rates must be within a 2% difference from the average to prove precision of the automated system and its hardware components. A 2% margin allows for miniscule errors when considering the inevitable dead space within the distal tip of the procedural syringe, medical grade tubing, and catheter. Dispensary times for each rate (30 seconds or 60 seconds) must be within 0.5 seconds of the target goal to ensure the device accurately delivers the given quantity of cells at the desired rate. This error margin will account for inaccurate syringe loading. The volume of fluid dispensed from the syringe after the completion of either injection rate (30 seconds or 60 seconds) must be within 5% of the 0.5 mL volume of fluid inserted in the syringe. The force sensor (includes electronics for monitoring) used to detect the syringe's injection force must provide readings that are within 5% of the actual applied force. All forces read from the device will come from a standardized curve generated via testing and will consist of the average of five different trials, each following the same applied force process. The aforementioned accuracy requirements must be met for each injection performed throughout the device's typical life cycle (see *Life in Service* below).

The MSC viability will be measured following thawing of the frozen cells, before use in the injection device, as well as after delivery through the procedural syringe-catheter

system via Trypan blue staining and a hemocytometer. In intramyocardial stem cell injection procedures, the typical MSC viability is ~88.9% directly after thawing [6]. To ensure successful treatment, the cell viability of MSCs following each injection can not be more than 5% lower than the viability found after thawing (~88.9%).

d. *Life in Service:*

The injector must be operable and maintain accurate injection rates for at least three years, aligning with current injection devices and pumps [7]. Any stepper DC/AC motors utilized in conjunction with the dispensing system will allow accurate and precise injection rates until 10,000 hours of operative use is exceeded. As a result, the injector will be able to perform 1.2 million injections when using the 30 second rate and 600,000 injections using the 60 second rate before motor replacement or repair is required [8]. If the device uses an exterior power supply, such as an outlet, it will be capable of functioning all day, performing procedures whenever required. The device must be small enough to allow for easy transport to different locations within the clinical operating room or hospital or different buildings without the need for mechanical assistance (see the *Size* and *Weight* sections below). If the injection device is powered by a rechargeable lithium-ion battery, it must be able to perform automated injections for at least 28 consecutive minutes, as this is the maximum amount of time required per procedure, correlating to 14 stem cell injections at 60 seconds each and a maximum 60 second dwell time in between each injection. See the *Shelf Life* section below for more details about the lifespan of stepper motors and rechargeable lithium-ion batteries. There are no restrictions on the power supply for the injector, so it can use a battery or exterior power source, such as an outlet or computer, during procedures as long as it can provide power for over 28 minutes.

e. *Shelf Life:*

When the injector is not in use, it will be stored within the clinical operating room used for intramyocardial stem cell injection procedures or in a storage room with environmental conditions that can be considered the same as the operating room. As a result, while in storage, the device will experience typical clinical operating room conditions; room temperature (20 °C to 25 °C), low and stable humidity (30% - 50% relative humidity) [9], and average atmospheric pressure (101.35 kPa) [10]. In this storage environment, the entire injector should be able to maintain functionality and efficacy for at least three years, consistent with current injection devices [7]. As a result, all components must be minimally affected by corrosion and should not experience any deterioration during the injector's typical life cycle.

Stepper DC/AC motors exhibit a life-time of about 10,000 operating hours, which corresponds to about 4.8 years if used for eight hours per day [11]. As the stepper motor is only utilized for 28 minutes per injection procedure and undergoes rest periods throughout the day due to the time between treatments (see the *Life in Service* section above), it will not consistently run for eight hours per day. This reduces the duty cycle for the stepper motor relative to a motor running constant eight hour shifts

each day. The lighter usage paired with the motor experiencing a minimal centric load (maximum force of 3.00 N [2]) prevents excessive bending and damage from being experienced throughout its service. This enables the stepper motor to meet and surpass the expected 4.8 year functioning duration when utilized in the injector, demonstrating that its shelf-life will be even longer as it does not have a duty cycle or load application, eliminating the need for replacement during the injection device's three year lifespan. Rechargeable lithium-ion batteries have a shelf-life of about five years (~2000 charge cycles) [12], so these batteries should not require replacement during the typical timetable of the injector if they are used within the design. The circuitry components, such as the wires, LEDs, and digital display, within the injector have a shelf-life of 50 - 70 years [13]. There should not be deterioration or loss of functionality concern with any component of the injector that is in storage throughout its typical usage cycle.

*f. Operating Environment:*

The injector device will be used for intramyocardial stem cell injections that are performed in typical clinical operating rooms. As a result, the injector base, its automatic and electrical components, and the feedback system will be exposed to room temperature (20 °C to 25 °C) and low and stable humidity (30% - 50% relative humidity) [9]. The average atmospheric pressure that the injector will experience is 101.35 kPa [10]. As the injector will rest on a table, a patient bed, or within a clinician's hand, it will be exposed to the dust particles and dirt contained on these surfaces and within the air. During the intramyocardial injection procedure, the device may interact with the physiological MSC aliquot solution used in each injection as well as patient blood. While the aliquot solution contains salt, the 0.5 mL injections present only a small exposure to the injector that enable its corrosiveness to be considered negligible. Blood is not corrosive and thus does not pose a concern for the injector.

Shock loading, vibration, and noise level are considered negligible. As the device is used for clinical injections, medical professionals will be the primary handlers of the injector. When not in use, the device will be kept within a sterile bag and either left in the clinical operating room or stored in a storage unit within the same or a similar room. As a result, the aforementioned operating conditions apply to the injector during storage and idle time.

*g. Ergonomics:*

The injector is used in conjunction with a syringe, medical grade tubing, and an intravenous catheter to inject MSCs through the syringe-catheter system at a controlled and adjustable rate. The injector should not be used for any other purpose or in conjunction with other devices. It should be properly connected to the syringe (see *Performance Requirements* section above) and positioned for the procedure following the insertion of the catheter into the target tissue and the connection of the injection syringe to the medical grade tubing and catheter. The



device should be kept within a sterile bag when not in use and throughout each intramyocardial stem cell injection procedure.

The injector base should not experience a stress value greater than 49.5 MPa [14] and the operator needs to pay close attention to the injector when it applies a force greater than 2.40 N (indicated by a visual feedback signal) to the syringe as catheter obstruction or MSC backflow is imminent [2]. If the operator suspects catheter obstruction or MSC backflow as a result of the detected force value or the stifling of aliquot solution movement, the injector must be manually stopped. The electrical components within the injector should not be modified or altered unless errors result during injector operation. Outside of blood and the physiological MSC aliquot solution, the injector should not be exposed to liquids. The injector should not be dropped from a height greater than one meter [15] and sharps should be treated with care when they are used in conjunction with the device.

h. *Size:*

The device should not be larger than 30 × 20 × 15 cm in order to fit within the desired operating table or drape location. A typical cardiac operating room ranges from 121.92 - 198.12 m<sup>2</sup> and contains large equipment such as anesthesia machines, a stretcher, monitors, sterilization equipment, and a surgical table [16]. The device will rest on any available space of the cathtable or be positioned on drapes in the patient's leg region. The device should also be easily transportable and moveable, especially since the device may need to be repositioned during a procedure. Additionally, all components of the device should be easily accessible for maintenance and sterilization.

i. *Weight:*

The device should be lightweight, ideally less than 3.00 kg, in order to make it easily transportable and comparable to other devices that are currently on the market such as the Baxter device (2.81 kg) [7]. A proper weight will ensure that the user does not incur a hand cramp if holding the device during the 10 - 14 cycles of 30 - 60 second injections.

j. *Materials:*

Materials used to fabricate the automatic injection device need to be compatible with standard 1 mL clinical syringes, medical grade tubing, therapeutic catheters, MSCs, and a sterile operating environment. A force sensor with a sensitivity of 0.01 N over a 0.00 N - 10.00 N range is required to properly read the force applied by the automatic injection device to the syringe and thus MSC aliquot solution [2]. The force application block system must contain a motor that can move the force application block forward at a rate that enables the injector to deliver the entire 0.5 mL MSC aliquot solution within 30 and 60 seconds. While the physiological MSC aliquot solution contains salt, the 0.5 mL injections present only a small exposure to the injector that enable its corrosiveness to be considered negligible. As a precautionary step to mitigate the corrosion risk of the device

via the aliquot solution, the injector should only contain metal where necessary [17].

k. *Aesthetics, Appearance, and Finish:*

The device should be able to produce visual feedback that is obvious and easy to interpret. It will notify the user that the threshold syringe pushing force (2.40 N) has been reached and that there may be a clog within the catheter that could result in product damage, inadequate delivery, or cell death. The operator should understand that they must slow the injection or stop the injection in order to ensure maximum cell viability, which can not decrease more than 5% from the starting viability. The force application system should have a smooth surface along all of its components, where applicable, to minimize the friction present between each material and thus enable a smooth and consistent force application to the syringe plunger. Other aesthetics associated with the device are not important.

## 2. Production Characteristics

a. *Quantity:*

One unit that is compatible with 1 mL syringes is needed.

b. *Target Product Cost:*

The injector should be manufactured at a cost of no more than \$500, demonstrating that it can be treated as a clinically disposable device [18]. Although there are not any automated injector devices used for the delivery of MSCs and thus there is not a direct price comparison that can be adequately made, there are similar devices that can be evaluated. For example, Baxter's Infus OR Syringe Pumps are used by anesthesiologists to deliver anesthesia from large syringes at a specified controlled rate. These products tend to sell for ~\$3000 - \$4000 [19]. See the *Competition* Section below for more information on the cost of similar devices.

## 3. Miscellaneous

a. *Standards and Specifications:*

The fabrication of the automatic injection device and the product itself should adhere to various standards and regulations in order to allow for the development of a successful product that interacts accurately, effectively, and safely with operators and patients and can be commercialized. The Code of Federal Regulations (CFR) Title 21 Part 820 provides quality system regulations, including the requirements related to the methods used in designing, manufacturing, packaging, labeling, storing, installing, and servicing of medical devices intended for human use [20]. As the injector will be used in conjunction with syringes, medical grade tubing, and

catheters that interact directly with patients, it should follow and meet the quality guidelines outlined in the CFR. This will allow good standard operating procedures to be followed in relation to the fabrication and commercialization of the product. The CFR Title 21 Part 870 identifies a Percutaneous Transluminal Coronary Angioplasty Catheter used for the treatment of acute myocardial infarction as a Class II medical device and specifies the procedure required for this class [21]. As the injector will be used for treating heart failure induced by myocardial infarction and provides an intermittent risk to patients (controls MSC injections into the myocardium), the injector can also be categorized as a Class II medical device and thus needs to adhere to the procedures outlined by this CFR. Current injection devices and syringe pumps used for drug delivery are identified as Class II medical devices [22]. This further supports the classification of the injector as a Class II device that must adhere to the process provided in CFR Title 21 Part 870, as MSC delivery will require considerations consistent with drug delivery.

The CFR Title 21 Part 3.2 categorizes the injection device as a combination product, due to its interaction with a medical device (syringe) and biological product (MSCs) in order to achieve its intended therapeutic effect. This standard provides the procedure for identifying the designated agency component and preparing it for premarket review and regulation [23]. If the injector device is pursued as a combination product rather than focusing on its design individually, this CFR will have to be followed in order to allow proper agency designation and to meet premarket review requirements.

The CFR Title 21 Part 610 provides the performance, testing, and safety requirements, labeling standards, and sterility expectations for biological products, such as MSCs [24]. As the injector will interact with a syringe that contains MSCs, it is important to have familiarity with the MSCs themselves and the performance and safety requirements they must adhere to. The CFR Title 21 Part 1271 describes the current good tissue practices that must be followed for cells, tissues, and cellular and tissue-based products, including their processing, manipulation, and associated manufacturing procedures, facilities, and equipment [25]. As the injector may interact directly with the MSCs via the force detection system, it must be designed in a manner that meets the requirements associated with the MSCs, limits the induction of cell apoptosis, and prevents the introduction, transmission, and spread of communicable diseases.

*b. Customer:*

The customers that would be using this product are cardiac surgeons, specifically, Dr. Amish Raval (the client). This product will be used during Dr. Raval's intramyocardial stem cell injection clinical trials and then during clinical procedures when stem cell injection therapy is approved for clinical use. Surgeons would like to be able to have less manual labor and thus fatigue (hand-cramping or freezing up) when performing these procedures and using the injector devices. As a result, having a simple device that can be programmed to automatically inject the cells at a certain injection rate over a specified

amount of time with a single click of a button (turns the device on and off) would be very beneficial for the surgeons. This product should provide a precise way to inject the cells over a steady rate and notify the surgeon at certain force differentials so that each surgery proceeds successfully.

Outside of use in clinical trials and procedures, the device will be used by researchers to conduct experiments to study the effectiveness, accuracy, and efficacy of the intramyocardial stem cell injection procedure that is currently being performed. For example, the device can be utilized to determine the amount of force the MSCs are experiencing while being injected into different tissue types and with various injection rates. It can also be used to determine the optimal injection rate for this procedure that maximizes localized cell retention at the site of interest within the myocardium and cell viability.

*c. Patient-related concerns:*

The device needs to be sterile as it will be in the operating room and on the table next to the patient or on a drape in the patient's leg region. The injection device must perform the required 30 and 60 second injection rates repeatedly and consistently for each procedure to prevent health risks to the patient associated with product dysfunction.

*d. Competition:*

There are currently products on the market that involve similar concepts to the automated stem cell injector, but no device has all of the components that will be included in the final design for this device. One type of device that is a competitor to the injector is an automated syringe pump. These systems are used by anesthesiologists to inject a controlled volume of anesthesia into the patient over time. The Baxter Infus OR Syringe Pump ABC 4100, is an infusion pump device that is compatible with 1, 3, 5, 10, 20, 30, 60 and 140 mL syringe sizes. To operate the device, the syringe is front loaded and locked into place. The anesthesiologist would then enter a flow rate and the type of drug being used, clicking start to initiate the injection. The advantage to the Baxter device is that it is able to sense syringe plunger force and movement and has a system to detect and monitor delivery accuracy as well as alarms with audio and LED lights [26]. The disadvantages and limitations include that this system is not tailored to eject fluid at the rate that is needed for intramyocardial stem cell delivery and has not been proven to maintain cell viability for MSCs. See Figure 1 below for this Baxter Syringe Pump along with an additional Baxter Syringe Pump.



Figure 1: The “Baxter Infus OR Syringe Pump ABC 4100” that is sold for ~\$3000 using the trade-in program (left image) [26] and the “Baxter Infus O.R. Syringe Pump Refurbished” that is sold for ~\$4000 (right image) [19].

Another competing device is the apparatus used to inject IV fluids into patients. This device is able to transfer fluids from a bag directly into the person through connection tubing at a programmed rate. There is also another similar device called the Contract Delivery System from ACIST Medical Group that is used for angiographic procedures to deliver an iopamidol injection. The advantages to this device include a controlled flow rate system that is compatible with catheters and has been used in procedures involving cardiology and radiology [27]. The disadvantages, however, is that this device is not tailored to eject the 0.5 mL volume of stem cells from a 1 mL syringe for 10-14 injections over a period of 30-60 seconds. In addition, similar to the Baxter device, the IV machines were not proven to be compatible with stem cells. This product can be seen in Figure 2 below.

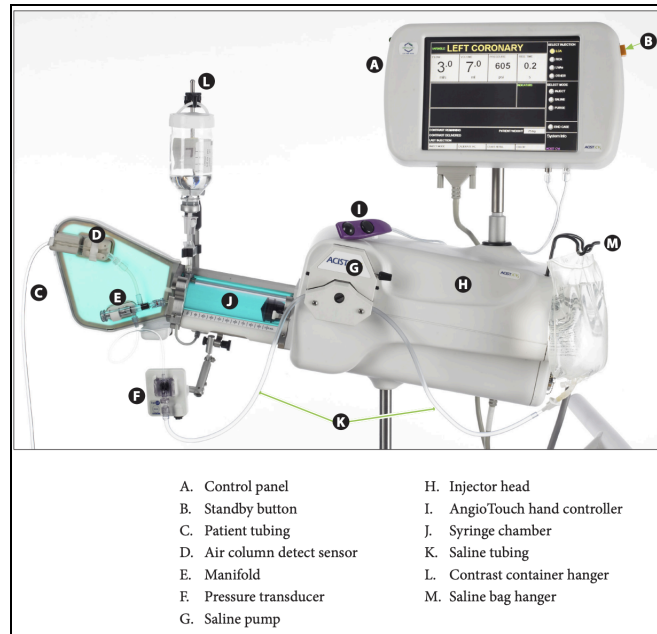


Figure 2: Diagram of the important user components in the Acist Contrast Delivery System a [36].

Lastly, there was a device in preclinical trials in 2017 that was fabricated to deliver cells. This product was called an “automated injection device for intradermal delivery of a cell-based therapy”. The current status of the product is unknown and the device is not currently patented or on the market. The limitation to this device is that it delivers solutions directly into a patient via the hypodermic needle and has not been proven to be compatible with the connection tubing / catheter system that is needed for the injections [28]. Although it may be easy to operate by pushing the trigger button, the disadvantage is that the flow rate of the solution is not tailored for the 30 and 60 second injection times for 0.5 mL of solution in the 1 mL syringe which is needed for intramyocardial stem cell injection procedure. The device can be seen in Figure 3 below.

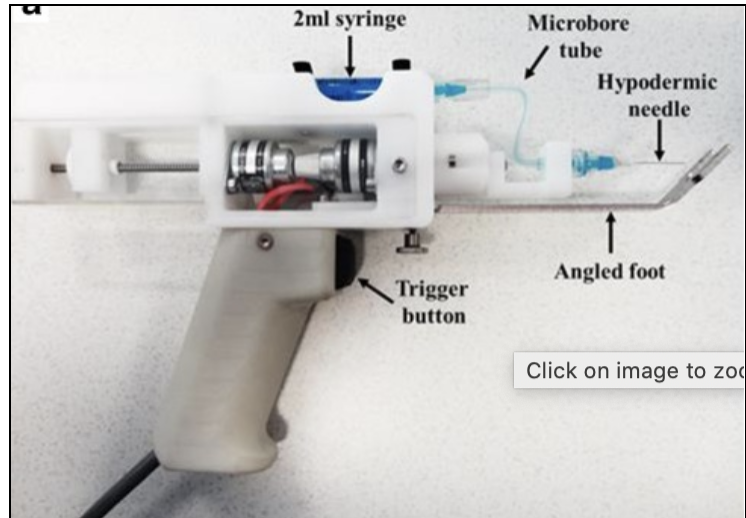


Figure 3: Automated injector device that was in preclinical development in 2017 [28].

Although these infusion pump systems and injection devices have positives when it comes to injecting a solution into a patient, they have not been proven to work well with stem cell delivery and in conjunction with the catheter system that goes into the myocardium. These features are important because MSC viability must be maintained for the intramyocardial stem cell injection procedures to be successful and the MSC aliquot solution must be able to transport through the catheter and into the heart. Additionally, the devices on the market do not contain force detection systems that provide accurate algorithms for determining the pressure needed for injecting cells into the myocardium.

The JP2019069165A patent (see Figure 4 below) involves a system which has an automatic injector device that uses cassettes to hold the injectate. This is an automatic device that could be engaged by the push of a button via its superior end. However, this apparatus is not extremely similar to the cardiac repair injector device that will be fabricated since it does not have syringe or catheter compatibility, it does not have a controlled injection rate, and does not have a pressure-detecting system that can trigger visual feedback [29].

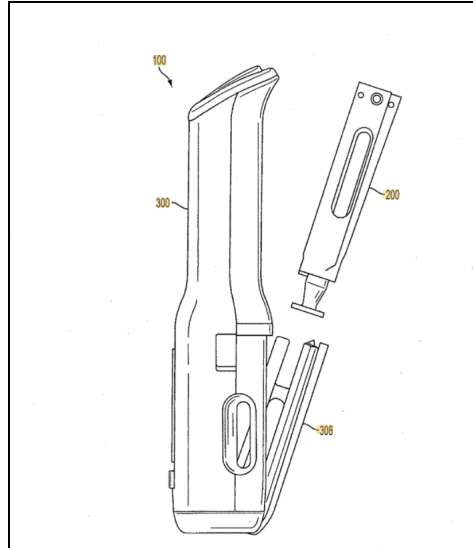


Figure 4: The cassette automatic injector device [29].

Lastly, the US Patent US4759750A (see Figure 5 below) is relevant to the current objective of detecting the force and / or pressure the cells are experiencing during the injections [30]. Specifically, the patent is for a Pressure Sensing Syringe which has a pressure sensitive piston between the syringe plunger and the thumb. The device also provides a tactile signal when a specified pressure is applied so that a person directing fluid somewhere can be alerted when a certain preset pressure is reached. This patent is interesting because it allows for a direct way to sense pressure in a fluid filled syringe. There are, however, other similar devices on the market that can also be used to get pressure readings.

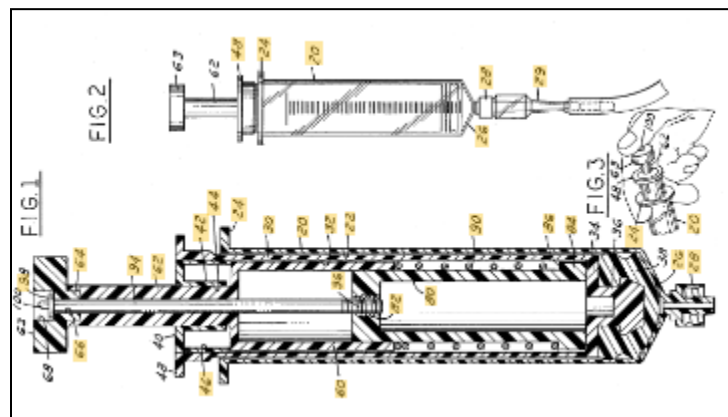


Figure 5: US Patent US4759750A [30]



## References:

- [1] A. N. Raval et al., “Point of care, Bone Marrow Mononuclear Cell Therapy in Ischemic Heart Failure Patients Personalized for Cell potency: 12-month Feasibility Results from CardiAMP Heart Failure roll-in Cohort,” *International Journal of Cardiology*, vol. 326, pp. 131–138, Mar. 2021, doi: 10.1016/j.ijcard.2020.10.043.
- [2] A. Vo, M. Doumit, and G. Rockwell, “The Biomechanics and Optimization of the Needle-Syringe System for Injecting Triamcinolone Acetonide into Keloids,” *Journal of Medical Engineering*, vol. 2016, 2016, doi: 10.1155/2016/5162394.
- [3] 14:00-17:00, “ISO 14971:2019,” *ISO*, Dec. 2019. <https://www.iso.org/standard/72704.html>.
- [4] ISO - International Organization for Standardization, “IEC 60601-1-11:2015,” *ISO*, 2015. <https://www.iso.org/standard/65529.html>.
- [5] 14:00-17:00, “ISO 10993-1:2018,” *ISO*, Oct. 2018. <https://www.iso.org/standard/68936.html>.
- [6] E. G. Schmuck et al., “Intravenous Followed by X-ray Fused with MRI-Guided Transendocardial Mesenchymal Stem Cell Injection Improves Contractility Reserve in a Swine Model of Myocardial Infarction,” *Journal of Cardiovascular Translational Research*, vol. 8, no. 7, pp. 438–448, Oct. 2015, doi: 10.1007/s12265-015-9654-0.
- [7] F. and D. Administration, “Guidance for Industry and FDA Staff: Technical Considerations for Pen, Jet, and Related Injectors Intended for Use with Drugs and Biological Products,” Food and Drug Administration, 10903 New Hampshire Avenue, WO-32 Hub 5129 Silver Spring, MD 20993, Jun. 2013. Accessed: Feb. 08, 2022. [Online]. Available: <https://www.fda.gov/files/about%20fda/published/Technical-Considerations-for-Pen--Jet--and-Related-Injectors-Intended-for-Use-with-Drugs-and-Biological-Products.pdf>.
- [8] “Brushless DC Motors | Low Prices, High Quality,” [www.anaheimautomation.com](http://www.anaheimautomation.com). <https://www.anaheimautomation.com/marketing/brushless-dc/brushless-dc-motors.php>.
- [9] Primex, “Laboratory Temperature and Humidity Requirements & Compliance | Primex,” [www.primexinc.com](http://www.primexinc.com), Dec. 22, 2020. <https://www.primexinc.com/en/blog/laboratory-temperature-humidity-requirements.html> (accessed Sep. 21, 2021).
- [10] M. Bell, “What is the average air pressure at the surface of the Earth?,” [Columbia.edu](http://Columbia.edu), 2019. [https://iridl.ldeo.columbia.edu/dochelp/QA/Basic/atmos\\_press.html](https://iridl.ldeo.columbia.edu/dochelp/QA/Basic/atmos_press.html) (accessed Sep. 21, 2021).
- [11] A. Automation, “Stepper Motor Guide | Anaheim Automation,” [www.anaheimautomation.com](http://www.anaheimautomation.com), 2021. <https://www.anaheimautomation.com/manuals/forms/stepper-motor-guide.php#:~:text=The%20typical%20lifetime%20of%20a%20stepper%20motor%20is%2010%2C000%20operating>

%20hours. (accessed Sep. 19, 2022).

- [12] A. Lerma, "Lithium-Ion Vs Lead Acid Battery Life," [www.fluxpower.com](http://www.fluxpower.com), Mar. 14, 2019. <https://www.fluxpower.com/blog/lithium-ion-vs.-lead-acid-battery-life> (accessed Feb. 09, 2022).
- [13] H. Miles, "How Long Does Electrical Wiring Last in a Home?," *Home Inspection Insider*, Jan. 08, 2022. <https://homeinspectioninsider.com/how-long-electrical-wiring-last/#:~:text=The%20average%20life%20expectancy%20of> (accessed Feb. 08, 2022).
- [14] Ultimaker, "Technical Data Sheet - PLA," Nov. 2018. Accessed: Dec. 02, 2021. [Online]. Available: <https://ultimaker.com/materials/pla>.
- [15] A. Schwartz and H. Seeger, "Are Adrenaline Autoinjectors Fit for purpose? a Pilot Study of the Mechanical and Injection Performance Characteristics of a cartridge- versus a syringe-based Autoinjector," *Journal of Asthma and Allergy*, vol. 3, p. 159, Nov. 2010, doi: 10.2147/jaa.s14419.
- [16] "Design distinctions for exam, procedure and operating rooms," [www.hfmmagazine.com](http://www.hfmmagazine.com), Oct. 08, 2019. <https://www.hfmmagazine.com/articles/3764-design-distinctions-for-exam-procedure-and-operating-rooms#:~:text=While%20the%20minimum%20requirements%20for> (accessed Feb. 06, 2022).
- [17] E. H. and Safety, "Ethylene Oxide," *Environmental Health & Safety | Baylor University*, 2022. <https://www.baylor.edu/ehs/index.php?id=93792> (accessed Sep. 19, 2022).
- [18] Dr. A. Raval, "Manufacturing cost of final automatic injection system product," Jan. 2022
- [19] "Baxter Infus O.R. Syringe Pump Refurbished." 4MD Medical Solutions, [https://www.4mdmedical.com/index.php/catalog/product/view/id/253457/s/infusor-syringe-pump-refurbished?CAWELAID=120141310000056386&CAGPSPN=pla&gclid=CjwKCAiAo4OQBhBBEiwA5KWu\\_8f3uyspUWEZJ9eX8-duXozZ5qbgAjz8DOYtmfDnjlz8zi4LdJ5RxoCcrIQAvD\\_BwE](https://www.4mdmedical.com/index.php/catalog/product/view/id/253457/s/infusor-syringe-pump-refurbished?CAWELAID=120141310000056386&CAGPSPN=pla&gclid=CjwKCAiAo4OQBhBBEiwA5KWu_8f3uyspUWEZJ9eX8-duXozZ5qbgAjz8DOYtmfDnjlz8zi4LdJ5RxoCcrIQAvD_BwE).
- [20] Food and Drug Administration, "CFR - Code of Federal Regulations Title 21," [Fda.gov](http://Fda.gov), 2019. <https://www.accessdata.fda.gov/scripts/cdrh/cfdocs/cfCFR/CFRSearch.cfm?CFRPart=820> (accessed Feb. 09, 2021)
- [21] F. and D. Administration, "CFR - Code of Federal Regulations Title 21 Part 870," [www.accessdata.fda.gov](http://www.accessdata.fda.gov), Jan. 06, 2022. <https://www.accessdata.fda.gov/scripts/cdrh/cfdocs/cfcfr/cfrsearch.cfm?fr=870.5100> (accessed Feb. 08, 2022).

- [22] U. S. Food and Drug Administration, “Product Classification,” <https://www.accessdata.fda.gov>, 2020.  
<https://www.accessdata.fda.gov/scripts/cdrh/cfdocs/cfPCD/classification.cfm?ID=FRN>  
(accessed May 01, 2022).
- [23] F. and D. Administration, “CFR - Code of Federal Regulations Title 21 3.2,” Code of Federal Regulations, Feb. 07, 2022.  
<https://www.ecfr.gov/current/title-21/chapter-I/subchapter-A/part-3/subpart-A/section-3.2>  
(accessed Feb. 08, 2022).
- [24] F. and D. Administration, “CFR - Code of Federal Regulations Title 21 Part 610,” U.S. Food and Drug Administration, Jan. 06, 2022.  
<https://www.accessdata.fda.gov/scripts/cdrh/cfdocs/cfcfr/cfrsearch.cfm?cfrpart=610>  
(accessed Feb. 08, 2022).
- [25] F. and D. Administration, “CFR - Code of Federal Regulations Title 21 Part 1271,” [www.accessdata.fda.gov](http://www.accessdata.fda.gov), Mar. 29, 2022.  
<https://www.accessdata.fda.gov/scripts/cdrh/cfdocs/cfcfr/CFRSearch.cfm?CFRPart=1271>  
(accessed Sep. 19, 2022).
- [26] “Baxter Infus or Syringe Pump ABC 4100 Trade in Program.” Wilburn Medical Equipment and Supplies,  
<https://wilburnmedicalusa.com/baxter-infus-or-syringe-pump-abc-4100-trade-in-program/>.
- [27] Acist | CVI® Contrast Delivery System.  
<http://acist.com/wp-content/uploads/2019/09/901418-00301-Users-Guide-CVi-MU-English-USA.pdf>.
- [28] Leoni, G., Lyness, A., Ginty, P., Schutte, R., Pillai, G., Sharma, G., Kemp, P., Mount, N., & Sharpe, M. (2017). Preclinical development of an automated injection device for intradermal delivery of a cell-based therapy. *Drug delivery and translational research*, 7(5), 695–708.  
<https://doi.org/10.1007/s13346-017-0418-z>
- [29] P. Mounce *et al.*, “Medicament cassette, automatic injector, and automatic injector system,” May 09, 2019
- [30] J. H. DeVries and R. J. VanPopering, “Pressure sensing syringe,” US4759750A, Jul. 26, 1988 Accessed: Oct. 03, 2022. [Online]. Available:  
<https://patents.google.com/patent/US4759750A/en>

## Section 2: Material Information and Calculations

### Section 2.1: Arduino Uno Rev 3 Technical Data Sheet

Arduino Uno is a microcontroller board based on the ATmega328P. It has 14 digital input/output pins (six can be used as PWM outputs), six analog inputs, a 16 MHz ceramic resonator (CSTCE16M0V53-R0), a USB connection, a power jack, an ICSP header and a reset button.

Table 1: Arduino Uno Rev 3 Technical Specifications [1].

MICROCONTROLLER	ATmega328P
OPERATING VOLTAGE	5V
INPUT VOLTAGE (RECOMMENDED)	7-12V
INPUT VOLTAGE (LIMIT)	6-20V
DIGITAL I/O PINS	14 (of which 6 provide PWM output)
PWM DIGITAL I/O PINS	6
ANALOG INPUT PINS	6
DC CURRENT PER I/O PIN	20 mA
DC CURRENT FOR 3.3V PIN	50 mA
FLASH MEMORY	32 KB (ATmega328P) of which 0.5 KB used by bootloader
SRAM	2 KB (ATmega328P)
EEPROM	1 KB (ATmega328P)
CLOCK SPEED	16 MHz
LED_BUILTIN	13

#### **References:**

- [1] A. Staff, "Arduino Uno Rev3," Arduino.cc, 2019.  
<https://store.arduino.cc/usa/arduino-uno-rev3> (accessed Feb. 25, 2021).

## Section 2.2: FSR 400 Series Round Force Sensing Resistor Technical Data Sheet

Interlink Electronics FSR 400 series is part of the single zone Force Sensing Resistor family. Force Sensing Resistors (FSRs) are robust polymer thick film (PTF) devices that exhibit a decrease in resistance with increase in force applied to the surface of the sensor. This force sensitivity is optimized for use in human touch control of electronic devices such as automotive electronics, medical systems, and in industrial and robotics applications. The standard 402 sensor is a round sensor 18.28 mm in diameter. Custom sensors can be manufactured in sizes ranging from 5 mm to over 600 mm. Female connector and short tail versions can also be ordered [1].

Table 1: FSR 400 Series Sensor characteristics [1].

Feature	Condition	Value*	Notes
<b>Actuation Force</b>		0.1 Newtons	
<b>Force Sensitivity Range</b>		0.1 - 10.0 <sup>2</sup> Newtons	
<b>Force Repeatability<sup>3</sup></b>	(Single part)	± 2%	
<b>Force Resolution<sup>3</sup></b>		continuous	
<b>Force Repeatability<sup>3</sup></b>	(Part to Part)	±6%	
<b>Non-Actuated Resistance</b>		10M W	
<b>Size</b>		18.28mm diameter	
<b>Thickness Range</b>		0.2 - 1.25 mm	
<b>Stand-Off Resistance</b>		>10M ohms	Unloaded, unbent
<b>Switch Travel</b>	(Typical)	0.05 mm	Depends on design
<b>Hysteresis<sup>3</sup></b>		+10%	$(R_{F+} - R_{F-})/R_{F+}$ .
<b>Device Rise Time</b>		<3 microseconds	measured w/steel ball
<b>Long Term Drift</b>		<5% per log <sub>10</sub> (time)	35 days test, 1kg load
<b>Temp Operating Range</b>	(Recommended)	-30 - +70 °C	
<b>Number of Actuations</b>	(Life time)	10 Million tested	Without failure

\*Specifications are derived from measurements taken at 1000 grams, and are given as one standard deviation / mean, unless otherwise noted.

1. Max Actuation force can be modified in custom sensors
2. Force Range can be increased in custom sensors. Interlink Electronics have designed and manufactured sensors with operating force larger than 50 kg
3. Force sensitivity depends on mechanics, and resolution depends on measurement electronics.

**References:**

- [1] I. Electronics, “FSR 400 Data Sheet Figure 1 -Typical Force Curve Industry Segments Interlink Electronics -Sensor Technologies FSR 400 Series Round Force Sensing Resistor,” 2021. Accessed: Feb. 15, 2022. [Online]. Available: <https://cdn.sparkfun.com/datasheets/Sensors/ForceFlex/2010-10-26-DataSheet-FSR400-Layout2.pdf>.

## Section 2.3: FSG020WNPB Series Force Sensor Technical Data Sheet

The FSG Series Force Sensor provides precise, reliable force sensing performance in a compact commercial-grade package. The sensor features a specialized piezoresistive micro-machined silicon sensing element. The piezoresistors are structured in a low power, unamplified, non-compensated Wheatstone bridge circuit design that provides inherently stable mV outputs over the 5 N force range. This force sensor operates on the principle that the resistance of the silicon-implanted piezoresistor will increase when the resistors flex under any applied force. The sensor concentrates force from the application, through the stainless steel plunger, directly to the silicon-sensing element. The amount of resistance changes in proportion to the amount of force applied to the sensor. This change in circuit resistance results in a corresponding mV output level change [1].

Table 1: FSG020WNPB Series Force Sensor performance characteristics [1].

Characteristic	Unit	FSG005WNPB			FSG010WNPB			FSG015WNPB			FSG020WNPB		
		Min.	Typ.	Max.	Min.	Typ.	Max.	Min.	Typ.	Max.	Min.	Typ.	Max.
Force sensing range	N	0 to 5			0 to 10			0 to 15			0 to 20		
Excitation <sup>2</sup>	Vdc	3.3	10	12.5	3.3	10	12.5	3.3	10	12.5	3.3	10	12.5
Null offset <sup>3</sup>	mV	-30	0	+30	-30	0	+30	-30	0	+30	-30	0	+30
Null shift <sup>4</sup> (25 to 0°, 25 to 50° C)	mV	-	±0.5	-	-	±0.5	-	-	±0.5	-	-	±0.5	-
Span <sup>5</sup>	mV	310	360	395	310	360	395	310	360	395	310	360	395
Linearity (BFSL) <sup>6</sup>	% span	-	±0.5	-	-	±0.5	-	-	±0.5	-	-	±0.5	-
Sensitivity <sup>7</sup>	mV/V/N	6.6	7.2	7.8	3.3	3.6	3.9	2.2	2.4	2.6	1.65	1.8	1.95
Sensitivity shift <sup>8</sup> (25 °C to 0°, 25 °C to 50 °C)	% span	-	±5.0	-	-	±5.0	-	-	±5.0	-	-	±5.0	-
Repeatability <sup>9</sup>	% span	-	±0.2	-	-	±0.2	-	-	±0.2	-	-	±0.2	-
Response time (10 %FS to 90 %FS)	ms	-	0.1	0.5	-	0.1	0.5	-	0.1	0.5	-	0.1	0.5
Input resistance	kΩ	4.0	5.0	6.0	4.0	5.0	6.0	4.0	5.0	6.0	4.0	5.0	6.0
Output resistance	kΩ	4.0	5.0	6.0	4.0	5.0	6.0	4.0	5.0	6.0	4.0	5.0	6.0
Plunger deflection	µm	-	31	-	-	40	-	-	51	-	-	63	-
Overforce <sup>10</sup>	N	-	-	15	-	-	30	-	-	45	-	-	60

### Notes:

1. All force-related specifications are established using dead weight or compliant force.
2. The range of voltage excitation which can be supplied to the product to produce an output which is proportional to force but due to ratiometricity errors may not remain within the specified performance limits. Non-compensated force sensors, excited by constant current (1.5 mA) instead of voltage, exhibit partial temperature compensation of span.
3. The output signal obtained when the zero force is applied to the sensor. Also known as "null" or "zero".
4. The change in the null resulting from a change in temperature. It is not a predictable error as it can shift up and down from unit to unit. Change in temperature causes the entire output curve to shift up or down along the voltage axis.
5. The algebraic difference between output signals measured at the upper and lower limits of the operating force range. Also known as "full scale output" or simply "span".
6. The maximum deviation of product output from a straight line fitted to output measured over the operating force range. The straight line through a set of points which minimizes the sum of the square of the deviations of each of the points from the straight line.

7. The ratio of output signal change to the corresponding input force change. Sensitivity is determined by computing the ratio of span to the specified operating force range multiplied by the supply voltage being used.
8. The maximum deviation in sensitivity due to changes in temperature over the operating temperature range, relative to sensitivity measured at 25 °C.
9. The maximum difference between output readings when the same force is applied consecutively, under the same operating conditions, with force approaching from the same direction within the operating force range.
10. The maximum force which may safely be applied to the product for it to remain in specification once force is returned to the operating force range. Exposure to higher forces may cause permanent damage to the product. Unless otherwise specified, this applies to all temperatures within the operating temperature range.

**References:**

- [1] H. Sensing and Productivity Solutions, “FSG020WNPB,” *Digi-Key Electronics*, 2022.  
<https://www.digikey.com/en/products/detail/honeywell-sensing-and-productivity-solutions/FSG020WNPB/3884049> (accessed Sep. 26, 2022).



## Section 2.4: LCMKD-10N Load Cell Technical Data Sheet

The LCMKD-10N Load Cell from Omega is a LCKD series subminiature industrial compression load cell. It has rugged all stainless steel construction and its high performance strain gauges assure superior linearity and stability. This unit is designed to be mounted on a smooth and flat surface. Temperature compensation is achieved through a miniature circuit board in the cable [1].

Table 1: LCMKD-10N Load Cell specifications and performance characteristics [1].

Specification	Values
Excitation	5 Vdc, 7 Vdc maximum
Output	2 mV/V nominal
5-Point Calibration	0%, 50%, 100%, 50%, 0%
Linearity	±0.25% FSO
Hysteresis	±0.25% FSO
Repeatability	±0.10% FSO
Zero Balance	±2% FSO
Operating Temperature Range	-54 to 121 °C
Compensated Temperature Range	16 to 71 °C
Thermal Effects	Span: ±0.018% FSO/°C Zero: ±0.009% FSO/°C
Safe Overload	150% of capacity
Ultimate Overload	300% of capacity
Bridge Resistance	350 Ω minimum
Full Scale Deflection	25.4 to 76.2 μm
Electrical Connection	1.5 m 4-conductor insulated cable with temperature compensation board
Weight	<14 g
Protection Class	IP54

**References:**

[1] Omega, “LCKD-1KG Load Cell,” *Newark*, 2022.

<https://www.newark.com/omega/lckd-1kg/load-cell-2mv-v-2-2lb-5vdc-rohs/dp/69AJ0415>.

## Section 2.5: Pressure Range Calculations

The distal tip of a typical 1 mL clinical syringe and medical grade tubing contain an inner diameter of ~ 4.50 mm [1]. As this is the diameter that the mesenchymal stem cell (MSC) aliquot solution flows through during each injection when the syringe plunger is compressed and the MSCs transport from the syringe to the medical grade tubing, the inner diameter of the flow module from the P30 Non-Invasive Pressure Sensor must also be ~ 4.50 mm to properly interface with the procedural system. To ensure that the expected pressure during a typical intramyocardial MSC injection procedure does not exceed the 0 kPa - 207 kPa range of the pressure sensor, pressure was calculated across the area that correlates to the tube's 4.03 mm diameter [2]. Using Equation 1 below, the pressure over the expected 0.00 N - 3.00 N force range for the procedure was established utilizing the flow module tube's cross-sectional area ( $1.590 \times 10^{-5} \text{ m}^2$ ) [3, 4].

$$[1] P = F / A$$

1 mL Syringe Distal Tip, P30 Pressure Sensor Tube, and Medical Grade Tubing:

$$\text{Cross-Sectional Area} = \pi * (0.00225 \text{ m})^2 = 1.590 \times 10^{-5} \text{ m}^2$$

$$\text{Minimum Force} = 0.00 \text{ N}$$

$$\text{Pressure} = 0.00 \text{ N} / 1.590 \times 10^{-5} \text{ m}^2 = 0.00 \text{ Pa} = 0.00 \text{ kPa}$$

$$\text{Cross-Sectional Area} = \pi * (0.00225 \text{ m})^2 = 1.590 \times 10^{-5} \text{ m}^2$$

$$\text{Maximum Force} = 3.00 \text{ N}$$

$$\text{Pressure} = 3.00 \text{ N} / 1.590 \times 10^{-5} \text{ m}^2 = 188628.08 \text{ Pa} = 188.63 \text{ kPa}$$

### **References:**

- [1] C. Inc., "BD Plastic Syringe | Maximum & Minimum Flow Rates," *Chemyx Inc*, Dec. 21, 2017.  
<https://www.chemyx.com/uncategorized/bd-plastic-syringe-minimum-maximum-flow-rates/> (accessed Feb. 15, 2022).
- [2] S. M. Devices, "NonInvasive Pressure Sensor," *Strain Measurement Devices*, 2017.  
<https://www.smdsensors.com/products/type/non-invasive-pressure-sensor/> (accessed Oct. 03, 2022).
- [3] F. P. Beer, E. R. Johnston Jr., J. T. DeWolf, and D. F. Mazurek, *Mechanics of Materials*, 8th Edition. McGraw Hill Education, 2020.
- [4] A. Vo, M. Doumit, and G. Rockwell, "The Biomechanics and Optimization of the Needle-Syringe System for Injecting Triamcinolone Acetonide into Keloids," *Journal of Medical Engineering*, vol. 2016, 2016, doi: 10.1155/2016/5162394.

Section 2.6: P30 Non-Invasive Pressure Sensor Technical Data Sheet

The P30 Non-Invasive Pressure Sensor is a small-diameter tubing sensor consisting of two parts assembled together. One part is a low-cost disposable flow module, while the other is a reusable pressure sensor. The sensor can be used to detect pressure in tubing up to 6.35 mm in diameter. The system is ideal for high sanitary applications in biopharmaceutical and medical device industries [1].

Table 1: P30 Non-Invasive Pressure Sensor design specifications [1].

<b><u>Product Specification:</u></b>	
<b>Pressure Range:</b>	0-30 psi
<b>Body Material:</b>	6061-T6 Aluminum, Black Anodize
<b>Pressure Interface:</b>	SMD7615 Disposable Membrane Housing
<b>Cable Part Number:</b>	SMD7720 (18" Length, Male Molex connector one end, other end flying leads)
<b>Overload Protection:</b>	>20 Pound Force
<b>Supply Voltage:</b>	5-24 VDC
<b>Sensor Pinout:</b> Pin # (Molex 53047-0510)	<b>Function</b>
1	VCC
2	I <sup>2</sup> C SCL
3	I <sup>2</sup> C SDA
4	Analog Out
5	GND
<b>Performance Specifications:</b>	
Output	I <sup>2</sup> C and 0-5 V Analog
Zero psi	3277 (I <sup>2</sup> C Counts 0.5 VDC)
Span (30 psi)	26214 (I <sup>2</sup> C Counts 4.0 VDC)

**References:**

- [1] S. M. Devices, "NonInvasive Pressure Sensor," *Strain Measurement Devices*, 2017. <https://www.smdsensors.com/products/type/non-invasive-pressure-sensor/> (accessed Oct. 03, 2022).

## Section 2.7: LED Serial 7-Segment Digital Display Technical Data Sheet

The Serial 7-Segment Display is an easy-to-use 4-digit display that is controlled using a serial interface and only requires a pin to control the LEDs. Using either a serial, I<sup>2</sup>C, or SPI interface, all digits, decimal points, the colon, and the apostrophe can be controlled [1].

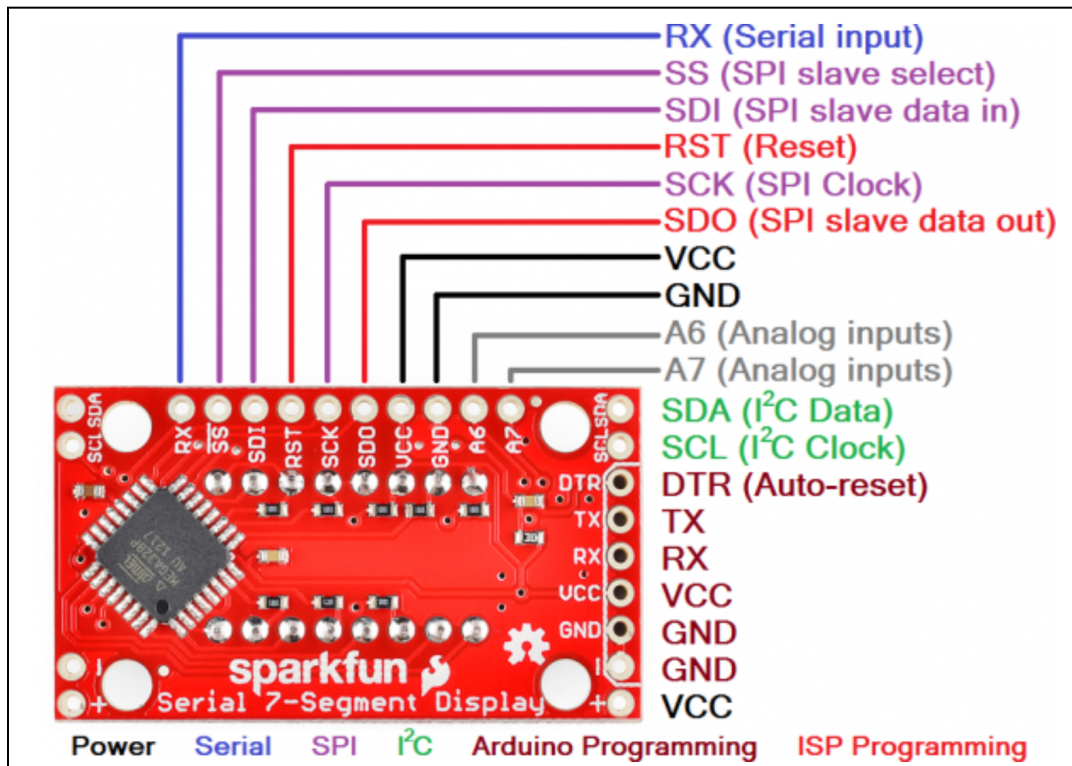


Figure 1: Pin-out schematic for the LED Serial 7-Segment Digital Display [1].

### References:

- [1] J. Blom, "Using the Serial 7-Segment Display," learn.sparkfun.com, 2022.  
<https://learn.sparkfun.com/tutorials/using-the-serial-7-segment-display/introduction>

## Section 2.8: INA129 Instrumentation Amplifier Technical Data Sheet

The INA129 Instrumentation Amplifier is a low-power, general-purpose instrumentation amplifier that offers excellent accuracy (50  $\mu\text{V}$  sensitivity). The versatile three op amp design and small size makes this amplifier an excellent choice for a wide range of applications. Current-feedback input circuitry provides wide bandwidth even at high gain (200 kHz at  $G = 100$ ). A single external resistor provides a gain ranging from 1 to 10,000. The INA129 gain equation uses a 49.4-k $\Omega$  resistor [1].

Table 1: INA129 Instrumentation Amplifier electrical characteristics [1].

PARAMETER		TEST CONDITIONS		MIN	TYP	MAX	UNIT
<b>INPUT</b>							
$V_{OS}$	Offset voltage (RTI)	$1 \leq G \leq 10000$	INA12xP, INA12xU	$\pm 10 \pm 100 / G$	$\pm 50 \pm 500 / G$		$\mu\text{V}$
			INA12xPA, INA12xUA	$\pm 25 \pm 100 / G$	$\pm 125 \pm 1000 / G$		
	Offset voltage drift (RTI)	$T_A = -40^\circ\text{C}$ to $+85^\circ\text{C}$	INA12xP, INA12xU	$\pm 0.2 \pm 2 / G$	$\pm 0.5 \pm 20 / G$		$\mu\text{V}/^\circ\text{C}$
			INA12xPA, INA12xUA	$\pm 0.2 \pm 5 / G$	$\pm 1 \pm 20 / G$		
PSRR	Power-supply rejection ratio (RTI)	$V_S = \pm 2.25 \text{ V}$ to $\pm 18 \text{ V}$	INA12xP, INA12xU	$\pm 0.2 \pm 20 / G$	$\pm 1 \pm 100 / G$		$\mu\text{V}/\text{V}$
			INA12xPA, INA12xUA		$\pm 2 \pm 200 / G$		
	Long-term stability			$\pm 0.2 \pm 3 / G$			$\mu\text{V}/\text{mo}$
	Input impedance	Differential		$10 \parallel 2$			$\text{G}\Omega \parallel \text{pF}$
		Common-mode		$100 \parallel 9$			
$V_{CM}$	Common-mode voltage <sup>(2)</sup>	$V_O = 0 \text{ V}$		$(V-) + 2$		$(V+) - 2$	V
		Safe input voltage	$R_S = 0 \Omega$			$\pm 40$	V
CMRR	Common-mode rejection ratio	$\Delta R_S = 1 \text{ k}\Omega$ , $V_{CM} = \pm 13 \text{ V}$	G = 1	INA12xP, INA12xU	80	86	dB
				INA12xPA, INA12xUA	73		
			G = 10	INA12xP, INA12xU	100	106	
				INA12xPA, INA12xUA	93		
			G = 100	INA12xP, INA12xU	120	125	
				INA12xPA, INA12xUA	110		
G = 1000	INA12xP, INA12xU	120	130				
INA12xPA, INA12xUA	110						
<b>INPUT BIAS CURRENT</b>							
$I_B$	Input bias current	INA12xP, INA12xU		$\pm 2$	$\pm 5$		nA
		INA12xPA, INA12xUA			$\pm 10$		
	Input bias current drift	$T_A = -40^\circ\text{C}$ to $+85^\circ\text{C}$		$\pm 30$			$\text{pA}/^\circ\text{C}$
$I_{OS}$	Input offset current	INA12xP, INA12xU		$\pm 1$	$\pm 5$		nA
		INA12xPA, INA12xUA			$\pm 10$		
	Input offset current drift	$T_A = -40^\circ\text{C}$ to $+85^\circ\text{C}$		$\pm 30$			$\text{pA}/^\circ\text{C}$
<b>NOISE</b>							
$e_N$	Voltage noise (RTI)	G = 1000, $R_S = 0 \Omega$	f = 10 Hz		10		nV/ $\sqrt{\text{Hz}}$
			f = 100 Hz		8		
			f = 1 kHz		8		
			$f_B = 0.1 \text{ Hz}$ to $10 \text{ Hz}$		0.2		$\mu\text{V}_{PP}$
$I_n$	Current noise	f = 10 Hz			0.9		$\text{pA}/\sqrt{\text{Hz}}$
		f = 1 kHz			0.3		
		$f_B = 0.1 \text{ Hz}$ to $10 \text{ Hz}$			30		$\text{pA}_{PP}$

### References:

[1] T. Instruments, "INA129P," Digi-Key Electronics, 2022.

<https://www.digikey.com/en/products/detail/texas-instruments/INA129P/254674>

## Section 2.9: Ultimaker PLA Technical Data Sheet

PLA for Ultimaker (FFF)

\$0.08 / g

Ultimaker PLA filament provides a no-hassle 3D printing experience thanks to its reliability and good surface quality. The PLA is made from organic and renewable sources. It's safe, easy to print with, and it serves a wide range of applications for both novice and advanced users.

Key Features: Good ultimate strength and surface quality, easy to work with at high print speeds, user-friendly for both home and office environments, and PLA allows the creation of high-resolution parts [1].

Table 1: Material and Mechanical Properties of Ultimaker PLA [1].

Mechanical properties*	Injection molding		3D printing	
	Typical value	Test method	Typical value	Test method
Tensile modulus	-	-	2,346.5 MPa	ISO 527 (1 mm/min)
Tensile stress at yield	-	-	49.5 MPa	ISO 527 (50 mm/min)
Tensile stress at break	-	-	45.6 MPa	ISO 527 (50 mm/min)
Elongation at yield	-	-	3.3%	ISO 527 (50 mm/min)
Elongation at break	-	-	5.2%	ISO 527 (50 mm/min)
Flexural strength	-	-	103 MPa	ISO 178
Flexural modulus	-	-	3,150 MPa	ISO 178
Izod impact strength, notched (at 23 °C)	-	-	5.1 kJ/m <sup>2</sup>	ISO 180
Charpy impact strength (at 23 °C)	-	-	-	
Hardness	-	-	83 (Shore D)	Durometer

\* Properties reported here are average of a typical batch. The 3D printed test specimens were printed in the XY plane, using the normal quality profile in Ultimaker Cura 2.1, an Ultimaker 2+, a 0.4 mm nozzle, 90% infill, 210 °C nozzle temperature, and 60 °C. The values are the average of five white and five black specimens for the tensile, flexural, and impact tests. The Shore hardness D was measured in a 7-mm-thick square printed using the normal quality profile in Ultimaker Cura 2.5, an Ultimaker 3, a 0.4 mm print core, and 100% infill. The electrical properties were measured on a 54-mm-diameter disk with 3 mm thickness printed in the XY plane, using the fine quality profile (0.1 mm layer height) in Ultimaker Cura 3.2.1, an Ultimaker 3, a 0.4 mm print core, and 100% infill. Ultimaker is constantly working on extending the TDS data.

### References:

[1] Ultimaker, "Technical Data Sheet - PLA," Nov. 2018. Accessed: Dec. 02, 2021. [Online]. Available: <https://ultimaker.com/materials/pla>.

## Section 2.10: NEMA-17 Stepper Motor Technical Data Sheet

A stepper motor to satisfy all your robotics needs! This 4-wire bipolar stepper has 1.8° per step for smooth motion and a nice holding torque. The motor was specified to have a max current of 350 mA so that it could be driven easily with an Adafruit motor shield for Arduino (or other motor driver) and a wall adapter or lead-acid battery. Some nice details include a ready-to-go cable and a machined drive shaft [1].

Table 1: NEMA-17 Stepper Motor Technical Specifications [1].

Item	Specifications
Step Angle	1.8°
Step Angle Accuracy	±5% ( full step, no load )
Resistance Accuracy	±10%
Inductance Accuracy	±20%
Temperatru Rise	80°CMax. ( rated current,2 phase on )
Ambient Temperatuar	-20°C~+50°C
Insulation Resistance	100M?Min.,500VDC
Dielectric Strength	500VAC/ for one minute
Shaft Radial Play	0.02Max. ( 450 g-load )
Shaft Axial Play	0.08Max. ( 450 g-load )
Max. radial force	28N ( 20mm foom the flange )
Max.axial force	10N

### References:

- [1] A. Industries, "Stepper Motor - NEMA-17 Size - 200 steps/rev, 12V 350mA," [www.adafruit.com](http://www.adafruit.com), 2022.  
[https://www.adafruit.com/product/324?gclid=Cj0KCCQiAjc2QBhDgARIsAMc3SqQi\\_8rpHenYK-iXt9KMn2Y-33zOxCpePZHou\\_C26oTArivpTp67CgQaArgPEALw\\_wcB](https://www.adafruit.com/product/324?gclid=Cj0KCCQiAjc2QBhDgARIsAMc3SqQi_8rpHenYK-iXt9KMn2Y-33zOxCpePZHou_C26oTArivpTp67CgQaArgPEALw_wcB) (accessed Feb. 21, 2022).



## Section 2.11: Grainger Zinc Coated Aluminum Fully Threaded Bolt Technical Data Sheet

Zinc coated aluminum fully threaded rods and studs are nonmagnetic and corrosion resistant with a clear finish. They have male threads running their entire length for full engagement of female-threaded nuts. Weighing less than steel, they are commonly used when a lightweight fastener is needed, such as with electronics or aircraft parts [1].

Table 1: Grainger Zinc Coated Aluminum Fully Threaded Bolt Technical Specifications [1].

Item	Fully Threaded Rod	Thread Direction	Right Hand
System of Measurement	Inch	Threaded Rod Thread Type	UNC
Threaded Rod Material	Aluminum	Min. Tensile Strength	42,000 psi
Thread Size	1/4"-20	Rockwell Hardness	Not Rated
Length	3 ft	Thread Class	1A

### **References:**

- [1] W. W. Grainger, Inc, "Fully Threaded Rod, Aluminum, 1/4"-20, 3 Ft Length," Grainger, 2022.  
<https://www.grainger.com/product/GRAINGER-APPROVED-Fully-Threaded-Rod-10P782>

## Section 2.12: Grainger Nylon Hex Nut Technical Data Sheet

The nylon hex nut has a temperature range from -40° to 85 °C. These lightweight, strong nylon nuts are for use with nylon machine screws in applications that require vibration, abrasion, and corrosion resistance. They also provide electrical insulation and meet IFI standards. These hex nuts are free-spinning, non-locking, and have right-hand thread direction for use with nylon male threaded parts [1].

Table 1: Grainger Nylon Hex Nut Technical Specifications [1].

Item	Hex Nut	Fastener Thread Direction	Right Hand
Nut Style	Machine Screw Nut	Dia./Thread Size	1/4"-20
System of Measurement	Inch	Fastener Thread Type	UNC (Coarse)
Basic Material	Nylon	Width Across Flats	27/64 in
Fastener Finish	Black Nylon coat	Nut Height	15/64 in

### References:

- [1] W. W. Grainger, "Hex Nut, Machine Screw Nut, Nylon, Not Graded, Black Nylon coat, 1/4"-20 Dia./Thread Size," Grainger, 2022.  
<https://www.grainger.com/product/GRAINGER-APPROVED-Hex-Nut-4AGF9> (accessed Feb. 26, 2022).

### Section 2.13: Maximum Stress Calculations

Using Equation 1 below, the maximum applied stress for the force application block in the location where the block comes into contact with the syringe plunger was calculated using the maximum expected applied force during injection (10.00 N) and the smallest plunger cross-sectional contact area ( $6.362 \times 10^{-5} \text{ m}^2$ ) [1].

$$[1] \sigma = F / A$$

Force Application Block:

$$\text{Cross-Sectional Area} = \pi * (0.0045 \text{ m})^2 = 6.362 \times 10^{-5} \text{ m}^2$$

$$\text{Maximum Force} = 10.00 \text{ N}$$

$$\text{Stress} = 10.00 \text{ N} / 6.362 \times 10^{-5} \text{ m}^2 = 157190.07 \text{ Pa} = 0.16 \text{ MPa}$$

### **References:**

[1] F. P. Beer, E. R. Johnston Jr., J. T. DeWolf, and D. F. Mazurek, Mechanics of Materials, 8th Edition. McGraw Hill Education, 2020.

Section 2.14: Materials List and Budget Table

Table 1: Itemized list of components used throughout fabrication and their purchasing information from the Spring 2022 semester.

Item	Description	Manufacturer	Part Number	Date	QTY	Cost Each	Total	Link
<b>Component 1</b>								
Hex Nut	¼" - 20 Nylon Black	Grainger	4AGF9	03/15	1	3.20	3.20	
<b>Component 2</b>								
Threaded Rod	Nylon 6/6 ¼" - 20 x 2 ft	Grainger	2KA63	03/15	1	14.06	14.06	
<b>Component 3</b>								
Stepper Motor	NEMA-17 size - 200 steps/rev, 12 V 350 mA	adafruit	324	03/15	1	14.00	14.00	
<b>Component 4</b>								
Aluminum Flex Shaft Coupler	5 mm to 5 mm	adafruit	1175	03/15	1	4.95	4.95	
<b>Component 5</b>								
Potentiometer	Panel Mount 10k	adafruit	562	03/15	1	0.95	0.95	
<b>Component 6</b>								
SN754410 Quad Half H-Bridge 1A Motor Driver IC	H-Bridge Microcontroller for NEMA-17 Stepper Motor	Banana Robotics	BR010086	03/15	2	1.75	3.50	
<b>Component 7</b>								
¼ in x 36 in Zinc Plated Threaded Rod	Threaded rod allows for motion of the nylon nut to move in a horizontal direction	UW Makerspace	6717	03/23	1	2.00	2.00	
<b>Component 8</b>								
Dasani Water Bottle	Force Application Device for FSR Calibration Curve Testing	Dasani Water	N/A	03/26	1	1.50	1.50	
<b>Component 9</b>								
Adafruit Motor/Stepper/Servo Shield for Arduino v2 Kit - v2.3	Intermediate connection between Arduino Uno and NEMA-17 Stepper Motor	adafruit	1438	03/29	1	19.95	19.95	
<b>Component 10</b>								
5 mm to ¼ inch Aluminum Alloy Coupling Set Screw	Allows for connection between the ¼ inch threaded rod and NEMA-17 Stepper Motor	uxcell	L25XD14	04/01	1	6.49	6.49	
<b>Component 11</b>								
Ultimaker PLA 3D printed Syringe clamp	Syringe clamp mold that tightly secures and locks the procedural 1 mL syringes in place,	Ultimaker and UW Makerspace	N/A	04/05	1	0.64	0.64	

	preventing any displacement throughout each procedure								
<b>Component 12</b>									
Ultimaker PLA 3D printed Motor Holder, Cylinder Rods and Force Application Block	Motor holder houses the NEMA-17 Stepper Motor, Cylinder Rods prevent rotation and enable horizontal motion of the Force Application Block, which pushes against the syringe	Ultimaker and UW Makerspace	N/A	04/08	1		20.41	20.41	
<b>Component 13</b>									
Ultimaker PLA 3D printed Syringe Base and Force Application Block	The Syringe Base will hold all other components as well as house all circuitry underneath the base. The updated Force Application Block will better hold the nylon nut and push against the syringe	Ultimaker and UW Makerspace	N/A	04/13	1		54.56	54.56	
<b>Component 14</b>									
12V 2A Power Supply Adapter	12V supply to the Arduino will better power the motor and create enough torque to supply the MSC's through the catheter	SANSUN	FBA-12000 01P	04/18	1		7.99	7.99	
<b>Component 15</b>									
Ultimaker PLA 3D printed Syringe Rods	Reprinted syringe rods	Ultimaker and UW Makerspace	N/A	04/22	1		9.44	9.44	
<b>TOTAL:</b>									<b>\$163.64</b>

Table 2: Itemized list of components used throughout fabrication and their purchasing information from the current Fall 2022 semester.

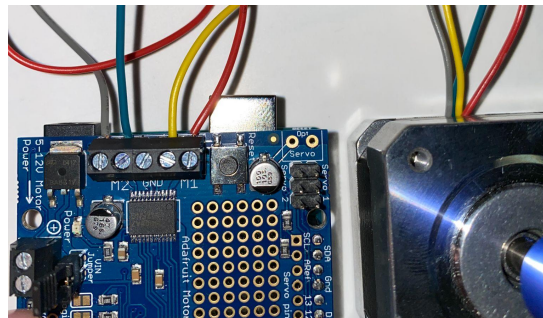
Item	Description	Manufacturer	Part Number	Date	QTY	Cost Each	Total	Link
<b>Component 1</b>								
FSG005WNPB	FSG Series Force Sensor	Honeywell Sensing and Productivity Solutions	480-5692-ND	10/21	1	163.12	163.12	<a href="#">Link</a>
<b>Component 2</b>								
SmartWater Bottle	591 mL SmartWater Bottle used to perform calibration testing for the FSG Sensor	Energy Brands	N/A	10/29	1	2.50	2.50	<a href="#">Link</a>
<b>Component 3</b>								
Updated Syringe Injector Components	Stepper motor holder, force blocks and rod holder	Makerspace	N/A	10/31	1	19.12	19.12	N/A
<b>Component 4</b>								
Reprinted force block and aortic arch prints		Makerspace	N/A	11/02	1	6.48	6.48	N/A
<b>Component 5</b>								
Instrumentation Amplifier	Instrumentation Amplifier 1 Circuit 8-PDIP	Texas Instruments	INA129PA	11/15	1	10.11	10.11	
<b>TOTAL:</b>							<b>201.33</b>	

## Section 3: Fabrication Protocols

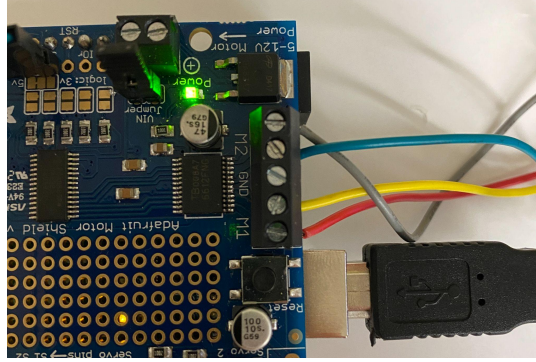
### Section 3.1: NEMA-17 Stepper Motor Circuit and General Fabrication

The NEMA-17 Stepper Motor is the main component that controls the injection rates within the device. The Stepper Motor and subsequent software coding will allow the injections to be programmed at 30 and 60 seconds, along with other features controlled by the buttons. The following protocol provides step-by-step instructions for how to assemble the Stepper Motor and incorporate it into the rest of the device.

1. Obtain a NEMA-17 Stepper Motor, breadboard, Arduino Uno Microcontroller, adafruit Motor Shield v2.3, 5 mm to 6.35 mm (¼ inch) coupler, 3.50 cm long 6.35 mm (¼ inch) threaded rod, 3 breadboard compatible buttons, 3 10k Ohm resistors, 15 connecting wires, 5/64 inch hexagonal screwdriver and small flathead screwdriver.
2. Connect the Stepper Motor with the Arduino Uno and Motor Shield
  - a. Connect the adafruit Motor Shield with the Arduino Uno Microcontroller by soldering the connecting pins onto the Motor Shield and placing the pins in the compatible compartments within the Arduino.
  - b. Connect the NEMA-17 Stepper Motor to the adafruit Motor Shield v2.3 by placing the wires in the M1 and M2 compartments with orientation as shown.



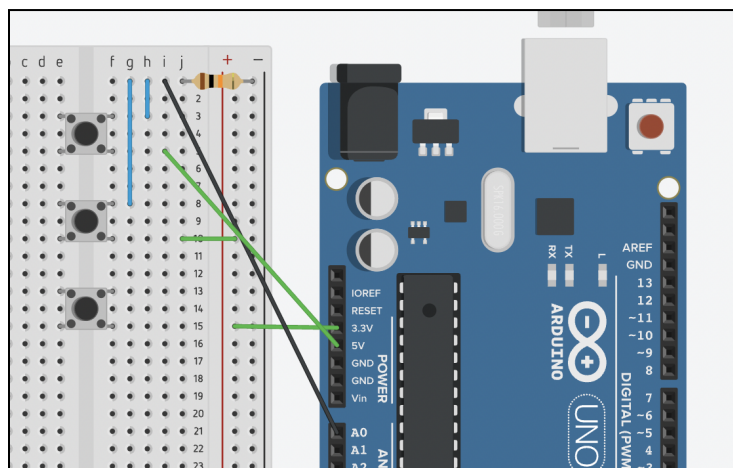
- c. Ensure the power supply from the Arduino is being transferred to the Stepper Motor by completing the jumper circuit with the jumper attachment provided with the Stepper Motor. This will be evident if the Motor Shield LED lights up upon providing the Arduino with power.



3. Assemble circuitry to control the Stepper Motor with 3 buttons
  - a. Each button will be used to either start or stop the motor by providing different voltage values to the Arduino Uno. Start by soldering 2 wires to each button, ensuring the wires are either diagonal or next to each other. Connect the buttons to the breadboard.

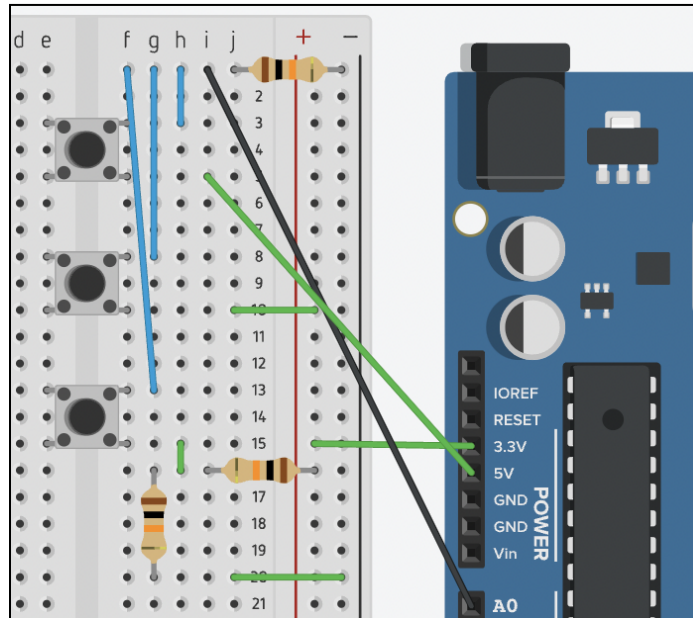


- b. Using power from the Arduino, connect 5V to button 1 and 3.3V to the positive rail. From the positive rail, connect 3.3V to button 2. Connect the adjacent legs of the buttons to ground (using a 10k Ohm resistor) and the A0 pin of the Arduino.

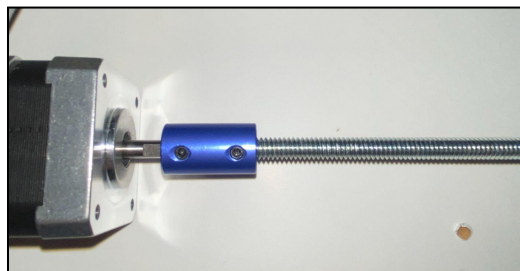




- c. Using power from the 3.3V of the Arduino, create a voltage divider circuit so that 1.65V of power is applied to button 3 (use 2 10k Ohm resistors). Connect the adjacent leg of the button to ground and A0 as well.



- d. Ensure the buttons and Arduino work by reading the ADC values off the serial monitor of the power being supplied to the A0 pin. When pressing each button, button 1 should read as 1023, button 2 should read as 512/513, and button 3 should read as 256 in the serial monitor.
4. Connect the threaded rod to the Stepper Motor
    - a. Place the 5 mm hole on the coupler onto the Stepper Motor cylinder. Use a small screwdriver to secure the coupler in place.
    - b. Place the 6.35 mm diameter threaded rod into the 6.35 mm side of the coupler that is attached to the Stepper Motor. Use the same screwdriver to secure the threaded rod in place. Ensure the rod is as vertical as possible.



5. Implement code into the Arduino software that allows each button to control different movements of the Stepper Motor (speed, step count, direction, etc.).

#### Arduino IDE Code

```
#include <Adafruit_MotorShield.h>
```

```
// Create the motor shield object with the default I2C address
```

```

Adafruit_MotorShield AFMS = Adafruit_MotorShield();
// Or, create it with a different I2C address (say for stacking)
// Adafruit_MotorShield AFMS = Adafruit_MotorShield(0x61);

// Connect a stepper motor with 200 steps per revolution (1.8 degree)
// to motor port #2 (M3 and M4)
Adafruit_StepperMotor *myMotor = AFMS.getStepper(200, 1);

void setup() {
  // put the setup code here, to run once:
  Serial.begin(9600);
  AFMS.begin();
}

void loop() {
  // put the main code here, to run repeatedly:
  int Repos = 1;
  int sensorValue = analogRead(A0);
  Serial.println(sensorValue);
  if (sensorValue > 1000) {
    myMotor->setSpeed(120); //SPEED FOR 30 SECONDS
    for (int i = 0; i <= 4656; i++) { //STEP COUNT FOR MM TRAVELING
      sensorValue = analogRead(A0);
      Serial.println(sensorValue);
      myMotor->step(1, BACKWARD, SINGLE);
      while (sensorValue > 1000) {
        delay(1);
        sensorValue = analogRead(A0);
      }
      if (sensorValue < 300 && sensorValue > 200) {
        delay(2000);
        myMotor->setSpeed(200);
        myMotor->step(i, FORWARD, SINGLE);
        Repos = 0;
        break;
      }
    }
  }
  if (Repos == 1) {
    delay(2000);
    myMotor->setSpeed(200);
    myMotor->step(4656, FORWARD, SINGLE); //STEP COUNT FOR MM RESET
  }
}

```

```

} else if (sensorValue < 800 && sensorValue > 500) {
  myMotor->setSpeed(34); //STEP SPEED FOR 60 SECONDS
  for (int i = 0; i <= 4656; i++) { //STEP COUNT FOR MM TRAVEL
    sensorValue = analogRead(A0);
    Serial.println(sensorValue);
    myMotor->step(1, BACKWARD, SINGLE);
    while (sensorValue < 800 && sensorValue > 500) {
      delay(1);
      sensorValue = analogRead(A0);
    }
    if (sensorValue < 300 && sensorValue > 200) {
      delay(2000);
      myMotor->setSpeed(200);
      myMotor->step(i, FORWARD, SINGLE);
      Repos = 0;
      break;
    }
  }
}
if (Repos == 1) {
  delay(2000);
  myMotor->setSpeed(200);
  myMotor->step(4656, FORWARD, SINGLE); //STEP COUNT FOR MM RESET
}

} else if (sensorValue < 300 && sensorValue > 200) {
  myMotor->setSpeed(15);
  for (int i = 0; i <= 4656; i++) { //STEP COUNT FOR MM TRAVEL
    sensorValue = analogRead(A0);
    Serial.println(sensorValue);
    //myMotor->step(1, BACKWARD, SINGLE);
    myMotor->step(1, FORWARD, SINGLE);

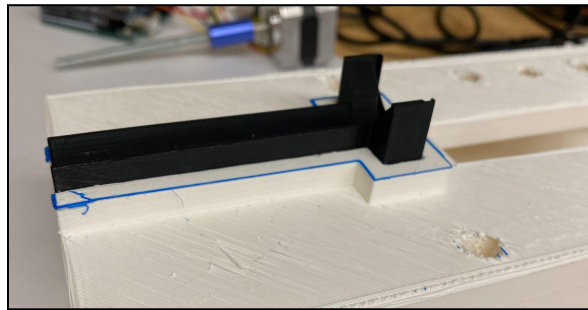
    if (sensorValue < 300 && sensorValue > 200) {
      break;
    }
  }
}
}
}

```

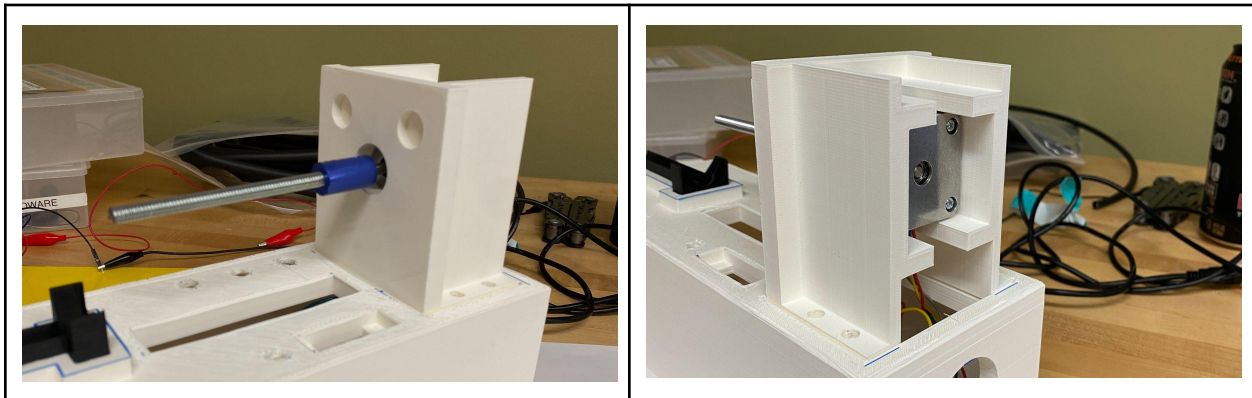
### Section 3.2: Cellringe Pump Fabrication

The final Cellringe Pump prototype was assembled by following this protocol in order to assemble all components into one functioning device. The following protocol provides step-by-step instructions for how to assemble the feedback system, FSR sensor, force application threaded system, the Stepper Motor, all 3D printed parts, and circuitry components into the Cellringe Pump.

1. Obtain the FSR Feedback System Circuit, NEMA-17 Stepper Motor Circuit, Cellringe Base, Motor Holder, Cylinder Rods, Force Application Block, 1 mL Syringe Mold, 3 nylon nuts (6.35 mm), and 2 bolts (6.35 mm).
2. Place the 1 mL Syringe Holder into the syringe holder compartment

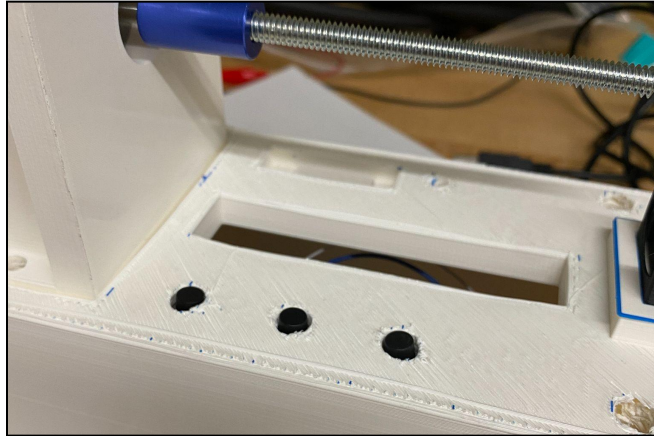


3. Assemble NEMA-17 Stepper Motor Circuit into Cellringe Base
  - a. With the circuitry system for both the Feedback System and Stepper Motor Circuit placed underneath the base, feed the motor through the large square hole on the top of the base.
  - b. Place the motor into the Motor Holder. The Motor Holder can now be placed onto the cut out in the base.

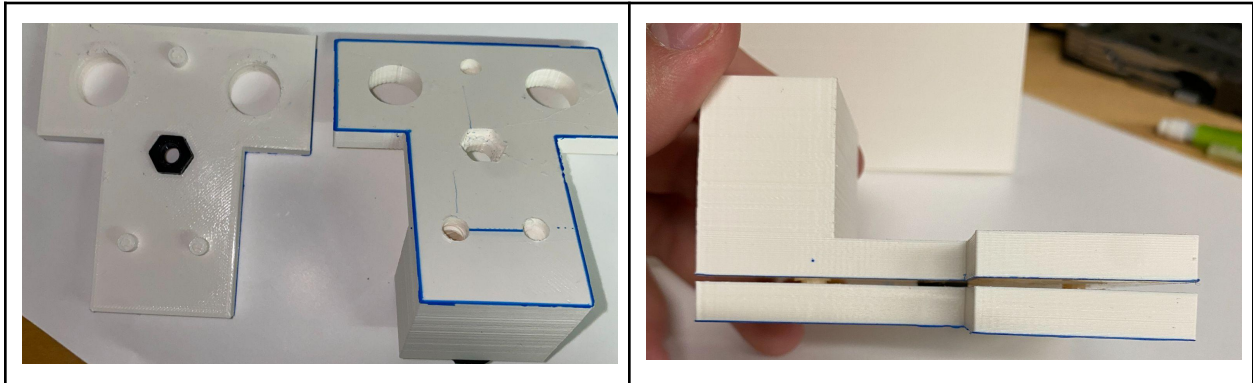


- c. Push the soldered buttons into the correct holes within the top of the base, with the 30 second button closest to the Motor Holder, 60 second button in

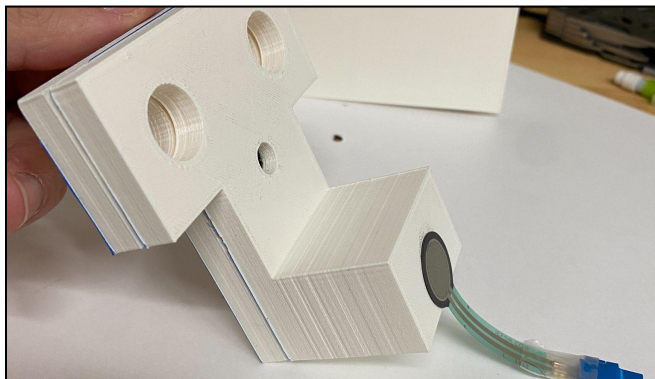
the middle, and the stop/reset button closest to the Cylinder Rod attachment.



4. Attach the Force Application Block
  - a. Place the 6.35 mm nylon nut into the cut out in one piece of the Force Application Block. Take the other conjoining piece and press them together, holding the nylon nut in place in the center of the 2 Force Application block pieces.

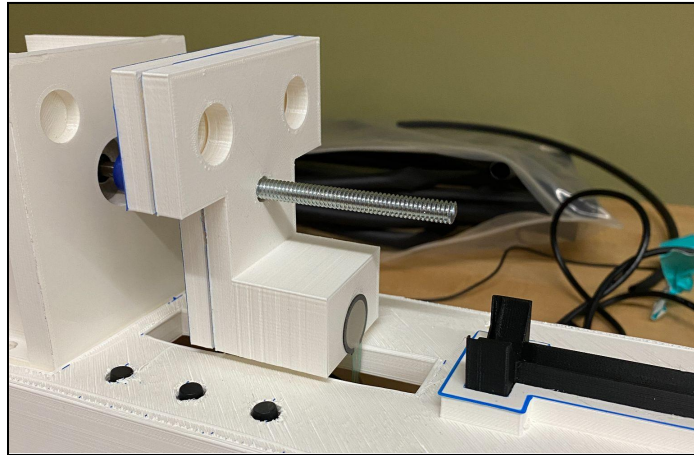


- b. Detach the FSR from the FSR circuit. Use the adhesive on the back side of the FSR to apply the FSR onto the face of the longer side of the FSR.

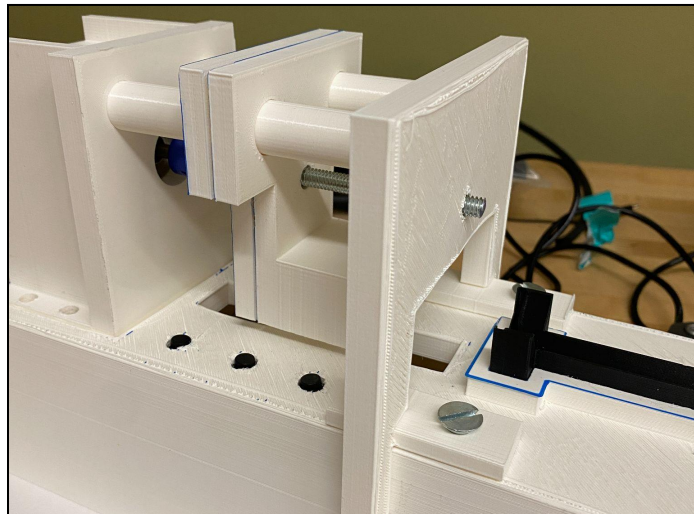




- c. Spin the Force Application block onto the 6.35 mm threaded rod until it is positioned over the rectangular hole in the center of the base. Reattach the FSR to the FSR circuit.



- d. Place the cylinder rods through the 2 holes in the Force Application Block. Further push the cylinder rods into the shallow holes in the Motor Holder. Use 2 of the 6.35 nylon nuts and bolts to secure the cylinder rods into the base.



5. Integrate the Feedback System's LED threshold light and LED digital display.
  - a. Bring the wires for the LED digital display from underneath the base up through the small rectangular hole designated for the LED digital display.
  - b. Attach the wires in the correct pins of the LED digital display.
  - c. Apply an adhesive to hold the LED digital display in place



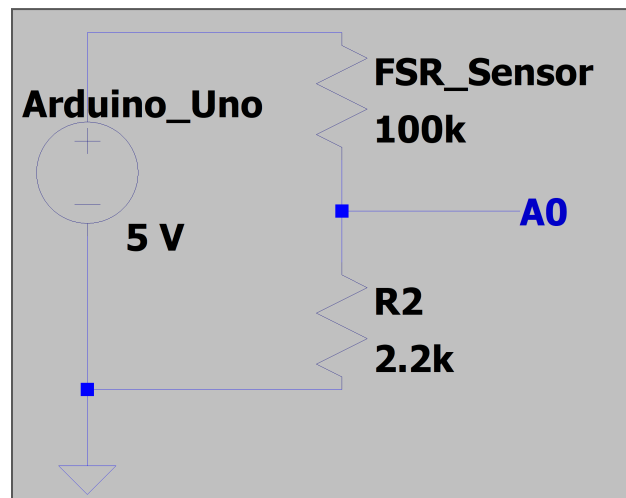
- d. Repeat steps a-b with the LED threshold light and corresponding wires.
- e. Set the LED threshold light firmly in place in the designated hole.



### Section 3.3: FSR Feedback System Circuit and General Fabrication

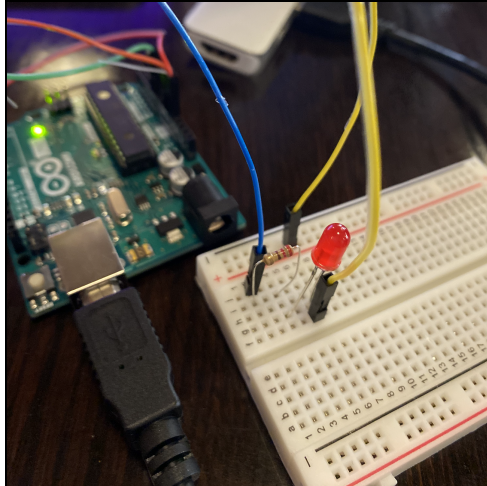
There are two components to the feedback system. The first is the red LED light that will turn on once the force is above the 2.4 N of force that identifies potential catheter obstruction and the second is the display scoreboard that will show the surgeon how much force they are applying. The following protocol provides step-by-step instructions for how to assemble the Feedback System and incorporate it into the rest of the device.

1. Obtain a breadboard, display scoreboard, Force Sensor, 200 Ohm resistor, 10kOhm resistor, red LED light, Arduino microcontroller, power supply for the Arduino and many wires.
2. Assemble the voltage divider circuit with the FSR using a 10 kOhm resistor.
  - a. The schematic shown below depicts the wiring that should be set up to obtain the voltage divider with the exception that the 2.2 kOhm resistor in the figure should be a 10 kOhm resistor.

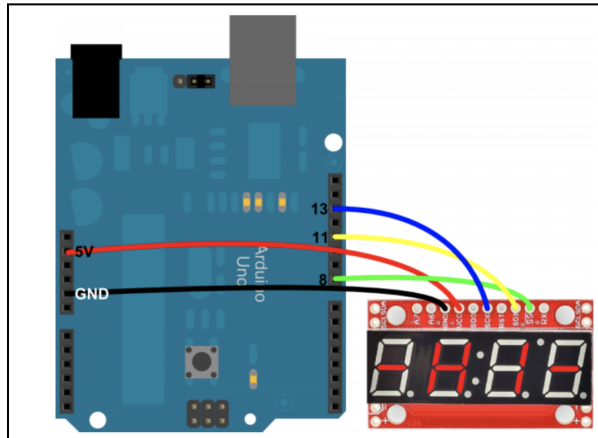


- b. Connect the 5V power from the Arduino to one side of the FSR and the other side of the FSR to the 10 kOhm resistor with room for a wire to go in between and connect to A0 of the Arduino to provide a Vout.
    - c. Connect the other leg of the 10 kOhm resistor to the ground which can be supplied by the Arduino as well.
3. Add the LED component of the circuit
  - a. Connect a red LED to a digital pin (digital pin 10 will work for the code below) where there will be a write out for whether the light should be on or off by giving it a HIGH output or LOW output
  - b. Use a 200 Ohm resistor before the red LED to prevent the LED from burning out.
  - c. Ground the other side of the red LED
  - d. The LED part of the circuit will look like the image below where the yellow wire is connected to the ground and the blue wire is connected to pin 10 of the Arduino

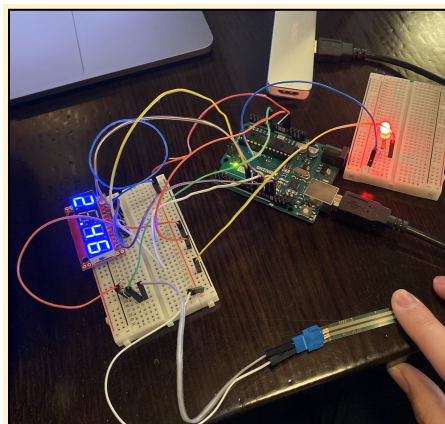




4. Add the Display component of the circuit
  - a. Connect the display to the breadboard and add the pins in the proper location as seen in the image below:



5. Make sure your breadboard looks as follows and begin the “FSR Feedback System Testing”



## Feedback System Code for the Spring 2022 Injector

```
/*  
  
Circuit:  
Arduino ----- Serial 7-Segment  
5V ----- VCC  
GND ----- GND  
8 ----- SS  
11 ----- SDI  
13 ----- SCK  
*/  
#include <SPI.h> // Include the Arduino SPI library  
  
// Define the SS pin  
// This is the only pin that can be moved around to any available  
// digital pin.  
const int ssPin = 8;  
char tempString[10]; // Will be used with sprintf to create strings  
  
int ledRed = 10; // pin that Orange LED is attached to  
int analogPin = A0; // pin that the sensor is attached to  
float force = 0; // initializing the force variable  
double power_series = 2.17; //power series exponent for the FSR curve  
  
void setup()  
{  
  
  Serial.begin(9600); // initialize serial communication at 9600 bits per second:  
  
  // ----- SPI initialization  
  pinMode(ssPin, OUTPUT); // Set the SS pin as an output  
  digitalWrite(ssPin, HIGH); // Set the SS pin HIGH  
  SPI.begin(); // Begin SPI hardware  
  SPI.setClockDivider(SPI_CLOCK_DIV64); // Slow down SPI clock  
  // -----  
  
  // Clear the display, and then turn on all segments and decimals  
  clearDisplaySPI(); // Clears display, resets cursor  
  
  // Custom function to send four bytes via SPI  
  // The SPI.transfer function only allows sending of a single  
  // byte at a time.  
  s7sSendStringSPI("-HI-");  
  setDecimalsSPI(0b111111); // Turn on all decimals, colon, apos
```

```

// Flash brightness values at the beginning
setBrightnessSPI(0); // Lowest brightness
delay(1500);
setBrightnessSPI(255); // High brightness
delay(1500);

// Clear the display before jumping into loop
clearDisplaySPI();
}

void loop()
{

    // read the input on analog pin 0:
    int sensorValue = analogRead(A0);
    float voltage = sensorValue * (5.0/1023.0); // initialize a variable that solves for the
    voltage value that corresponds to the read ADC value from pin A0
    Serial.print("FSR Voltage Output = "); // Prints "FSR Voltage Output = " to the serial
    monitor
    Serial.println(voltage); // Prints the voltage value read from the A0 pin to the serial
    monitor

    if (voltage <= 3.05) {
        force = (0.0707 * pow(voltage, 5)) - (0.00348 * pow(voltage, 6)) - (0.419 * pow(voltage,
        4)) + (1.10 * pow(voltage, 3)) - (1.33 * pow(voltage,2)) + (0.795 * voltage) - 0.000185; //
        will use the flipped 6th-degree polynomial curve when equal to or below a voltage value
        of 3.05 V
    }

    else {
        force = (0.19 * pow(voltage, 4)) - (1.5 * pow(voltage, 3)) + (3.89 * pow(voltage,2)) -
        (2.97 * voltage) - 0.0000245; // will use a 4th-degree polynomial curve for voltage
        values above 3.05 V
    }

    Serial.print("Force = "); // Prints "Force = " to the serial monitor

    Serial.println(force); // Displays the force value on a monitor

    if (force < 2.4) {
        digitalWrite(ledRed, LOW); // should keep the light off if the force is below 2.4 N
    }

    else { // should be 2.4 and up
        digitalWrite(ledRed, HIGH);
    }
}

```

```
Serial.println("Stop"); // turns light on and prints stop on serial monitor when above 2.4
N
}
```

```
// Delay the code for 10 millisecond to allow for the Vout reading to be picked up by the
user
```

```
// Magical sprintf creates a string for us to send to the s7s.
```

```
// The %4d option creates a 4-digit integer.
```

```
//int forceInt = force * 100;
String forceString = String(force, 4);
```

```
sprintf(tempString, "%4d", force);
```

```
// This will output the tempString to the S7S
s7sSendStringSPI(forceString);
```

```
// Print the decimal at the proper spot
```

```
if (force < 10000)
```

```
    setDecimalsSPI(0b00000010); // Sets digit 3 decimal on
```

```
else
```

```
    setDecimalsSPI(0b000000100);
```

```
delay(1000); // This will make the display update at 100Hz.*/
}
```

```
// This custom function works somewhat like a serial.print.
```

```
// You can send it an array of chars (string) and it'll print
```

```
// the first 4 characters in the array.
```

```
void s7sSendStringSPI(String toSend)
```

```
{
    digitalWrite(ssPin, LOW);
```

```
    for (int i=0; i<4; i++)
```

```
    {
        SPI.transfer(toSend[i]);
```

```
    }
    digitalWrite(ssPin, HIGH);
```

```
}
```

```
// Send the clear display command (0x76)
```

```
// This will clear the display and reset the cursor
```

```
void clearDisplaySPI()
```

```
{
    digitalWrite(ssPin, LOW);
```

```
    SPI.transfer(0x76); // Clear display command
```

```

    digitalWrite(ssPin, HIGH);
}

// Set the displays brightness. Should receive byte with the value
// to set the brightness to
// dimmest----->brightest
// 0-----127-----255
void setBrightnessSPI(byte value)
{
    digitalWrite(ssPin, LOW);
    SPI.transfer(0x7A); // Set brightness command byte
    SPI.transfer(value); // brightness data byte
    digitalWrite(ssPin, HIGH);
}

// Turn on any, none, or all of the decimals.
// The six lowest bits in the decimals parameter sets a decimal
// (or colon, or apostrophe) on or off. A 1 indicates on, 0 off.
// [MSB] (X)(X)(Apos)(Colon)(Digit 4)(Digit 3)(Digit2)(Digit1)
void setDecimalsSPI(byte decimals)
{
    digitalWrite(ssPin, LOW);
    SPI.transfer(0x77);
    SPI.transfer(decimals);
    digitalWrite(ssPin, HIGH);
}

```

## Section 4: SolidWorks Drawings

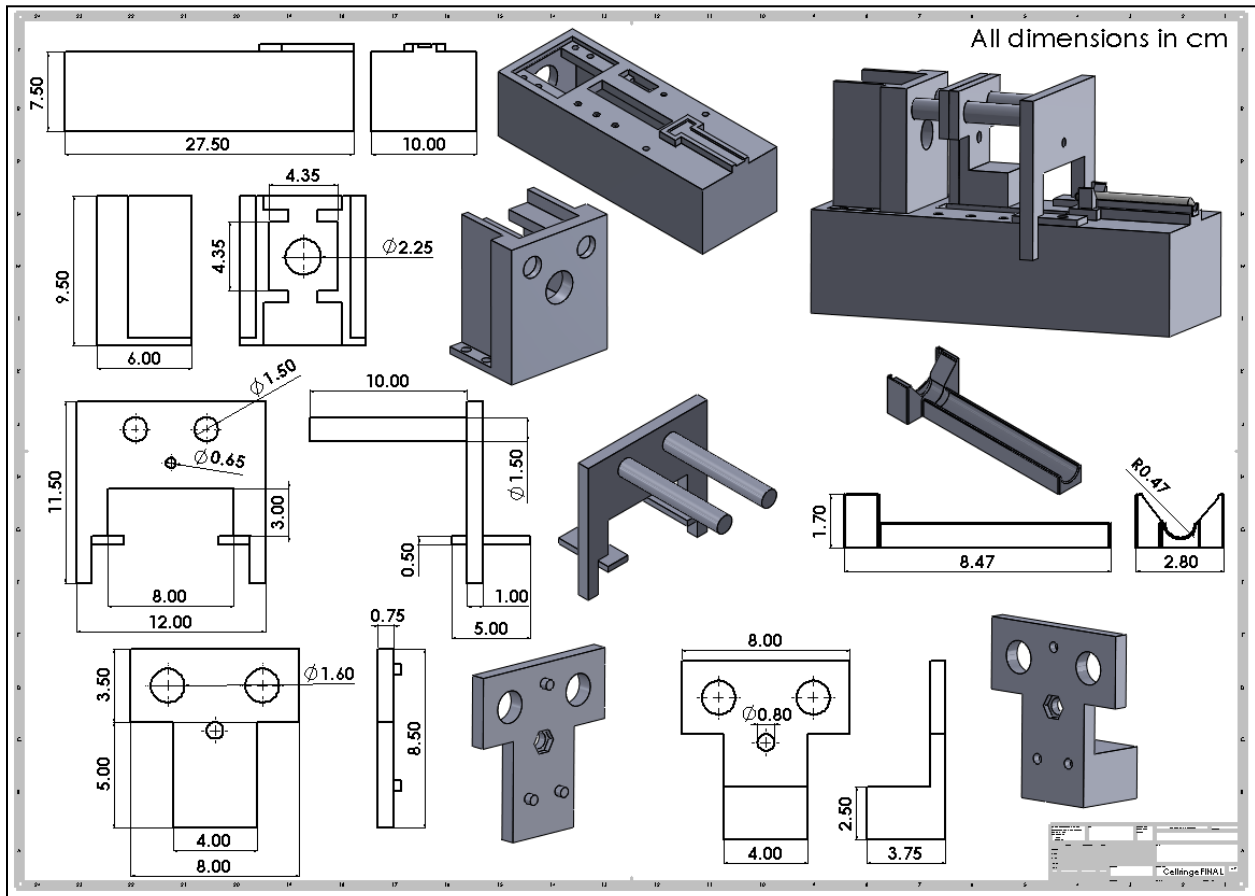


Figure 1: SolidWorks designs of individual components. Each piece is displayed and dimensioned, with the full assembly reference seen in the upper right corner. Individual pieces starting from the top to bottom: Cellringe Base, Motor Holder, Cylinder Rods (left), 1 mL Syringe Holder (right), Force Application Block pt. 1 (bottom left), and Force Application Block pt. 2 (bottom right).

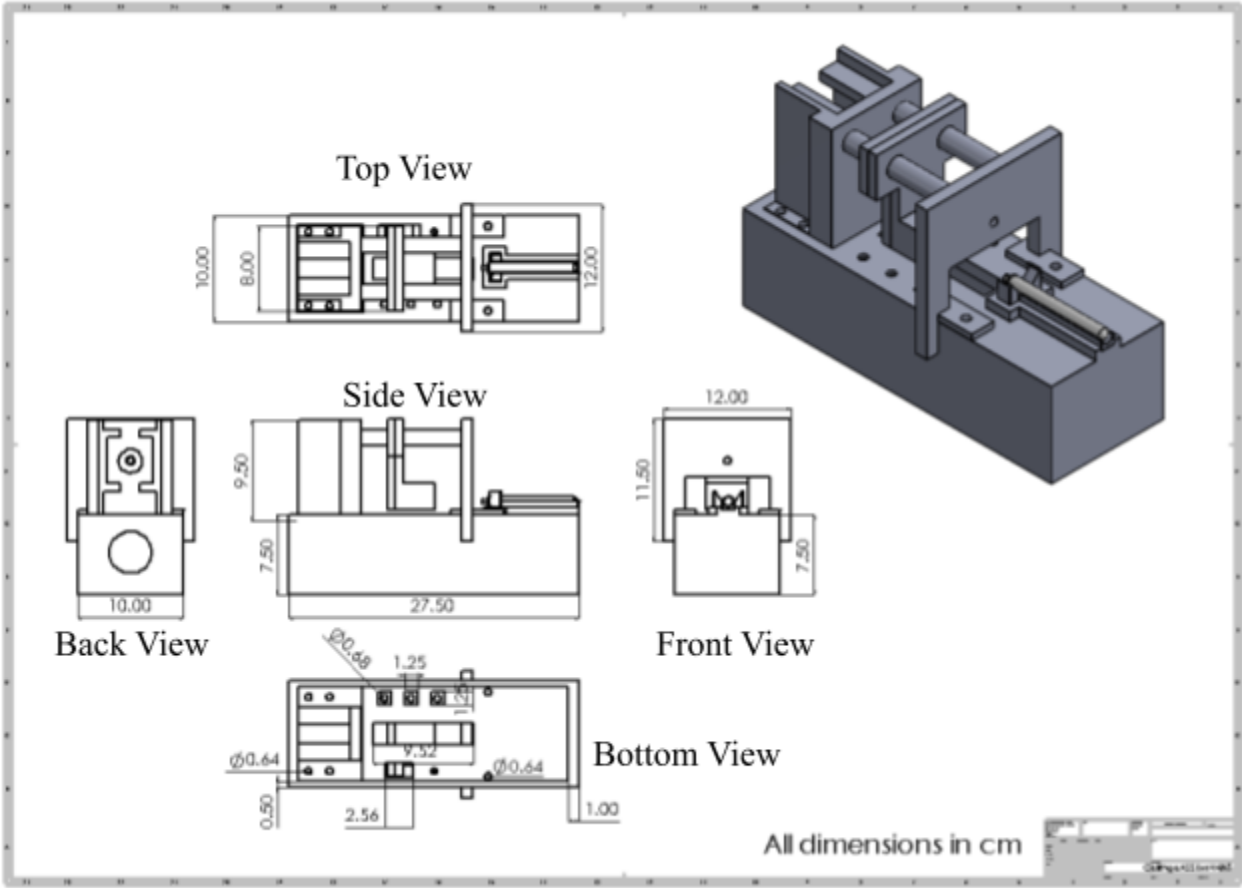


Figure 2: SolidWorks dimensions and reference drawings of the entire assembly.

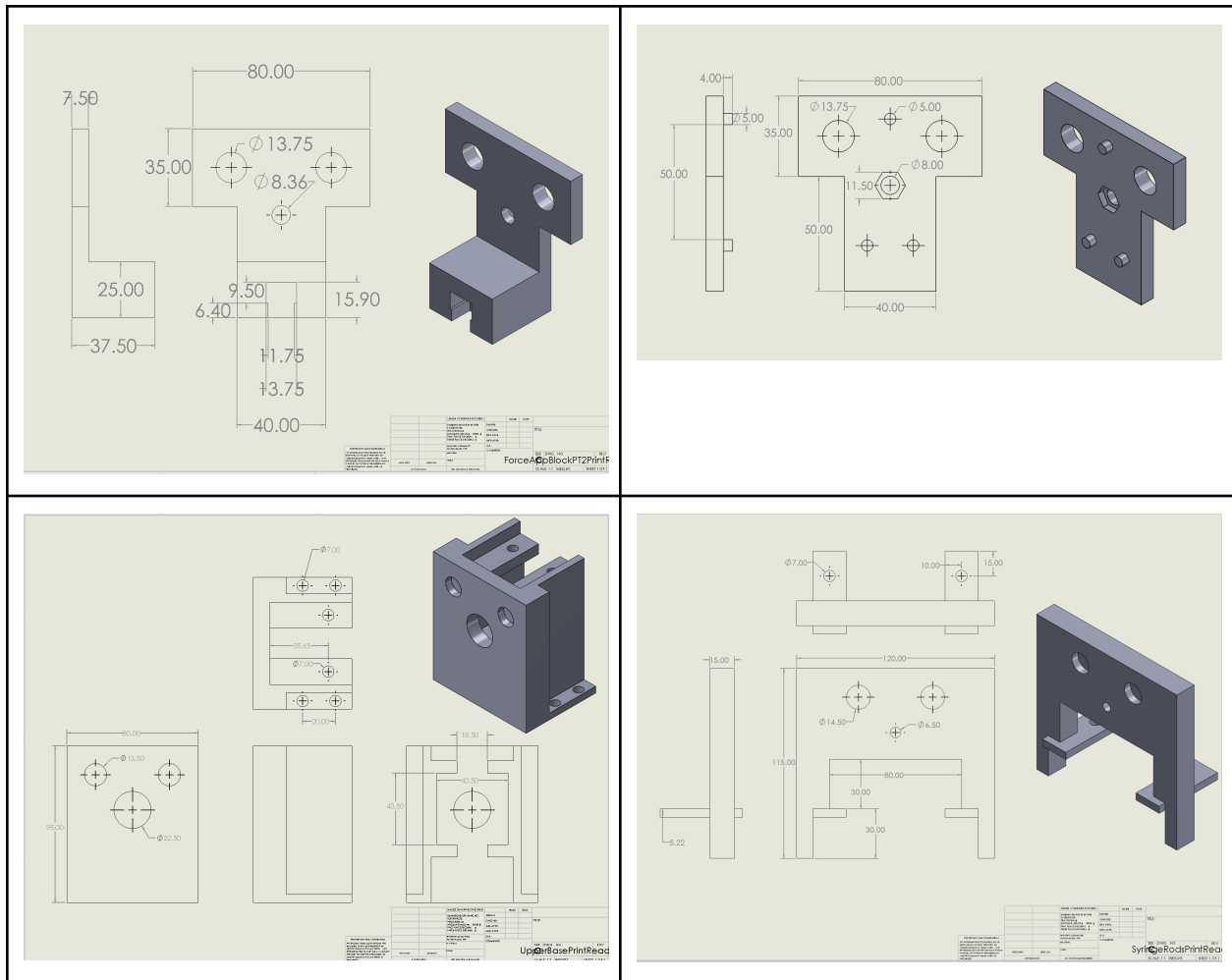


Figure 3: Solidworks dimensions and reference drawings of the new pieces made for the updated prototype. The new additions are the new force application block to house the FSG force sensor (upper left), other half of the force application block (upper right), new motor holder designed to secure the motor in place (bottom left), and a new cylinder rod holder to secure the aluminum rods (bottom right). All dimensions are in mm.



## Section 5: Testing Protocols

### Section 5.1: Sensor Calibration Curve Testing Protocol

To provide an equation to accurately and reliably establish the injector force applied to the syringe plunger throughout each injection, a calibration curve was created based on the sensor feedback system testing force and voltage data. Using a line of best fit that takes into account noise, an equation was identified that correlates voltage (V) to weight (N) and thus allows the force to be determined based on each voltage input to the Arduino Uno microcontroller. The purpose of the calibration curve is primarily to derive the linear trendline which can then be used to calculate the unknown applied force during the injection. The linear trendline from the sensor calibration curve will be used to calculate the force being applied to the sensor by measuring the output voltage. The independent variable (x) in the line of best fit equation represents the applied force and the dependent variable (y) describes the output voltage.

1. Prior to testing, a digital caliper battery case (includes battery inside), 500 mL water bottle, scale (in grams), and various sized micropipettes and graduated cylinders will need to be obtained.
2. Open the “FSR\_Feedback\_System\_Vout” within Arduino IDE on the computer that will be used for testing.
3. After the feedback system is set-up, attach the Arduino Uno microcontroller to the testing computer via the Arduino Uno microcontroller USB cord.
4. Upload the Arduino IDE code and open the serial monitor of the Arduino IDE program. Keep the serial monitor open for the entirety of the testing.
  - a. Verify that no error messages pop-up when the upload button was selected in the software to run the code
  - b. Verify that the serial monitor is displaying voltage and that it is 0.0 V, to confirm that the code is running properly
5. Place the digital caliper battery case (including battery) on top of the active zone of the sensor with the rounded, smallest diameter end of the battery in contact with the sensor active zone.
  - a. **Ensure that the battery is only in contact with the active zone of the sensor throughout the testing. If the battery moves and is only partially in contact with the active zone of the sensor, the results will be inaccurate**
6. Weigh an empty 500 mL water bottle on the scale (keep the cap on the water bottle during this measurement) . Record this value so it can be referenced later when determining the proper water amounts that need to be added to the water bottle in order to apply a specified force to the sensor.
7. Choose a force value to test within the 0.14 N - 5.00 N force range that corresponds to the typical injector force application range.

8. Remove the cap off of the water bottle and add the required amount of water to it based on the selected force application value. Use micropipettes and graduated cylinders for this addition.
  - a. Use Newton's Second Law ( $F = ma$ ) [1] to calculate the required weight to add to the water bottle. Keep units in mind when performing these calculations as the mass used for this equation is in kilograms rather than grams
    - i. 1 mL = 1 g
    - ii. 1 mL = 1000  $\mu$ L
    - iii. Take into account the weight of the water bottle when calculating the amount of water that needs to be added
9. Put the cap back on the water bottle and use the scale to measure the new weight of the bottle.
  - a. Verify that the weight of the water bottle correlates to the desired force and thus that the correct amount of water has been added to the water bottle
10. Ensure that the cap is tightly secured onto the bottle. Balance the water bottle on the battery case with the bottle cap in contact with the flat end (contains the largest surface area) of the digital caliper battery case.
  - a. Make sure the water bottle is only in contact with the digital caliper battery case
  - b. **Ensure that the battery is only in contact with the active zone of the sensor. If the battery is only partially in contact with the active zone of the sensor, the force detection results will be inaccurate**
11. When the water bottle is properly balancing on the sensor via the battery case without any support, view the voltage value output by the system as displayed on the Arduino IDE serial monitor.
12. Record the voltage value that is settled on or that is most consistently displayed (if the value is constantly shifting between multiple values) by the serial monitor. This may take a couple of seconds.
13. Repeat steps 7-12, three times each for each new force value applied.
  - a. Calculate the average voltage applied between the three trials for each weight used.
  - b. Calculate the standard deviation for each weight used as well.
14. Calculate the average applied pressure using Equation 1 below [1].

[1] Applied Pressure = $N/m^2 = \text{Total Applied Force} / \text{Area}$
---

- a. The area is equal to the area of the battery which was applying the pressure to the sensor, this area is calculated as seen in Equation 2 below.

[2] Area = $(6/1000)^2 * \pi = 113.10 \text{ mm}^2 = 1.13 * 10^{-4} \text{ m}^2$
--

15. Create a graph of the Total Force (N) vs Vout (V) and generate a line of best fit that will have the highest  $R^2$  value, an equal distribution of residuals about the line of best fit, and a Gaussian distribution of residuals about 0.

16. This calibration curve line of best fit equation can then be rearranged and used to calculate the applied force based on the voltage value the Arduino is reading.

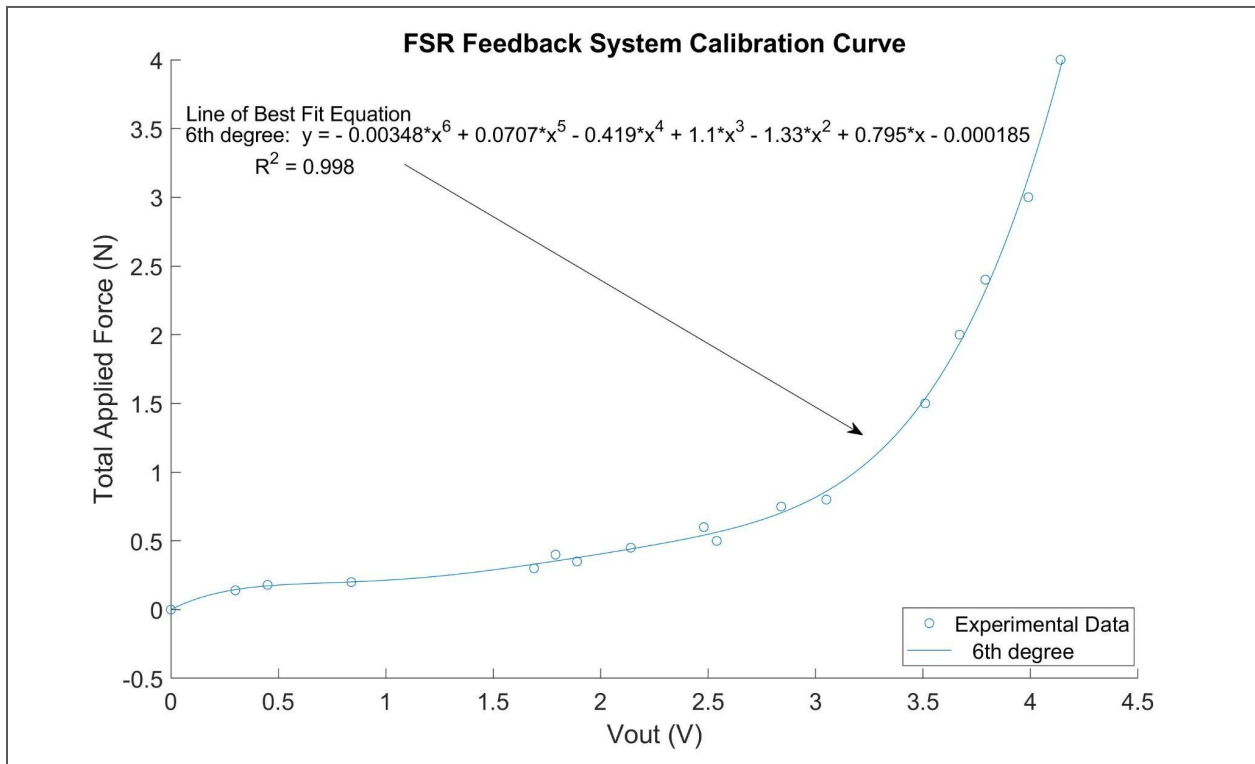


Figure 1: Calibration curve for the FSR feedback system under various loading enabling applied force calculation. The line of best fit equation was integrated with the Arduino IDE software to calculate the force output for all voltage values less than or equal to 3.05 V delivered to the Arduino Uno microcontroller.

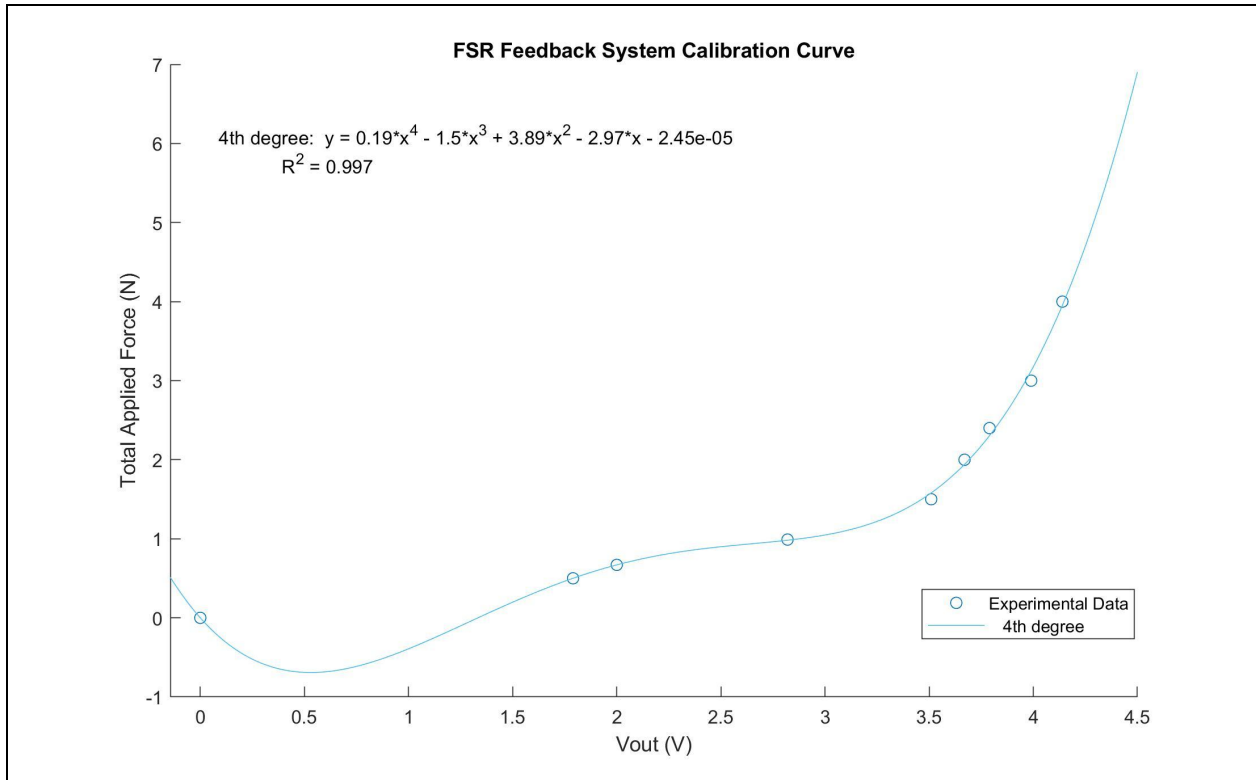


Figure 2: 4th Degree calibration curve FSR feedback system under various loading enabling applied force calculation. The line of best fit equation was integrated with the Arduino IDE software to calculate the force output for all values greater than 3.05 V delivered to the Arduino Uno microcontroller.

### References

- [1] F. P. Beer, E. R. Johnston Jr., J. T. DeWolf, and D. F. Mazurek, Mechanics of Materials, 8th Edition. McGraw Hill Education, 2020.

## Section 5.2: Feedback System Force Detection Accuracy Testing Protocol

The feedback system consists of a voltage divider circuit, force sensor, Arduino Uno microcontroller, red LED, and an Arduino Uno compatible scoreboard. The LED and scoreboard are not used in this test (see the Feedback System Testing protocol for their testing). The feedback system is fabricated as described in the Feedback System Circuit Fabrication protocol. The following provides a step-by-step protocol to test the accuracy of the feedback system and if it is within the required error margin relative to the actual applied force to the sensor. This testing protocol is used prior to incorporation of the sensor and feedback system into the injector base in order to confirm that the force detection system contains the required accuracy. Read through the protocol before performing the steps.

1. Prior to testing, a digital caliper battery case (includes battery inside), 500 mL water bottle, scale (in grams), and various sized micropipettes and graduated cylinders will need to be obtained.
2. Open the “Modified\_FSR\_Feedback\_System\_Force\_Output” within Arduino IDE on the computer that will be used for testing.
3. After the feedback system is set-up, attach the Arduino Uno microcontroller to the testing computer via the Arduino Uno microcontroller USB cord.
4. Upload the Arduino IDE code and open the serial monitor of the Arduino IDE program. Keep the serial monitor open for the entirety of the testing.
  - a. Verify that no error messages pop-up when the upload button was selected in the software to run the code
  - b. Verify that the serial monitor is displaying voltage and force values and that they are 0.0 V and 0.0 N, respectively, to confirm that the code is running properly
5. Place the digital caliper battery case (including battery) on top of the active zone of the sensor with the rounded, smallest diameter end of the battery in contact with the sensor active zone.
  - a. **Ensure that the battery is only in contact with the active zone of the FSR sensor throughout the testing. If the battery moves and is only partially in contact with the active zone of the sensor, the results will be inaccurate**
6. Weigh an empty 500 mL water bottle on the scale (keep the cap on the water bottle during this measurement) . Record this value so it can be referenced later when determining the proper water amounts that need to be added to the water bottle in order to apply a specified force to the sensor.
7. Choose a force value to test within the 0 N - 5.00 N force range that corresponds to the typical injector force application range.
8. Remove the cap off of the water bottle and add the required amount of water to it based on the selected force application value. Use micropipettes and graduated cylinders for this addition.

- a. Use Newton's Second Law ( $F = ma$ ) [1] to calculate the required weight to add to the water bottle. Keep units in mind when performing these calculations as the mass used for this equation is in kilograms rather than grams
  - i. 1 mL = 1 g
  - ii. 1 mL = 1000  $\mu$ L
  - iii. Take into account the weight of the water bottle when calculating the amount of water that needs to be added
9. Put the cap back on the water bottle and use the scale to measure the new weight of the bottle.
  - a. Verify that the weight of the water bottle correlates to the desired force and thus that the correct amount of water has been added to the water bottle
10. Ensure that the cap is tightly secured onto the bottle. Balance the water bottle on the battery case with the bottle cap in contact with the flat end (contains the largest surface area) of the digital caliper battery case.
  - a. Make sure the water bottle is only in contact with the digital caliper battery case
  - b. **Ensure that the battery is only in contact with the active zone of the sensor. If the battery is only partially in contact with the active zone of the sensor, the force detection results will be inaccurate**
11. When the water bottle is properly balancing on the sensor via the battery case without any support, view the force and voltage value output by the system as displayed on the Arduino IDE serial monitor.
12. Record the force and voltage value that is settled on or that is most consistently displayed (if the value is constantly shifting between multiple values) by the serial monitor. This may take a couple of seconds.
  - a. Verify that the force value output by the feedback system is within a 20% error margin of the actual applied force as calculated by the weight of the bottle for all applied forces below 1.00 N and an error margin of 15% for all forces greater than or equal to 1.00 N
    - i. Calculate the error margin using Equation 1 below, with the theoretical value corresponding to the calculated weight [2]

$[1] \text{ Percent Error} = (  V_{\text{theoretical}} - V_{\text{experimental}}  / V_{\text{theoretical}} ) * 100$
---

13. Repeat steps 7 - 12 at least four more times, selecting a new force value each time this step sequence is repeated.
  - a. For each new force value, verify that the force value output by the feedback system is within a 20% error margin of the actual applied force as calculated by the weight of the bottle for all applied forces below 1.00 N and an error margin of 15% for all forces greater than or equal to 1.00 N
    - i. Calculate the error margin using Equation 1 below, with the theoretical value corresponding to the calculated weight [2]

$$[1] \text{ Percent Error} = ( |V_{\text{theoretical}} - V_{\text{experimental}}| / V_{\text{theoretical}} ) * 100$$

If any of the steps can not be completed as outlined above or the verification steps fail, reevaluate the design and determine how the feedback circuit can be modified in order to allow for the force detection accuracy tests to pass. If there is an error within the test protocol or a modification is required, a deviation can be made within the protocol in order to allow a verification step to pass or a step to be completed.

### References

- [1] Britannica, “Newton’s Laws of Motion - Newton’s Second law:  $F = ma$ ,” Encyclopedia Britannica, 2022.  
<https://www.britannica.com/science/Newtons-laws-of-motion/Newtons-second-law-F-ma>
- [2] Dr. A. M. Helmenstine, “How to Calculate Percent Error,” ThoughtCo, Nov. 02, 2020.  
<https://www.thoughtco.com/how-to-calculate-percent-error-609584> (accessed Dec. 03, 2021).

### Section 5.3: Feedback System Testing Protocol

This testing procedure aims at establishing whether the feedback system and display are working properly. The following protocol includes a step-by-step procedure for how to conduct the testing. The tests include applying constant forces and recording what the values are to see if they compare to the serial monitor output as well as applying a force that exceeds that 2.4 N of force to see if the red light turns on.

1. Assemble the circuit which was outlined in the “Feedback System Circuit and General Fabrication” protocol document
2. Follow a similar procedure as done with the “Sensor Calibration Curve Testing Protocol” where you begin by obtaining a digital caliper battery case (includes battery inside), 500 mL water bottle, scale (in grams), and various sized micropipettes and graduated cylinders for testing and set the caliper battery case on top of the sensor while it lays on a flat surface.
3. Instead of looking for the accuracy for the force that is being applied to the sensor as is done in the “Sensor Calibration Curve Testing Protocol”, the accuracy of the display in comparison to the serial monitor values will be compared
4. Slowly add water in increments of 50 - 200 mL at a time. The exact amount of water does not matter because all that needs to be confirmed is that the force values on the display should be similar to the force value on the serial monitor.
5. Record the value from the serial monitor corresponding to the force applied to the sensor by the water as well as record the value that is output on the scoreboard display over a period of five seconds where the delay time in the code is one second
6. Calculate the percent difference between the display and the serial monitor and ensure there is less than 5% difference
7. Check that the LED lights up if the force value is at or above 2.4 N (this is also when the serial monitor will display a line that says “Stop”)
8. Repeat steps 4 - 8 with five different aliquots of water, doing three trials per aliquot.

After testing is finished, a conclusion can be made about whether or not the display shows accurate force values in comparison to the serial monitor where the voltage values are converted into force values and outputted. A conclusion can also be made about where the red LED warning light works to alert the surgeon that they have exceeded the 2.4 N of force and there may be potential catheter blockage.



#### Section 5.4: Syringe Clamp Connection and Locking Testing Protocol

The syringe clamp is a 3D printed material composed of Ultimaker PLA [1]. The following provides a step-by-step protocol to test if the syringe clamp mold enables an easy removal and insertion of the required 1 mL syringe (less than 20 seconds) and if it creates a firm and secure connection, ensuring that user and design requirements are met. This testing protocol is used prior to incorporation of the syringe clamp into the injector base in order to confirm that the mold contains the correct connection system. Read through the protocol before performing the steps.

1. Place the syringe clamp mold on a flat surface, preferably a table, with its entire inferior side (does not contain the semi-circle cut-out) sitting flush with the smooth, flat surface.
  - a. The direction and orientation of the syringe clamp does not matter for this test as long as it is in an appropriate position for efficient syringe insertion, force application, and removal
2. Prior to inserting the 1 mL syringe into the clamp, properly connect it to the procedural medical grade tubing (fasten it into place, ensuring a tight connection is present) and then connect the medical grade tubing to the needle-tipped catheter.
  - a. Connections should be made and tightened following the current clinical process
3. Pull the syringe plunger out as far as it can go without popping out of the proximal end of the 1 mL syringe.
4. With this syringe-tubing-catheter complex kept intact, place the 1 mL syringe into the syringe clamp, with the widest diameter portion of the syringe located on the proximal end of the syringe, inserting into the slit on the proximal end of the clamp. The body and distal end of the syringe should be sitting in the semi-circle mold.
  - a. Verify that the syringe's widest diameter segment fits within the mold's slot
  - b. Verify that the entire body of the syringe sits within the semi-circle mold
  - c. Verify that the syringe rests completely horizontal within the syringe clamp mold without requiring intervention
5. Lay the medical grade tubing-catheter complex connected to the syringe on the table in a location just distal of the syringe and the clamp as well as in a position and orientation that mimics clinical injections (the catheter sits flat initially and then eventually rotates in the superior direction relative to the flat surface). The system can be held in place in order to replicate the clinical orientation if required
  - a. Verify that the syringe's widest diameter segment still sits within the mold's slot
  - b. Verify that the entire body of the syringe still rests within the semi-circle mold
  - c. Verify that the syringe still sits horizontally in the syringe clamp mold without requiring intervention
6. Secure the syringe clamp mold in place on the flat surface with either hands or a temporary adhesive that can be easily removed following the end of the procedure.

- a. If an adhesive is used, ensure that there are not any residues left on the syringe clamp that will disrupt its ability to connect to the injector base following the removal of the adherent material
  - b. The syringe clamp should be tightly secured to the surface, preventing any movement of the clamp during the following steps of the protocol**
- 7. With the syringe clamp secured in place, apply a minimum of 5.00 N of force to the syringe plunger until it completely inserts into the plunger. The force application should be applied horizontally in the axial direction of the syringe plunger's circular end to simulate the injector's force application to the syringe plunger.
  - a. Verify that the clamp and syringe are able to withstand this force without breaking or cracking
  - b. Verify that the syringe does not experience any displacement (horizontal, vertical, rotational, etc.) throughout this force application
- 8. After full compression of the syringe plunger, continue applying at least 5.00 N of force to the syringe plunger for 10 seconds (can use a stopwatch)
  - a. Verify that the clamp and syringe are able to withstand this force without breaking or cracking
  - b. Verify that the syringe does not experience any displacement (horizontal, vertical, rotational, etc.) throughout this force application

Read the rest of the steps prior to performing them as they need to be performed sequentially in a timely manner.

- 9. Following the completion of the compression testing and verification that all steps passed, remove the syringe from the syringe clamp mold. As soon as the syringe removal process is initiated (when the syringe is first touched), another individual needs to begin a stopwatch.
  - a. Verify that the syringe can be removed from the clamp without catching on the clamp or becoming stuck
- 10. After the syringe is completely removed from the clamp, disconnect the medical grade tubing-catheter complex from the syringe and place both the medical grade tubing and syringe on the surface next to the syringe clamp mold.
- 11. Pick up either the same 1 mL syringe that was just removed from the syringe clamp mold or a different 1 mL syringe and properly connect it to the procedural medical grade tubing (fasten it into place, ensuring a tight connection is present).
  - a. Connections should be made and tightened following the current clinical process
- 12. Pull the syringe plunger out as far as it can go without popping out of the proximal end of the 1 mL syringe.
- 13. With this syringe-tubing-catheter complex kept intact, place the 1 mL syringe into the syringe clamp, with the widest diameter portion of the syringe located on the proximal end of the syringe, inserting into the slit on the proximal end of the clamp. The body and distal end of the syringe should be sitting in the semi-circle mold. Stop the stopwatch

when the syringe insertion is complete and it is properly located within the syringe clamp mold.

- a. Verify that the syringe's widest diameter segment fits within the mold's slot
- b. Verify that the entire body of the syringe sits within the semi-circle mold
- c. Verify that the syringe rests completely horizontal within the syringe clamp mold without requiring intervention
- d. Ensure that the syringe removal and insertion process took less than 20 seconds

If any of the steps can not be completed as outlined above or the verification steps fail, reevaluate the design and determine how the syringe clamp mold can be modified in order to allow for the connection and locking tests to pass. If there is an error within the test protocol or a modification is required, deviation can be made within the protocol in order to allow a verification step to pass or a step to be completed.

## **References**

- [1] Ultimaker, "Technical Data Sheet - PLA," Nov. 2018. Accessed: Dec. 02, 2021. [Online]. Available: <https://ultimaker.com/materials/pla>.

### Section 5.5: Injection Rate Testing Protocol

The following provides a step-by-step protocol to test if the stepper motor consistently provides a 30 and 60 second injection rate while also traveling the appropriate distance to fully eject 0.5 mL of solution. This protocol is used to evaluate the accuracy and consistency of the two injection rates the device provides. Read through the protocol before performing the steps.

1. Power on the device
2. Measure the distance between the force application block and the end of the syringe that is set to 0.5 mL in mm
3. Set up a timer and press start and at the same time press the 60 second flow rate button
4. Stop the timer when the device stops
5. Record the time
6. Record the distance that the force application block traveled in mm
7. Press the reset button and record the time it takes for the device to fully reset back to the original position
8. Repeat five times and calculate the average injection time to ensure that each trial is within 5% error
  - a. Calculate the error margin using Equation 1 below, with the theoretical value corresponding to the required 60 second injection time [1]

$$[1] \text{ Percent Error} = (|V_{\text{theoretical}} - V_{\text{experimental}}| / V_{\text{theoretical}}) * 100$$

9. Perform one more trial and press the pause button multiple times throughout the injection to ensure that the injection comes to a full stop whenever the pause button is pressed
10. Follow the previous steps using the 30 second injection rate
11. Repeat five times calculate the average injection time to ensure that it is within 2.5% error
  - a. Calculate the error margin using Equation 1 below, with the theoretical value corresponding to the required 30 second injection times [1]

$$[1] \text{ Percent Error} = (|V_{\text{theoretical}} - V_{\text{experimental}}| / V_{\text{theoretical}}) * 100$$

### **References**

- [1] Dr. A. M. Helmenstine, "How to Calculate Percent Error," ThoughtCo, Nov. 02, 2020.  
<https://www.thoughtco.com/how-to-calculate-percent-error-609584> (accessed Dec. 03, 2021).

## Section 5.6: Cell Viability Testing Protocol

The cell viability testing protocol is outlined in this document. The protocol includes thawing the cells, using trypan blue and conducting tests with the automatic device at 30 and 60 seconds, manually with the 30 and 60 second rates, and a rapid test.

1. Start with five vials full of pig MSCs that are at 5 million cells / dose and remove them from the liquid N<sub>2</sub>
  2. Pig MSCs are more robust than other cell types so the sterility shouldn't matter as much but use gloves throughout the course of the experiments if directly dealing with the cells and spray down hands using 70% EtOH if working in the hood.
  3. Thaw the cells in a 37 degrees C water bath while continuously mixing them by hand.
  4. In the hood, obtain two 20 mL empty and sterile vials and add 2 mL of MCDB 131 media with FBS for the cells to begin with (Note: Cells are frozen in DMSO media so use different media to wash it off)
  5. Add two of the cell vials (about 1 mL of solution) to one of the media-containing vials and three of the cell vials to the other media-containing vials.
  6. After the cells are added, fill the vials with media until there is 7mL of total solution for each of the 2 vials
  7. Place both vials on opposite ends of a centrifuge machine and set on 1000 RCF for 5 minutes
  8. Aspirate the supernatant using a vacuum in the hood and combine the 2 vials with cells adding 1 mL of MCDB 131 media and resuspend so they can be counted via Trypan Blue staining
  9. In a 1.5-2 mL tube, add trypan blue and cell suspension according to the appropriate dilution (Note: dilution may need to be adjusted depending on if cells were cultured in a smaller flask, how many flasks are accounted for in each tube, or if cell count may be low).
  10. Using a hemacytometer, count cells in all four quadrants.
    - a. Count the initial number of cells that are alive (clear looking) and dead (blue)
  11. To determine the total cell count: cell count x dilution factor x 2500 = cell count
  12. Add media to the rest of the cells and get 40mL of solution
  13. Load up the syringe with 0.5 mL
  14. Test at 30 seconds with machine x5
  15. Test at 60 seconds with machine x5
  16. Test at 30 seconds with manual x3
  17. Test at 60 seconds with manual x3
  18. Test at rapid rate x3
  19. Record the cell viability after each testing using protocol in steps 9 and 10.
  20. Repeat steps 9 and 10 after all testing is finished to get the end cell viability
-

## Section 5.7: Catheter Obstruction Testing Protocol

The catheter obstruction testing protocol is outlined below. This protocol includes establishing the force values that correspond to catheter obstruction. The force values detected on the injector will be used to establish the threshold reflective of catheter obstruction and cell reflux. This test aims to determine the catheter obstruction force level for different myocardium Young's Modulus values corresponding to different extents of myocardial infarction (healthy, diseased, and scarred). The Young's modulus of a healthy human heart is below 50 kPa and increases to more than 100 kPa for scar tissue [1].

1. Set up the injector (integrated with the FSG Sensor)
2. Connect a 1 mL syringe loaded with 0.5 mL of water to the procedural catheter
3. Create an obstruction in the catheter by creating a kink
4. Before beginning the injections ensure the force detected by the FSG Sensor is being properly plotted by the Arduino into a file
5. Test at 30 seconds with the Cellringe Pump integrated with the FSG Sensor
  - a. Repeat this step three times ensuring there is an obstruction in the catheter for each trial
6. Save the force data file after each trial and name appropriately
7. Test at 60 seconds with the Cellringe Pump integrated with the FSG Sensor
  - a. Repeat this step three times ensuring there is an obstruction in the catheter for each trial
8. Save the force data file after each trial and name appropriately

If any of the steps can not be completed as outlined above or the force detection steps fail, reevaluate the design and determine how the catheter obstruction testing can be modified in order to allow for proper catheter interference and force value determination. If there is an error within the test protocol or a modification is agreed upon, a deviation can be made within the protocol in order to allow a step to be completed

## **References**

- [1] Allijn, Iris, Marcelo Ribeiro, André Poot, Robert Passier, and Dimitrios Stamatialis. "Membranes for Modeling Cardiac Tissue Stiffness In Vitro Based on Poly(Trimethylene Carbonate) and Poly(Ethylene Glycol) Polymers." *Membranes* 10, no. 10 (October 3, 2020): E274. <https://doi.org/10.3390/membranes10100274>.

### Section 5.8: Bovine Steak Injection Testing Protocol

The bovine steak injection testing protocol is outlined below. This protocol includes obtaining a bovine steak and cooking with various temperatures. Then conducting tests with the Cellringe Pump integrated with the FSG Sensor, at 30 and 60 seconds. This test aims to mimic the Young's Modulus of various states of heart tissue: healthy, diseased, and scarred.

The Young's modulus of a healthy human heart is below 50 kPa and increases to more than 100 kPa for scar tissue [1]. While the Young's Modulus for raw steak is around 70 kPa and cooked steak is around 260 kPa [2].

1. Start by obtaining one steak from the grocery store
2. Cut the steak into four sections
  - a. Leave one section uncooked
3. Using a stovetop, cook one section rare, one medium, and one well done
  - a. Rare: ensure the stovetop is at 130° F then grill 3 minutes per side, ensure the internal temperature is between 125° - 130° F with a meat thermometer [3]
  - b. Medium: ensure the stovetop is at 130° F then grill 4 minutes per side, ensure the internal temperature is between 140° - 150° F with a meat thermometer [3]
  - c. Well-Done: ensure the stovetop is at 140° F then grill 4 minutes per side, ensure the internal temperature is over 160° F with a meat thermometer [3]
4. Set up the Cellringe Pump integrated with the FSG Sensor
5. Connect a 1 mL syringe filled with 0.5 mL of DI water to the procedural catheter
6. Insert the needle-tipped end of the procedural catheter into the one of the bovine steak sections
7. Before beginning the injections ensure the force detected by the FSG Sensor is being properly plotted by the Arduino into a file
8. Test at 30 seconds with the Cellringe Pump integrated with the FSG Sensor
  - a. Repeat 3 times
  - b. Save the force data file after each trial and name appropriately
9. Test at 60 seconds with the Cellringe Pump integrated with the FSG Sensor
  - a. Repeat 3 times
  - b. Save the force data file after each trial and name appropriately
10. Repeat steps 6 - 9 for each steak condition

## References

- [1] Allijn, Iris, Marcelo Ribeiro, André Poot, Robert Passier, and Dimitrios Stamatialis. “Membranes for Modeling Cardiac Tissue Stiffness In Vitro Based on Poly(Trimethylene Carbonate) and Poly(Ethylene Glycol) Polymers.” *Membranes* 10, no. 10 (October 3, 2020): E274. <https://doi.org/10.3390/membranes10100274>.
- [2] James, Bryony, and Seo Won Yang. “Testing Meat Tenderness Using an in Situ Straining Stage with Variable Pressure Scanning Electron Microscopy.” *Procedia Food Science*, 11th International Congress on Engineering and Food (ICEF11), 1 (January 1, 2011): 258–66. <https://doi.org/10.1016/j.profoo.2011.09.041>.
- [3] “Steak Temperatures | The Majestic Restaurant and Jazz Club.” Accessed October 31, 2022. <https://majesticc.com/steak-temperatures/>.



## Section 5.9: Ex Vivo Cervine Heart Injection Testing Protocol

The ex vivo injection testing protocol is outlined below. This protocol includes obtaining a cervine heart and measuring the force within the heart. Then conducting tests with the Cellringe Pump integrated with the FSG Sensor, at 30 and 60 seconds. This test aims to mimic the Young's Modulus of various states of heart tissue: healthy, diseased, and scarred. The Young's modulus of a healthy human heart is below 50 kPa and increases to more than 100 kPa for scar tissue [1]. Deer hearts mimic the anatomy of human hearts as they are very similar in size, structure, and function. Porcine hearts consist of four chambers and also have four valves and an aorta [2].

1. Start by obtaining a cervine heart
2. Set up the Cellringe Pump integrated with the FSG Sensor
3. Connect a 1 mL syringe loaded with 0.5 mL of water to the procedural catheter
4. Insert the needle-tipped end of the procedural catheter into the internal aortic arch of the deer heart
5. Before beginning the injections ensure the force detected by the FSG Sensor is being properly plotted by the Arduino into a file
6. Test at 30 seconds with the Cellringe Pump integrated with the FSG Sensor
7. Save the force data file after each trial and name appropriately
  - a. Repeat steps 3-5 for 3 trials with each trial at a different location inside the aortic arch
  - b. Repeat but test with 60 seconds with the Cellringe Pump integrated with the FSG Sensor for 3 trials
8. Save the force data file after each trial and name appropriately

## **References**

- [1] Allijn, Iris, Marcelo Ribeiro, André Poot, Robert Passier, and Dimitrios Stamatialis. "Membranes for Modeling Cardiac Tissue Stiffness In Vitro Based on Poly(Trimethylene Carbonate) and Poly(Ethylene Glycol) Polymers." *Membranes* 10, no. 10 (October 3, 2020): E274. <https://doi.org/10.3390/membranes10100274>.
- [2] "Circulatory System and Respiratory System," *WhiteTail Deer*. <http://whitetailsmo.weebly.com/circulatory-system-and-respiratory-system.html> (accessed Dec. 04, 2022).

## Section 5.10: Viscosity Testing Protocol

The viscosity correlation testing protocol is outlined below. This protocol includes obtaining various solutions ranging in viscosity and conducting tests with the Cellringe Pump integrated with the FSG sensor at 30 and 60 seconds.

Viscosity corresponds to the concept of ‘thickness’ while also providing a measure of the resistance of a fluid to deformation or flow with application of shear or tensile stress, defined by the following equation [1]:

$$\text{viscosity } \mu = \frac{\text{shear stress}}{\text{strain rate}} \text{ (Pa. s)}$$

%FBS (v/v)	Density (g/cm <sup>3</sup> )		Dynamic Viscosity (mPa.s)	
	DMEM (high glucose)	RPMI-1640	DMEM (high glucose)	RPMI-1640
0	1.000 ± 0.001	0.999 ± 0.003	0.731 ± 0.015	0.733 ± 0.006
5	1.002 ± 0.003	1.002 ± 0.002	0.862 ± 0.029	0.848 ± 0.021
10	1.009 ± 0.003	1.007 ± 0.002	0.930 ± 0.034	0.958 ± 0.032
20	1.023 ± 0.005	1.020 ± 0.005	1.050 ± 0.027	1.089 ± 0.044
Water		0.995 ± 0.002	0.659 ± 0.017	
PBS		0.998 ± 0.002	N/A	
H460 spent medium		1.015 ± 0.003	0.954 ± 0.070	
HN6 spent medium		1.013 ± 0.003	1.086 ± 0.073	

1. Start by obtaining a 5 mL aliquot of deionized water control at 20 degrees Celsius (known viscosity of 10<sup>-3</sup> Pa. s)
2. Load up the syringe with 0.5 mL of the DI water
3. Before beginning the injections ensure the force detected by the FSG Sensor is being properly plotted by the Arduino into a file
4. Test at 30 seconds with the Cellringe Pump integrated with the FSG Sensor
  - a. Repeat the test for a total of 3 trials
5. Save the force data file after each trial and name appropriately
6. Test at 60 seconds with the Cellringe Pump integrated with the FSG Sensor
  - a. Repeat the rest for a total of 3 trials
7. Repeat steps 1-5 using canola oil at 20 degrees Celsius (known viscosity of 46.2 mPa. S [2])
  - a. Record the maximum force exhibited as well as an average force range
8. Save the force data file after each trial and name appropriately

## References

- [1] Poon, Christine. “Measuring the Density and Viscosity of Culture Media for Optimized Computational Fluid Dynamics Analysis of in Vitro Devices.” bioRxiv, August 25, 2020. <https://doi.org/10.1101/2020.08.25.266221>.
- [2] L. M. Diamante and T. Lan, “Absolute Viscosities of Vegetable Oils at Different Temperatures and Shear Rate Range of 64.5 to 4835 s<sup>-1</sup>,” Journal of Food Processing, vol. 2014, pp. 1–6, Aug. 2014, doi: 10.1155/2014/234583.

## Section 6: Testing Results and Data Analysis

### Section 6.1: FSR Feedback System Force Detection Accuracy Results

#### **Calculations:**

$1 \text{ mL} = 1 \text{ g}$ $1 \text{ mL} = 1000 \text{ } \mu\text{L}$ $[1] \text{ Weight of Water Bottle} = 9.440 \text{ g}$ $\text{Total Weight} = 9.440 \text{ g} + \text{mL}$ $\text{Force} = (\text{Total Weight} / 1000) * 9.81$
---

$[2] \% \text{ Difference} = ( \text{Actual Value} - \text{Theoretical Value}  / \text{Theoretical}) * 100$ $\text{Theoretical Value} = \text{Estimated Force}$
---

Table 1: Feedback system's force output error margin relative to their respective applied forces over the typical 0.14 N - 3.00 N injector force range.

Unknown sample of water	Force of the bottle + water (N)	Measured Force of the bottle + water using FSR and Arduino (N)	% Difference between Force Values in Column 2 and 3 Using Estimate as Theoretical
1	0.14	0.16	14%
2	0.32	0.27	15.6%
3	0.55	0.64	16.4%
4	0.70	0.82	17.1%
5	1.00	1.15	13%
6	1.30	1.31	0.77%
7	1.75	1.82	3.43%
8	2.15	1.99	7.44%
9	2.30	2.03	11.74%
10	2.40	2.29	4.58%
11	3.00	2.72	9.33%

#### **Scatter Plot Matlab Code**

```
%% BME 400 - FSR Feedback System Force Detection Results
% Author - Parker Esswein
%%
```

```
x = [0.14 0.32 0.55 0.70 1.00 1.30 1.75 2.15 2.30 2.40 3.00] % Applied Voltage Values
y = [14.00 15.60 16.40 17.10 13.0 0.77 3.43 7.44 11.74 4.58 9.33] % Corresponding error
provided by the feedback system in detecting the force value
```

```
figure (1);
hold on;
plot(x, y, 'o')
title('FSR Feedback System Force Detection Accuracy')
xlabel('Total Applied Force (N)')
ylabel('Percent Error Between Applied Force and Feedback System (%)')
hold off;
%%
lforce = [14.00 15.60 16.40 17.10];
mean(lforce)
std(lforce)
hforce = [13.0 0.77 3.43 7.44 11.74 4.58 9.33];
mean(hforce)
std(hforce)
nlforce = [14.00 15.60 16.40 17.10 13.0 0.77 3.43 7.44 11.74 4.58];
mean(nlforce)
std(nlforce)
```

## References

- [1] F. P. Beer, E. R. Johnston Jr., J. T. DeWolf, and D. F. Mazurek, *Mechanics of Materials*, 8th Edition. McGraw Hill Education, 2020.
- [2] Dr. A. M. Helmenstine, "How to Calculate Percent Error," ThoughtCo, Nov. 02, 2020. <https://www.thoughtco.com/how-to-calculate-percent-error-609584> (accessed Dec. 03, 2021).

Section 6.2: FSG Feedback System Force Detection Accuracy Results

**Calculations:**

$$1 \text{ mL} = 1 \text{ g}$$

$$1 \text{ mL} = 1000 \text{ }\mu\text{L}$$

$$[1] \text{ Weight of Water Bottle} = 30.09 \text{ g}$$

$$\text{Total Weight} = 30.09 \text{ g} + \text{mL}$$

$$\text{Force} = (\text{Total Weight} / 1000) * 9.81$$

$$[2] \% \text{ Difference} = (|\text{Actual Value} - \text{Theoretical Value}| / \text{Theoretical}) * 100$$

$$\text{Theoretical Value} = \text{Estimated Force}$$

Table 1: Feedback system's force output error margin relative to their respective applied forces over the typical 0.14 N - 5.00 N injector force range.

Unknown sample of water	Force of the bottle + water (N)	Measured Force of the bottle + water using FSR and Arduino (N)	% Difference between Force Values in Column 2 and 3 Using Estimate as Theoretical
1	0.41	0.39	4.88%
2	0.66	0.64	3.03%
3	0.76	0.74	2.63%
4	0.98	0.96	2.04%
5	1.41	1.37	2.83%
6	1.90	1.89	0.53%
7	2.45	2.44	0.41%
8	2.91	2.90	0.34%
9	3.24	3.22	0.62%
10	3.69	3.69	0.00%
11	4.39	4.41	0.46%
12	4.96	4.83	2.62%

**Scatter Plot Matlab Code**

```
%% BME 400 - Force Detection Accuracy Results
```

```
% Author - Parker Esswein
```

```
%%
```

```
x = [0.41 0.66 0.76 0.98 1.41 1.90 2.45 2.91 3.24 3.69 4.39 4.96] % Applied Force Values
```

y = [4.88 3.03 2.63 2.04 2.83 0.53 0.41 0.34 0.62 0.00 0.46 2.62] % Corresponding error provided by the feedback system in detecting the force value

```
figure (1);  
hold on;  
plot(x, y, 'o')  
title('FSR Feedback System Force Detection Accuracy')  
xlabel('Total Applied Force (N)')  
ylabel('Percent Error Between Applied Force and Feedback System (%)')  
legend('Experimental Data')  
hold off;  
%%  
mean(y)  
std(y)
```

```
lforce = [4.88 3.03 2.63 2.04 2.83 0.53 0.41];  
mean(lforce)  
std(lforce)
```

```
terror = [0.53 0.41 0.34];  
mean(terror)  
std(terror)
```

### References

- [1] F. P. Beer, E. R. Johnston Jr., J. T. DeWolf, and D. F. Mazurek, Mechanics of Materials, 8th Edition. McGraw Hill Education, 2020.
- [2] Dr. A. M. Helmenstine, "How to Calculate Percent Error," ThoughtCo, Nov. 02, 2020. <https://www.thoughtco.com/how-to-calculate-percent-error-609584> (accessed Dec. 03, 2021).

### Section 6.3: FSR vs FSG Feedback System Force Detection Accuracy Comparison Results

#### **Matlab Boxplot and t-test Code**

```
%% BME 400 - FSG and FSR Feedback System Force Detection Comparison
% Author - Parker Esswein
%%
FSG = [4.88 3.03 2.63 2.04 2.83 0.53 0.41 0.34 0.62 0.00 0.46 2.62] % Error provided by the
FSG feedback system in detecting the force value
FSR = [14.00 15.60 16.40 17.10 13.0 0.77 3.43 7.44 11.74 4.58 9.33] % Error provided by the
FSR feedback system in detecting the force value
%%
mean(FSR)
std(FSR)
[h,p,ci, stats] = ttest2(FSG, FSR)
%% Box Plot Generation
FSG = [4.88 3.03 2.63 2.04 2.83 0.53 0.41 0.34 0.62 0.00 0.46 2.62]' % Error provided by the
FSG feedback system in detecting the force value
FSR = [14.00 15.60 16.40 17.10 13.0 0.77 3.43 7.44 11.74 4.58 9.33 NaN]' % Error provided by
the FSR feedback system in detecting the force value (Added additional 10.31 percent
difference)
name = ["FSG Sensor", "FSR Sensor"];
figure(1)
boxplot([FSG, FSR], name)
ylabel('Percent Error Between Applied Force and Feedback System (%)')
title('Force Detection Accuracy of the FSR and FSG Feedback Systems Across Various Applied
Forces (0.14 N - 5.00 N)')
```

Section 6.4: FSR Feedback System Testing Results

Table 1: Results for each of the three trials that were done over the course of five seconds where both the display and serial monitor force values were recorded

		Trial 1		Trial 2		Trial 3	
		Display	SM	Display	SM	Display	SM
Aliquot of water #1	1 sec	0.20	0.20	0.21	0.20	0.23	0.23
	2 sec	0.20	0.20	0.20	0.19	0.23	0.23
	3 sec	0.21	0.22	0.19	0.20	0.23	0.23
	4 sec	0.22	0.21	0.20	0.21	0.23	0.23
	5 sec	0.21	0.20	0.21	0.22	0.23	0.23
Aliquot of water #2	1 sec	0.67	0.67	0.68	0.68	0.69	0.69
	2 sec	0.67	0.67	0.69	0.69	0.68	0.69
	3 sec	0.67	0.67	0.69	0.69	0.67	0.68
	4 sec	0.67	0.68	0.68	0.69	0.68	0.68
	5 sec	0.68	0.68	0.68	0.68	0.68	0.68
Aliquot of water #3	1 sec	1.20	1.21	1.21	1.21	1.21	1.20
	2 sec	1.22	1.23	1.21	1.21	1.20	1.20
	3 sec	1.20	1.21	1.21	1.21	1.20	1.20
	4 sec	1.22	1.22	1.20	1.21	1.20	1.20
	5 sec	1.21	1.21	1.20	1.20	1.20	1.20
Aliquot of water #4	1 sec	1.93	1.93	1.93	1.93	1.93	1.93
	2 sec	1.93	1.93	1.92	1.93	1.93	1.93
	3 sec	1.94	1.94	1.93	1.93	1.93	1.94
	4 sec	1.93	1.94	1.93	1.93	1.94	1.94
	5 sec	1.93	1.93	1.92	1.92	1.94	1.94



Aliquot of water #5 (light was on)	1 sec	2.47	2.47	2.48	2.48	2.47	2.47
	2 sec	2.47	2.47	2.48	2.48	2.47	2.47
	3 sec	2.48	2.48	2.48	2.48	2.47	2.47
	4 sec	2.49	2.49	2.48	2.48	2.48	2.47
	5 sec	2.49	2.49	2.48	2.48	2.48	2.48

The mean and standard deviation of the display and serial monitor for the three trials (over five seconds) per each aliquot of water was taken (15 data points for each aliquot of water). The percent difference was calculated to indicate how much difference there was between the serial monitor and the display using the following equation [1]:

$$\left( \frac{|SM_{\text{avg}} - \text{Display}_{\text{avg}}|}{\left( \frac{SM_{\text{avg}} + \text{Display}_{\text{avg}}}{2} \right)} \right) * 100 = \text{Percent Difference}$$

SM = Serial Monitor  
Display = Scoreboard

#### References:

[1] “Percent Difference Calculator - with Step-by-Step Guide,” Inch Calculator.

<https://www.inchcalculator.com/percent-difference-calculator/> (accessed May 03, 2022).

Section 6.5: Syringe Clamp Connection and Locking Results

Table 1: Syringe Clamp Connection and Locking force testing and exchange time results.

Trial	Force Testing Result	Exchange Time (seconds)
1	Pass	14.67
2	Pass	10.56
3	Pass	13.31
4	Pass	14.78
5	Pass	14.17

## Section 6.6: Injection Rate Testing Results

### 30 Second Injection Rate Testing

Run 1

Injection time: 30.5 seconds

Traveled: 30.86 mm

Run 2

Injection time: 30.4 seconds

Traveled: 30.31 mm

Run 3

Injection time: 30.34 seconds

Traveled: 30.34 mm

Run 4

Injection time: 30.26 seconds

Traveled: 30.36 mm

Run 5

Injection time: 30.12 seconds

Traveled: 30.52 mm

### Results:

Time: Mean = 30.324, standard deviation  $s=0.1438$ , percent error from 30 seconds: 1.08%

Distance Traveled: Mean = 30.478mm, standard deviation  $s=0.2285$ mm, percent error from 30.5mm = 0.0721%

### 60 Second Injection Rate

Run 1

Injection time: 1 min 2 sec

Traveled: 30.25 mm

Run 2

Injection time: 1 min 1 sec

Traveled: 30.51 mm

Run 3

Injection time: 1 min 1 sec

Traveled: 30.49 mm

Run 4

Injection time: 1 min

Traveled: 30.55 mm

Run 5

Injection time: 1 min

Traveled: 30.65 mm

**Results:**

Time: Mean = 60.8, standard deviation  $s = 0.83666$ , percent error from 30 seconds: 1.333%

Distance Traveled: Mean = 30.49mm, standard deviation  $s=0.1476$ mm, percent error from 30.5mm = 0.03281%

\*Note: The following percent error equation was used for calculations.

$$[1] \text{ Percent Error} = ( |V_{\text{theoretical}} - V_{\text{experimental}}| / V_{\text{theoretical}} ) * 100$$

**References:**

[1] Dr. A. M. Helmenstine, "How to Calculate Percent Error," ThoughtCo, Nov. 02, 2020.

<https://www.thoughtco.com/how-to-calculate-percent-error-609584> (accessed Dec. 03, 2021).

Section 6.7: Cell Viability Testing Results and Analysis

Table 1: Cell Viability of Porcine-derived MSCs following automatic and manual injections at various rates. All injections were performed with a 25 gauge needle containing a length of 2.22 cm unless otherwise noted.

Injection Type	Trial Number	Injection Rate (Seconds)	Force Range (N)	Maximum Force (N)	Cell Viability (%)
Automatic	1	30 (20 gauge needle)	~ 0.16 N	0.29 N	88.0
Automatic	2	30 (20 gauge needle)	0.14 - 0.18 N	0.21 N	88.0
Automatic	3	30 (20 gauge needle)	0.16 - 0.18 N	0.29 N	78.9
Automatic	4	30 (20 gauge needle)	~ 0.19 N	0.33 N	100.0
Automatic	5	30	0.32 N - 0.61 N	1.43 N	92.0
Automatic	1	60	~ 0.14 N	0.17 N	85.0
Automatic	2	60	0.21 - 0.22 N	0.41 N	83.0
Automatic	3	60	0.21 - 0.22 N	0.67 N	90.0
Automatic	4	60	0.29 - 0.42 N	0.52 N	80.0
Automatic	5	60	~ 0.30 N	1.02 N	87.0
Manual	1	30	0.29 - 0.31 N	1.03 N	90.0
Manual	2	30	0.59 - 0.63 N	0.73 N	93.0
Manual	3	30	0.59 - 0.62 N	1.05 N	80.0
Manual	4	30	0.28 - 0.34 N	0.39 N	83.0
Manual	1	60	0.42 - 0.54 N	0.71 N	86.0
Manual	2	60	0.30 - 0.51 N	1.91 N	83.0
Manual	3	60	0.28 - 0.43 N	0.46 N	78.0
Manual (Rapid)	1	1.03	Initial Force $\approx$ 0.39 N	3.21 N	86.0

Manual (Rapid)	2	1.15	Initial Force ≈ 0.21 N	3.34 N	92.0
Manual (Rapid)	3	0.44	Initial Force ≈ 0.30 N	8.17 N	90.0
Manual (Rapid)	4	0.37	Initial Force ≈ 0.49 N	9.30 N	77.0

Table 2: One-way ANOVA table comparing the viability of MSCs following automatic and manual 30 and 60 second injections. The p-value when comparing all four groups as separate is 0.41, demonstrating that there is not a significant difference between the automatic and manual injections when using a significance value of  $p = 0.05$ .

ANOVA Table					
Source	SS	df	MS	F	Prob>F
Groups	102.961	3	34.3202	1.03	0.4113
Error	432.955	13	33.3042		
Total	535.915	16			

Table 3: Comparison of all four injection groups (automatic and manual) via pairs and each pair's respective p-value.

Group 1	Group 2	Lower Confidence Interval of the Difference	Estimated Difference in the Means	Upper Confidence Interval of the Difference	p-value (CType correction)
1	2	-6.334	4.380	15.093	0.637
1	3	-8.483	2.880	14.243	0.878
1	4	-5.323	7.047	19.417	0.376
2	3	-12.863	-1.500	9.863	0.979
2	4	-9.703	2.667	15.037	0.920
3	4	-8.770	4.167	17.104	0.782

## Cell Viability Box Plot, ANOVA, and Comparison Matlab Code

```
%% BME 301 - Cell Viability ANOVA
% Author - Parker Esswein
%% Variable Initialization
A30 = [88.00 88.00 78.90 100.00 92.00]' % Cell Viability for the 30 second automatic injections
A60 = [85.00 83.00 90.00 80.00 87.00]' % Cell Viability for the 60 second automatic injections
M30 = [90.00 93.00 80.00 83.00 NaN]' % Cell Viability for the 30 second manual injections
M60 = [86.00 83.00 78.00 NaN NaN]' % Cell Viability for the 60 second manual injections
SV = [81.10 81.10 81.10 81.10 81.10]' % Cell Viability after Thawing
EV = [80.0 80.0 80.0 80.0 80.0]' % Final Cell Viability
%% Average and Std for each injection group
mean(A30)
std(A30)
mean(A60)
std(A60)
mean(M30(1:4,:))
std(M30(1:4,:))
mean(M60(1:3,:))
std(M60(1:3,:))
%% Box Plot Generation
name = ["Initial Viability", "30 Second Automatic Injections", "30 Second Manual Injections",
"60 Second Automatic Injections", "60 Second Manual Injections", "Final Viability"];
figure(1)
boxplot([SV, A30, M30, A60, M60, EV], name)
ylabel('MSC Viability (%)')
title('Cell Viability of Porcine-derived MSCs Following Automatic and Manual Injections at
Various Rates')
%% ANOVA between automatic and manual injection values
viability = [A30 A60 M30 M60]
name = ["30 Second Automatic Injections", "60 Second Automatic Injections", "30 Second
Manual Injections", "60 Second Manual Injections"];
figure(2)
hold on;
[p, tbl, stats] = anova1(viability, name)
hold off;
figure (5)
hold on;
[c,m,h,gnames] = multcompare(stats)
hold off;
```

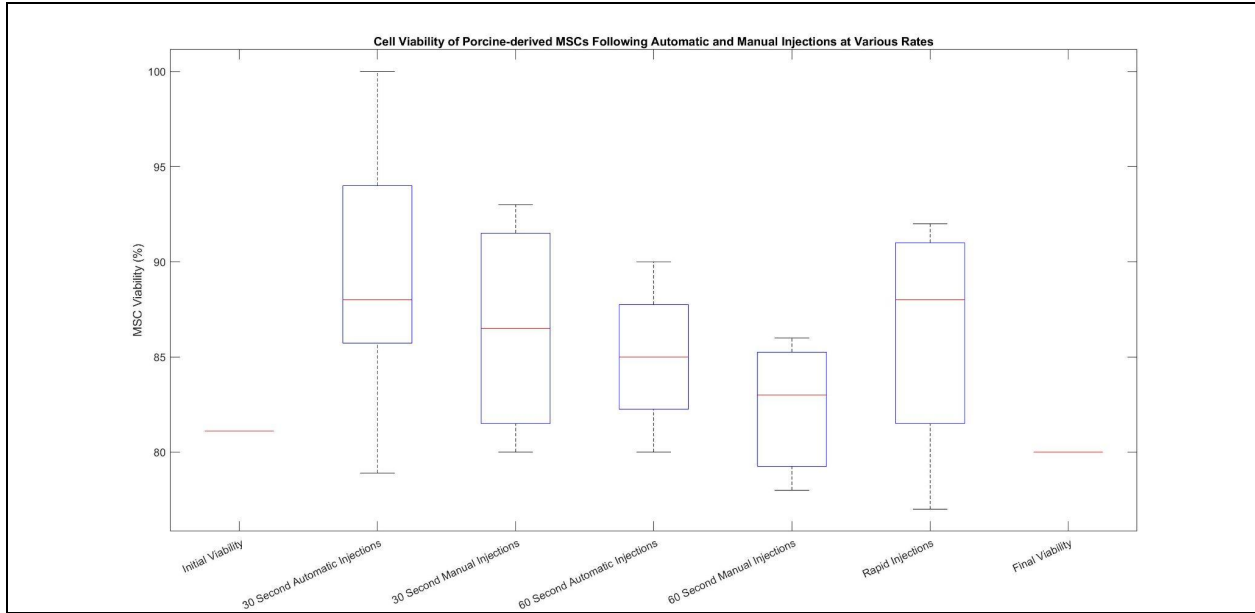


Figure 1: Boxplot comparing the viability of MSCs following automatic and manual 30 and 60 second injections as well as rapid injections to each other and to the starting and final MSC viability. The rectangles represent the interquartile range, the whiskers display the full range of MSC viability, and the red lines locate the median for each rate and injection modality (manual and automatic).

Table 4: One-way ANOVA table comparing the viability of MSCs following automatic and manual 30 and 60 second injections as well as rapid injections. The p-value when comparing all five groups as separate is 0.59, demonstrating that there is not a significant difference between the automatic and manual injections when using a significance value of  $p = 0.05$ .

ANOVA Table					
Source	SS	df	MS	F	Prob>F
Groups	102.981	4	25.7453	0.73	0.5857
Error	565.705	16	35.3565		
Total	668.686	20			

Table 5: Comparison of all five injection groups (automatic and manual) via pairs and each pair's respective p-value.

Group 1	Group 2	Lower Confidence Interval of the Difference	Estimated Difference in the Means	Upper Confidence Interval of the Difference	p-value (CType correction)
1.0000000000000000	2.0000000000000000	-7.141454155022577	4.3799999999999995	15.901454155022568	0.770507398690263
1.0000000000000000	3.0000000000000000	-9.340347543219583	2.8799999999999995	15.100347543219574	0.948273148098677
1.0000000000000000	4.0000000000000000	-6.257162649049764	7.046666666666667	20.350495982383098	0.504930748924941
1.0000000000000000	5.0000000000000000	-9.090347543219583	3.1299999999999995	15.350347543219574	0.931385677226005
2.0000000000000000	3.0000000000000000	-13.720347543219578	-1.5000000000000000	10.720347543219578	0.995302029608716
2.0000000000000000	4.0000000000000000	-10.637162649049760	2.6666666666666671	15.970495982383103	0.970723753334347
2.0000000000000000	5.0000000000000000	-13.470347543219578	-1.2500000000000000	10.970347543219578	0.997677655194277
3.0000000000000000	4.0000000000000000	-9.746811068698481	4.1666666666666671	18.080144402031824	0.886030466159960
3.0000000000000000	5.0000000000000000	-12.631377345138937	0.2500000000000000	13.131377345138937	0.999996820763444
4.0000000000000000	5.0000000000000000	-17.830144402031824	-3.9166666666666671	9.996811068698481	0.906398343857326



## Cell Viability Box Plot, ANOVA, and Comparison including Rapid Injections Matlab Code

```
%% BME 301 - Cell Viability ANOVA with Rapid Injections
% Author - Parker Esswein
%% Variable Initialization
A30 = [88.00 88.00 78.90 100.00 92.00]' % Cell Viability for the 30 second automatic injections
A60 = [85.00 83.00 90.00 80.00 87.00]' % Cell Viability for the 60 second automatic injections
M30 = [90.00 93.00 80.00 83.00 NaN]' % Cell Viability for the 30 second manual injections
M60 = [86.00 83.00 78.00 NaN NaN]' % Cell Viability for the 60 second manual injections
RI = [86.00 92.00 90.00 77.00 NaN]' % Cell Viability for the 60 second manual injections
SV = [81.10 81.10 81.10 81.10 81.10]' % Cell Viability after Thawing
EV = [80.0 80.0 80.0 80.0 80.0]' % Final Cell Viability
%% Average and Std for each injection group
mean(A30)
std(A30)
mean(A60)
std(A60)
mean(M30(1:4,:))
std(M30(1:4,:))
mean(M60(1:3,:))
std(M60(1:3,:))
mean(RI(1:4,:))
std(RI(1:4,:))
%% Box Plot Generation
name = ["Initial Viability", "30 Second Automatic Injections", "30 Second Manual Injections",
"60 Second Automatic Injections", "60 Second Manual Injections", "Rapid Injections", "Final
Viability"];
figure(1)
boxplot([SV, A30, M30, A60, M60, RI, EV], name)
ylabel('MSC Viability (%)')
title('Cell Viability of Porcine-derived MSCs Following Automatic and Manual Injections at
Various Rates')
%% ANOVA between automatic and manual injection values
viability = [A30 A60 M30 M60 RI]
name = ["30 Second Automatic Injections", "60 Second Automatic Injections", "30 Second
Manual Injections", "60 Second Manual Injections", "Rapid Injections"];
figure(2)
hold on;
[p, tbl, stats] = anova1(viability, name)
hold off;
figure (5)
hold on;
[c,m,h,gnames] = multcompare(stats)
hold off;
```

## Cell Viability Force Variance Matlab Code

```
%% BME 301 - Cell Viability Force Variation
```

```

% Author - Parker Esswein
%% Minimum Force Values
FA30 = [0.16 0.14 0.16 0.19 0.32];
FM30 = [0.29 0.59 0.59 0.28];
FA60 = [0.14 0.21 0.21 0.29 0.30];
FM60 = [0.42 0.30 0.28];
%% Average of Minimum Force Values
mean(FA30)
std(FA30)
mean(FM30)
std(FM30)
mean(FA60)
std(FA60)
mean(FM60)
std(FM60)
%% Maximum Force Values
FA30 = [0.16 0.18 0.18 0.19 0.61];
FM30 = [0.31 0.63 0.62 0.34];
FA60 = [0.14 0.22 0.22 0.42 0.30];
FM60 = [0.54 0.51 0.43];
%% Average of Maximum Force Values
mean(FA30)
std(FA30)
mean(FM30)
std(FM30)
mean(FA60)
std(FA60)
mean(FM60)
std(FM60)
%% Variance Across Maximum and Minimum Force Values
TFA30 = [0.16 0.14 0.16 0.19 0.32];
TFM30 = [0.29 0.59 0.59 0.28];
TFA60 = [0.14 0.21 0.21 0.29 0.30];
TFM60 = [0.42 0.30 0.28];
var(TFA30)
var(TFM30)
var(TFA60)
var(TFM60)
%% ANOVA between automatic and manual injection values
TFA30 = [0.16 0.14 0.16 0.19 0.32]';
TFM30 = [0.29 0.59 0.59 0.28 NaN]';
TFA60 = [0.14 0.21 0.21 0.29 0.30]';
TFM60 = [0.42 0.30 0.28 NaN NaN]';
force = [TFA30 TFA60 TFM30 TFM60]
name = ["30 Second Automatic Injections", "60 Second Automatic Injections", "30 Second
Manual Injections", "60 Second Manual Injections"];

```

```
figure(2)
hold on;
[p, tbl, stats] = anova1(force, name)
hold off;
figure (5)
hold on;
[c,m,h,gnames] = multcompare(stats)
hold off;
```

## Section 6.8: Overall Device - 25 Gauge Needle Testing Results

### 30 second Overall Testing

**Trial 1:**

Actual delivery time: 30.72 seconds

Force Value Ranges: 0.14-0.49

Volume ejected: 0.49 mL

**Trial 2:**

Actual delivery time: 30.61 seconds

Force Value Ranges: 0.14-0.54

Volume ejected: 0.49 mL

**Trial 3:**

Actual delivery time: 30.60 seconds

Force Value Ranges: 0.13-0.55

Volume ejected: 0.47 mL

**Trial 4:**

Actual delivery time: 30.40 seconds

Force Value Ranges: 0.18-0.41

Volume ejected: 0.47 mL

**Trial 5:**

Actual delivery time: 30.50 seconds

Force Value Ranges: 0.23-0.50

Volume ejected: 0.46 mL

---

### 60 second Overall Testing

**Trial 1:**

Actual delivery time: 60.40 seconds

Force Value Ranges: 0.23-0.40

Volume ejected: 0.47 mL

**Trial 2:**

Actual delivery time: 60.11 seconds

Force Value Ranges: 0.11-0.50

Volume ejected: 0.47 mL

**Trial 3:**

Actual delivery time: 60.30 seconds

Force Value Ranges: 0.18-0.45  
Volume ejected: 0.47 mL

**Trial 4:**

Actual delivery time: 60.04 seconds  
Force Value Ranges: 0.13-0.46  
Volume ejected: 0.47 mL

**Trial 5:**

Actual delivery time: 60.12 seconds  
Force Value Ranges: 0.13-0.50  
Volume ejected: 0.47 mL

The mean of the ejection time, force ranges and volume ejected were calculated using the typical mean equation for a sample of five trials and the standard deviation was calculated using the standard deviation equation for samples rather than populations. The percent error was calculated to indicate how much error there was for the 30 and 60 second time settings respectively using the following equation:

$$[1] \text{ Percent Error} = (|V_{\text{theoretical}} - V_{\text{experimental}}| / V_{\text{theoretical}}) * 100$$

The serial plots were also obtained for this round of testing and can also be seen in the figures below.

### Serial Plot for a 30 Second Injection: 25 Gauge Needle

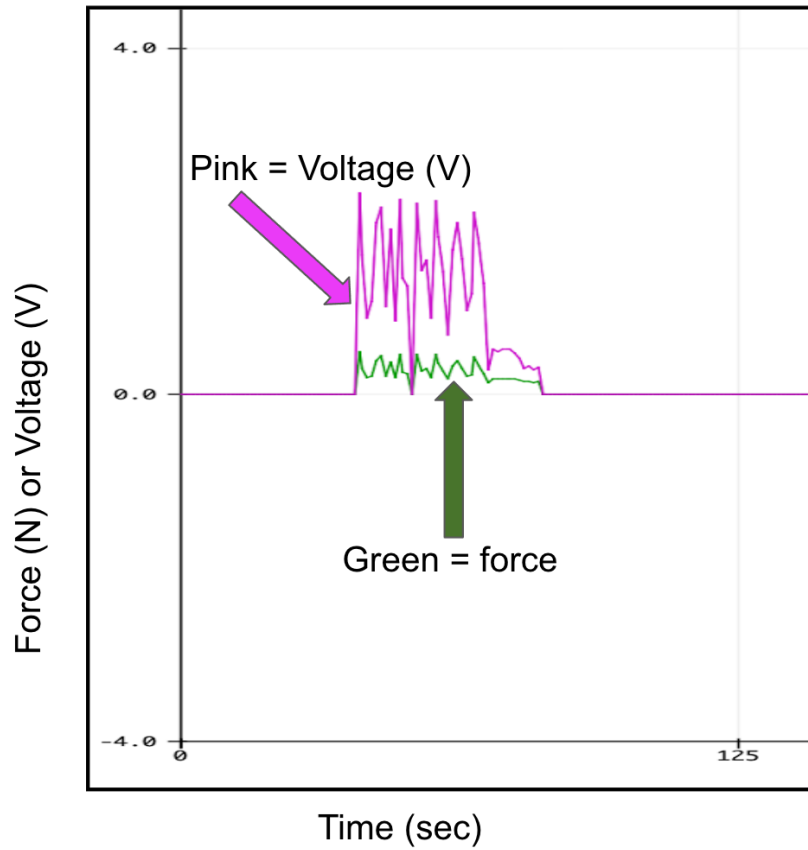


Figure 1: The serial plot with force values vs. time for the 25 gauge for one of the 30 second trials. The green line is the force values.

### Serial Plot for a 60 Second Injection: 25 Gauge Needle

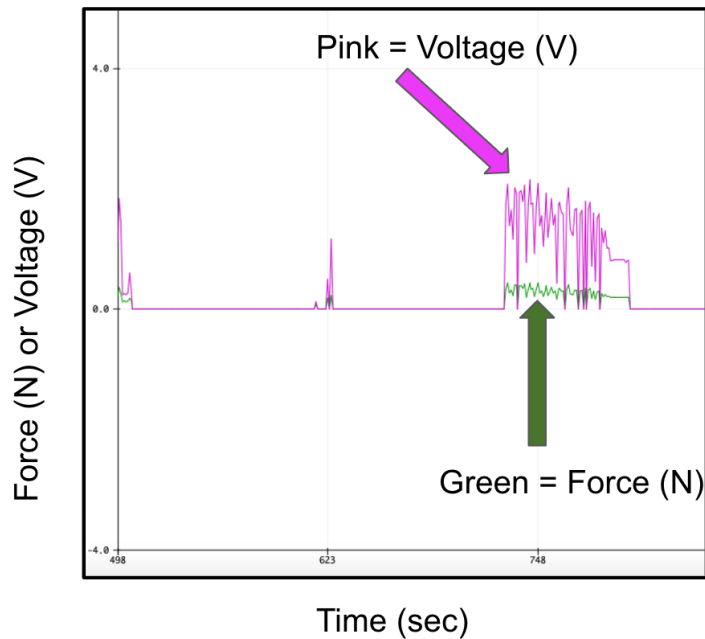


Figure 2: The serial plot with force values vs. time for the 25 gauge for one of the 60 second trials. The green line is the force values.

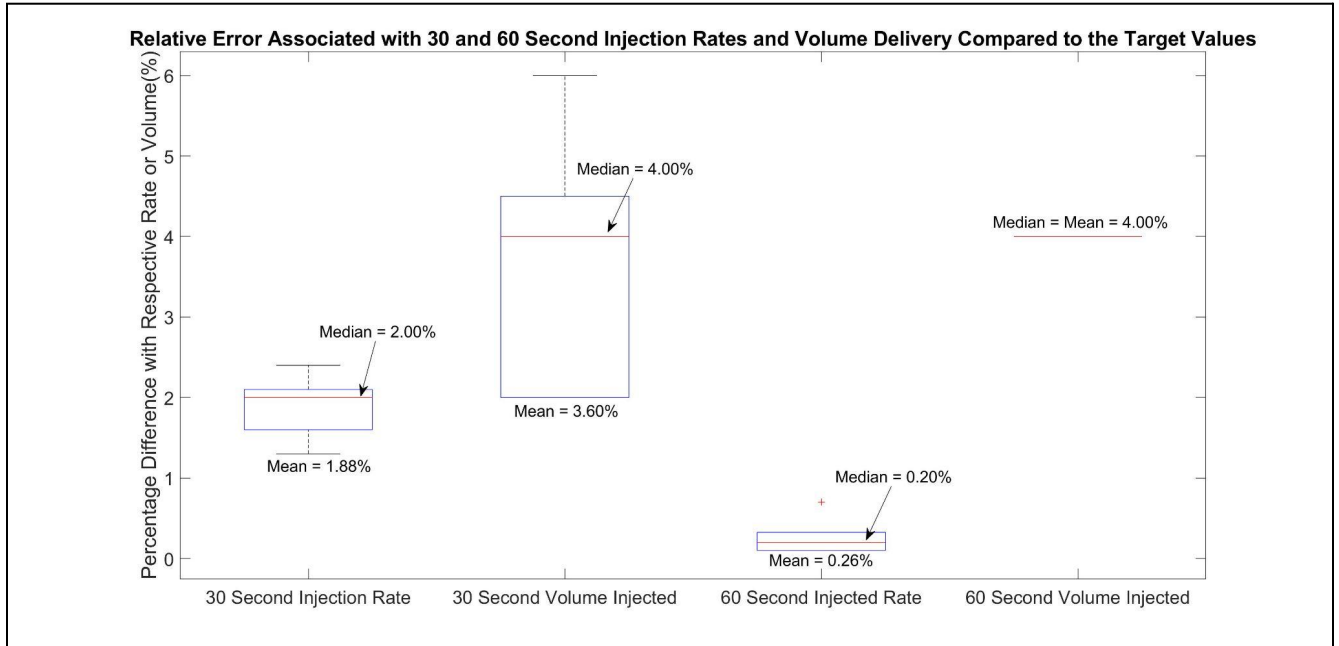


Figure 3: Boxplot displaying the percentage difference between the injection rates and delivery volumes to their respective 30 second, 60 second, and 0.5 mL target values. The rectangles represent the interquartile range, the whiskers display the full range of MSC viability, the red lines locate the median, and the plus signs resemble outliers for each rate and injection volume.

## Injection Rate and Volume Analysis Matlab Code

```
%% BME 301 - Injection Testing Results
% Author - Parker Esswein
%%
A30t = [2.4 2.0 2.0 1.3 1.7]' % Percentage difference between injection time for the 30 second
automatic injection setting and 30 seconds
A30v = [2.0 2.0 4.0 4.0 6.0]' % Percentage difference between the corresponding volume
injected by the device over the injection time and the required 0.5 mL
A60t = [0.7 0.2 0.1 0.1 0.2]' % Percentage difference between injection time for the 60 second
automatic injection setting and 60 seconds
A60v = [4.0 4.0 4.0 4.0 4.0]' % Percentage difference between the corresponding percent area
volume injected by the device over the injection time and the required 0.5 mL

figure(1);
hold on;
name = ["30 Second Injection Rate", "30 Second Volume Injected", "60 Second Injected Rate",
"60 Second Volume Injected"];
figure(1)
boxplot([A30t, A30v, A60t, A60v], name)
ylabel('Percentage Difference with Respective Rate or Volume(%)')
title('Relative Error Associated with 30 and 60 Second Injection Rates and Volume Delivery
Compared to the Target Values')
hold off;
```

## References:

- [1] Dr. A. M. Helmenstine, "How to Calculate Percent Error," ThoughtCo, Nov. 02, 2020.  
<https://www.thoughtco.com/how-to-calculate-percent-error-609584> (accessed Dec. 03, 2021).



Section 6.9: Overall Device - Clinical Simulation Testing

Table 1: 30 Second Clinical Simulation Data for Overall Device Testing.

		Results	Percent Error (%)
Trial 1	Ejection Time	30.5 seconds	1.67
	Force Range	0.30-0.54 N	-
	Reverse time	24.15 seconds	-
Trial 2	Ejection Time	30.65 seconds	2.17
	Force Range	0.27-0.48 N	-
	Reverse time	23.25 seconds	-
Trial 3	Ejection Time	30.85 seconds	2.83
	Force Range	0.18-0.42 N	-
	Reverse time	23.30 seconds	-
Trial 4	Ejection Time	30.39 seconds	1.30
	Force Range	0.20-0.50 N	
	Reverse time	23.55 seconds	
Trial 5	Ejection Time	30.67 seconds	2.23
	Force Range	0.23-0.48 N	
	Reverse time	23.62 seconds	-

Table 2: 60 Second Clinical Simulation Data for Overall Device Testing.

		Results	Percent Error (%)
Trial 1	Ejection Time	60.42 seconds	0.70
	Force Range	0.13-0.41 N	-
	Reverse time	24.67 seconds	-
Trial 2	Ejection Time	60.45 seconds	0.75
	Force Range	0.17-0.42 N	-
	Reverse time	24.69 seconds	-
Trial 3	Ejection Time	60.01 seconds	0.017
	Force Range	0.15-0.50 N	-
	Reverse time	24.62 seconds	-
Trial 4	Ejection Time	60.45 seconds	0.75
	Force Range	0.16-0.48 N	-
	Reverse time	24.23 seconds	-
Trial 5	Ejection Time	60.32 seconds	0.53
	Force Range	0.23-0.43 N	-
	Reverse time	24.28 seconds	-

The mean of the ejection time, force ranges and reverse times were calculated using the typical mean equation for a sample of five trials and the standard deviation was calculated using the standard deviation equation for samples rather than populations. The percent error was calculated to indicate how much error there was for the 30 and 60 second time settings respectively using the following equation:

$$[1] \text{ Percent Error} = (|V_{\text{theoretical}} - V_{\text{experimental}}| / V_{\text{theoretical}}) * 100$$

The serial plots were also obtained for this round of testing and can also be seen in the figures below.

**Serial Plot for a 30 Second Injection: Clinical Stimulation**

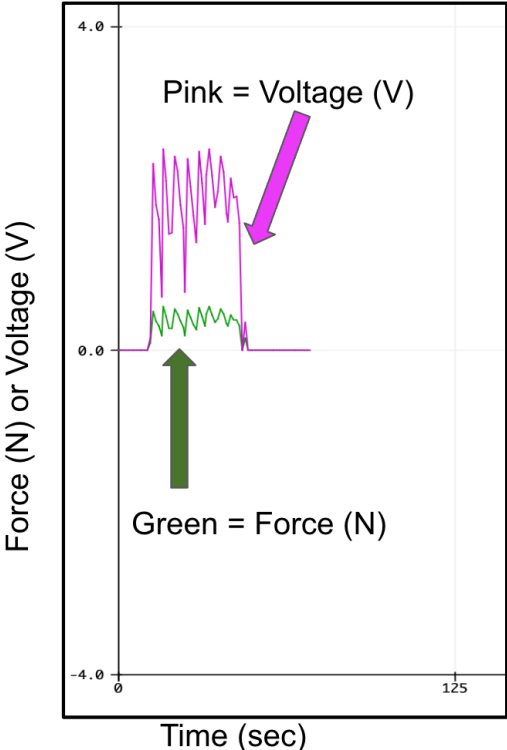


Figure 1: The serial plot with force values vs. time for the clinical simulation testing for one of the 30 second trials. The green line is the force values.

## Serial Plot for a 60 Second Injection: Clinical Stimulation

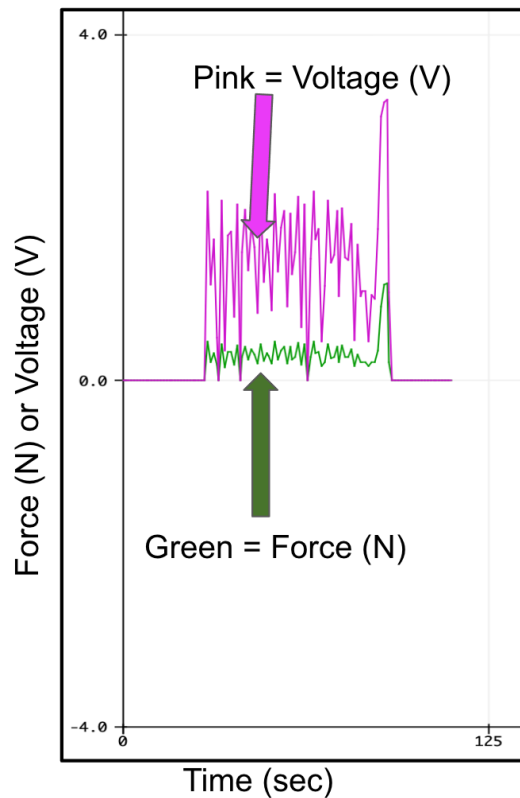


Figure 2: The serial plot with force values vs. time for the clinical simulation testing for one of the 60 second trials. The green line is the force values.

### **References:**

- [1] Dr. A. M. Helmenstine, "How to Calculate Percent Error," ThoughtCo, Nov. 02, 2020.  
<https://www.thoughtco.com/how-to-calculate-percent-error-609584> (accessed Dec. 03, 2021).

Section 6.10: Catheter Backup Data and Analysis

Table 1: Maximum threshold force values that correspond to catheter obstruction for both 30 and 60 second injection rates as well as the average threshold (n = 3).

Injection Rate	Trial Number	Maximum Threshold Force Value (N)	Average Threshold Force Value (N)	Standard Deviation (N)
30 Second Injections	1	3.84	3.47	± 0.33
	2	3.23		
	3	3.33		
60 Second Injections	1	4.24	4.29	± 0.07
	2	4.37		
	3	4.27		

**Average and Standard Deviation Matlab Code**

%% BME 400 - Catheter Obstruction Testing Results

% Author - Parker Esswein

%%

x = [3.84 3.23 3.33] % 30 second automatic injection threshold force values

y = [4.24 4.37 4.27] % 60 second automatic injection threshold force values

mean(x) % Average threshold force value for the 30 second injections

std(x) % Sample standard deviation for the 30 second injection rates

mean(y) % Average threshold force value for the 60 second injections

std(y) % Sample standard deviation for the 60 second injection rates

**Two-Sample Student t-test Matlab Code**

%% BME 400 - Catheter Obstruction Force Value t-test

% Author - Parker Esswein

%%

sPF = [3.84 3.23 3.33] % Peak force values for the 30 second injection rate

IPF = [4.24 4.37 4.27] % Peak force values for the 60 second injection rate

%%

mean(sPF)

std(IPF)

[h,p,ci, stats] = ttest2(sPF, IPF)

## References

- [1] F. P. Beer, E. R. Johnston Jr., J. T. DeWolf, and D. F. Mazurek, Mechanics of Materials, 8th Edition. McGraw Hill Education, 2020.
- [2] Dr. A. M. Helmenstine, “How to Calculate Percent Error,” ThoughtCo, Nov. 02, 2020. <https://www.thoughtco.com/how-to-calculate-percent-error-609584> (accessed Dec. 03, 2021).

Section 6.11: Bovine Steak Injection Testing Results

Well Done Results

Table 1: 60 second Well Done Steak Testing Results with the Force Range (lower and upper boundaries), peak force and injection rate.

	Lower Boundary of Force Range (N)	Upper Boundary of Force Range (N)	Peak Force (N)	Rate (s)
Trial 1	0.90	1.25	1.36	60.47
Trial 2	0.85	1.20	1.41	60.87
Trial 3	1.07	1.50	1.69	60.45
Trial 4	1.20	1.60	1.85	60.27
Average ± Standard Deviation	1.01 ± 0.161	1.39 ± 0.193	1.58 ± 0.233	60.52 ± 0.253

Table 2: 30 second Well Done Steak Testing Results with the Force Range (lower and upper boundaries), peak force and injection rate.

	Lower Boundary of Force Range (N)	Upper Boundary of Force Range (N)	Peak Force (N)	Rate (s)
Trial 1	1.20	1.70	1.92	30.90
Trial 2	1.30	1.60	1.99	30.90
Trial 3	1.30	1.60	1.93	30.93
Average ± Standard Deviation	1.27 ± 0.058	1.63 ± 0.058	1.95 ± 0.0379	30.91 ± 0.0173

Medium Well Results

Table 3: 60 second Medium Well Steak Testing Results with the Force Range (lower and upper boundaries), peak force and injection rate.

	Lower Boundary of Force Range (N)	Upper Boundary of Force Range (N)	Peak Force (N)	Rate(s)
Trial 1	1.30	1.60	1.98	60.53

Trial 2	1.50	1.70	2.03	60.56
Trial 3	1.30	1.80	2.06	60.62
Average ± Standard Deviation	1.37 ± 0.115	1.70 ± 0.100	2.02 ± 0.0404	60.57 ± 0.0458

Table 4: 30 second Medium Well Steak Testing Results with the Force Range (lower and upper boundaries), peak force and injection rate.

	Lower Boundary of Force Range (N)	Upper Boundary of Force Range (N)	Peak Force (N)	Rate (s)
Trial 1	1.40	1.90	2.04	30.90
Trial 2	1.50	2.00	2.30	30.49
Trial 3	1.30	2.20	2.44	30.70
Average ± Standard Deviation	1.40 ± 0.100	2.03 ± 0.153	2.26 ± 0.203	30.70 ± 0.205

#### Medium Results

Table 5: 60 second Medium Steak Testing Results with the Force Range (lower and upper boundaries), peak force and injection rate.

	Lower Boundary of Force Range (N)	Upper Boundary of Force Range (N)	Peak Force (N)	Rate (s)
Trial 1	1.60	2.30	2.52	60.51
Trial 2	1.00	1.80	2.40	60.72
Trial 3	1.00	2.00	2.33	60.50
Average ± Standard Deviation	1.20 ± 0.346	2.03 ± 0.252	2.42 ± 0.0961	60.58 ± 0.124

Table 6: 30 second Medium Steak Testing Results with the Force Range (lower and upper boundaries), peak force and injection rate.



	Lower Boundary of Force Range (N)	Upper Boundary of Force Range (N)	Peak Force (N)	Rate (s)
Trial 1	1.00	2.00	2.45	30.73
Trial 2	1.20	2.30	2.54	30.90
Trial 3	1.20	2.30	2.53	30.33
Average ± Standard Deviation	1.13 ± 0.115	2.20 ± 0.173	2.51 ± 0.0493	30.65 ± 0.293

Raw Results

Table 7: 60 second Raw Steak Testing Results with the Force Range (lower and upper boundaries), peak force and injection rate.

	Lower Boundary of Force Range (N)	Upper Boundary of Force Range (N)	Peak Force (N)	Rate (s)
Trial 1	0.80	1.19	1.24	60.14
Trial 2	1.26	1.26	1.36	60.54
Trial 3	1.04	1.40	1.49	60.53
Average ± Standard Deviation	1.03 ± 0.230	1.28 ± 0.107	1.36 ± 0.125	60.40 ± 0.228

Table 8: 30 second Raw Steak Testing Results with the Force Range (lower and upper boundaries), peak force and injection rate.

	Lower Boundary of Force Range (N)	Upper Boundary of Force Range (N)	Peak Force (N)	Rate (s)
Trial 1	1.10	1.40	1.68	30.60
Trial 2	1.14	1.60	1.72	30.39
Trial 3	1.15	1.50	1.67	30.92
Average ± Standard Deviation	1.13 ± 0.0265	1.50 ± 0.100	1.69 ± 0.0265	30.64 ± 0.267

Section 6.12: Viscosity Testing Injection Results

Table 1: 30 second Water Injection Testing Results with the Force Range (lower and upper boundaries), and peak force.

30 Second Trial #	Maximum Force (N)	Range Minimum (N)	Range Maximum (N)
Trial 1	2.06	1	1.8
Trial 2	1.06	0.7	0.9
Trial 3	1.2	0.71	1
Average ± Standard Deviation	1.44 ± 0.54	0.803 ± 0.17	1.23 ± 0.49

Table 2: 60 second Water Injection Testing Results with the Force Range (lower and upper boundaries), and peak force.

60 Second Trial #	Maximum Force (N)	Range Minimum (N)	Range Maximum (N)
Trial 1	1.06	0.5	0.8
Trial 2	1.21	0.7	1
Trial 3	1.1	0.75	0.95
Average ± Standard Deviation	1.12 ± 0.077	0.65 ± 0.13	0.917 ± 0.104

Table 3: 60 second Oil Injection Testing Results with the Force Range (lower and upper boundaries), and peak force.

60 Second Trial #	Maximum Force (N)	Range Minimum (N)	Range Maximum (N)
Trial 1	2.08	1.5	1.85
Trial 2	2.03	1.5	1.8
Trial 3	1.99	1.4	1.7
Average ± Standard Deviation	2.03 ± 0.045	1.46 ± 0.048	1.78 ± 0.076

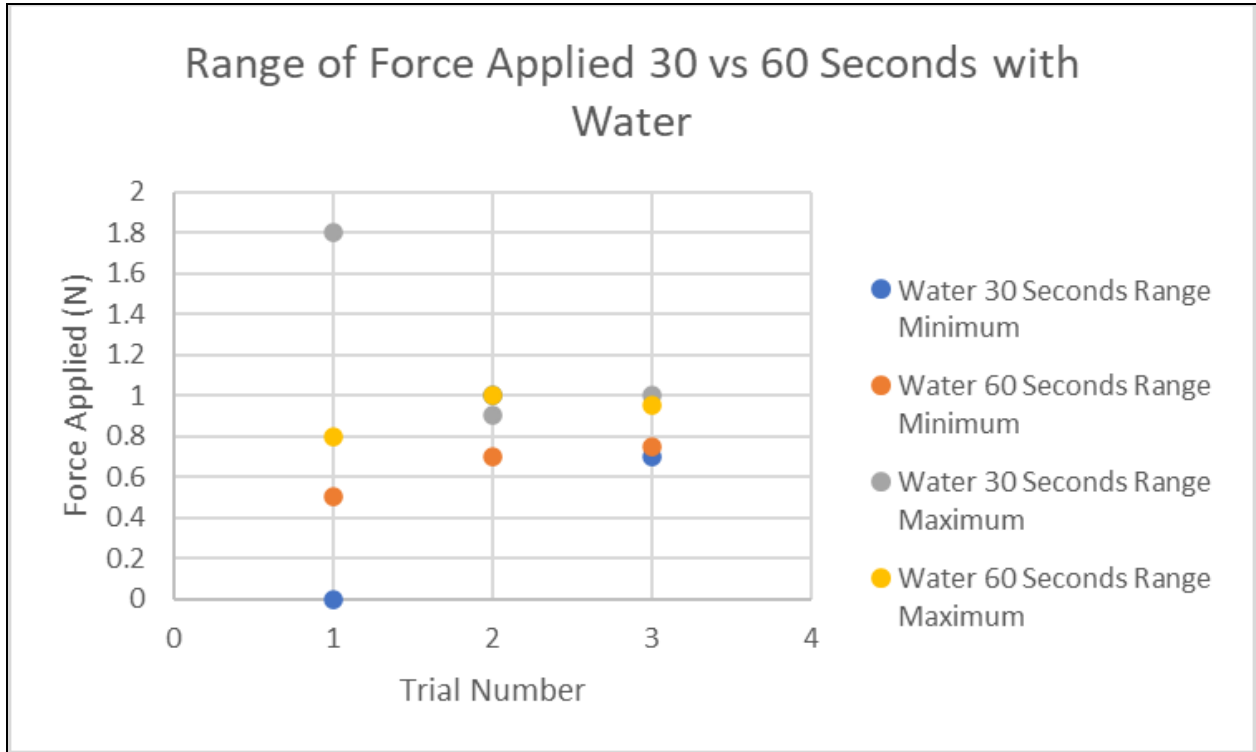


Figure 1: Viscosity Injection Testing Results for water force range (N) at the 30 and 60 second injection rates.

Section 6.13: Pressure Sensing Catheter Data and Analysis

Table 1: Force Range, Peak Force, and Peak Pressure as established during pressure sensing catheter testing for both the 30 second and 60 second injection rates (n = 3).

Injection Rate and Average	Trial Number	Force Range (N)	Peak Force (N)	Peak Pressure (mmHg)
30 Second Injections	1	1.40 - 2.50	2.98	429
	2	1.50 - 2.80	3.20	429
	3	1.50 - 5.00	6.00	429
Average	-	1.47 ± 0.06 - 3.43 ± 1.37	4.06 ± 1.68	429
60 Second Injections	1	1.20 - 2.20	2.72	429
	2	1.40 - 1.80	2.22	429
	3	2.20 - 4.00	4.35	429
Average	-	1.60 ± 0.53 - 2.67 ± 1.17	3.10 ± 1.11	429

**Force Range and Peak Force Average and Standard Deviation Matlab Code**

%% BME 400 - Pressure Sensor Average Value

% Author - Parker Esswein

%%

sPF = [2.98 3.20 6.00] % Peak force values for the 30 second injection rate

IPF = [2.72 2.22 4.35] % Peak force values for the 60 second injection rate

lsFR = [1.40 1.50 1.50] % Lower force values for force range associated with 30 second injection rate

usFR = [2.50 2.80 5.00] % Upper force values for force range associated with 30 second injection rate

lfFR = [1.20 1.40 2.20] % Lower force values for force range associated with 60 second injection rate

ufFR = [2.20 1.80 4.00] % Upper force values for force range associated with 60 second injection rate

%%

mean(sPF)

std(sPF)

mean(IPF)

std(IPF)

mean(lsFR)

std(lsFR)

mean(usFR)  
std(usFR)

mean(lIFR)  
std(lIFR)

mean(uIFR)  
std(uIFR)

Table 2: Force Values that correlate to the onset of Peak Pressure as established during pressure sensing catheter testing for both the 30 second and 60 second injection rates (n = 2).

Injection Rate and Average	Trial Number	Peak Pressure Onset Force (N)	Peak Pressure (mmHg)
30 Second Injections	1	2.20	429
	2	2.22	429
Average	-	2.21 ± 0.01	429
60 Second Injections	1	2.26	429
	2	2.17	429
Average	-	2.22 ± 0.06	429

### Onset Peak Pressure Force and t-test Matlab Code

```
%% BME 400 - Pressure Sensor Force Value t-test
% Author - Parker Esswein
%%
sPF = [2.20 2.21] % Peak force values for the 30 second injection rate
IPF = [2.26 2.17] % Peak force values for the 60 second injection rate
%%
mean(sPF)
std(sPF)
mean(IPF)
std(IPF)
[h,p,ci, stats] = ttest(sPF, IPF)
```